Pre-clinical and clinical evaluation of the malaria vaccines RH5-VLP and PfSPZ Vaccine



Andrew Scott Ishizuka

Keble College

University of Oxford

A thesis submitted for the degree of

Doctor of Philosophy

Trinity Term 2016

This thesis is dedicated to:

Gene N. Peterson, M.D., Ph.D.

for his unending support and inspiration.

Acknowledgements

Personal

This work was conducted under the supervision of Profs. Simon Draper and Adrian Hill at the Jenner Institute, Oxford, and Dr. Robert Seder at the Vaccine Research Center, NIH, in Bethesda, Maryland.

I had the privilege of working with over 100 scientists who contributed ideas, materials, and experimental support over the course of this degree. Their contributions are recognized throughout the text. I am grateful for the contributions of each of them. In particular, I wish to thank:

Bob Seder, for his endless enthusiasm, keen insights, tireless support, and tailored mentorship in the face of my progressive obstinancy.

Simon Draper and Adrian Hill, for their patience, selflessness, and deft experimental planning.

My VRC colleagues Tricia Darrah, Barbara Flynn, Joe Francica, Ayako Yamamoto, and Tracy Abram, for emotional, experimental, and administrative support, and Mario Roederer, for definitive guidance on everything related to flow cytometry.

Steve Hoffman, Kim Lee Sim, and their outstanding teams at Sanaria, in particular Sumana Chakravarty, Adam Ruben, Eric James, and Tao Li, for - among other efforts - producing over 300 million sporozoites for me.

Kirsten Lyke at the University of Maryland, and Julie Ledgerwood and Barney Graham at the VRC, for coordinating the clinical protocols, teams, and study volunteers.

Benjamin Mordmüller at the University of Tübingen for the opportunity to study the clinical samples from a brilliantly designed and executed study.

Sumi Biswas and the Blood-stage group at the Jenner, in particular, Jing Jin, Darren Leneghan, Lee Li, Rebecca Dabbs, and Daniel Alanine, for helping me produce my first recombinant proteins.

Katie Soucy, Rick Fairhurst, Mike Lenardo, Richard Siegel, Tom Wynn, and Richard Cornall, for their service to the NIH-Oxford-Cambridge Scholars program, and for giving me the opportunity to be a member of the program.

My friend and colleague Geoff Lynn, for countless contributions to my personal and professional life.

Finally, I wish to thank my family and friends for their unwavering support through the daily ups and downs of my training as a physician-scientist.

Institutional

This work was supported by an Intramural Research Training Award through the NIH-Oxford-Cambridge Scholars Program. My training was also supported by a grant from the Medical Scientist Training Program in collaboration with the Duke University School of Medicine.

Declaration of Authentication

The work presented herein was performed by me and in no way forms part of another thesis from this or any other university. Contributions made by others are acknowledged in the text. This work was performed under the supervision of Professors Simon Draper and Adrian Hill within the Nuffield Department of Clinical Medicine under the Division of Medical Sciences at the University of Oxford.

Andrew Scott Ishizuka

University of Oxford

Trinity Term 2016

Abstract

Despite progress through expanded use of bed nets and anti-malarial drugs, *Plasmodium falciparum* (Pf) malaria caused about 200 million cases and 500,000 deaths in 2015. An ideal vaccine would reduce the burden of disease and interrupt transmission. Despite decades of effort, there is no vaccine that can adequately address the global burden of malaria.

This thesis focuses on two potential weaknesses in the parasite life-cycle. First, I investigate two vaccination strategies aimed at improving the antibody response to RH5, an essential and conserved protein for erythrocyte invasion. Due to instability of the resultant recombinant vaccine constructs, these efforts have required re-engineering of the vaccine platform, which remains an ongoing effort.

Second, the immunogenicity and mechanism of protection of a live-attenuated whole sporozoite vaccine, PfSPZ Vaccine, was assessed. In a study that examined PfSPZ Vaccine at intravenous (IV) doses between 1.35×10^5 to 4.5×10^5 PfSPZ, I demonstrate that PfSPZ antibody responses correlated with durable sterile protection against controlled human malaria infection (CHMI). Surprisingly, the *pre-vaccine* frequency of $V\gamma9^+V\delta2^+$ T cells, an innate T cell that recognizes conserved *Plasmodium* phosphoantigens, also correlated with durable sterile protection. Regarding the mechanism of protection, PfSPZ-specific antibodies as well as CD8 and CD4 T cells in the blood decreased substantially over time, yet sterile protection was maintained. In non-human primates, the CD8 T cell response in the liver at a memory time point was measured to be about 100-fold higher than found in the blood. Collectively, these data suggest that PfSPZ Vaccine confers durable protection in humans by long-lived, tissue-resident CD8 T cells.

These findings were extended with a study using 9.0×10^5 PfSPZ, wherein I demonstrate that T cell responses peaked immediately after the first vaccination

with minimal T cell activation despite additional immunizations. This suggests that anti-PfSPZ immunity may be limiting the effectiveness of subsequent immunizations.

Finally, I examined the T cell response to PfSPZ attenuated by chloroquine (termed PfSPZ-CVac). T cell responses were substantially higher than achieved with comparable PfSPZ Vaccine doses. Additionally, a significantly higher proportion of PfSPZ-specific CD4 T cells were polyfunctional, simultaneously expressing IFN-γ, IL-2, and TNF-α, in subjects that were protected from CHMI.

In sum, these studies provide insight into the immunobiology of a protective immune response that may guide future malaria vaccine development efforts.

Contents

List of Figures **xii**

List of Tables **xiv**

List of Abbreviations **xv**

1 Introduction **1**

1.1 Vaccines and public health 2

1.1.1 Major global diseases for which vaccines do not currently exist 5

1.2 Vaccine composition 6

1.2.1 Whole organism vaccines 6

1.2.2 Subunit vaccines 6

1.3 Vaccine immunology 8

1.3.1 Innate immune system 8

1.3.2 Innate and semi-innate lymphocytes 9

1.3.3 Adaptive immune system 10

1.3.4 Tissue-resident T cells 11

1.4 Malaria 11

1.4.1 Burden of disease 12

1.4.2 Life cycle 12

1.4.3 Pathogenesis 14

1.4.4 Naturally acquired immunity 15

1.4.5 Malaria control interventions 16

1.5 Malaria vaccines 17

1.5.1 Pre-erythrocytic vaccines 17

1.5.2 Blood stage vaccines 26
1.5.3 Transmission blocking vaccines 29
1.6 Hypothesis and specific aims 30
1.6.1 Approach and principal aims 30
1.6.2 Principal hypotheses 30
1.6.3 Specific aims 31
1.6.4 Outline 32

2 Materials and methods **33**
2.1 Materials 34
2.1.1 Solutions and reagents 34
2.2 Methods in molecular biology 39
2.2.1 Cloning 39
2.2.2 Transfections and transformations 40
2.2.3 Protein expression and purification 41
2.2.4 Protein characterization 43
2.3 Methods in immunology 45
2.3.1 Human immunology 45
2.3.2 Functional assessment of IgG from vaccine recipients 51
2.3.3 T cell responses in vaccinated non-human primates 53
2.4 Statistical analyses 54
2.4.1 Data analysis 54
2.4.2 Efficacy analysis 56
2.4.3 Immunogenicity 56
2.4.4 Immune correlates 56

3 RH5 VLPs **58**
3.1 Introduction 59
3.1.1 RH5 as a blood stage vaccine target 59
3.1.2 Study rationale 59
3.1.3 Study aims 60

3.1.4 Authorship 60
3.1.5 Summary of findings 61
3.2 Results 61
3.2.1 Construct design: sv3 and sv3-IMX313 61
3.2.2 sv3 and sv3-IMX313 expression and purification 62
3.2.3 SpyTag-SpyCatcher rationale 64
3.2.4 Construct design: sv3-SpyTag and Pfs25-SpyTag 66
3.2.5 sv3-SpyTag and Pfs25-SpyTag expression and purification . 66
3.2.6 Construct design: SpyCatcher-HBsAg 66
3.2.7 SpyCatcher-HBsAg expression and purification 69
3.2.8 HBsAg conjugation 69
3.2.9 AP205 conjugation 70
3.3 Discussion 71
3.3.1 RH5-IMX313 71
3.3.2 sv3-SpyTag 72
3.3.3 Future directions 72

4 PfSPZ Vaccine correlates and mechanism of protection 74
4.1 Introduction 75
4.1.1 Durability of PfSPZ Vaccine efficacy is unkonwn 75
4.1.2 Study design 75
4.1.3 Study aims 76
4.1.4 Authorship 76
4.1.5 Summary of findings 77
4.2 Results 77
4.2.1 Study population 77
4.2.2 Vaccine efficacy over 1 year 80
4.2.3 Immunogenicity 81
4.2.4 Correlates of sterile protection 83
4.2.5 Role of PfSPZ antibodies in protection 86

4.2.6 PfSPZ-specific T cell activation after CHMI is dependent on timing of CHMI . . . 88
4.2.7 Longitudinal T cell responses . . . 90
4.2.8 Tissue-resident T cell responses in NHP. . . . 91
4.3 Discussion . . . 94
4.3.1 Vaccine efficacy . . . 94
4.3.2 Immunogenicity . . . 94
4.3.3 Correlates of sterile protection . . . 95
4.3.4 Mechanism of protection . . . 96
4.3.5 Study limitations and future directions . . . 97

5 Immunogenicity and efficacy against heterologous PfSPZ 98
5.1 Introduction . . . 98
5.1.1 Study aims . . . 99
5.1.2 Authorship . . . 100
5.1.3 Summary of findings . . . 100
5.2 Results . . . 100
5.2.1 Study population . . . 100
5.2.2 Vaccine efficacy, homologous CHMI . . . 100
5.2.3 Vaccine efficacy, heterologous CHMI . . . 101
5.2.4 Antibody responses . . . 102
5.2.5 CD8 and CD4 T cell responses . . . 103
5.2.6 $\gamma\delta$ T cell responses . . . 104
5.2.7 T cell responses against 7G8 . . . 106
5.3 Discussion . . . 107
5.3.1 Efficacy . . . 107
5.3.2 Immunogenicity . . . 109
5.3.3 Study limitations and future directions . . . 110

6 PfSPZ-CVac T cell immunology **111**

6.1 Introduction 111

6.1.1 Clinical study design and efficacy 112

6.1.2 Immunogenicity study rationale 113

6.1.3 Study aims 113

6.1.4 Authorship 113

6.1.5 Summary of findings 114

6.2 Results 114

6.2.1 T cell immunogenicity 114

6.2.2 Correlates of sterile protection 120

6.3 Discussion 123

6.3.1 Immunogenicity 123

6.3.2 Correlates of sterile protection 123

6.3.3 Study limitations and future directions 123

7 Conclusions **127**

7.1 Summary and conclusions 127

7.2 Future directions 130

7.2.1 RH5 vaccines 130

7.2.2 Immunological studies of PfSPZ Vaccine 130

7.2.3 PfSPZ Vaccine regimen optimizations 132

Bibliography **134**

List of Figures

2.1 Human flow cytometry gating 48
2.2 Phenotypic flow cytometry gating 49
2.3 ICS assay reproducibility 50
2.4 FRG experimental scheme 52
2.5 NHP flow cytometry gating 55

3.1 RH5 and RH5-IMX313 construct design 62
3.2 sv3 and sv3-IMX313 expression and purification 63
3.3 SpyTag assembly scheme 65
3.4 sv3-SpyTag and Pfs25-SpyTag construct design, expression, and purification 67
3.5 SpyCatcher-HBsAg construct design, expression, and purification . 68
3.6 sv3 and Pfs25 conjugation to HBsAg VLP 70
3.7 sv3 and Pfs25 conjugation to AP205 VLP 71

4.1 VRC 314 Consort diagram 78
4.2 Sterile protection following CHMI at 59 weeks after PfSPZ vaccination 79
4.3 Pf-specific antibody and cellular immune responses 2 weeks after final immunization. 82
4.4 $\gamma\delta$ T cell subset and phenotypic changes 84
4.5 Correlation between immune responses and CHMI outcome. 85
4.6 Functional role of PfSPZ-specific antibodies. 87
4.7 Activation of PfSPZ-specific CD4 T cells following CHMI. 89
4.8 Longitudinal assessment of Pf-specific T cells. 91
4.9 Circulating and tissue-resident Pf-specific T cells in NHP. 92

4.10 Composition of lymphocytes in NHP and human liver 93

5.1 Efficacy of PfSPZ Vaccine against homologous and heterologous CHMI. 101
5.2 PfSPZ-specific antibody responses. 102
5.3 PfSPZ-specific CD8 and CD4 T cell responses. 105
5.4 PfSPZ-specific $\gamma\delta$ T cell responses. 106
5.5 T cell responses to PfSPZ NF54 and 7G8. 108

6.1 Clinical study design and estimated efficacy 112
6.2 Cytokine profiles of post-vaccination PBMC supernatants 115
6.3 T_H1 CD4 T cell immunogenicity 116
6.4 CD4 T_H1 cytokine polyfunctionality 117
6.5 IL-4^+ and IL-10^+ CD4 T cell immunogenicity 117
6.6 CD8 T cell immunogenicity 118
6.7 $\gamma\delta$ T cell immunogenicity 118
6.8 $\gamma\delta$ T cell sub-family analysis 119
6.9 Phenotypic analysis of $\gamma\delta$ T cells 120
6.10 Correlation of CD4 T cell responses with sterile protection 121
6.11 CD4 T cell IFN-γ MFI 121
6.12 Correlation of CD4 T cell polyfunctionality with sterile protection . 122
6.13 Correlation of CD8 T cell responses with sterile protection 122

List of Tables

1.1 FDA approved vaccines 3
1.2 FDA approved vaccines (cont.) 4

2.1 Commercially available reagents 36
2.2 Fluorescently-labeled antibodies used for flow cytometry 37
2.3 Flow cytometry panels 38

6.1 Correlation of CD4, CD8, and $\gamma\delta$ T cell responses with sterile protection. 124

List of Abbreviations

aIFA . . . . . automated immunofluoresence assay

ACUC . . . . . animal care and use committee

ACD . . . . . acid citrate dextrose

APC . . . . . allophycocyanin dye

APC . . . . . antigen-presenting cell

AS01 . . . . . liposomes with 50 μg MPL and 50 μg QS21

AS02A . . . . an oil-in-water emulsion with 50 μg MPL and 50 μg QS21

Ax . . . . . Alexa Fluor dye

BCA . . . . . bicinchoninic acid

BSA . . . . . bovine serum albumin

BV . . . . . Brilliant Violet dye

CBC . . . . . complete blood count

CCR . . . . . CC chemokine receptor

CD . . . . . cluster of differentiation

CHMI . . . . . controlled human malaria infection

CPS . . . . . chloroquine prophylaxis with sporozoites

CSP . . . . . circumsporozoite protein

CXCR . . . . . CXC chemokine receptor

Cy . . . . . cyanine dye

DC . . . . . dendritic cell

DVI . . . . . direct venous inoculation

EDTA . . . . . ethylenediaminetetraacetic acid

ELISA . . . . . enzyme linked immunosorbent assay

FACS . . . . . fluorescence-activated cell sorting

FDA . . . . . U.S. Food and Drug Administration

FITC . . . . . fluorescein isothiocyanate dye

FPLC . . . . . fast protein liquid chromatography

GAP . . . . . genetically-attenuated parasites

GPI . . . . . glycophosphatidylinositol

HEK293 . . . human embryonic kidney cell line 293

HI-FCS . . . . heat-inactivated fetal calf serum

HIV . . . . . human immunodeficiency virus

HLA . . . . . human leukocyte antigen

HSA . . . . . human serum albumin

ICS . . . . . intracellular cytokine staining

ID . . . . . intradermal

IFN . . . . . interferon

Ig . . . . . immunoglobulin

IHL . . . . . intrahepatic lymphocytes

IND . . . . . investigational new drug

IL . . . . . interleukin

IM . . . . . intramuscular

IRB . . . . . institutional review board

IV . . . . . intravenous

iNKT . . . . . invariant natural killer T cell

KLRG1 . . . . killer cell lectin-like receptor subfamily G member 1

LN . . . . . lymph node

LNVP . . . . . liquid nitrogen vapor phase

mAb . . . . . monoclonal antibody

MAIT . . . . . mucosal associated invariant T cell

MHC . . . . . major histocompatibility complex

MPL . . . . . monophosphoryl lipid A, an immunostimulant

MVA . . . . . modified vaccinia Ankara

NHP . . . . . non-human primate

NK . . . . . natural killer cell

PAGE . . . . . polyacrylamide gel electrophoresis

PBMC . . . . peripheral blood mononuclear cells

PBS . . . . . phosphate buffered saline

PCR . . . . . polymerase chain reaction

PD-1 . . . . . programmed death receptor-1

PE . . . . . phycoerythrin dye

PEXEL . . . . *Plasmodium* export element

PTEX . . . . . *Plasmodium* translocon of exported proteins

PerCP . . . . . peridinium chlorophyll protein dye

Pf . . . . . *Plasmodium falciparum*

QD . . . . . quantom dot dye

QS21 . . . . . an immunostimulant from *Quillaja saponaria* tree bark

RAS . . . . . radiation-attenuated sporozoite

RIFIN . . . . . repetitive interspersed families of polypeptides

SAGE . . . . . Strategic Advisory Group of Experts (SAGE) on Immunization

SC . . . . . subcutaneous

SDS . . . . . sodium dodecyl sulfate

SPZ . . . . . sporozoite

STEVOR . . . subtelomeric variable open reading frame

TB . . . . . *Mycobacterium tuberculosis*

TBS . . . . . thick blood smear

TBS . . . . . Tris buffered saline

$\mathbf{T_{CM}}$ . . . . . central memory T cell

TCR . . . . . T cell receptor

TE . . . . . terminal effector memory T cell

$\mathbf{T_{EM}}$ . . . . . effector memory T cell

Th . . . . . T helper cell

TLR . . . . . Toll-like receptor

$\mathbf{T_{REG}}$ . . . . . regulatory T cell

VTS . . . . . vacuolar transport signal

VRC . . . . . Vaccine Research Center

VLP . . . . . virus-like particle

WHO . . . . . World Health Organization

YPD . . . . . yeast, peptone, dextrose

1 Introduction

Contents

1.1 Vaccines and public health 2
1.1.1 Major global diseases for which vaccines do not currently exist 5
1.2 Vaccine composition 6
1.2.1 Whole organism vaccines 6
1.2.2 Subunit vaccines 6
1.3 Vaccine immunology 8
1.3.1 Innate immune system 8
1.3.2 Innate and semi-innate lymphocytes 9
1.3.3 Adaptive immune system 10
1.3.4 Tissue-resident T cells 11
1.4 Malaria 11
1.4.1 Burden of disease 12
1.4.2 Life cycle 12
1.4.3 Pathogenesis 14
1.4.4 Naturally acquired immunity 15
1.4.5 Malaria control interventions 16
1.5 Malaria vaccines 17
1.5.1 Pre-erythrocytic vaccines 17
1.5.2 Blood stage vaccines 26
1.5.3 Transmission blocking vaccines 29
1.6 Hypothesis and specific aims 30
1.6.1 Approach and principal aims 30
1.6.2 Principal hypotheses 30
1.6.3 Specific aims 31
1.6.4 Outline 32

1.1 Vaccines and public health

Vaccines have been instrumental in preventing disease and death against a wide array of infectious pathogens. The widespread use of the smallpox vaccine led to its eradication [1]. Additionally, considerable progress has been made in suppressing infections with polio [2], measles [3], and tetanus [4], among other diseases. Vaccines have now been developed for dozens of infectious diseases (see **Table 1.1**). However, 5 million deaths globally per year are caused by infectious diseases for which there is no vaccine or for which the vaccine is inadequately effective or deployed [5]. The disproportionate share of these deaths fall on populations in low- and middle-income countries.

Thus, efforts to develop new vaccines – aided by continuously improving understanding of the mechanistic determinants of the induction and functionality of protective immune responses – are continuing with vigor. These advances have caused a shift in vaccine discovery from a process of empiricism to one of rational design of each component [6]. In particular, there is a vibrant effort directed against HIV [7], TB [8], and malaria.

The list of FDA approved vaccines, their trade names, and composition are described in **Tables 1.1** and **1.2**; **Tables 1.1** and **1.2** adapted from [9].

Disease (vaccine target)	Vaccine trade name	Vaccine composition
Adenovirus-associated acute respiratory disease	No trade name	Live, oral adenovirus type 4 and type 7
Anthrax	Biothrax	Bacillus anthracis antigen (PA) adsorbed on alum
Cholera	Vaxchora	Live, oral V. cholerae CVD 103-HgR
Diphtheria and tetanus	TENIVAC, and no trade name	Diphtheria and tetanus toxoids adsorbed on alum
Diphtheria, tetanus, and pertussis	Infanrix, DAPTACEL, Tripedia	Diphtheria and tetanus toxoids and pertussis antigens adsorbed on alum
Diphtheria, tetanus, pertussis, and poliomyelitis	KINRIX , Quadracel	Diphtheria and tetanus toxoids, pertussis antigens and inactivated poliovirus adsorbed on alum
Diphtheria, tetanus, pertussis, hepatitis B, and poliomyelitis	Pediarix	Diphtheria and tetanus toxoids, pertussis antigens, HBsAg VLP, and inactivated poliovirus adsorbed on alum
Diphtheria, tetanus, pertussis, poliomyelitis, and Haemophilus influenza type b	Pentacel	Diphtheria and tetanus toxoids, pertussis antigens, inactivated poliovirus adsorbed, and Haemophilus influenza type b conjugated to tetanus toxoid on alum
Haemophilus influenza type b	PedvaxHIB	Capsular polysaccharide of Haemophilus influenza type b conjugated to an outer membrane protein complex (OMPC) of Neisseria meningitidis serogroup B
Haemophilus influenza type b	ActHIB, Hiberix	Capsular polysaccharide of Haemophilus influenza type b conjugated to tetanus toxoid
Haemophilus influenza type b and hepatitis B	Comvax	Components from PedvaxHIB plus Recombivax HB
Hepatitis A	Havrix, VAQTA	Inactivated hepatitis A virus
Hepatitis A and Hepatitis B	Twinrix	Components from Havrix plus Engerix-B
Hepatits B	Recombivax HB, Engerix-B	HBsAg VLP
Human Papillomavirus associated cancers	Gardasil	VLP of recombinant major capsid (L1) from Human Papillomavirus (HPV) types 6, 11, 16 and 18
Human Papillomavirus associated cancers	Gardasil 9	VLP of recombinant major capsid (L1) from Human Papillomavirus (HPV) types 6, 11, 16, 18, 31, 33, 45, 52, and 58
Human Papillomavirus associated cancers	Cervarix	VLP of recombinant L1 from HPV types 16 and 18
Influenza A H1N1 (2009)	No trade name	Inactivated, split virion of influenza A H1N1
Influenza A H5N1	No trade name	Inactivated, split viron of influenza A H5N1
Influenza A and B	Afluria, FluLaval, Fluarix, Fluvirin, Agriflu, Fluzone, Flucelvax, Flublok, Fluarix Quadrivalent, Fluzone Quadrivalent, FluLaval Quadrivalent	Inactivated, split viron of selected influenza A and influenza B strains
Influenza A and B	FluMist, FluMist Quadrivalent	Live, attenuated influenza A and influenza B virus of selected strains

Table 1.1: FDA approved vaccines

Disease (vaccine target)	Vaccine trade name	Vaccine composition
Japanese Encephalitis Virus	Ixiaro, JE-Vax	Inactivated whole virus (Ixiaro adsorbed to alum)
Measles and mumps	M-M-Vax	Live, attenuated virus
Measles, mumps, and rubella	M-M-R II,	Live, attenuated virus
Measles, mumps, varicella, and rubella	ProQuad	Live, attenuated virus
Meningococcal (Groups A, C, Y, and W-135)	Menveo	Oligosaccharides from N. meningitidis serogroup A, C, Y and W-135 conjugated to Corynebacterium diphtheriae CRM197 protein
Meningococcal (Groups A, C, Y, and W-135)	Menactra	Polysaccharides from N. meningitidis serogroup A, C, Y and W-135 conjugated to diphtheria toxoid
Meningococcal (Groups A, C, Y, and W-135)	Menomune-A/C/Y/W- 135	Soluble polysaccharides from N. meningitidis serogroup A, C, Y and W-135
Meningococcal (Groups C and Y) and Haemophilus influenza type b	MenHibrix	Polysaccharides from N. meningitidis serogroup C and Y plus Capsular polysaccharide of Haemophilus influenza type b conjugated to tetanus toxoid
Meningococcal Group B	TRUMENBA	Recombinant lipidated factor H binding protein (fHbp) from N. meningitidis serogroup B, subfamily A05 and B01
Meningococcal Group B	BEXSERO	fHbp, Neisserial adhesin A (NadA), Neisserial heparin-binding antigen (NHBA), and PorA P1.4 immunodominant antigen of OMV NZ (strain NZ98/254)
Pneumococcal infection	Pneumovax 23, Prevnar, Prevnar 13	Saccharides from capsular antigens of different Streptococcus pneumoniae serotypes conjugated to diphtheria CRM197 protein (Pneumovax 23 not conjugated)
Poliovirus	Poliovax, IPOL	Inactivated poliovirus
Rabies	Imovax, RabAvert	Inactivated virus
Rotavirus	ROTARIX, RotaTeq	Live, attenuated virus
Smallpox	ACAM2000	Live vaccinia virus
Tetanus	No trade name	Tetanus toxoids adsorbed on alum
Typhoid	Vivotif	Live, attenuated Salmonella typhi Ty21a
Typhoid	TYPHIM Vi	Capsular polysaccharide from Salmonella enterica serovar Typhi, S typhi Ty2 strain
Tuberculosis	BCG Vaccine / TICE BCG	Live attenuated Mycobacterium bovis
Varicella virus	Varivax	Live, attenuated varicella virus
Yellow fever	YF-Vax	Live, attenuated 17D-204 strain of yellow fever virus
Herpes zoster	Zostavax	Live, attenuated varicella-zoster virus

Table 1.2: FDA approved vaccines (cont.)

1.1.1 Major global diseases for which vaccines do not currently exist

Campylobacter

Chlamydia

Cytomegalovirus

Ebola

Epstein-Barr (mononucleosis)

Helicobacter pylori: Gastrointestinal ulcers

Hepatitis C

Herpes Simplex

HIV

Influenza (universal flu vaccine)

Leishmaniasis

Malaria

Respiratory syncytial virus

Rhinovirus

Schistosomiasis

Shigella

Streptococcus groups A and B

Tuberculosis

Urinary tract infections

Zika virus

Other: Immunotherapies for allergies and autoimmune diseases

Other: Cancers (therapeutic vaccination)

(Adapted from Koff, *et al.* [10])

1.2 Vaccine composition

1.2.1 Whole organism vaccines

The first vaccines were developed empirically from whole organisms that were either inactivated/killed or attenuated [6]. Whole organism vaccines make up the majority of currently licensed vaccines [11] and have contributed immeasurably to reduce the burden of certain infections, notably smallpox [1]. Whole pathogen vaccines are useful in that they recapitulate certain aspects of the immune response to natural infection. For example, certain live attenuated vaccines have tropism for select tissues, which allows for the induction of a tissue-specific immune response that is focused to the site of natural transmission. The oral polio vaccine, oral typhoid, and live attenuated influenza vaccines have this property, at least in principle. Furthermore, whole organism vaccines contain a wide breadth of antigens. Wherein protection is mediated by multiple antigenic determinants, *e.g.*, pre-erythrocytic malaria [12], this approach allows one to develop a vaccine for which a clear target of protective immunity is unknown. Whole organism vaccination, however, does not work for many infections because the immunodominant immune response to the whole attenuated pathogen is not itself protective. Vaccines for HIV and influenza, wherein the natural immune response does not confer cross-strain protection, will likely require vaccines that focus the immune response on precisely defined antigens [13, 14]. More saliently, some live attenuated vaccines can revert to virulence (*e.g.*, polio [15]), or may be unsafe for immunocompromised individuals [16]. Additionally, some live attenuated vaccines require special storage (typhoid), creating logistical barriers, whereas others can be lyophilized and reconstituted at the point of care (*e.g.*, Cholera vaccine).

1.2.2 Subunit vaccines

Advances in molecular biology and recombinant engineering have allowed vaccinologists to design and test vaccines that aim to focus the immune response against a small set of well-defined antigens. These subunit vaccines often contain a single,

highly purified antigenic target. Such vaccines offer a more defined platform than whole organism vaccines [17]. The principal advantages of such an approach are their safety and high chemical definition. Moreover, delivery of a single, well defined antigen may also allow the immune response to focus on an otherwise subdominant component of the pathogen.

The nature of the subunit vaccine composition varies, but in the majority of cases is either a purified recombinant protein or polysaccharide, or encoded by a gene (either enclosed in a viral vector or administered as purified DNA/RNA).

DNA vaccines – due to their high degree of chemical definition – are the easiest to develop in principle, but many DNA vaccines have suffered from poor immunogenicity [18]. Viral vectors are considerably more efficient in the induction of T cell responses, but are often limited to single administration due to the generation of anti-vector immunity [19, 20, 21].

Polysaccharide or protein-based vaccines – when delivered as soluble components alone – are weakly immunogenic. Therefore, these antigens require formulation with adjuvants (delivery vehicles and immunostimulants) or require linkage to protein carriers to improve the stimulation of innate immune system and antigen delivery necessary to prime adaptive immune responses [22].

Virus-like particles

Subunit vaccines aimed at inducing antibody responses can be improved if the antigen is presented as a virus-like particle (VLP). VLPs present repetitive and densely-spaced epitopes that can efficiently cross-link B cell receptors [23]. Certain proteins will spontaneously form VLPs after expression, and several VLP-based vaccines have been licensed. The hepatitis B vaccine is based on the HBV surface antigen, which spontaneously forms 42 nm lipid-containing particles. These particles can be found in the blood of HBV infected patients, and indeed, the original vaccine was based on these isolated particles [24]. Now, the particles are expressed in yeast. RTS,S, described in detail below, is also a VLP, and is comprised of a fragment of *P. falciparum* CSP on an HBsAg particle. The human papillomavirus vaccine,

which consists of recombinantly expressed L1 capsid protein, also spontaneously forms VLPs [25]. The immunogenicity and success of these vaccine exemplifies the utility of multimeric display of B cell epitopes by VLPs for vaccines designed to elicit effective antibody responses.

1.3 Vaccine immunology

Vaccines function by inducing the adaptive immune system to generate a memory response. To successfully induce an adaptive immune response, it is essential to coordinate the activation and trafficking of both innate and adaptive arms of the immune system. Broadly speaking, the innate immune system comprises a set of cells that are specialized to recognize and rapidly respond to invariant chemical motifs on pathogens or stressed cells. The adaptive immune system comprises B cells and T cells, which express a diverse receptor repertoire and undergo selective expansion to confer immunological memory to the individual. Most licensed vaccines to date rely primarily on antibodies to mediate protection. CD4 T cells primarily provide help to B cells in currently licensed vaccines. There is currently no licensed vaccine that relies on CD8 T cells for protective immunity.

1.3.1 Innate immune system

The innate immune system specializes in providing a rapid response to invading pathogens. Innate immune cells include monocytes/macrophages, dendritic cells, eosinophils, neutrophils, basophils, mast cells, natural killer cells, and invariant T cells. These cells recognize invariant chemical motifs or stress signals associated with infection. Such pathogen-associated molecular patterns, or PAMPS, bind to conserved families of pathogen-recognition receptors (PRRs) expressed by these cells, including the Toll-like receptors (TLR), nod-like receptors (NLRs), and RIG-I-like receptors (RLRs) [26]. Macrophages, granulocytes, and NK cells can respond immediately to invading pathogens, mediating phagocytosis, inhibition of pathogen growth, or directly killing of infected cells. Monocyte/macrophages, dendritic cells, and – in certain cases – $\gamma\delta$ T cells are able to phagocytose dead or dying cells or

infectious agents, process their components into peptide fragments, and present the foreign peptides in the context of MHC molecules to T cells. They may also present entire foreign proteins on the surface of their cells for recognition by B cells. These cells are also programmed to migrate to secondary lymphoid organs for efficient encounter with circulating T cells and B cells [27].

1.3.2 Innate and semi-innate lymphocytes

Natural killer (NK) cells are strongly inhibited by tonic signaling by surface-expressed MHC Class I. Thus, in the event a cell downregulates MHC, NK cells recognize this as a strong signal and kill the affected cell. Certain pathogens down-regulate MHC class I to avoid detection by T cells.

$\gamma\delta$ T cells often bridge the gap between the innate and adaptive immune system. At the cell population level, $\gamma\delta$ T cells express a diverse TCR repertoire, however, certain clonotypes occur commonly and expand to large numbers [28]. There are two major expanded populations in humans, the V$\delta1^+$ and V$\delta2^+$ populations. V$\delta2^+$ predominant in adults, whereas V$\delta1^+$ are more common in infants [29]. V$\delta2^+$ T cells recognize phosphoantigens (lipid metabolites, such as hydroxyl-methyl-butenyl-pyrophosphate (HMBPP)) from stressed cells or pathogen-infected cells, including *Plasmodium*-infected cells [30, 31]. $\gamma\delta$ T cells may serve as antigen-presenting cells [32], leading to enhanced CD8 T cell priming [33]. $\gamma\delta$ T cells have also been shown to provide help to dendritic cells to facilitate protective responses to blood-stage malaria [34]. IFN-γ-secreting $\gamma\delta$ T cells are a correlate of protection against blood-stage malaria [35].

Invariant natural killer T cells (iNKT) are a family of closely related innate T cells that express an invariant T cell receptor encoded by the Vα24-Jα18 TCR alpha chain. iNKT cells recognize lipid antigens from bacteria and some fungi, most classically, α-galactosylceramide, in the context of CD1d, an MHC-Class I-like molecule. They cells express CXCR6 and are present in much higher frequencies in the mouse liver than mouse blood [36].

Mucosal-associated invariant T cells (MAIT) are another type of innate T cell that expresses an invariant T cell receptor encoded by the Vα7.2-Jα33 TCR alpha chain. MAIT cells recognize invariant micro-organism-derived riboflavin metabolites presented in the context of the highly-conserved MHC-Class-I-related molecule MR1. MAIT cells are present in higher percentages in humans compared to mice, and are particularly enriched in the liver. Like iNKT cells, MAIT cells express CXCR6, but not CCR7 [37].

1.3.3 Adaptive immune system

The adaptive immune system is comprised of B cell and T cells. B cells express a B cell receptor (BCR) on their surface, which allows these cells to recognize conformational epitopes present in polypeptides, proteins, polysaccharides and haptens. B cell activation requires B cell receptor cross-linking and co-stimulation, often from an activated professional antigen-presenting cell (often a follicular dendritic cell [38]), or through TLR signaling from phagocytosed antigen [23]. Following BCR cross-linking, the recognized cargo is phagocytosed, processed, and presented on the B cell surface in the context of MHC Class II. Thereafter, CD4 T cells (termed T follicular helper cells, Tfh) specific for the phagocytosed antigen can further license the B cell to undergo class switch recombination (to change the effector function of the antibody constant region) and affinity maturation (to increase the affinity of the antibody for the antigen) [39]. This process occurs within the primary lymphoid follicles of secondary lymphoid organs (*e.g.*, lymph nodes and spleen). As this process is ongoing, some cells receive signals to leave the lymph node, differentiate into plasma cells and similar antibody secreting cells, and home to the bone marrow. Still others remain as memory B cells and persist in secondary lymphoid organs awaiting re-encounter with antigen.

T cells express a T cell receptor on their surface, which allows these cells to recognize 8–24 amino acid long peptide sequences presented in the context of MHC. Generally, T cells express either CD8 or CD4. CD8 T cells recognize shorter peptide fragments on MHC Class I, which is expressed by all nucleated cells. CD4 T

cells, however, can recognize longer peptide fragments on MHC Class II, which is expressed by cells of the myeloid and lymphoid lineages only. CD8 T cells specialize in eliminating infected cells by secretion of effector cytokines (IFN-γ [40]), death signals (FAS–FAS-ligand), or pro-apoptotic factors (perforin, granzyme) [41].

CD4 T cells, however, have more diverse functions [42, 43]. CD4 T cells are now broadly classified into T_H1, T_H2, T_H17, T_{FH}, and T_{REG} cells. There are several other T_H subset that have more recently been described. T_H1 cells form in response to IL-12 and IFN-γ and classically secrete IFN-γ, IL-2, and TNF-α, mediate direct effector function on pathogen-infected cells, and facilitate the differentiation of CD8 T cells and isotype switching to IgG2a and IgG3 [44]. T_H2 cells form in response to IL-4 and IL-2 and classically secrete IL-4, IL-5, and IL-13. These cells are involved in anti-helminth immunity, and aberrantly, atopy. T_H17 cells form in response to TGF-β and IL-6 and these cells secrete IL-17, IL-21, and IL-22 as effector functions against extracellular bacteria and fungi. T_{REG} cells form in response to TGF-β and secrete TGF-β and IL-10, a major anti-inflammatory regulator [45]. These cells help maintain tolerance to self-antigens and prevent autoimmune disease.

1.3.4 Tissue-resident T cells

Recently, a subset of T cells was identified that reside within tissues and does not recirculate [46]. These tissue-resident cells constitutively express CD69 [47]. Tissue-resident T cells are often primed at the tissue site [48] or are pulled there by antigen expression [49]. Heath and collagues recently showed in mice that protection against liver-stage malaria was mediated by tissue-resident CD8 T cells, not effector memory CD8 T cells, and that prime-and-trap vaccination, wherein T cells are primed in the spleen but trapped in the liver by liver-specific transgene expression, is an effective modality for protecting against liver-stage malaria [49].

1.4 Malaria

Malaria is caused by a single-cell, eukaryotic protozoan of the genus *Plasmodium*. It is transmitted by *Anopheles* mosquitoes in tropical and subtropical countries.

There are five species that cause nearly all cases of malaria in humans: *falciparum*, *vivax*, *malariae*, *ovale*, and *knowlesi* [50], with *falciparum* and *vivax* responsible for the majority of cases.

1.4.1 Burden of disease

P. falciparum is the cause of the majority of deaths from malaria. Global malaria incidence peaked in 2003–2004 at an estimated 232 million cases and 1.2 million deaths, predominantly (>80%) in sub-Saharan Africa [51]. Malaria incidence has fallen steadily, and there were an estimated 165 million cases and 855,000 deaths in 2013 [51]. The WHO World Malaria Report 2015 estimates there were 214 million cases and 438,000 deaths in 2015. The majority of deaths occur in children under age 5, who also face a substantially higher burden of cases. Though, because of the cumulative age distribution, children older than age 5 and adults account for an estimated 33% of all malaria deaths [51], despite far lower rates of clinical malaria at any given age.

Malaria causes a substantial economic burden, accounting for $12 billion in direct costs of care and indirect costs of lost productivity [52]. However, the year-over-year burden of malaria is greater than the sum of these costs. Critically, malaria exerts a powerful economic drag through a series of interlocking social and economic feedback loops. For example, in the setting of high infant mortality, fertility decisions may favor excessively high parity, which exacerbates gender disparities in educational investment [53].

1.4.2 Life cycle

Plasmodium has two hosts: mammals and mosquitoes.

Sporozoite stage

Malaria is transmitted to human hosts by the bite of infected mosquitoes, which carry sporozoites in their salivary glands. While probing for a blood meal, the mosquito injects sporozoites into the dermis [54]. Sporozoites exhibit gliding motility and traverse the endothelial wall of capillaries to enter the blood stream [55].

During gliding motility, CSP protein is formed at the apical end of the parasite [56] and translocates along its surface. CSP is release in large quantities from the distal end [57]. Anti-CSP antibodies can cause a distinct morphological change in the sporozoite, termed the circumsporozoite precipitation reaction [58], associated with decreased motility and hepatocyte invasiveness.

Liver stage

Sporozoites that reach the liver adhere to the liver sinusoids and again exhibit gliding motility. Sporozoites invade Kupffer cells, and then iteratively invade several hepatocytes [59]. CSP is shed by sporozoites upon entering Kupffer cells [60], and the shed CSP modulates cAMP and reactive oxygen species (ROS) production. Sporozoite traversal of Kupffer cells also decreases the secretion of pro-flammatory cytokines (TNF-α, IL-6, and MCP-1) and increases secretion of the anti-inflammatory cytokine, IL-10 [61]. This may serve to further shield the parasite from the immune system by creating an immuno-suppressive micro-environment. Traversal of hepatocytes has been shown to be necessary for the final hepatocyte invasion event [62].

During the next 6–8 days, the parasite substantially remodels the hepatocyte and its metabolic machinery [63]. It undergoes a process of asexual replication called schizogony and develops approximately 30,000 daughter merozoites, which are ultimately released into the blood stream. Hypnozoites, or dormant parasites can develop during the liver-stage of *P. vivax* and *P. ovale*.

Blood stage

Merozoites are dedicated erythrocyte invasion machines [64]. Several Plasmodium proteins are involved, including MSPs (merozoite surface proteins), PfEBAs (*P. falciparum* erythrocyte binding antigens), PfRHs (*P. falciparum* reticulocyte binding protein homologs), and AMA1–RON2 (apical membrane antigen 1 – rhoptry neck protein 2). Circulating parasites have developed redundant invasion pathways (in the case of the EBAs and RHs) or highly polymorphic variants (in the case of AMA1) that allow the parasite to escape elimination [64].

After invasion, the merozoite undergoes several morphological changes, progressing from a ring to a trophozoite to a schizont. Each schizont yields 12–16 daughter merozoites, which are eventually released by erythrocyte lysis. The duration of the blood stage life cycle varies for each species of malaria, and is typically 48 hours in *P. falciparum*.

Mosquito stage

During the blood stage of infection, some parasites differentiate into sexual forms called male and female gametocytes. If ingested by a mosquito during a blood meal, these parasite forms can fuse (fertilize), becoming a zygote within the mosquito mid-gut. After fusion, the zygote differentiates into a motile ookinete, which invades the midgut wall and further differentiates into a oocyst. Here, a third type of replication occurs, and haploid sporozoites are formed by meiosis. The sporozoites spread throughout the mosquito body. Sporozoites that reach the salivary gland undergo additional differentiation, which is required to become fully infectious [65].

1.4.3 Pathogenesis

Clinical malaria is classically characterized by cyclical fevers and chills that coincide with the lysis of erythrocytes [66]. Anemia is a major contributor of symptoms in clinical malaria. The length of each cycle is dependent on the species of malaria, which have different replication times.

Symptoms of severe malaria include respiratory distress, prostration, severe anemia, and convulsions, though these symptoms are often non-overlapping [67]. Interestingly, parasite density does not correlate with severe malaria [67]. An overly vigorous immune response is thought to be a major driver of the symptoms of cerebral malaria, which are often precipitated by parasite sequestration along the endothelium of the central nervous system [66]. Systemic cytokine release, including TNF-α, IFN-γ, and lymphotoxin-α, have been identified as key contributors to the pathogenesis of this disease phenotype [68, 69].

Parasite proteins containing the PEXEL/VTS motif [70] are exported to the surface of the parasite by PTEX machinery [71]. One family of highly variant surface antigens, encoded by so-called *var* genes in *Plasmodium*, is the *P. falciparum* erythrocyte membrane protein 1 (PfEMP1) family. These proteins provide antigenic variation [72], and mediate cyto-adherence and rosetting [73], allowing the parasite to sequester away from phagocytic cells present in the spleen and liver [74]. Still other *var* genes that provide additional antigenic diversity include the STEVOR and RIFIN families [75, 76], and contribute to the parasite's ability to avoid immune-mediated clearance.

1.4.4 Naturally acquired immunity

Naturally-acquired immunity to malaria develops over time in residents of malaria endemic regions. Naturally acquired immunity in heavily exposed adults is very efficient at protecting against severe malaria and death [77]. However, young children and especially infants generally lack naturally acquired immunity and are thus highly susceptible to severe malaria disease. Natural history studies highlight that naturally acquired immunity is correlated with age. However, studies of malaria-naive migrants to malaria endemic areas show an age dependence of the severity of disease, suggesting that host factors also play a role [78].

Merozoites, which must traverse the plasma, and parasitized erythrocytes are highly susceptible to antibody-mediated neutralization [64]. Naturally-acquired immunity has been associated with antibodies targeting one of several proteins exported to the surface of the infected erythrocyte, including PfEMP1 [79] and rifins [76]. Merozoite proteins are also targets of naturally-acquired immunity, including AMA-1 [80], MSP-1 [81, 82, 83, 84], MSP-2 [85], MSP-3 [86], and GLURP [87].

Antibodies to RH5 only occasionally develop in natural infection [88]. This is in stark contrast to antibody responses against other merozoite surface antigens, such as AMA1, which increase progressively with age in naturally exposed cohorts [88]. In another study, acquisition of RH5 antibodies was correlated with age, though, <25% of children and adolescents had anti-RH5 antibodies [89]. Affinity purified

antibodies from naturally-exposed individuals can mediated parasite inhibition *in vitro* [90]. Importantly, in the rare individuals that do develop RH5 antibodies in the field, time from initial infection (as determined by active PCR surveillance) until development of clinical malaria is significantly delayed [89]. This suggests that naturally-acquired RH5 antibodies can mediate biologically-meaningful delay in blood stage parasite growth.

1.4.5 Malaria control interventions

Collectively, malaria control interventions have had a dramatic impact on the burden of malaria [91]. Between 2000 and 2015, malaria prevalence (median prevalence of *P. falciparum* parasitemia in children age 2 to 10, also known as $PfPR_{2-10}$) was reduced by approximately 50% and malaria clinical cases were reduced by approximately 40%. During this time period, malaria control interventions averted an estimated 632 million clinical cases, which was driven largely by insecticide treated bed nets (68% of cases averted) [91]. Expanded access to ACT accounted for 22% of cases averted and Indoor Residual Spraying accounted for 10% [91].

Insecticide-treated bed-net (ITN) and indoor residual spraying (IRS)

Insecticide treated bed-nets have been shown to reduce mortality in children when deployed at scale [92, 93]. However, bed nets only work partially, and only work when they are used regularly. Indoor residual spraying – the application of insecticides to indoor spaces to reduce the density of mosquitoes around the home – also has demonstrable efficacy [94]. As could be expected from applying a single selective pressure on a large genetically diverse population, there is growing resistance to the insecticides used in bed-nets and indoor residual spraying, which may limit their effectiveness in the future [95].

Artemisinin-based combination therapies (ACT)

Artemisinin combination therapies are important tools for the treatment of uncomplicated and severe malaria. The efficacy of ACTs, however, is threatened by drug resistance. Chloroquine resistance spread rapidly throughout Africa and South

America after originating at the Thai-Cambodia border around 1960 [96]. Now, an artemisinin resistance phenotype has emerged, wherein parasite clearance is slowed [97]. This phenotype is growing in prevalence, particularly in Cambodia, Thailand, and Myanmar, and is associated with single point mutations in *P. falciparum* kelch13 gene [98].

1.5 Malaria vaccines

The unique biology of *Plasmodium* offers numerous opportunities to interfere with parasite growth or pathogenesis [99].

1.5.1 Pre-erythrocytic vaccines

Pre-erythrocytic vaccines aim to induce sterilizing immunity that targets the sporozoite and/or infected hepatocytes.

Subunit vaccines for pre-erythrocytic malaria

RTS,S

The most extensively studied candidate malaria vaccine is RTS,S. RTS,S is a subunit vaccine based on the Pf circumsporozoite protein (CSP), the immunodominant protein on the surface of sporozoites [100]. RTS,S consists of two polypeptide components that assemble into particles. The first component consists of *P. falciparum* strain 3D7 CSP residues 207 to 395. These residues encompass 19 of the NANP tetrapeptide repeats as well as the entire C-terminal domain (except the GPI anchor), which contains putative T cell epitopes. The CSP fragment is genetically fused to the N-terminus of HBsAg. The second component is the unaltered HBsAg, which itself is 226 amino acids [101]. The two components are both integrated into the same yeast (*Saccharomyces cerevisiae*) genome at a ratio of 1:4, which upon expression, yields stable chimeric particles [101].

During its initial development, RTS,S was tested with several different adjuvants in controlled human malaria infection (CHMI) trials. In the initial report, RTS,S (7G8 strain) was mixed with alum or alum + MPL, and 6/6 and 6/8 subjects

developed parasitemia after homologous CHMI 3 weeks after the final vaccination [101]. In a subsequent study, RTS,S (3D7 strain) was mixed with either alum + MPL, an oil-in-water emulsion, or an oil-in-water emulsion containing two potent immunostimulants, QS21 and MPL [102]. In this study, parasitemia developed in 7/8, 5/7, and 1/7 subjects, respectively, after homologous CHMI 3 weeks after final vaccination. In still another follow-up study, the adjuvant was changed to AS01B, which replaced the oil-in-water component with liposomes, but kept the QS21 and MPL components unaltered [103]. With AS01, 18/36 subjects developed parasitemia after homologous CHMI 3 weeks after final vaccination. With each adjuvant adjustment, the CSP titer increased. Additional studies with RTS,S have demonstrated about 30–50% efficacy against homologous CHMI 3 weeks after vaccination [104, 105, 106, 107]. Upon rechallenge at 5 months in one of these studies, sterile efficacy was estimated at 22% [103].

In the field, efficacy results have generally been consistent with the efficacy results in malaria-naive adults. CSP titers were identified as a potential correlate of protection [108, 109]. In a collaboration between GlaxoSmithKline and the Bill and Melinda Gates Foundation, the three monthly dose regimen of RTS,S/AS01 was taken forward into phase III field efficacy studies beginning in March 2009. 15,460 children were enrolled in two age groups 6 to 12 week olds and 5 to 17 month olds across 11 centers in 7 African countries in a double-blind trial with the rabies vaccine as comparator [110]. Vaccine efficacy, as measured by the incidence of the first episode of clinical malaria between the RTS,S and comparator vaccine group, was 50.4% in the 5 to 17 month olds in the first 12 months after final vaccination [110], and 30.1% in the 6 to 12 month old infants [111]. Extended follow-up of the same cohort, which split the original RTS,S into two groups either receiving a booster dose 18 months after the third vaccination or receiving a comparator vaccine, showed that vaccine efficacy was 36.3% through four years of follow-up in the 5 to 17 month old children. Without the booster dose, efficacy was 28.3%. In the 6 to 12 week old infants, vaccine efficacy was 25.9% and 18.3%, with and without the booster dose, respectively, through 38 months of follow-up [112].

On the basis of these findings, RTS,S/AS01 was given a positive scientific opinion by the Europeans Medicines Association, meaning the benefits of a vaccination outweighed the adverse events. The decision on whether RTS,S should be implemented and to what extent fell to the World Health Organization Strategic Advisory Group of Experts (SAGE) on Immunization (WHO SAGE). In 2015, SAGE advised that additional field studies were needed prior to widespread deployment of the vaccine. As such, the fate of RTS,S is currently uncertain, as these studies will take several additional years and considerable resources to conduct.

Cost effective analyses trained on the Phase III data set were used to estimate the costs of routine roll out in African settings. Using an ensemble of four models, the incremental cost-effectiveness of rolling out the four dose regimen was calculated as $87 per DALY averted in transmission settings where the parasitemia rate of children age 2–10 years old is 10–65% [113], assuming $5 purchase cost per dose. This is similar to the cost-effectiveness of bed-nets and considered highly cost-effective.

Extended follow up of the Phase II studies with RTS,S has shown that vaccine efficacy wanes over time, reaching –0.4% during the fourth year after vaccination [114]. More strikingly, it appears that vaccine efficacy is actually negative thereafter, reaching a nadir in year 5 with vaccine efficacy of –43.5% among children in high transmission settings [115]. Efficacy over the entire 7 year follow-up period was 4.4%. It should be noted that this analysis was not pre-specified in the original study protocol, and was dependent on comparison to the malaria incidence in the community, not a blinded control group.

Nonetheless, this seminal study should give all malaria vaccine developers pause. It has been well documented that immunity to the blood stage of malaria develops over many years, and that the development of naturally acquired immunity confers a partial but real benefit to children as they age. Furthermore, it has previously been shown that both age and level of exposure influence severity of disease presentation [116]. Thus, delaying naturally-acquired immunity may have unintended consequences on both the prevalence and severity of malaria. Mechanistically, RTS,S likely functions primarily through antibodies directed against

the CSP repeat region, with CD4 T cells targeting the C-terminal region playing a minor role [117]. RTS,S/AS01 is a partially protective vaccine with a defined mechanistic correlate of immunity. High concentrations of CSP-specific antibodies are required to prevent sporozoite infection of the liver. These antibodies typically wane to non-protective levels over time. This conversion from protective to non-protective CSP antibody levels appears to gradually leave the child with neither functional pre-erythrocytic immunity nor naturally-acquired blood stage immunity.

Future field trials of all partially protective pre-erythrocytic malaria vaccines may be significantly influenced by this result, because the development cycle now demands long-term (>5 years) follow-up to determine the magnitude of vaccine rebound.

Some safety issues have also been raised with RTS,S/AS01. The key issue seems to be related to the AS01 adjuvant. AS01 consists of a liposomal formulation of QS21 (a saponin) and MPL (a TLR4 agonist). A similar protein and adjuvant subunit vaccine, the herpes zoster subunit vaccine (HZ/su) containing recombinant varicella–zoster virus glycoprotein E and the AS01B adjuvant system, showed grade 3 (severe) injection site reactions in 8.5% of vaccine recipients compared to 0.2% of placebo recipients in a phase 3 study of patients >70 years of age. Grade 3 systemic symptoms occurred in 6.0% of vaccine recipients compared to 2.0% in the placebo group. Grade 3 injection site reactions include redness and swelling >10 cm. Grade 3 systemic reactions include >39.0 °C or symptoms that prevent normal activity [118]. In a phase 3 study of the same vaccine in participants >50 years old, grade 3 systemic symptoms were present in 11.4% of vaccine recipients compared to 2.4% of placebo recipients and local symptoms occurred in 9.5% of vaccine recipients compared to 0.4% of placebo recipients [119].

In children 5 to 17 months of age receiving RTS,S/AS01, fever >37.5% °C was reported within 7 days of vaccination in 31% compared to 13% [110]. In infants 6 to 12 weeks of age, fever was reported within 7 days of vaccination after 30.6% of doses in the RTS,S/AS01 group and after 21.1% of doses in the rabies vaccine group [111]. Additionally, within 7 days after the booster dose, generalized convulsive seizures occurred in 2.5 per 1000 doses in the RTS,S group, compared to 1.2 and 0.4 per 1000

doses in the two groups that received the comparator vaccine [112]. Furthermore, in the phase III study, meningitis was reported in 21 children who received either three or four doses of RTS,S/AS01 and 1 child who received rabies vaccine (2:1 allocation) [112], though, this finding requires additional study because there was no clear temporal association with vaccination. There is data to suggest that there may be detrimental sex specific effects in girls who receive RTS,S/AS01 compared to the comparator vaccine [120]. In comparing all-cause mortality in the RTS,S group compared to the comparator vaccine group, girls had a higher mortality ratio (1.91, 95% CI: 1.30–2.79), which was not found in boys (0.84, 95% CI: 0.61–1.17). This association was found in both age groups tested [120]. Therefore, additional studies to determine the validity of the findings – particularly the higher incidence of meningitis and the excess mortality in girls receiving RTS,S – are warranted.

It should be noted that RTS,S targets a single protein. As is often the case when applying a selective pressure against a single microbial vulnerability, escape mutants will emerge. The CSP gene was sequenced from parasites isolated following clinical infection in the phase III study and compared between vaccine and placebo group. Vaccine efficacy was 50.3% against perfectly matched strains and 33.4% against mismatched strains [121]. Whether and how this affects transmission at the parasite population level and therefore vaccine efficacy over successive generations is yet to be determined.

Most recently, efforts to improve the quality and quantity of the immune response have led investigators to attempt an RTS,S regimen termed delayed fractional dose. In this regimen the third dose is given five months rather than one month after the second immunization, and one fifth the vaccine dose is administered. The hypothesis is that the reduced dose results in greater competition among B cells in the germinal centers of draining lymph nodes, and therefore, improved affinity maturation. Using this regimen, 26/30 (87%) subjects were protected in the fractional dose group administered at 0, 1, and 7 months (abbreviated Fx017M) compared to 10/16 (63%) subjects protected in the standard dose group administered at 0, 1, and 2 months

[122]. Antibodies from the Fx017M group showed greater somatic hypermutation and avidity. Efforts to test this in the field are ongoing.

Finally, still other investigators are testing RTS,S in combination with alternative vaccines. When given as a five vaccination regimen staggered with ME-TRAP expressed by ChAd63 and MVA (vaccine described in the next section), 14/17 (82%) subjects were protected 4 weeks after final vaccination compared to 12/16 subjects (75%) of subjects who received RTS,S/AS01 alone. While the addition of ME-TRAP did not significantly improve sterile efficacy of RTS,S in this study, the short-term efficacy of RTS,S alone was higher than prior experience with this vaccine, and thus, there was little window to demonstrate improved efficacy. Additional studies of this regimen will determine if there is truly a benefit to the combination.

Heterologous prime-boost vaccines

A different subunit vaccine approach using a heterologous prime-boost vaccination with DNA and/or viral vectors has shown promise in CHMI and field studies. The initial iterations of this approach showed little success, likely because the regimens were based on less immunogenic vaccination strategies. For example, a DNA vaccine expressing the ME-TRAP antigen (Multiple epitope string and thrombospondin-related adhesion protein also known as SSP2) or modified vaccinia Ankara (MVA) expressing the same antigen protected 0/22 vaccine recipients against CHMI, even when the two vaccines were administered as a heterologous prime-boost regimen [123]. However, changing the vectors to fowlpox and MVA resulted in 3/16 subjects protected against CHMI at 2–7 weeks after final vaccination in one study [124], but 0/8 protected in another where CSP antigen was co-administered with ME-TRAP [125]. Similarly disappointing results have occurred when using CSP as the antigen insert, either with DNA-MVA [126] or fowlpox-MVA [125]. More recently, the CSP and ME-TRAP antigens have been tested using chimpanzee adenovirus serotype 63 (ChAd63) followed by MVA. This regimen was shown to be safe and highly immunogenic in malaria naive UK adults and semi-immune Kenyan adults [127, 128]. In one CHMI study, sterile protection was observed in 1/15 and 2/15 subjects vaccinated with CSP and ME-TRAP, respectively [129]. In a second

study, protection was observed in 3/14 subjects 3 weeks after vaccination with ME-TRAP using the same vectors. Importantly, of the three sterilely protected subjects rechallenged at 8 months, one was again sterilely protected [130].

In a field study, the heterologous prime-boost vaccination regimen of ChAd63-MVA expressing ME-TRAP demonstrated 67% efficacy against heterogeneous field transmission through eight weeks of follow-up after vaccination [131]. The durability of this protective efficacy is unknown, since there was minimal transmission beyond the first 1–2 weeks after vaccination.

Other subunit vaccines

Other attempts at subunit vaccines have largely yielded disappointing results. Adenovirus serotype 5 expressing CSP or CSP-AMA1 protected 0/11 subjects [132] and 0/18 subjects [133], respectively; DNA-Ad5 expressing CSP and AMA1 protected 4/15 subjects [134]; DNA expressing five liver stage antigens and GM-CSF protected 0/31 subjects [135]; and TRAP protein or CSP/TRAP mixed with AS02 protected 0/5 subjects or 1/11 subjects, respectively [136].

Whole sporozoite vaccines

Live attenuated vaccines have primarily been an academic curiosity in the malaria vaccine development field. The initial proof of concept studies were performed in the 1960s and 1970s, but were never pursued at scale because of the intractable nature of producing sporozoites for injection.

Radiation-attenuated sporozoites

The initial trial was performed by exposing Pf-infected mosquitoes to radiation and then having these mosquitoes bite subjects. The exposure to radiation-attenuated sporozoites (RAS) conferred sterile protection against a subsequent exposure to non-attenuated sporozoites [137]. Additional studies through the 1980s and 1990s defined that this approach generally required >1000 mosquito bites to confer high level (>80%) sterile protection against CHMI 2–4 weeks after the final vaccination [138]. Importantly, 5/6 subjects challenged 23–42 weeks

after final vaccination were sterilely protected [138], suggesting that protection could be durable.

The level and durability of efficacy by RAS vaccination was the highest seen to that point (1990s) of any malaria vaccine strategy, but vaccination by means of mosquito bite is impractical for widespread use. Hoffman and colleagues proposed a strategy by which radiation-attenuated sporozoites would be isolated from infected mosquitoes, purified, and frozen in a process that meets all regulatory requirements [139]. By 2010, these efforts met FDA requirements for an initial human study using injectable sporozoites [140].

The first clinical study enrolled 80 vaccine recipients who received up to 1.35×10^5 PfSPZ 4–6 times by the SC or ID routes. Low level antibody and CD4 T cell responses against PfSPZ were detected, but CD8 T cell responses were undetectable. 2 of 44 vaccinated subjects were protected from CHMI at 3 weeks after final vaccination [141]. These findings raised the question of whether the dose and route of vaccination were correct for this specific vaccine. On the basis of the low level immunogenicity and protective efficacy, PfSPZ Vaccine at 1.35×10^5 PfSPZ was administered to non-human primates (NHP) by either the SC or IV route to determine if the route of vaccination influenced immunogenicity. Importantly, IV vaccination resulted in substantially higher levels of IFN-γ secreting CD8 T cells in the liver than SC vaccination [141]. On the basis of this finding, a second clinical study examined the safety, immunogenicity, and efficacy of PfSPZ Vaccine at doses of up to 1.35×10^5 PfSPZ administered by the IV route (the VRC 312 study, ClinicalTrials.gov # NCT01441167). 6/9 and 6/6 subjects who received 4 or 5 doses of 1.35×10^5 PfSPZ IV did not develop parasitemia following homologous CHMI 3 weeks after final vaccination [12]. PfSPZ-specific antibody and CD4 T cell responses were considerably higher than measured following SC or ID vaccination [141], but CD8 T cell responses were still low to undetectable in the majority of volunteers, including in a number of subjects that did not develop parasitemia. Nevertheless, this study demonstrated that PfSPZ Vaccine – a vialed product that meets all regulatory standards – conferred high level (>80%), short-term protection

against CHMI. Subjects from this study underwent repeat CHMI at 5 months, and, among those who were previously protected, only 2/6 were again protected [142]. This indicated that doses of 1.35×10^5 PfSPZ were inadequate to confer high-level, long-term protection. The immunogenicity and efficacy of additional dose-escalations are described herein.

Drug-attenuated parasites

More recently, an alternative whole sporozoite vaccination strategy was proven efficacious in humans. The malaria parasite – being a multi-stage, eukaryotic, transcriptionally- and metabolically-active parasite – offers a wide array of potential targets for attenuation. Roestenberg and colleagues demonstrated that humans exposed to 15 sporozoite-infected mosquito bites at monthly intervals three times while taking continuous chloroquine prophylaxis – so-called CPS immunization – led to sterile protection in 10/10 subjects who underwent CHMI [143]. Chloroquine is active against the blood stage of infection, and thus, the parasite is given the opportunity to infect hepatocytes, replicate unhindered (approximate 30,000-fold expansion in parasite numbers), and infect erythrocytes. Arrest occurs in the latter half of the blood stage, wherein toxic heme metabolites from hemoglobin proteolysis inhibit parasite growth [144]. The protection afforded by this vaccination approach was shown to be remarkably durable, as 3/5 subjects were sterilely protected following repeat CHMI at 28 months [145].

Mechanistically, the protection following CPS immunization was shown to be pre-erythrocytic, as all 5/5 vaccinated subjects challenged with infected mosquitoes were protected but 0/9 were protected against a small blood stage challenge (<2000 infected erythrocytes) [146]. As chloroquine has well known but ill-defined immunomodulatory properties, the efficacy of this approach was demonstrated using an alternative quinolone: using a partially-protective vaccination dose (8 mosquito bites instead of 15), chloroquine protected 3/5 subjects and mefloquine protected 7/10 subjects [147]. Heterologous protection was also assessed by this vaccination strategy. In subjects that received three rounds of 5, 10, or 15 mosquito bites with chloroquine co-administration who were previously protected against

homologous challenge at 4.5 months, only 2/13 were again sterilely protected against a heterologous CHMI at 14 months after vaccination [148]. This low level efficacy against a temporally distant heterologous CHMI may be explained by the relatively low doses of SPZ administered by the vaccination regimens (only 5, 10, and 15 mosquito bites per immunization). The immunogenicity of this vaccination strategy using vialed, cryopreserved PfSPZ is described herein.

Genetically-attenuated parasites

Genetically-attenuated parasites (GAP) represent still another means of attenuating the parasite. As the parasite has stringent metabolic requirements throughout its life cycle, there are a number of potential targets – in particular essential enzymes in metabolic pathways – that could be disrupted by genetic means.

A first-generation genetically-attenuated sporozoite vaccine in a first-in-human study revealed that the GAP was immunogenic, but not sufficiently attenuated [149]. 1 of 6 vaccine recipients developed parasitemia after receiving 200 bites from mosquitos carrying PfGAP. The breakthrough infection was confirmed to harbor the genetic lesions that were intended to attenuate it. This first generation GAP was deficient in the *P36/P52* homologous genes [150]. A next generation GAP was generated that is deficient in *SAP1* and *P36/P52* [151]. This GAP shows complete attenuation in humanized mice and cultures. A first-in-human study has been completed with results pending (ClinicalTrials.gov # NCT02313376). Such a vaccine may confer a similar dose sparing benefit as CPS immunization, while avoiding the need to co-administer a prophylactic drug.

1.5.2 Blood stage vaccines

Considerable effort has been spent on strategies to develop blood stage immunity through vaccination. There is compelling clinical evidence that antibodies directed against the infected erythrocyte surface and merozoites are capable of mediating clinically-meaningful control of blood stage malaria after natural exposure. Moreover, passive transfer of antibodies from semi-immune adults reduced parasitemia and fever in children with severe malaria [152, 153]. Such antibodies prevent binding

of infected erythrocytes to endothelial cells [154]. Other mechanisms include opsonization [155] and ADCI in cooperation with phagocytic cells [156].

Most early studies with blood stage vaccines focused on two antigens: AMA-1 and MSP-1. Numerous studies have been performed using either protein in adjuvant formulations [157, 158, 159, 160] or vectored constructs [161, 162]. However, AMA-1 and MSP-1 are highly polymorphic antigens [163], and protection – when seen – is typically strain specific [164]. Therefore, alternative targets are needed.

Studies with the blood stage antigens RESA, MSP-1, and MSP-2 in Montanide ISA720 showed strain-specific efficacy in the field [165, 166]. An MSP-3 and GLURP fusion protein vaccine in alum, termed GMZ2, was safe and immunogenic [167]. However, a phase II field efficacy study showed only 14% efficacy against natural transmission [168]. Still other vaccines against additional blood stage targets are in the early stages of development, including erythrocyte-binding antigen (EBA)-175 as a recombinant protein adsorbed to alum [169]. To date, these vaccines have been hindered by the high genetic diversity of the target antigen in the field.

RH5 based vaccines

Importantly, there is one parasite ligand that appears to function through non-redundant invasion pathways and to have relatively low polymorphism, RH5.

RH5 is a 62.5 kDa protein, expressed in the rhoptries of the merozoite [170]. Efforts to knock-out RH5 resulted in no viable progeny, suggesting it is an essential protein for blood stage growth [170]. RH5 is highly conserved in field isolates. Of the 526 amino acids, only 5 non-synonymous mutations were identified at >10% allelic frequency in a panel of 227 clinical isolates [171].

The receptor for RH5 is basigin, an erythrocyte membrane protein [172]. Monoclonal antibodies directed against basigin inhibit parasite invasion and growth of all tested laboratory strains and several field isolates [172].

Structurally, unlike other members of the PfRH family, RH5 lacks a transmembrane domain and a GPI anchor [170]. RH5 is presented on the surface as part of a larger protein complex, which includes *P. falciparum* RH5 interacting protein

(PfRipr) [173] and the cysteine-rich protective antigen (PfCyRPA) [174]. CyRPA has a GPI anchor, and like RH5, is refractory to knock out [174].

Vaccination with RH5 expressed in adenovirus and MVA resulted in the development of antibodies with *in vitro* growth inhibitory activity (GIA) in rabbits [88]. In an *Aotus* monkey model of *P. falciparum* infection, a similar heterologous prime-boost vaccination regimen with adenovirus and MVA resulted in high levels of antibodies that mediated *in vivo* GIA upon heterologous parasite challenge [175]. In this same study, a full-length recombinant protein mixed with a potent adjuvant (albeit, one that is not suitable for use in humans) achieved higher antibody levels and correspondingly higher *in vivo* GIA. However, this protein construct required the genetic fusion of RH5 to a rat CD4 domain, which improved protein stability and yield. Such a fusion is not suitable for use in humans. Nonetheless, this study revealed that biologically-meaningful GIA could be achieved when anti-RH5 antibody levels reached >165 μg/mL in the serum. This clearly demonstrated the mechanistic importance of RH5 antibodies in mediating GIA.

Vectored vaccines are easier to produce and translate to the clinic, however, it is possible that this heterologous prime-boost regimen will not achieve sufficiently high antibody levels in humans to mediate GIA. Prior experience in humans with this viral vector regimen expressing the blood stage antigen MSP1 shows that antibody levels reach approximately 30–40 μg/mL at the peak after vaccination [162]. As antibody responses to different antigens using the same vaccine platform cannot be precisely predicted, this result does not preclude testing of the vectored RH5 regimen in humans. However, alternative regimens should be pursued, particularly, recombinant protein and adjuvant formulations.

Experience with the RTS,S vaccine, a recombinant virus like particle containing a truncated version of the circumsporozoite protein (CSP) shows that quantitatively higher antibody responses can be generated with this approach. Vaccination with RTS,S results in a geometric mean antibody concentration of approximately 75 μug/mL when formulated with AS02 and approximately 150 μg/mL when formulated with AS01, when administered to healthy malaria-naive adults [103].

Thus, efforts to test vectored RH5 are proceeding in parallel with efforts to develop recombinant RH5 vaccine formulations.

1.5.3 Transmission blocking vaccines

Plasmodium must pass through the mosquito before being transmitted to another mammalian host. Thus, there are potentially additional susceptible targets during the life cycle that could be amenable to vaccination. It has been demonstrated that antibodies ingested during the blood meal can interfere with parasite development in the mosquito [176]. This strategy may be particularly effective because many of the proteins expressed in mosquitoes are never expressed in the human host, and thus, there may be fewer adaptations (such as antigenic diversity or redundant pathways) to avoid human immune pressure.

Several candidate transmission blocking vaccine antigens have been tested in animals and humans, with Pfs25 being a particularly promising candidate [177]. Clinical studies with several Pfs25-based candidates are ongoing or recently completed (ClinicalTrials.gov # NCT02532049, NCT01867463, NCT01434381).

Further development faces several hurdles, however, including the lack of a simple read out for functional immunity (the standardized membrane feeding assay is challenging to implement [178]), difficulty of monitoring effectiveness in the field (*e.g.*, monitoring infectivity of field mosquitoes by direct skin feeds is equally challenging), and the ethical considerations (given that a monovalent vaccine containing only a transmission blocking component confers no direct benefit to the vaccine recipient).

1.6 Hypothesis and specific aims

Collectively, prior studies have established that RH5 is a promising blood stage vaccine target, but the quality and magnitude of the antibody response needs to be improved to attain meaningful efficacy. Also, prior studies have established that whole sporozoite vaccines are a promising pre-erythrocytic vaccine. However, it is currently unknown how the whole sporozoite vaccines PfSPZ Vaccine and PfSPZ-CVac interact with the human immune system to induce protective immunity and how the primed immune system mediates protective immunity against naturally-transmitted sporozoites.

1.6.1 Approach and principal aims

Using recombinantly-engineered variants of RH5, the principal aim of this thesis is to define whether and how the antibody response is affected by RH5-multimerization and use of a truncated structural variant of RH5. Additionally, using clinical samples from several human studies of PfSPZ Vaccine and PfSPZ-CVac as well as animal studies, the second principal aim of this thesis is to precisely define the immunogenicity, correlates of protection, and mechanisms of protection of whole sporozoite vaccination. Regimens will be evaluated in parallel for efficacy and immunogenicity in humans and non-human primates, and the utility of different immune responses to predict protection will be evaluated.

1.6.2 Principal hypotheses

1. RH5-sv3-multimers will yield greater quality and magnitude of antibody neutralization compared to monomeric full length RH5.
2. Pf-specific CD8 T cells are the mechanistic correlate of protection.
3. Higher doses of PfSPZ Vaccine will lead to greater vaccine immunogenicity and more durable protective efficacy against homologous and heterologous CHMI.
4. PfSPZ-CVac will be more immunogenic than comparable doses of PfSPZ Vaccine

1.6.3 Specific aims

1A Design, produce, and characterize two distinct RH5 virus-like particles

1B Characterize and compare the mouse antibody response to RH5 for neutralizing activity

2A Define antibody and cellular correlates of short-term and long-term sterile protection of PfSPZ Vaccine

2B Define the mechanism of protection of PfSPZ Vaccine

3A Assess the cellular immune activation in humans vaccinated three times with 9.0×10^5 PfSPZ IV

3B Determine the cross-reactivity of T cells between the vaccinating and heterologous CHMI strains

4A Describe the cellular immune activation in humans vaccinated with PfSPZ-CVac and compare this to humans vaccinated with PfSPZ Vaccine

4B Identify immune signatures that associate with sterile protection

1.6.4 Outline

Chapter 2 details the reagents, solutions, and methods used in this study. Chapter 3 describes the production, purification, and characterization of multimeric RH5 subunit vaccine constructs. Chapter 4 describes the efficacy, correlates of protection, and mechanism of protection of the live attenuated PfSPZ Vaccine. Chapter 5 describes the efficacy of PfSPZ Vaccine against heterologous challenge and describes the cross-reactivity of the T cell response to the heterologous strain. Chapter 6 describes the immunogenicity and T cell correlates of protection of PfSPZ-CVac. Chapter 7 summarizes the results of this thesis and discusses its central limitations as well as possible future directions.

2
Materials and methods

Contents

2.1 Materials 34
2.1.1 Solutions and reagents 34
2.2 Methods in molecular biology 39
2.2.1 Cloning 39
2.2.2 Transfections and transformations 40
2.2.3 Protein expression and purification 41
2.2.4 Protein characterization 43
2.3 Methods in immunology 45
2.3.1 Human immunology 45
2.3.2 Functional assessment of IgG from vaccine recipients . . 51
2.3.3 T cell responses in vaccinated non-human primates . . . 53
2.4 Statistical analyses 54
2.4.1 Data analysis 54
2.4.2 Efficacy analysis 56
2.4.3 Immunogenicity 56
2.4.4 Immune correlates 56

2.1 Materials

2.1.1 Solutions and reagents

YPD media

1% w/v yeast extract, 2% w/v peptone, 20 mM dextrose in deionized H_2O.

BMGY

1% w/v yeast extract, 2% w/v peptone, 1.34% w/v yeast nitrogen base with ammonium sulfate, 0.0004% w/v biotin, 1% v/v glycerol, 100 mM potassium phosphate (pH 6.0) in deionized H_2O.

BMMY

1% w/v yeast extract, 2% w/v peptone, 1.34% w/v yeast nitrogen base with ammonium sulfate, 0.0004% w/v biotin, 2% v/v methanol, 100 mM potassium phosphate (pH 6.0) in deionized H_2O.

Yeast lysis buffer

0.1% v/v Triton, 1 mM EDTA, 1 mM $MgCl_2$, 1 mM EDTA, 10 mM Tris pH 7.8 in deionized H_2O.

1 M potassium phosphate buffer

132 mL of 1 M K_2HPO_4 and 868 mL 1 M KH_2PO_4, pH was adjusted to 6.0.

Tris-buffered saline (TBS)

20 mM TRIZMA HCl pH 7.4, 15 mM NaCl in deionized H_2O.

C-tag column elution buffer

2 M $MgCl_2$, 20 mM Tris in deionized H_2O.

SpyCatcher-SpyTag reaction buffer

40 mM Na_2HPO_4, 200 mM sodium citrate, pH 6.2.

R10

Filter sterilized RPMI-1640 containing 2 mM L-glutamine, 10% v/v HI-FCS, 100 U/mL penicillin, and 100 μg streptomycin.

cRPMI

Filter sterilized RPMI-1640 containing 2 mM L-glutamine, 10% v/v HI-FCS, 100 U/mL penicillin, 100 μg streptomycin, 25 mM HEPES buffer, and 0.1% v/v β-mercapto-ethanol.

FACS buffer

Filter sterilized 2% v/v HI-FCS in PBS.

Material	Supplier	Catalog
Phusion® High-Fidelity PCR Master Mix with HF Buffer	New England BioLabs	M0531S
Agarose	Sigma-Aldrich	A9539
SYBR® Safe DNA Gel Stain	Life Technologies	S33102
In-Fusion® HD Cloning Plus	Clontech	638909
NEB 5-α Competent *E. coli* (High Efficiency)	New England BioLabs	C2987H
Ampicilin	Sigma-Aldrich	A9539
QIAprep Spin Miniprep Kit	Qiagen	27104
QIAGEN Plasmid Midi Kit	Qiagen	12143
QIAquick PCR Purification Kit	Qiagen	28104
PichiaPink™ Expression Strain Set	Life Technologies	A11154
PinciaPink™ Media Kit	Life Technologies	A11156
Yeast extract	Sigma-Aldrich	Y1625-1KG
Peptone	Sigma-Aldrich	P0431-1KG
Yeast nitrogen base	Sigma-Aldrich	Y1251-1KG
Biotin	Sigma-Aldrich	B4501-500MG
Corning® Erlenmeyer baffled cell culture flasks (2 L)	Sigma-Aldrich	CLS431256-6EA
Corning® Erlenmeyer cell culture flasks (125 mL)	Sigma-Aldrich	CLS431143-50EA
PureLink® air porous tape	Life Technologies	12262-010
HiLoad 16/600 Superdex 200 pg	GE Healthcare	28-9893-35
Amicon Ultra-15 Centrifugal Filter Units (10kDa cut-off)	Merck Millipore	UFC901024
Phosphate buffered saline (PBS)	Sigma-Aldrich	D8537
Trizma® HCL buffer solution (pH 7.8, 1M)	Sigma-Aldrich	T2569
Glass beads, acid-washed	Sigma-Aldrich	G8772-500G
Expi293 expression media	ThermoFisher Scientific	A1435101
EX-CELL® 420 serum-free media	Sigma-Aldrich	14420C-1000ML
Benzonase® nuclease	Sigma-Aldrich	E1014-25KU
$MgCl_2$ (1M)	Sigma-Aldrich	63069-100ML
Potassium phosphate monobasic	Sigma-Aldrich	P5655-1KG
Potassium phosphate dibasic	Sigma-Aldrich	P3786-1KG
Sodium chloride	Sigma-Aldrich	S7653-1KG
Magnesium chloride	Sigma-Aldrich	208337-1KG
CaptureSelect™ C-tag affinity matrix	Life Technologies	191307005
Precise Tris-HEPES gels	ThermoFisher Scientific	25221
20× Tris-HEPES-SDS buffer	ThermoFisher Scientific	28368
NuPAGE® LDS sample buffer	Life Technologies	NP0007
DTT	Life Technologies	P2325
Trans-Blot® Turbo™ Mini Nitrocellulose Transfer	Bio-Rad	170-4158
Trans-Blot® Turbo™ Midi Nitrocellulose Transfer	Bio-Rad	170-4159
Goat anti-HBV monoclonal antibody	AbD serotec	4940-1484
Bovine serum albumin	Sigma-Aldrich	05470-1G
Sodium azide	Sigma-Aldrich	S2002
Alkaline phosphatase-conjugated rabbit anti-goat IgG	Sigma-Aldrich	A4062-1ML
Alkaline phosphatase-conjugated goat anti-rabbit IgG	Sigma-Aldrich	A3687
BCIP®/NBT	Sigma-Aldrich	B5655-25TAB
TWEEN® 20	Sigma-Aldrich	P2287-500ML
Ficoll-Paque PLUS	GE Healthcare	17-1440-02
PBS	GE Healthcare	SH30256.02
RPMI-1640 with L-glutamine	GE Healthcare	SH30027.02
Heat-inactivated fetal calf serum	Atlanta Biologicals	S11150H
Penicllin, Streptromycin, L-glutamine (100×)	ThermoFisher Scientific	10378016
HEPES buffer (1M)	ThermoFisher Scientific	15630080
β-mercaptoethanol	Sigma-Aldrich	M7522
Dimethyl sulfoxide for molecular biology	Sigma-Aldrich	D8418
Benzonase	Novagen	71205-3
Paraformaldehyde	Electron Microscopy Sciences	15710
Brefeldin A	Sigma-Aldrich	B7651
Cytofix/Cytoperm solution kit	BD	554714

Table 2.1: Commercially available reagents

Antibody clones and manufacturers.				
Specificity	**Fluorophore**	**Clone**	**Manufacturer**	**Catalog**
CD3	Cy7APC	SP34.2	BD	557757
CD4	BV785	OKT4	BioLegend	317441
CD8	Cy7PE	RPA-T8	BioLegend	301012
CD8	BV570	RPA-T8	BioLegend	301038
CD14	BV510	M5E2	BioLegend	301842
CD20	Ax700PE	2H7	VRC	--
CD25	BV605	BC96	BioLegend	302632
CD38	Cy5PE	HIT2	BD	555461
CD45RA	Cy5.5PE	MEM-56	Invitrogen	MHCD45RA18
CD56	BV711	NCAM16.2	BD	563169
CD57	QD705	NK-1	VRC	--
CD127	BV421	A019D5	BioLegend	351310
CD137	PE	4B4-1	BD	555956
CD159a	APC	Z199	Beckman	A60797
CD161	Cy5PE	DX12	BD	551138
CD161	Cy7PE	HP-3G10	BioLegend	339918
CCR7	Ax680	150503	VRC	--
CXCR5	Ax488	RF8B2	VRC	--
CXCR6	PE	K041E5	BioLegend	356004
HLA-DR	BV711	L243	BioLegend	307644
PD-1	BV421	EH12.2H7	BioLegend	329920
TCR-Vα7.2	PerCPCy5.5	3C10	BioLegend	351710
TCR-Vγ9	APC	B3	BioLegend	331310
TCR-γδ	CF594PE	B1	BD	562511
TCR-Vδ1	FITC	TS8.2	ThermoScientific	TCR2730
TCR-Vδ2	Cy5PE	B6	VRC	--
IFN-γ	APC	4S.B3	BioLegend	502512
IFN-γ	BV421	4S.B3	BioLegend	502532
IL-2	BV605	MQ1-	BioLegend	500331
IL-4	BV421	MP4-25D2	BD	564110
IL-10	PE	JES3-9D7	BioLegend	501404
TNF-α	BV650	MAb11	BioLegend	502937
Perforin	PE	B-D48	BioLegend	353303
Ki-67	FITC	B56	BD	556026
Foxp3	Ax647	259D	BioLegend	320214

Table 2.2: Fluorescently-labeled antibodies used for flow cytometry

Flow cytometry panels.							
#	Detector	Fluorophore	Panel 1 Stim: PfSPZ/HSA	Panel 2 Stim: PfRBC/uRBC	Panel 3 Stim: PfSPZ/HSA	Panel 4 Human liver	Panel 5 NHP liver
1	B515	FITC	Ki-67		TCR-Vδ1		
2	B710	Cy5.5PerCP	TCR-Vα7.2			TCR-Vα7.2	
3	V440	BV421					IFN-γ
4	V510	Aqua/BV510#	Viability/CD14#	Viability/CD14#	Viability/CD14#	Viability/CD14#	Viability/CD14#
5	V570	BV570					CD8
6	V605	BV605	IL-2	IL-2			IL-2
7	V650	BV650	TNF-α	TNF-α			TNF-α
8	V710	BV711	CD56			CD56	
9	V750	BV750					
10	V800	BV785	CD4	CD4	CD4	CD4	CD4
11	R660	APC	IFN-γ	IFN-γ	TCR-Vγ9		NKG2a
12	R710	Ax680	CCR7	CCR7	CCR7	CCR7	CCR7
13	R780	Cy7APC	CD3	CD3	CD3	CD3	CD3
14	G560	PE	CXCR6	Perforin			TCR-Vα7.2
15	G610	CF594PE	TCR-γδ	TCR-γδ	TCR-γδ	TCR-γδ	TCR-γδ
16	G660	Cy5PE	CD161	CD38	TCR-Vδ2	CD161	
17	G710	Cy5.5PE/Ax700PE#	CD45RA	CD45RA	CD45RA	CD20#	CD45RA
18	G780	Cy7PE	CD8	CD8	CD8	CD8	CD161

Flow cytometry panels.							
#	Detector	Fluorophore	Panel 6 Stim: PfSPZ/HSA	Panel 7 Stim: PfSPZ/HSA	Panel 8 Stim: PfSPZ/HSA	Panel 9 Stim: PfRBC/uRBC	Panel 10 Stim: PfRBC/uRBC
1	B515	FITC/Ax488*	CXCR5*	TCR-Vδ1	Ki-67		TCR-Vδ1
2	B710	Cy5.5PerCP			TCR-Vα7.2		
3	V440	BV421	PD-1		PD-1	CD127	IL-4
4	V510	Aqua/BV510#	Viability/CD14#	Viability/CD14#	Viability/CD14#	Viability/CD14#	Viability/CD14#
5	V570	BV570					
6	V605	BV605	IL-2		IL-2	IL-2	
7	V650	BV650	TNF-α		TNF-α	TNF-α	
8	V710	BV711/QD705¶	HLA-DR		CD56	CD57¶	
9	V750	BV750					
10	V800	BV785	CD4	CD4	CD4	CD4	CD4
11	R660	APC	IFN-γ		IFN-γ	IFN-γ	TCR-Vγ9
12	R710	Ax680	CCR7	CCR7	CCR7	CCR7	CCR7
13	R780	Cy7APC	CD3	CD3	CD3	CD3	CD3
14	G560	PE	CD137		CXCR6	Perforin	IL-10
15	G610	CF594PE	TCR-γδ	TCR-γδ	TCR-γδ	TCR-γδ	TCR-γδ
16	G660	Cy5PE	CD38	TCR-Vδ2	CD161	CD38	TCR-Vδ2
17	G710	Cy5.5PE	CD45RA	CD45RA	CD45RA	CD45RA	CD45RA
18	G780	Cy7PE	CD8	CD8	CD8	CD8	CD8

Table 2.3: Flow cytometry panels: chapter 4 used panels 1–5, chapter 5 used panels 6–7, chapter 6 used panels 8–10.

2.2 Methods in molecular biology

2.2.1 Cloning

Expression constructs were cloned using standard PCR methods, site directed mutagenesis, or In-Fusion HD Cloning Plus kit (ClonTech). Inserts were verified by Sanger sequencing.

Site directed mutagenesis of RH5-sv3

RH5-sv3 of the Pf3D7 strain differs from Pf7G8 by one amino acid, having a cysteine at residue 203 in place of a tyrosine. To generate the 3D7 strain, site-directed mutagenesis of pExpreS^2-1 Pf7G8-RH5-sv3 plasmid [179] was achieved using the QuikChange II Site-Directed Mutagenesis Kit per manufacturer's instructions.

RH5, Pfs25, and HBsAg constructs

pExpreS^2-1-Pf3D7-RH5-sv3-IMX313-Ctag was derived from Pf3D7-RH5-sv3-Ctag by In-fusion cloning per the manufacturer's instructions. The 56 amino acid IMX313 sequence (GSKKQGDADVCGEVAYIQSVVSDCHVPTAELRTLLEIRKLFLEIQK-LKVELQGLSK) was placed between sv3 and the Ctag, and is as described in [180].

pENTR4-Pfs25-SpyTag-Ctag was derived from Pfs25 as described in [177] by In-fusion cloning. The 13 amino acid SpyTag sequence (AHIVMVDAYKPTK) was placed between Pfs25 and the Ctag, and is as described in [181].

pPinkα-HD-SpyCatcher-HBsAg-Ctag was derived from pPinkα-HD-RTS-HBsAg-Ctag as described in Collins, DPhil thesis, Oxon, 2015 by In-fusion cloning. The truncated SpyCatcherδN1δC2 (hereafter referred to as SpyCatcher) and its non-catalytic variant SpyCatcher-EQ (which contains a single E to Q mutation at residue 57) were placed at the N-terminus of the fusion protein and separated from HBsAg by a four amino acid linker, PVTN. The SpyCatcher sequences are as described [182]. The constructed had a C-terminal Ctag for affinity purification.

2.2.2 Transfections and transformations

Stably transfected S2 lines

Stably-transfected Schneider S2 (*Drosophila melanogaster*) cell lines were generated by ExpreS^{2}ions Biotechnologies (Horsholm, Denmark) using pExpreS^2-1 plasmid constructs and G418 selection media.

Stably transformed *Pichia*

Pichia pastoris yeast was transformed using 10 μg of gel purified EcoRI linearized pPinkα plasmid according to manufacturer's instructions.

Briefly, *Pichia* strains 1, 2, 3 and 4 from the PichiaPink Kit were streaked on YPD agar (1% w/v yeast extract, 2% w/v peptone, 2% w/v dextrose, and 2% w/v agar). The plates were incubated at 25°C for 5 days. Single colonies from each strain were expanded in 10 mL YPD media at 30°C and 300 rpm. After 2 days, the starter culture was transferred to 100 mL YPD at 30°C and 300 rpm.

When the cell suspension OD600 density reached 1.3–1.5 (log phase growth), the cultures were harvested at 1,500 g for 5 minutes, washed twice with 250 mL ice-cold sterile water, and then washed with 10 mL ice-cold 1M sorbitol. Cells were resuspended in 500 μL ice-cold 1M sorbitol. 80 μL of the solution was mixed with 10 μg linearized plasmid and transferred to a 0.2 cm electroporation cuvette (Bio-Rad). The cuvette was incubated on ice for 5 minutes and electroporated in a Bio-Rad GenePulser Xcell using manufacturer's recommended pulse sequence.

Cells were rescued with 1 mL ice-cold YPDS media, incubated at 25 °C for 2 hours, and plated on PAD selection plates. The plates were incubated at 25 °C for 5 days until colonies formed.

Transiently transfected HEK293E

Suspension HEK293E cells were grown to 2 million cells per mL in Expi293 Expression Medium with penicillin/streptomycin at 37 °C and 8% CO_2 at 125 rpm. Cells were transiently transfected with 1 μg plasmid complexed to polyethylenimine per million cells and incubated for 72 hours.

2.2.3 Protein expression and purification

Supernatant processing

Cell culture (S2 and HEK293E) suspensions were centrifuged at 3,000 g for 15 minutes. Pichia lysates were centrifuged at 13,000 g for 20 minutes. Supernatants were harvested and filtered through a 0.22 μm polyethersulfone (PES) filter immediately before affinity purification.

Tangential flow filtration

Prior to affinity purification, cell supernatants were filtered and concentrated by tangential flow filtration, as indicated in the text, using a Pellican Biomax-10 (Merck Millipore) filter, according to manufacturer's instructions. Briefly, the membrane was washed with 0.1M NaOH, flushed with deionized H_2O, and equilibrated using 20 mM TRIS pH 7.4 in deionized H_2O. The supernatant was run over the filter continuously until concentrated approximately 15 fold, recovered, and refiltered through a 0.22 μm PES filter.

C-tag affinity purification

Cell supernatants were purified by C-tag affinity purification on an FPLC (*ÄKTA* Pure, GE Healthcare) according to manufacturer's instructions. Briefly, the CaptureSelect C-tag Affinity Matrix (Life Technologies) column (5 mL) was equilibrated with 3 column volumes of TBS. The clarified supernatant was then bound to the column and washed with 10 column volumes of TBS. The sample was eluted in 5 column volumes of C-tag column elution buffer. Elution was continuously monitored by in-line UV-Vis spectroscopy and conductivity measurements.

Size exclusion chromatography

Protein-containing fractions recovered after C-tag elution were pooled and resolved by size exclusion chromatography using FPLC (*ÄKTA* Pure, GE Healthcare) using a HiLoad 16/600 Superdex 200 pg (GE Healthcare) column. Briefly, the column was equilibrated using 3 column volumes of TBS. The sample was applied in 5 mL

maximum volume and resolved with TBS. Elution was continuously monitored by in-line UV-Vis spectroscopy and conductivity measurements.

Protein concentration and buffer exchange

Fractions recovered from the FPLC that contained protein were pooled and, if needed, concentrated using Amicon 10,000 kDa molecular weight cut-off ultrafiltration units (Millipore). Amicon filters were also used for buffer exchange by three rounds of centrifugation and buffer replacement. Alternatively, protein solutions were buffer exchanged using PD-10 columns (GE Healthcare) or size exclusion chromatography, as indicated in the text.

RH5 variants expression and purification

Stably-transfected S2 cells were cultured in EX-CELL 420 serum-free media to a final volume of 2.5–5.0 L. Cells were split every 3 days, re-seeding to a density of 8×10^6 cells per mL. Supernatants were harvested by centrifugation, filtered, and concentrated by tangential flow filtration. RH5 variants were purified by CaptureSelect C-tag Affinity Matrix (Life Technologies) using an *ÄKTA* Pure per the manufacturer's instructions, followed by size-exclusion chromatography (HiLoad 16/600 Superdex 200 pg column, GE Healthcare).

Pfs25-SpyTag expression and purification

Transiently transfected HEK293E cells were cultured for 72 hours. Supernatants were harvested by centrifugation. Pfs25-SpyTag was purified by CaptureSelect C-tag Affinity Matrix (Life Technologies) per the manufacturer's instructions, followed by size-exclusion chromatography (HiLoad 16/600 Superdex 200 pg column, GE Healthcare).

Small scale HBsAg expression

6 colonies from each transformation were inoculated into 5 mL BMGY medium and grown for 2 days at 25 °C and 300 rpm. Cells were centrifuged at 1500 g for 5 minutes at room temperature. BMGY medium were decanted and replaced with 1

mL of BMMY medium. Cells were incubated at 25 °C at 300 rpm. Cultures were supplemented with 0.5% v/v methanol every 24 hours. After 72 hours, cells were harvested by centrifugation and processed. The expression of different constructs was determined by SDS-PAGE of the cell lysate.

Large scale HBsAg expression

The clone with the highest protein expression was selected for large scale protein expression. A single colony was inoculated into 25 mL of BMGY and further expanded after 2 days into 2 L BMGY. After two days, the cells were centrifuged and resuspended in 800 mL BMMY. The culture was supplemented with 0.5% methanol every 24 hours. After 72 hours, the cells were harvested by centrifugation and processed.

Pichia lysis

Pichia cell pellets were washed with 100 mL ice-cold deionized H_2O, and resuspended in 36 mL yeast lysis buffer. Resuspended cells were split between four 50 mL conical vials containing 4.5 g acid washed glass beads and 2000 U Benzonase each. Cells were vortexed for 1 minute, followed by a 1 minute rest on ice. This process was repeated 10 times with vigorous vortexing. The cell lysate wass centrifuged at 1,500 g at 4 °C for 5 minutes, and the supernatant was transferred to a 50 mL conical vial. The supernatant was clarified by centrifugation at 13,000 g for 20 minutes and filtered before proceeding to Ctag purification.

SpyCatcher-AP205

SpyCatcher-AP205 VLPs were cloned and expressed as previously described [181].

2.2.4 Protein characterization

Protein quantification

Purified protein concentration was determined by nanodrop (ThermoFisher Scientific) or BCA assay (ThermoFisher Scientific) per the manufacturer's instructions.

SDS-PAGE and Coomassie staining

Proteins were prepared in 4× LDS sample loading buffer. To reduce the samples, 250 mM DTT was added as indicated. The samples were heated at 95 °C for 3 minutes and resolved on precast Precise SDS Tris-HEPES gels. Gels were stained with Coomassie Brilliant Blue and destained with water.

Western blots

Proteins on PAGE gels were transferred to nitrocellulose paper using the Trans-Blot Turbo kit (Bio-Rad), followed by blocking in 3% BSA in PBS for 1 hour. The primary antibody (goat anti-HBsAg monoclonal antibody, 1:200 dilution; or rabbit anti-RH5 polyclonal serum, 1:500 dilution) was added diluted in blocking buffer for 1 hour. After washing three times with PBS + Tween, the secondary antibody (donkey anti-mouse alkaline phosphatase, or goat anti-rabbit alkaline phosphatase) was added at 1:1000 dilution in blocking buffer for 1 hour. After washing three times, the blot was developed with BCIP in water. The reaction was stopped by washing with water.

SpyCatcher-SpyTag interaction

SpyCatcher constructs were mixed with SpyTag constructs in a 1.5 × molar ratio in the SpyCatcher-SpyTag reaction buffer for 2 hours.

Transmission electron microscopy

Transmission electron microscopy (TEM) was performed by Errin Johnson at the Dunn School BioImaging Facility (Sir William Dunn School of Pathology, University of Oxford). Samples were stained with 2% uranyl acetate for 30 seconds, blotted and air dried. Girds were imaged in a FEI Tecnai T12 transmission electron microscope at 120 kV using a Gatan US1000 CCD camera.

2.3 Methods in immunology

2.3.1 Human immunology

PfCSP ELISA

For ELISA measurement of IgG against PfCSP, a recombinant Pf circumsporozoite protein (rPfCSPv2) was used. The rPfCSP (3D7 strain) is a 48 kDa protein with an N-terminal sequence SLGEND, 299 amino acids in length, the first amino acid being residue 50 at the N-terminus and comprising the rest of the N- and C-termini with 22 NANP and 4 NVDP intervening repeats. 96-well plates (Nunc MaxiSorp Immuno Plate) were coated overnight at 4°C with 2.0 μg rPfCSP/mL in 50 μL per well in coating buffer (KPL). Plates were then washed three times with 1× imidazole-based wash solution containing 2 mM imidazole, 160 mM NaCl, 0.02% Tween-20, 0.5 mM EDTA and blocked with 1% Bovine Serum Albumin (BSA) blocking buffer (KPL) containing 1% non-fat dry milk at 37°C for 1 hour. Plates were washed three times and serially diluted samples (in triplicates) were added and incubated at 37°C for 1 hour. After washing three times, peroxidase-labeled goat anti-human IgG (KPL) was added at a dilution of 0.1 μg/mL and incubated at 37°C for 1 hour. After washing three times, ABTS peroxidase substrate was added for plate development, and the plates were incubated at 22°C for 75 minutes. The plates were read with a Spectramax Plus384 microplate reader (Molecular Devices) at 405 nm. The data were collected using Softmax Pro GXP v5. Data were fit to a 4-parameter sigmoidal curve, and the reciprocal serum dilution at which the optical density was 1.0 (OD1.0) calculated. To serve as assay controls, a negative control (pooled serum from non-immune individuals from a malaria-free area) and a positive control (serum from an individual with anti-PfCSP antibodies) were always included. The results are reported as net OD1.0, which was the OD1.0 of the post-immunization serum minus the OD1.0 of the pre-immunization serum. Samples were considered positive if the difference between the post-immunization OD1.0 and the pre-immunization OD1.0 (net OD1.0) was >50 and the ratio of post-immunization OD1.0 to pre-immunization OD1.0 (ratio) was >2.5.

PfSPZ aIFA

Preparation of slides with air-dried PfSPZ. Purified PfSPZ (NF54 strain) from aseptic *A. stephensi* mosquitoes produced by Sanaria were resuspended in phosphate buffered saline (PBS, pH 7.4). 0.5×10^4 PfSPZ in 40 μL were added to each well of Greiner CELLSTAR clear-bottom black 96-well plates (Sigma-Aldrich). After addition of the suspension, plates were left at room temperature for 12–18 hour for air-drying.

IFA procedure. 50 μL of sera diluted in PBS with 2% BSA were added to each well of the 96-well plate containing air-dried PfSPZ. Sera samples were added at 2-fold dilutions starting at 1:50. After adding samples, plates were incubated at 37°C for 1 hour. Plates were washed in PBS three times on an Aquamax Microplate washer. Ax488-conjugated goat anti-human IgG (Molecular Probes) was diluted to 1:250 in PBS with 2% BSA and 40 μL was added to each well. The plates were then incubated for 1 hour at 37°C . Plates were washed three times with PBS on an Aquamax Microplate washer. 100 μL PBS was added to each well. The plates were sealed using a plate sealer and stored in the dark at 4°C until data acquisition. Samples were assessed by scanning the plates using an Acumen eX3 laser scanning imaging cytometer. The positive control was pooled human serum taken 2 weeks after the last immunization from 12 protected volunteers immunized 4 or 5 times with PfSPZ Vaccine in the VRC 312 clinical trial [12]. The Acumen image cytometer scans the entire surface area of each well in a 96-well plate and the fluorescence measured therefore represents the signal from all 0.5×10^4 PfSPZ that were seeded in each well.

Analysis. The data obtained from the Acumen image cytometer was plotted to fit a 4-parameter sigmoidal curve in Prism using serum dilution as the x-axis and arbitrary fluorescence units (AFU) on the y-axis. Sera from malaria-naïve volunteers in the USA and Europe, including pre-immune sera, always register an AFU value less than 2.0×10^5 even at the highest concentration used in this assay (1:50 dilution). For sera that do bind to PfSPZ, 2.0×10^5 AFU falls in the exponential portion of the sigmoidal curves. Therefore 2.0×10^5 was chosen as the threshold in the aIFA

assay, and the level of anti-PfSPZ antibodies for each volunteer is reported as the reciprocal serum dilution at which fluorescence intensity was equal to 2.0×10^5 AFU.

T cell assays and flow cytometry

Antigen stimulations. Assessment of cellular immune responses using multi-parameter flow cytometry was done from PBMCs on cryopreserved samples at the completion of each study. PBMCs were isolated by density-gradient centrifugation from EDTA anti-coagulated whole blood. PBMCs were then rested for 8 hours in complete RPMl containing 25 U/mL Benzonase, and plated in 200 μL of media at 1.5×10^6 cells per well in a 96-well V-bottom plate and stimulated for 17 hours with: (a) PfSPZ Vaccine diluent (1% Human Serum Albumin, CSL Behring); (b) 1.5×10^5 viable, irradiated, aseptic, purified, cryopreserved PfSPZ from a single production lot; (c) 2.0×10^5 lysed, infected RBC consisting of >90% parasitemic late-stage schizonts (PfRBC) from a single production lot; or (d) 2.0×10^5 donor-matched uninfected erythrocytes from a single production lot (uRBC). PfSPZ and PfRBC were titrated for optimal sensitivity and specificity of detection of Pf-specific responses. For the last 5 hours of the stimulation, 10 μg/mL Brefeldin A (BD) was added to the culture. A positive control sample from a subject vaccinated with 5 doses of 1.35×10^5 PfSPZ IV and negative malaria-naive control were included for each day subjects were analyzed to determine the consistency of antigen stimulation.

Intracellular cytokine staining. After stimulation, cells were stained as previously described [183]. The staining panels and antibody clones and manufacturers are shown in **Table 2.2** and **2.3**. Briefly, cells were surface stained with CCR7 at 37°C for 20 min. Dead cells were identified by Aqua Live/Dead dye (Invitrogen) per manufacturer's instructions. This was followed by 15 min surface staining at room temperature. Cells were washed, fixed, and permeabilized using Cytofix/Cytoperm kit (BD) and stained intracellularly. Cells were washed, fixed in 0.5% paraformaldehyde in PBS, and acquired on a modified LSR II (BD Biosciences). All antigen-specific cytokine frequencies are reported after background subtraction of

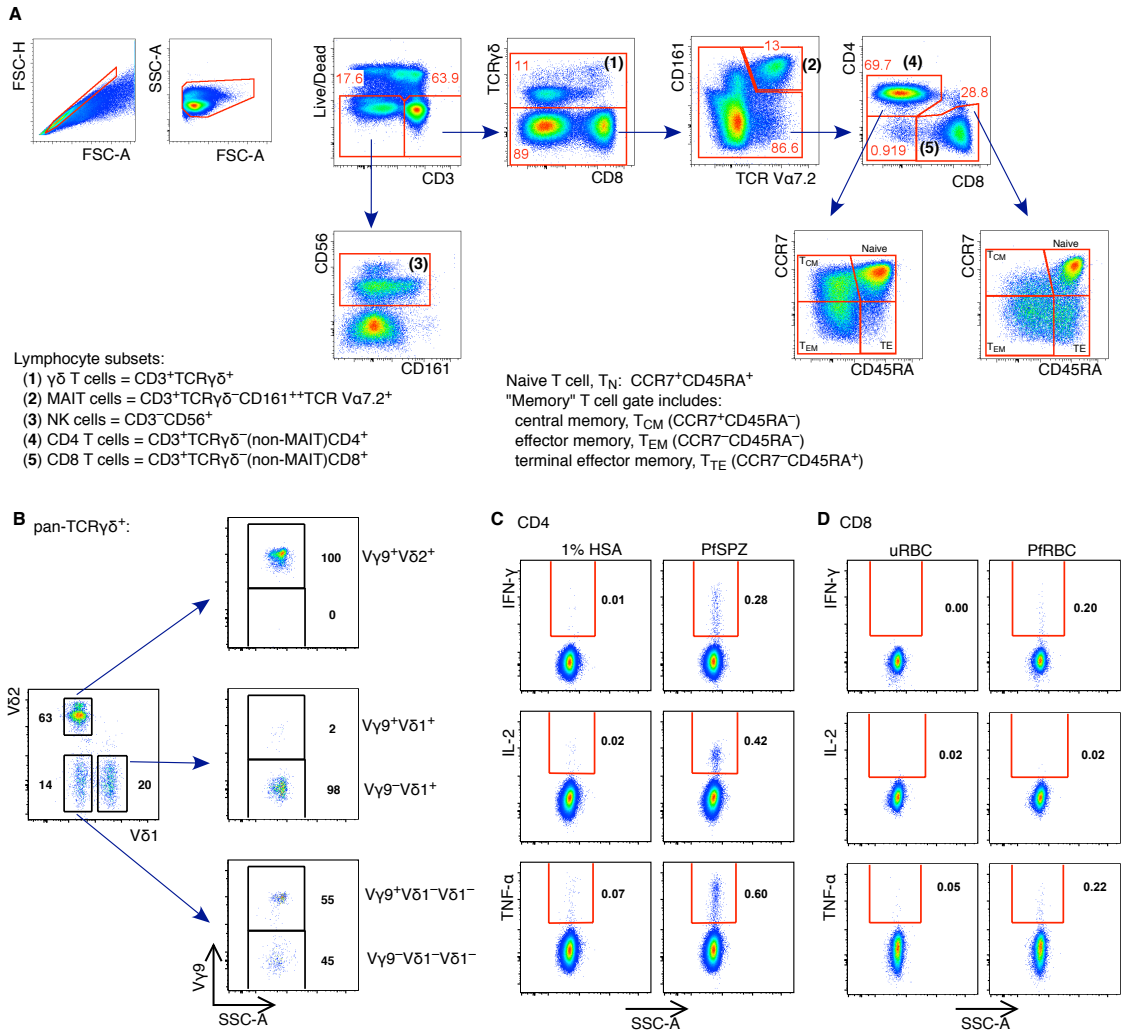


Figure 2.1: Flow cytometry gating tree for analysis of human PBMCs. Flow cytometry staining panels were developed to assess the magnitude, quality, and phenotype of Pf-specific lymphocytes. (**A**) General gating tree for all staining panels, with the following exceptions: For Panels 2, 3, 5, 6, 7, 9, and 10, the CD4 vs. CD8 T cell gate directly follows TCR-$\gamma\delta^-$ gate. References to 'total memory' or 'memory' in the thesis refer to all non-naive T cells, specifically T_{CM}, T_{EM}, and TE combined. (**B**) For Panel 3 and 7, TCR-$\gamma\delta^+$ cells are subdivided into $V\delta2^+$ vs. $V\delta1^+$ vs. $V\delta2^-V\delta1^-$ cells, and then, for Panel 3, further subdivided into $V\gamma0^+$ vs. $V\gamma9^-$ subsets. (**C**) PBMCs were stimulated with PfSPZ or vaccine diluent (1% HSA) and assessed for intracellular cytokine expression by flow cytometry. PfSPZ-specific T cells are identified by expression of any combination of IFN-γ, IL-2, or TNF-α. (**D**) PBMCs were stimulated with Pf-infected erythrocyte lysate (PfRBC) or uninfected control lymphocytes (uRBC) and assessed for intracellular cytokine expression by flow cytometry. PfRBC-specific T cells are identified by expression of any combination of IFN-γ, IL-2, or TNF-α.

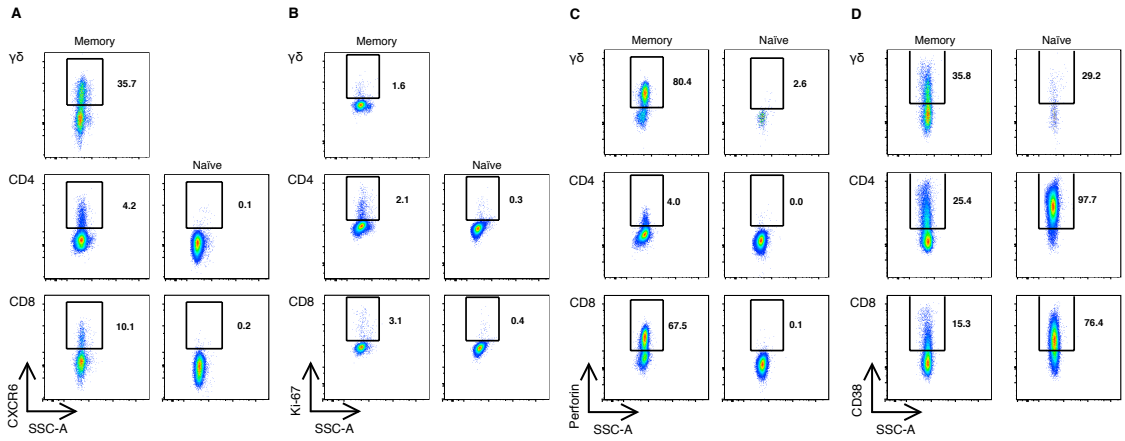


Figure 2.2: Flow cytometry gating of phenotypic markers. (**A**–**D**) Phenotype gates for markers in Panels 1, 2, 6, 8, and 9. Gates are shown for expression of the indicated markers on memory (left) or naive (right) cells from the $\gamma\delta$, CD4, or CD8 T cell lineages.

identical gates from the same sample incubated with the control antigen stimulation (HSA or uRBC).

Luminex cytokine bead array

After PBMCs were stimulated with antigen or control stimulations for 17 hours, the plate was centrifuged at 700 g for 10 minutes. With care not to disturb the cell pellet, the supernatant was removed and frozen at –80 °C until use. Supernatants were assessed for the secreted analytes by Milliplex MAP human cytokine / chemokine 30-plex magnetic bead array (EMD Millipore) according to the manufacturer's instructions. Briefly, culture supernatants (25 μL were incubated overnight with a mixture of magnetic beads that each recognize a unique cytokine or chemokine. The beads were washed, followed by addition of biotin-conjugated detection antibodies and then PE-conjugated streptavidin. Samples were washed and then run on a Luminex FLEX MAP3D (Austin, Texas). Concentrations of individual cytokines were determined from standard curves.

Human liver samples

Human liver samples were obtained under a clinical protocol unrelated to the PfSPZ vaccination protocol. The regional Ethical Review Board in Stockholm, Sweden, approved the study. Oral and written informed consent was obtained

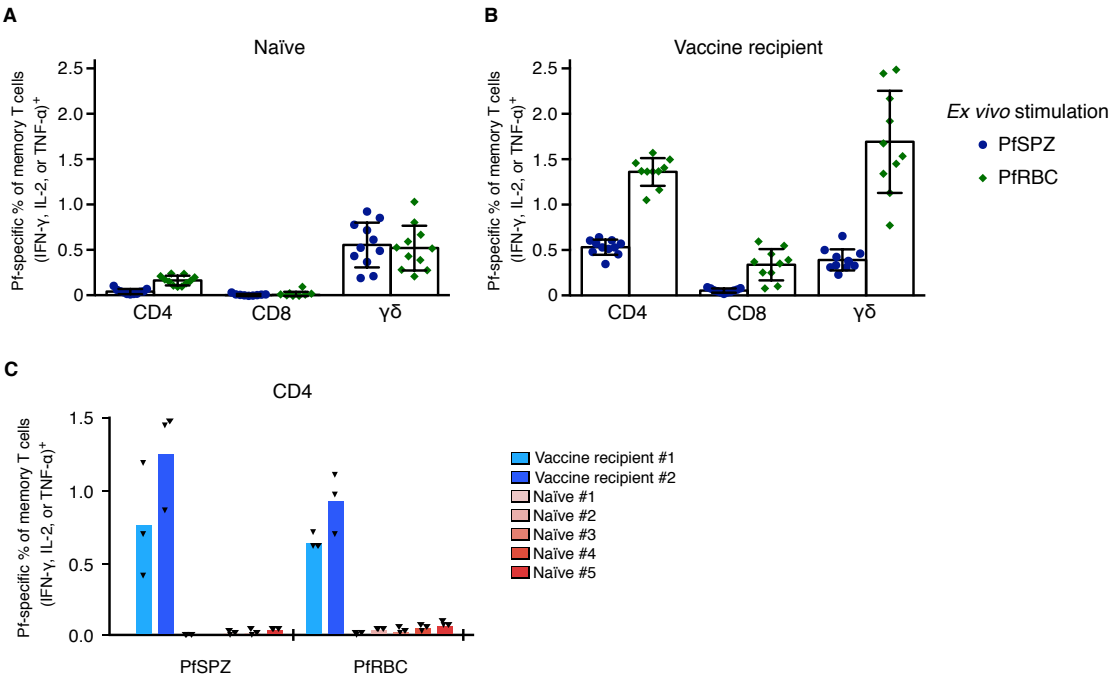


Figure 2.3: Reproducibility of intracellular cytokine staining (ICS) assay. For **A**–**B**, frozen PBMCs from one malaria-naive donor and one PfSPZ Vaccine recipient were included in 10 consecutive assays on separate days analyzing PfSPZ or PfRBC responses from vaccinated and control subjects. The measured cytokine responses are reported for each lineage as mean ± standard deviation. For **C**, three different operators stimulated and stained PBMCs from two vaccine recipients and five naïve controls, using two different staining panels and two different LSR IIs to further determine the variability in stimulation and staining. Bar denotes mean. For the ICS assay, cytokine percentages are always reported after background subtraction of identical gates on the same sample after control stimulation (HSA or uRBC). Across the entire data set herein, the frequency of any cytokine positive cell (IFN-γ, IL-2, or TNF-α) in the control stimulation (the background) is as follows: for CD4, 0.20% ± 0.10% and 0.20% ± 0.10% (mean ± standard deviation) for HSA and uRBC, respectively; and for CD8, 0.13% ± 0.09% and 0.15% ± 0.10% for HSA and uRBC, respectively.

from all subjects. Livers were obtained during partial hepatectomy from living donors undergoing therapeutic tumor excision where only tumor-free nonaffected tissue was used for isolation of immune cells. Immune cells were isolated using a previously described protocol. In brief, excess sinusoidal blood was removed by flushing liver tissues with injections of ice-cold EMEM (Lonza) into blood vessels on the cut surface. Subsequently, tissues were cannulated and perfused at 37°C in a three-step-perfusion protocol. First, the tissue was perfused with 500 mL perfusion buffer 1 ($Ca^{2+}Mg^{2+}$-free HBSS (Sigma) supplemented with 5 mM EGTA (Lonza)

and 25 mM HEPES (Lonza)), followed by perfusion buffer 2 (HBSS, supplemented with 25 mM HEPES). Finally, 500 mL of perfusion buffer 3 (EMEM, supplemented with collagenase XI (Sigma) and DNase (Sigma)) was recirculated for 20–30 min until the parenchyma was loosened from the liver capsula. The digested tissue was filtered with ice-cold EMEM into centrifuge bottles and washed at 75 *g* at 4°C for 5 min. The supernatant contained the non-parenchymal cells from which mononuclear cells were isolated by density gradient centrifugation (Lymphoprep, Stemcell Technologies), washed twice, and cryopreserved for subsequent analyses.

2.3.2 Functional assessment of IgG from vaccine recipients

Antibody purification

Total IgG serum antibodies were purified from serum or plasma by affinity chromatography using Pierce Protein G Plus Agarose (Thermo Scientific) according to manufacturer's instructions. Column eluted IgG was concentrated and buffer-exchanged into phosphate-buffered saline (pH 7.4) using Amicon Ultra 30,000 MWCO centrifugal filters (EMD Millipore). Protein concentration of the purified IgG was calculated by BCA assay (Thermo Scientific).

FRG-huHep mouse challenges

Animals. Human hepatocyte donor-matched FRG-huHep mice (male and female, age 5–9 months) were purchased from Yecuris, Inc. FRG-huHep mice are *Fah*$^{-/-}$ (fumarylacetoacetate hydrolase), *Rag2*$^{-/-}$, and *Il2rg*$^{-/-}$ mice engrafted by intravenous injection of primary human hepatocytes. All animals were cared for in accordance with the NIH Guide for the Care and Use of Laboratory Animals. The Institutional Animal Care and Use Committee approved all animal procedures. Animals were randomly allocated to experimental and control groups.

Mice were intravenously injected with 8 mg/mouse of total IgG purified from vaccinated subjects or 150 μg of anti-PfCSP mouse monoclonal antibody (IgG3, clone 3C1) 16–24 hours before challenge. For mosquito bite challenge, *Anopheles* mosquitoes infected with *P. falciparum* expressing GFP-luciferase were generated as

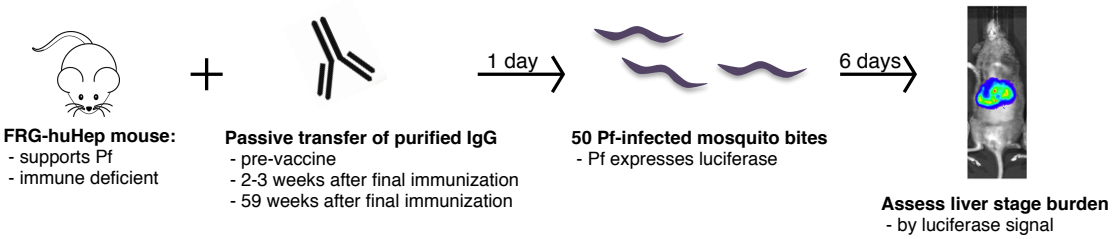


Figure 2.4: Experimental scheme for functional assessment of purified IgG *in vivo*. Total IgG was purified before vaccination, and 2–3 and 59 weeks after final vaccination from all 5 subjects that were not parasitemic at 59 week CHMI. Purified IgG (8 mg) was injected intravenously into individual immune deficient mice capable of supporting the liver stage development of Pf (FRG-huHep mice). One day after injection, animals were infected with luciferase-expressing PfSPZ by 50 mosquito bites. On day 6 post-infection, liver stage burden was assessed by In Vivo Imaging System (IVIS). As a negative control, mice ($n = 7$) received 8 mg of pre-vaccination total IgG pooled from all 5 subjects. As a positive control, mice ($n = 2$) received 150 μg of a monoclonal antibody (clone 3C1) against the repeat region of PfCSP.

previously described [184]. Mosquito infection was quantified at day 10 post-blood meal and were used only if infection was >50% prevalence with an average of >10 oocysts/midgut. All qualifying mosquitoes were then pooled and distributed into cages with 50 mosquitoes/mouse, up to 250 mosquitoes. Mice, in groups of up to 5, were then anesthetized with isoflurane and placed on a mesh screen covering the container of mosquitoes while under isoflurane anesthesia. Mosquitoes were then allowed to feed for 10 minutes with lifting of mice every minute to encourage probing and injection of sporozoites rather than blood feeding. After 10 minutes mice were returned to normal activity.

At day 6 post-infection (peak of liver burden), mice were imaged for liver stage burden using bioluminescence and IVIS imaging as previously described [185]. Briefly, mice were intraperitoneally injected with 100 μL of RediJect *D*-Luciferin (PerkinElmer) and, after 5 minutes, imaged with a 5-minute exposure. Liver stage burden was assessed by placing a region of interest (ROI) around the liver of each mouse and measuring total flux in photons/second. An identical ROI was placed over the thorax, which was used to subtract background luminescence signal. Liver stage burden of all mice was normalized to the mean of the negative control group, which received pre-immune IgG. Sample size was based on prior

passive transfer experiments and calculated using Prism (GraphPad) and JMP Design of Experiment functionality (SAS). Pearson correlation coefficient was used to determine the relationship between Pf liver stage burden and PfCSP level. Investigators were blinded to treatment group during passive transfer of IgG, Pf infection, and measurement of luminescence.

2.3.3 T cell responses in vaccinated non-human primates

Animals

Thirty healthy male and female Indian origin rhesus macaques (*Macaca mulatta*) with a mean (s.d.) age and weight of 6.1 (1.5) years and 8.7 (3.1) kg were singly housed in animal biosafety level 2 facilities and were monitored throughout the study for physical health, food consumption, body weight, and temperature. All animals were cared for in accordance with the NIH Guide for the Care and Use of Laboratory Animals. The Institutional Animal Care and Use Committee approved all animal procedures.

Vaccinations

Study groups were balanced with respect to age, weight, and gender (equal numbers of males and females in each group). Sample size was based on prior NHP immunogenicity studies and calculated using Prism (GraphPad) and JMP Design of Experiment functionality (SAS). PfSPZ Vaccine was formulated and administered as for human injection with the following exceptions. For IV groups, PfSPZ in 500 μL was administered by direct venous inoculation into the saphenous vein. For the IM group, PfSPZ was administered to the left and right deltoid, and each injection was 500 μL in volume. For the ID group, PfSPZ was administered in the skin over the left and right deltoid, and each injection was 100 μL in volume. Immunizations and blood sampling occurred with the animal under anesthesia (10 mg/kg ketamine HCl).

PBMC processing

PBMCs were isolated by density-gradient centrifugation from ACD anti-coagulated whole blood using Ficoll-Paque PLUS (GE Healthcare) according to manufacturer's instructions. Briefly, Buffy layers were washed in PBS, resuspended in R10, and counted. PBMCs were frozen at 10^7 cells per mL in filter sterilized 10% v/v DMSO in HI-FCS using a controlled rate freezer and stored in LNVP until use.

T cell assays and flow cytometry

Immune assays on PBMCs were batch-analyzed on cryopreserved samples at the completion of the study. Ten weeks after final immunization, animals were euthanized and liver tissue was processed as previously described [141]. For immune analysis, samples were thawed, rested, stimulated, stained, and analyzed using identical reagents, stimulation antigens, and protocol as the intracellular cytokine staining assay used for human PBMC samples (described above). The staining panel and the antibody clones and manufacturers are shown in **Tables 2.2** and **2.3**. Investigators were blinded to treatment group during lymphocyte stimulations and flow cytometry gating. All antigen-specific cytokine frequencies are reported after background subtraction of identical gates from the same sample incubated with the control antigen stimulation (HSA or uRBC).

2.4 Statistical analyses

2.4.1 Data analysis

Flow cytometry data was analyzed using FlowJo v9.9.3 (Tree Star). Statistical analyses were performed with Pestle v1.7 and SPICE v5.3 (M. Roederer) [186], JMP 11 (SAS), Prism 7 (GraphPad), and R v3.2.2 with RStudio v0.99.483. Graphs were rendered in FlowJo, SPICE, and Prism.

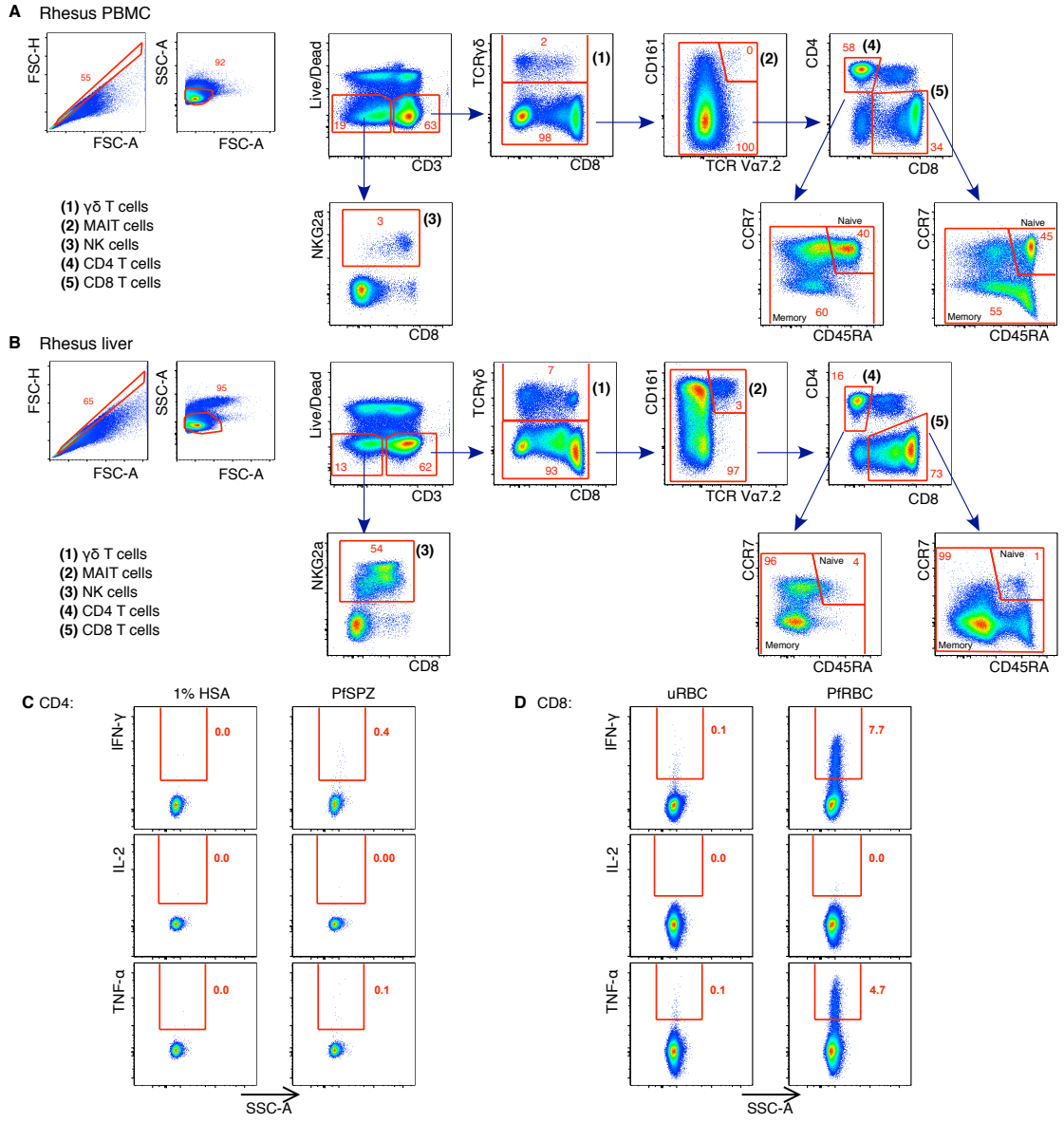


Figure 2.5: Gating tree for rhesus PBMCs and liver lymphocytes. (**A**) Gating tree for NHP PBMCs identifies the same lymphocyte populations as in human PBMCs. (**B**) Gating tree for NHP liver lymphocytes identifies the same lymphocyte populations as in human PBMCs and rhesus PBMCs (**B**). (**C**) Liver lymphocytes were stimulated with PfSPZ or vaccine diluent (1% HSA) and assessed for intracellular cytokine expression by flow cytometry. PfSPZ-specific CD4 T cells are identified by expression of any combination of IFN-γ, IL-2, or TNF-α. (**D**) Liver lymphocytes were stimulated with Pf-infected erythrocyte lysate (PfRBC) or uninfected control lymphocytes (uRBC) and assessed for intracellular cytokine expression by flow cytometry. PfRBC-specific CD8 T cells are identified by expression of any combination of IFN-γ, IL-2, or TNF-α.

2.4.2 Efficacy analysis

For the primary efficacy analysis, the results of the first CHMI for each vaccine group were compared to controls who underwent CHMI concurrently using a one-sided Fisher's exact test. Secondary efficacy analyses compare the results from the different groups as well as describe the results of repeated challenges among those who remained parasite free in each group. No formal multiple comparison adjustment were employed for secondary endpoints. When determining vaccine efficacy (VE), *first* VE was the VE (VE = 1 – relative risk) for the first CHMI. In instances in which a group underwent two CHMIs, vaccine recipients that developed parasitemia during the first CHMI did not undergo repeat CHMI. This was based on data showing that vaccinated subjects that were parasitemic following CHMI and treated remained parasitemic following a second CHMI [142]. *Subgroup* VE was VE among the subgroup of subjects that were not parasitemic at the prior CHMI. We also report *cumulative* VE, a composite of *first* VE and *subgroup* VE (*first* VE multiplied by *subgroup* VE).

2.4.3 Immunogenicity

For vaccine immunogenicity, all statistical comparisons were with non-parametric tests, as specified in the figure legends. Comparisons between three or more groups were performed using Kruskal-Wallis with Dunn's post-test correction for multiple comparisons. If no differences between vaccines groups were identified by Kruskal-Wallis, then difference from pre-vaccination was assessed by Wilcoxon matched-paired signed rank test with Bonferroni correction for multiple comparisons. Comparisons between two groups was by Mann Whitney U-test, Wilcoxon's signed rank test, or Spearman's rank correlation.

2.4.4 Immune correlates

For Chapter 4, immune responses were assessed 2 weeks after final immunization or pre-vaccination (as described in the figure legends) and compared to outcome at either 3 week CHMI or 21–25 week CHMI. For Chapter 6, immune responses were

assessed prior to vaccination, 2 weeks after final immunization, and at the time of CHMI. Assessment of immune responses that correlate with outcome at CHMI (parasitemia or no parasitemia) was made using a stratified Wilcoxon test (R 3.2.2 with RStudio 0.99.483) controlling for vaccine regimen as a co-variate.

3

RH5 VLPs

Contents

3.1 Introduction 59
3.1.1 RH5 as a blood stage vaccine target 59
3.1.2 Study rationale 59
3.1.3 Study aims 60
3.1.4 Authorship 60
3.1.5 Summary of findings 61
3.2 Results 61
3.2.1 Construct design: sv3 and sv3-IMX313 61
3.2.2 sv3 and sv3-IMX313 expression and purification 62
3.2.3 SpyTag-SpyCatcher rationale 64
3.2.4 Construct design: sv3-SpyTag and Pfs25-SpyTag 66
3.2.5 sv3-SpyTag and Pfs25-SpyTag expression and purification 66
3.2.6 Construct design: SpyCatcher-HBsAg 66
3.2.7 SpyCatcher-HBsAg expression and purification 69
3.2.8 HBsAg conjugation 69
3.2.9 AP205 conjugation 70
3.3 Discussion 71
3.3.1 RH5-IMX313 71
3.3.2 sv3-SpyTag 72
3.3.3 Future directions 72

3.1 Introduction

3.1.1 RH5 as a blood stage vaccine target

Erythrocyte invasion is a multi-step process involving several receptor ligand interactions between the *Plasmodium* merozoite and the mammalian erythrocyte [187]. Vaccines targeting most blood stage antigens have been limited by the high genetic diversity of the target antigen in the field. There is one parasite ligand that appears to function through non-redundant invasion pathways and to have relatively low polymorphism, RH5. A vectored RH5 vaccines is currently being evaluated in the clinic, and a recombinant RH5 version is also being pursued [188]. It is possible that this recombinant protein-in-adjuvant version will not meet the required antibody level for clinically-meaningful growth inhibitory activity.

3.1.2 Study rationale

On the basis of the immunological challenges remaining for an RH5 vaccine, I set out to improve the quality and magnitude of the RH5 antibody response.

Antibodies targeting non-neutralizing, immunogenic / immunodominant epitopes present on RH5 may increase the overall antibody levels to RH5 but provide no improvement in neutralization efficiency. Recently, the Higgins and Draper labs solved the structure of RH5 with its native ligand (basigin) and two distinct neutralizing monoclonal antibodies by x-ray crystallography [179]. To facilitate crystal formation, the full-length RH5 protein was modified by removing regions of predicted disorder, residues 1–140 and 248–296. The resultant protein, which was able to form crystals suitable for crystallography, retained the ability to bind basigin with comparable affinity to the wildtype protein and retained the ability to bind neutralizing monoclonal antibodies. I selected this variant of the protein on the basis of these properties.

Antibody responses to monomeric proteins can be improved by multimeric antigen display and the use of carriers and immuno-stimulants [23]. These improvements occur as a result of recruitment of additional precursor B cells, more

efficient expansion, and/or facilitation of germinal center formation that promotes somatic hypermutation and class-switch recombination.

In this study, I sought to multimerize the truncated structural variant (sv3) of RH5 using two distinct protein engineering strategies. Specifically, RH5 was multimerized by (1) direct fusion with the heptamerization domain IMX313, and (2) ligation to a virus-like-particle by a site-specific, covalent, isopeptide bond created between the recombinant protein tags SpyTag and SpyCatcher.

I hypothesized that using the truncated protein will reduce off-target antibody responses to immunodominant, non-neutralizing RH5 epitopes present on the full-length protein, thereby improving the *quality* of the overall antibody response.

I hypothesized that multimerization would improve the *quantity* of the antibody response by improving B cell receptor cross-linking and – due to its larger size – improving pharmacokinetics of the construct within the draining lymphatics.

3.1.3 Study aims

In this study, I sought to:

1 Design, produce, and characterize two distinct RH5 virus-like particles

2 Characterize and compare the mouse antibody response to RH5 for neutralizing activity

3.1.4 Authorship

Profs. Simon Draper and Mark Howarth conceived of the project. Prof. Draper, Prof. Howarth, and I designed the experiments. I conducted the experiments. Jing Jin, Darren Leneghan, Lee Li, Karl Brune, Rebecca Dabbs, Joe Illingworth, and Daniel Alanine assisted with the conduct of experiments. Prof. Adrian Hill, Prof. Sumi Biswas, Julie Furze, Rebecca Ashfield, and Fay Nugent provided scientific oversight and administrative support. Stably transfected S2 cells were generated at ExpreS^{2}ions Biotechnologies (Horsholm, Denmark). Technical guidance with the use of IMX313 was provided by Dr. Fergal Hill and Imaxio.

3.1.5 Summary of findings

1 Pf3D7-RH5-sv3-IMX313 purification was hindered by impurities and degradation products.

2 Pf3D7-RH5-sv3-SpyTag produces a stable monomeric protein that rapidly forms aggregates when multimerized on HBsAg-VLP and AP205-VLP. Multimerization of Pfs25-SpyTag, a different, highly-glycosylated malaria antigen, does not result in aggregation.

3.2 Results

3.2.1 Construct design: sv3 and sv3-IMX313

PfRH5 is a 526 amino acid, 62.5 kDa protein containing 2 disulfide bonds and four predicted glycosylation sites [179]. As with many other malaria proteins, there has been substantial difficulty in expressing full length RH5 in the commonly used recombinant systems, including bacterial, mammalian, and yeast systems [188].

Recently, a truncated version was designed that can be expressed in S2 insect cells [179]. This variant retains the key epitopes of the protein that bind to basigin and two neutralizing antibodies (**Fig. 3.1A**). The structural variant, sv3, contains 338 amino acids from RH5 with all glycosylation sites removed (**Fig. 3.1B**). All constructs herein were based on the Pf3D7 strain of the sv3 variant.

To improve the immunogenicity of the sv3 construct, I first attempted to append a multimerization domain, known as IMX313 to the C-terminus of RH5 (**Fig. 3.1C**). IMX313 is a C4bp (complement protein 4 binding protein) subdomain of avian origin that facilitates heptamerization of the antigen and improves antibody responses [180]. This multimerization likely improves B cell receptor cross-linking and may also – depending on the delivery system used – improve the pharmacokinetics of the antigen, and thereby lead to improved local retention and antigen persistence in the draining lymphatics. Such appendages have demonstrably improved the antibody response of the malaria antigen Pfs25, either expressed in viral vectors or as a recombinant protein [177].

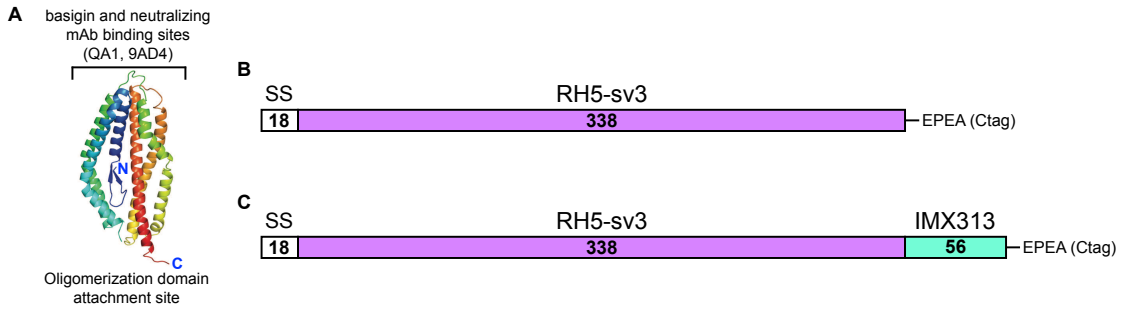


Figure 3.1: (**A**) Crystal structure of RH5-sv3, showing the site of basigin and neutralizing monoclonal antibody (mAb) binding, and the N- and C-termini, adapted from Wright et al., 2014 [179]. (**B**) Pf3D7-RH5-sv3-Ctag, and (**C**) Pf3D7-RH5-sv3-IMX313-Ctag were cloned into the S2 vector pExpreS^2-1. The constructs contain an N-terminal signal sequence (SS) for secretion, and a C-terminal Ctag containing the four amino acid sequence EPEA, which was used to purify the antigen on a Ctag affinity column. IMX313 is a truncated hybrid avian C4bp domain that enables heptamerization of the antigen.

3.2.2 sv3 and sv3-IMX313 expression and purification

The sv3 and sv3-IMX313 variants were expressed in stably transfected S2 cells. After growing to 2.5–5.0 L, the supernatant was harvested, concentrated and filtered by tangential flow filtration (TFF), purified by Ctag affinity column, and further purified by size exclusion chromatography (SEC) (**Fig. 3.2A**). The process was monitored by SDS-PAGE, Coomassie staining, and Western blot.

The sv3 construct was recovered at high purity at approximately 0.6 mg per L of S2 culture (**Fig. 3.2B**).

The sv3-IMX313 construct could not be purified by SEC. The product that was recovered from the Ctag column was loaded on the SEC column and revealed two broad peaks (**Fig. 3.2A**). The first peak also appeared in the monomeric sv3 SEC trace. Evaluation by SDS-PAGE revealed that Peak 1 contained a large amount of a 100 kDa protein that did not react with RH5 anti-sera (**Fig. 3.2C,D**). The fully-assembled covalently-linked multimeric RH5-IMX313 construct is expected to be 345.1 kDa (49.3 kDa per monomer). As this protein would be expected to elute at the same time as Peak 1, it was not possible to isolate the protein from the 100 kDa non-RH5 impurity.

Peak 1 also contained RH5 protein of approximately the expected molecular weight. Reduced sv3-IMX313 monomer is expected to be 49.3 kDa. However, Peak

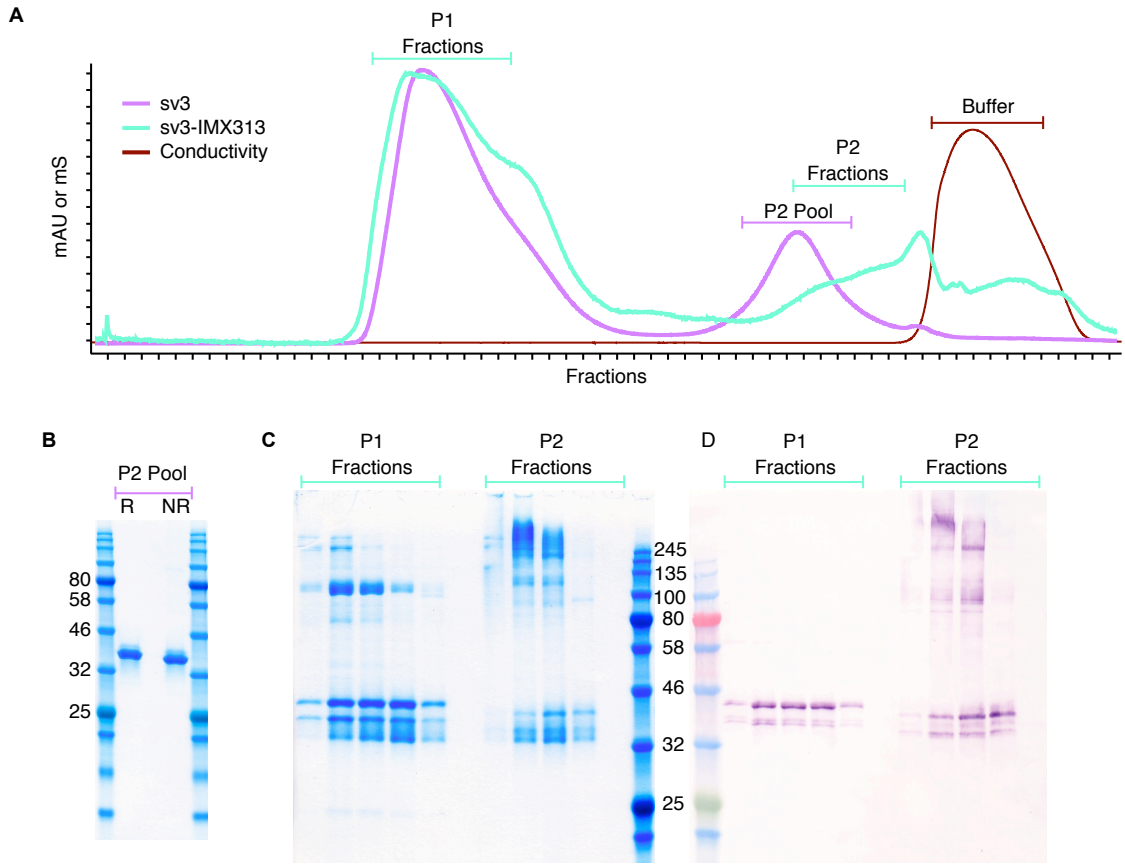


Figure 3.2: (**A**) Overlaid SEC profiles of Pf3D7-RH5-sv3-Ctag ('sv3', purple tracing) and Pf3D7-RH5-sv3-IMX313-Ctag ('sv3-IMX313', teal tracing). The constructs had previously undergone concentration by TFF and affinity purification on a Ctag resin. For sv3, a large amount of high molecular weight material is seen as the first peak eluting from the column. The second peak, P2 Pool, contains highly purified, monomeric sv3, of the expected molecular weight (43.1 kDa), as confirmed by coomassie staining in **B** and subsequently by Western blot (not shown). For sv3-IMX313, there is a large peak that elutes first (P1) and a much smaller dispersed peak that elutes later (P2). Fractions from P1 reveal a large amount of a 100 kDa protein (**C**), which is not identified by Western blot using RH5 polyclonal mouse serum (**D**). P2 contains three bands that bind RH5 anti-sera: a high molecular weight variant that is refractory to disulfide reduction, and two bands of approximately the expected molecular weight (49.3 kDa). Both peaks contain RH5 degradation products of sv3-IMX313, possibly from the cleavage of the multimerization domain from sv3. R, reduced with DTT; NR, no reducing DTT added. For **C** and **D**, all wells contained DTT.

1 also contained an RH5 protein that is approximately 5–7 kDa smaller than the other RH5 protein band present in the sample.

Peak 2 did not contain the 100 kDa impurity, but did contain the same RH5 doublet banding pattern (with the 5–7 kDa difference) as seen in Peak 1 (**Fig. 3.2C,D**). As the IMX313 domain is 6.2 kDa, it is likely that this doublet band represents a degradation product resultant from cleavage of the IMX313 domain from RH5.

As there appears to be considerable degradation of the RH5-IMX313 fusion protein, further development of this approach for this version of RH5 was abandoned.

3.2.3 SpyTag-SpyCatcher rationale

A second multimerization strategy was designed, which utilized the SpyTag-SpyCatcher system. The *Streptococcus pyogenes* fibronectin-binding protein contains a spontaneous, intramolecular isopeptide amide bond between the epsilon amino group of lysine and an aspartic acid. The Howarth group previously split and engineered the domain into two fragments, each of which can be expressed as tags on different proteins. SpyTag is 13 amino acids in length, and SpyCatcher is 84 amino acids in length and contains a domain with micromolar affinity for SpyTag and a domain with catalytic activity [182]. When a protein tagged with SpyTag is mixed under aqueous conditions with a protein fused to the SpyCatcher domain, an isopeptide amide bond is formed spontaneously. The tag can be fused at either terminus or internally. The isopeptide bond is not reversed by boiling or under reducing conditions [189].

A key strategy to improve the immunogenicity of soluble monomeric proteins is to link the antigens to VLPs [23]. Linkage is typically achieved by genetic fusion or conjugation through chemical means [190, 191]. While there are several examples of successful genetic fusion (*e.g.*, the pre-erythrocytic malaria vaccine RTS,S), this approach often fails due to misfolding of the fusion protein [192]. This is further compounded by compromises when the optimal expression system for the capsid is incompatible with the antigen. Chemical strategies of antigen attachment, which typically utilize activated amino–, carboxy–, or sulfhydryl–

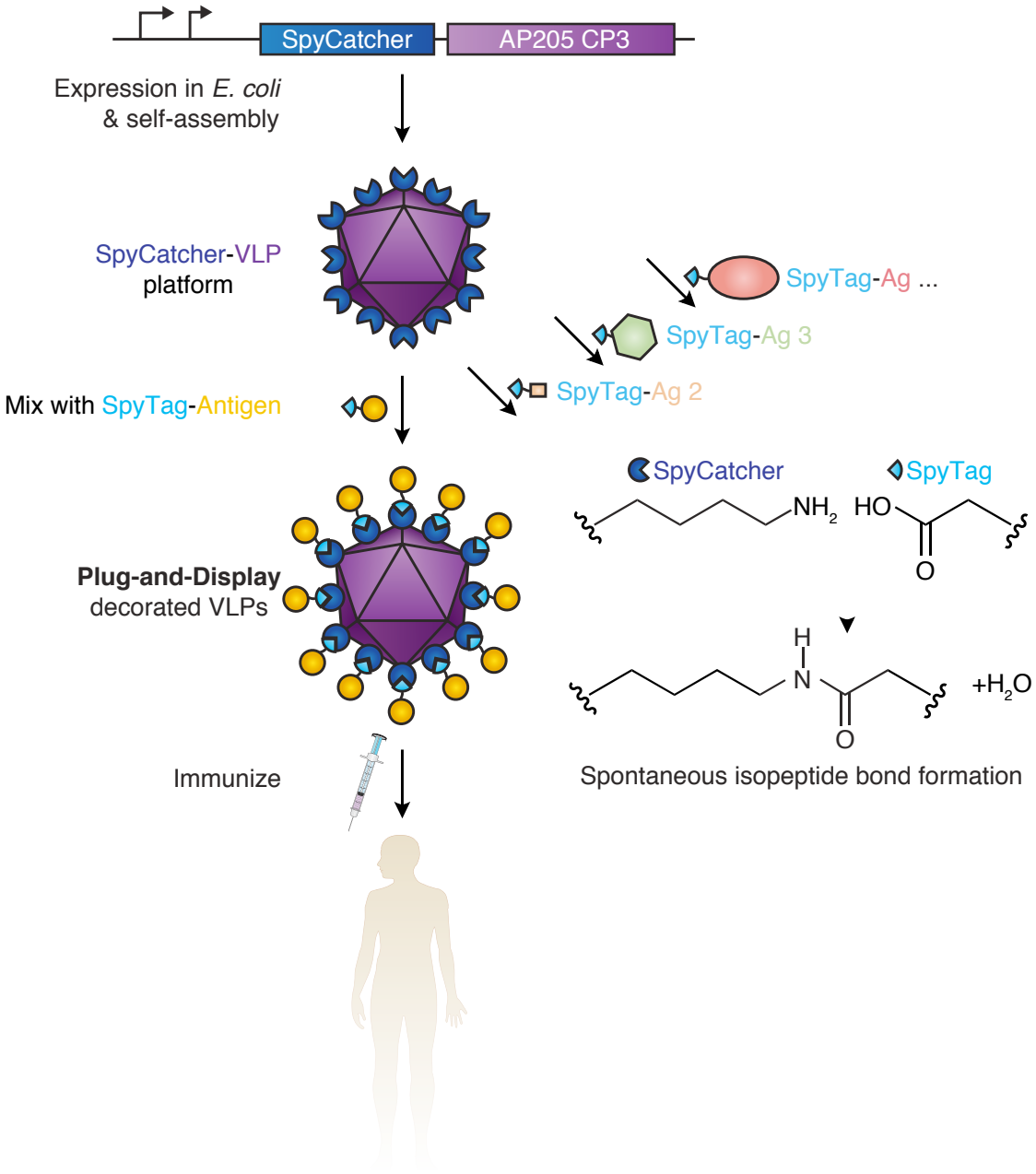


Figure 3.3: Spy assembly scheme. Figure from Brune K, *et al.* 2016 [181]

groups, suffer from incomplete reactivity and heterogenous products [193, 194]. This makes manufacturing at scale and compliance with regulatory preferences for a well defined product difficult.

To address these problems, we conceived of a process wherein the antigen and VLP would be expressed separately (**Fig. 3.3**). Fusion of the two would occur by SpyTag-SpyCatcher interaction, which would allow site-specific, irreversible attachment and complete antigen loading. This strategy also has the advantage of allowing the antigen and VLP to be produced in the optimal expression system, which is particularly important for malaria antigens.

3.2.4 Construct design: sv3-SpyTag and Pfs25-SpyTag

SpyTag (13 amino acids) was appended to the C-terminal end of the antigen sv3 (**Fig. 3.4A**). SpyTag was also appended to the C-terminal end of Pfs25, the transmission blocking malaria antigen (**Fig. 3.4B**) [177]. Both constructs were capped with a C-terminal Ctag for affinity purification.

3.2.5 sv3-SpyTag and Pfs25-SpyTag expression and purification

sv3-SpyTag was expressed in stably transfected S2 cells. After growing to 5.0 L, the supernatant was harvested and concentrated and filtered by TFF. Pfs25-SpyTag was expressed in transiently-transfected HEK293E cells. Both constructs were purified by Ctag affinity column and further purified by SEC (**Fig. 3.4C**). The process was monitored by SDS-PAGE, Coomassie staining, and Western blot.

Highly-purified sv3-SpyTag was recovered at approximately 1.9 mg per L of S2 culture (**Fig. 3.4D**). Highly-purified Pfs25-SpyTag was recovered at approximately 7.8 mg per L of HEK293E culture (**Fig. 3.4E**).

3.2.6 Construct design: SpyCatcher-HBsAg

The hepatitis B virus is enclosed by a lipid envelope which is stabilized by a transmembrane protein called Hepatitis B surface antigen (HBsAg). The particles

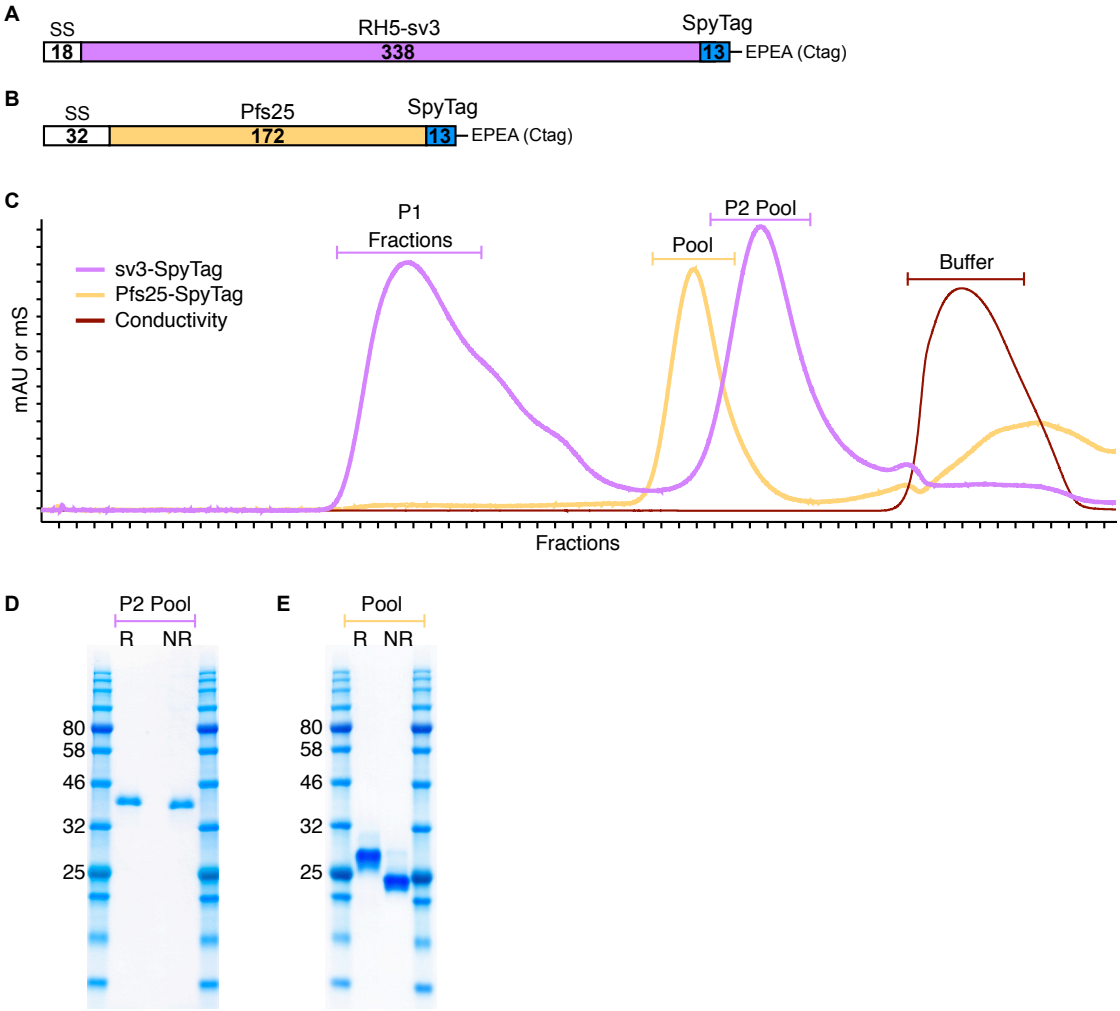


Figure 3.4: (**A**) Pf3D7-RH5-sv3-SpyTag-Ctag (sv3-SpyTag) was cloned into the S2 vector pExpreS^2-1. (**B**) Pfs25-SpyTag-Ctag was cloned into the HEK293 vector pENTR4. Both constructs contain an N-terminal signal sequence (SS) for secretion, and a C-terminal Ctag for affinity purification. (**C**) Overlaid SEC profiles of sv3-SpyTag and Pfs25-SpyTag. The constructs had previously undergone concentration by TFF and/or affinity purification on a Ctag resin. As for sv3 without SpyTag, a large amount of high molecular weight material (identified as an RH5 aggregate by Western) is seen as the first peak (P1) eluting from the column (gels not shown). The second peak, P2 Pool, contains highly purified, monomeric sv3-SpyTag, of the expected molecular weight (44.5 kDa), as confirmed by coomassie staining in **D** and subsequently by Western blot (not shown). Pfs25-SpyTag eluted as a single, narrow peak (labeled Pool), containing highly purified, monomeric Pfs25-SpyTag of the expected molecular weight (24.3 kDa) with substantial disulfide bonding, as expected (**E**). R, reduced with DTT; NR, no DTT added.

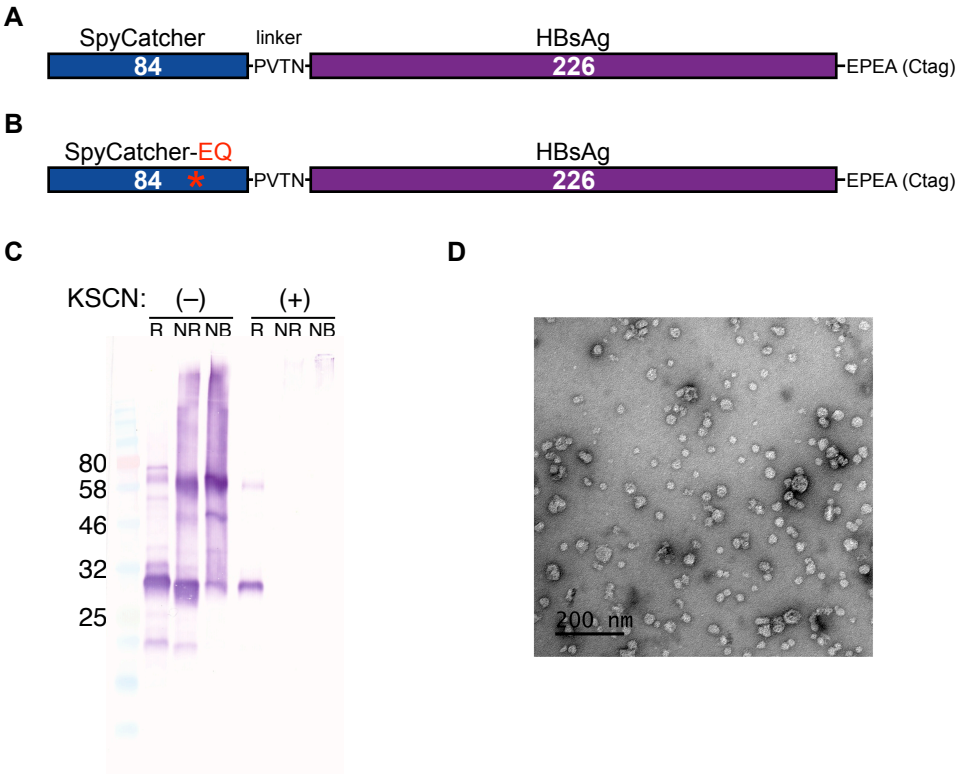


Figure 3.5: (**A**) SpyCatcher-HBsAg and (**B**) SpyCatcher-EQ-HBsAg were cloned into the *Pichia* expression vector pPinkα-HC. Each construct contains a PVTN-linker sequence between the SpyCatcher domain and the HBsAg domain and a C-terminal Ctag for affinity purification. SpyCatcher-EQ-HBsAg contains an E to Q substitution to eliminate the catalytic activity of SpyCatcher. (**C**) After Ctag affinity purification, the eluant was incubated in 1.2M KSCN at 37 °C overnight. As assessed by Western blot, the KSCN treatment resulted in loss of a low-molecular weight variants in the NR (not reduced) and NB (not boiled and not reduced) conditions, consistent with fully assmbled particles. In the reduced lane (R), a band of the expected size (34.5 kDa) is found. (**D**) Transmission electron micrograph of KSCN-treated SpyCatcher-HBsAg showing polydisperse particles.

form approximately 42 nm spheres. RTS,S, a pre-erythrocytic malaria vaccine, consists of a truncated version of CSP fused to the N-terminus of HBsAg [102]. As protein fusions to the N-terminus have already been demonstrated, I chose to append the SpyCatcher domain to the N-terminus of HBsAg. I included a four amino acid short linker (-PVTN-) between the SpyCatcher domain and the HBsAg domain, which is the same as the linker used in RTS,S. The construct was capped with a C-terminal Ctag for purification (**Fig. 3.5A,B**).

3.2.7 SpyCatcher-HBsAg expression and purification

SpyCatcher-HBsAg was expressed in stably transfected *Pichia* yeast by methanol induction. The cells were harvested and lysed with glass beads and lysis buffer. After filtration, the lysate was purified by Ctag affinity column. The process was monitored by SDS-PAGE, Coomassie staining, and Western blot.

As a heterogeneous mixture of HBsAg was identified by SDS-PAGE under non-reducing conditions, KSCN treatment was tested (**Fig. 3.5C**). Incubation of the HBsAg eluant in 1.2M KSCN has been shown to mature the particles, likely by reducing the activation energy needed to refold and reorganize the HBsAg/lipid constructs [195]. After incubation, the low-molecular weight products were no longer identified by SDS-PAGE (**Fig. 3.5C**). Rather, the product is identified as a high-molecular weight species that barely enters the gel, consistent with fully assembled particles. Transmission electron microscopy confirmed particle formation with moderate heterogeneity (**Fig. 3.5D**).

3.2.8 HBsAg conjugation

To determine if the isopeptide bond would form between either sv3-SpyTag or Pfs25-SpyTag and SpyCatcher-HBsAg, 1.5 molar equivalents of sv3-SpyTag or Pfs25-SpyTag were separately mixed with 1 molar equivalent of SpyCatcher-HBsAg in SpyCatcher-SpyTag reaction buffer for two hours at room temperature. The reaction was assessed by SDS-PAGE after reduction. If a successful SpyTag-SpyCatcher isopeptide bond formed, it would be refractory to reduction by boiling in the presence of DTT.

The gel shows a new band corresponding to the combined expected molecular weight of the sv3-HBsAg adduct and the Pfs25-HBsAg adduct. Excess sv3-SpyTag and Pfs25-SpyTag monomers remain, as expected. This signifies that a non-reducible, covalent linkage is formed between sv3-SpyTag and SpyCatcher-HBsAg as well as between Pfs25-SpyTag and SpyCatcher-HBsAg (**Fig. 3.6**). The sv3-HBsAg product aggregated after mixing, and could not be resolved by transmission electron microscopy.

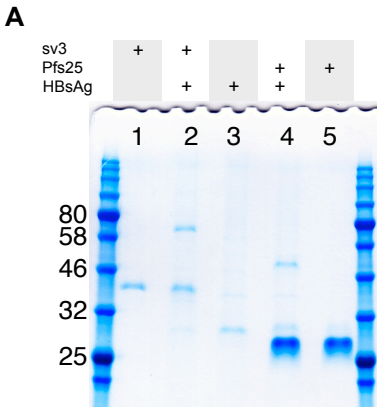


Figure 3.6: (**A**) sv3-SpyTag and Pfs25-SpyTag was mixed at room temperature for 2 hours with SpyCatcher-HBsAg, as specified, prior to reducing with DTT. A new band is found after the reaction, which corresponds with the approximate expected molecular weight of the antigen-VLP conjugate (79.0 kDa for the sv3-HBsAg conjugate; 58.8 kDa for the Pfs25-HBsAg conjugate). The gel shows that a non-reducible, covalent linkage is formed between sv3-SpyTag and SpyCatcher-HBsAg (lane 2). Similar results are obtained with Pfs25 (lane 4). Excess, unreacted monomeric antigen is also seen in the lanes 2 and 4, as expected.

3.2.9 AP205 conjugation

As an alternative to HBsAg, a second VLP carrier was made by the Howarth lab based on the bacteriophage coat protein AP205 [181]. To test the reactivity of sv3-SpyTag and Pfs25-SpyTag, the antigens were reacted with SpyCatcher-AP205 and assessed by SDS-PAGE.

The gel shows that a non-reducible, covalent linkage is formed between sv3-SpyTag and SpyCatcher-AP205 as well as between Pfs25-SpyTag and SpyCatcher-AP205 (**Fig. 3.7A,B**). There is no appreciable amount of unreacted AP205, suggesting that the reaction went to completion. Again, unreacted antigen monomer is seen in the reaction mixture. However, dialysis by spin column with 100 kDa molecular weight cut-off removed the free monomer, leaving only fully-formed, fully-conjugated antigen-VLP conjugate.

Pfs25-AP205 formed stable, uniform particles, as determined by TEM (**Fig. 3.7C**). However, sv3-AP205 rapidly formed a cloudy mixture on reaction, suggesting that protein aggregation was occurring. TEM of the reaction mixture showed large protein aggregates and no free particles (**Fig. 3.7D**).

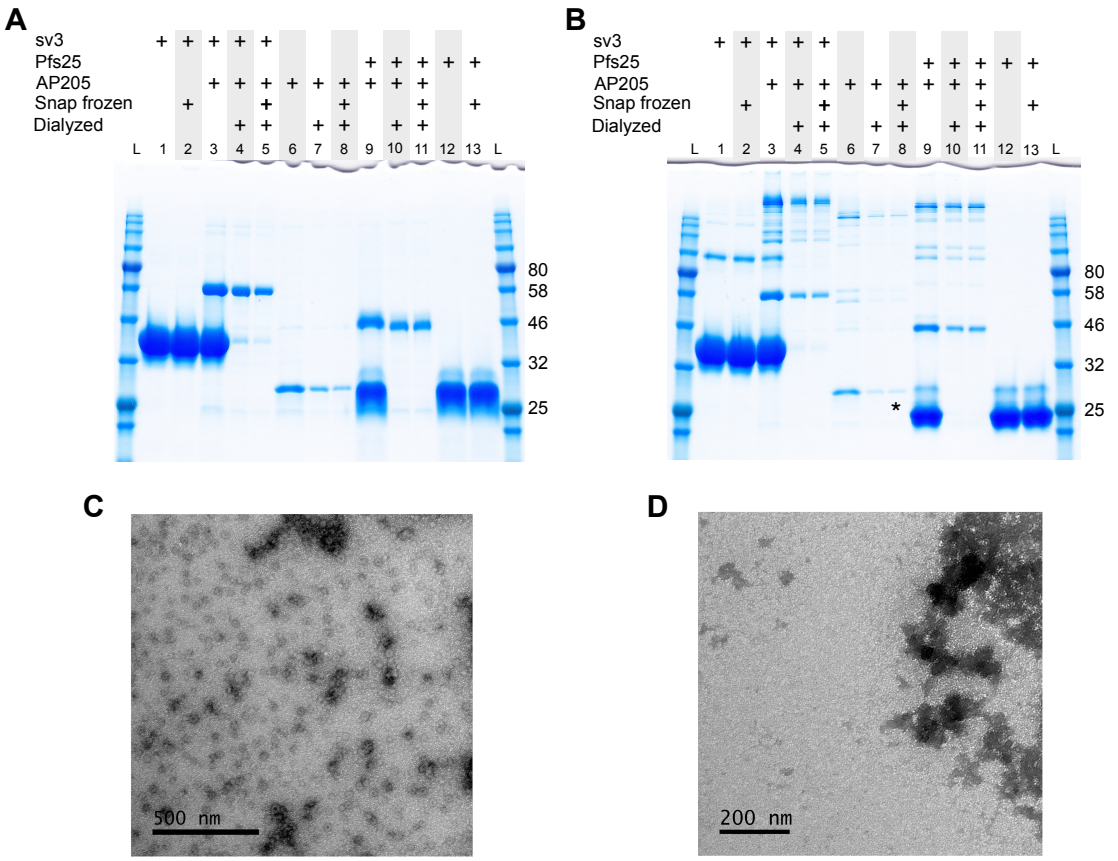


Figure 3.7: (**A**) Protein was mixed at room temperature for 2 hours, dialyzed by spin column, and snap frozen, as specified, prior to reducing with DTT. The gel shows that a non-reducible, covalent linkage is formed between sv3-SpyTag and SpyCatcher-AP205 (lane 3), that the monomer sv3-SpyTag can be dialyzed away (lane 4), and the product can be snap frozen for storage (lane 5). Similar results are obtained with Pfs25 (lanes 9, 10, 11). (**B**) Non-reduced image of same conjugations as in **A**, showing higher molecular weight convalent conjugates. (**C**) TEM image of Pfs25-AP205 showing discrete, uniform particles. (**D**) TEM image of sv3-AP205 showing protein aggregates.

3.3 Discussion

3.3.1 RH5-IMX313

Monomeric sv3 was produced from S2 cells, however, sv3-IMX313 was not able to be produced, due to degradation products and persistent impurities after Ctag and SEC purification steps. Degradation issues could potentially be addressed by expression of the protein in the presence of a protease inhibitor cocktail. The impurities could be addressed by alternative purification strategies, including ion-exchange chromatography.

3.3.2 sv3-SpyTag

Monomeric sv3 and monomeric sv3-SpyTag were recovered as highly-purified proteins at modest yield. However, while sv3-SpyTag was successfully conjugated to two distinct VLPs, the resultant product rapidly aggregated. Much effort has been spent on expressing stable RH5 proteins [188]. It is likely that aggregation on multimerization is reflecting a broader issue with the sv3 immunogen, which often aggregates on synthesis and colocalizes with impurities.

3.3.3 Future directions

First, the importance of the co-crystal structure of RH5 with neutralizing antibodies cannot be understated [179]. It is now possible to rationally design structural variants with improved properties, including yield, solubility, and stability on a pre-formed particle. Modifications, such as introduction of hydrophilic amino acids and glycosylation motifs on the solvent exposed surface of the protein, could be pursued. The four glycosylation sites on the sv3 protein were mutated away to facilitate crystallization. Reintroduction of these could be tested, especially since they do not conflict with the basigin or neutralizing mAb binding domains. sv3 has two free thiol groups. It could be tested how mutation of either of these affects yield, stability, and antigenicity. Additionally, non-native disulfide bridges could be introduced using predictive software on the basis of the crystal structure (Disulfide by Design 2.0, [196]), which can stabilize the protein in solution. Flexibility in the molecule can – when the effective concentration of the protein increases during multimerization -– expose hydrophobic patches that precipitate aggregation. Constraining the antigen with disulfide bridges or other stabilizing interactions may mitigate this issue.

Second, since the current structural variant of RH5 leads to aggregation when multimerized, I have designed an alternative strategy that avoids pre-formed multimers during manufacture and storage, but allows multimeric display *in vivo*. This approach utilizes a thermo-responsive polymeric nanoscaffold as the carrier for the recombinant protein antigen [197]. These polymers-antigen conjugates remain as soluble unimolecular species at room temperature, allowing for facile

manufacturing and stable storage and avoiding the pre-formed multimers that have proved problematic with the current structural variant of RH5. Importantly, the polymer-antigen conjugate undergoes spontaneously self-assemble into multimers upon heating to body temperature. While the previously reported approach utilized non-covalent coiled-coil interactions [197], I will adapt the SpyTag system for use with the platform.

4

PfSPZ Vaccine correlates and mechanism of protection

Contents

4.1 Introduction 75
4.1.1 Durability of PfSPZ Vaccine efficacy is unkonwn 75
4.1.2 Study design 75
4.1.3 Study aims 76
4.1.4 Authorship 76
4.1.5 Summary of findings 77
4.2 Results 77
4.2.1 Study population 77
4.2.2 Vaccine efficacy over 1 year 80
4.2.3 Immunogenicity 81
4.2.4 Correlates of sterile protection 83
4.2.5 Role of PfSPZ antibodies in protection 86
4.2.6 PfSPZ-specific T cell activation after CHMI is dependent on timing of CHMI 88
4.2.7 Longitudinal T cell responses 90
4.2.8 Tissue-resident T cell responses in NHP. 91
4.3 Discussion 94
4.3.1 Vaccine efficacy 94
4.3.2 Immunogenicity 94
4.3.3 Correlates of sterile protection 95
4.3.4 Mechanism of protection 96
4.3.5 Study limitations and future directions 97

4.1 Introduction

In the previous chapter, I presented data on the synthesis of a subunit vaccine for blood stage malaria. In the next three chapters, I will discuss the efficacy and immunological evaluations of a live attenuated whole sporozoite vaccine for pre-erythrocytic malaria.

4.1.1 Durability of PfSPZ Vaccine efficacy is unkonwn

Attenuated PfSPZ immunization consistently achieves high-level (>80%), short-term sterile protection against CHMI with homologous Pf parasites [12, 138, 143].

There is also some evidence that PfSPZ immunization can confer protection for several months, though, this data has only been demonstrated using mosquitoes for vaccination. In a study of malaria-naive adults, 5/6 subjects exposed to >1000 irradiated mosquitoes carrying attenuated PfSPZ were protected when CHMI occurred 23–42 weeks after immunization [138]. Additionally, 4/6 subjects vaccinated with 15 infected mosquito bites with chloroqiune prophylaxis were protected 28 months after vaccination [145]. To date, however, high-level, long-term sterile protection has not been demonstrated with an injectable malaria vaccine.

The following immunological data is derived from a large clinical study conducted between the Vaccine Research Center, NIH, and the University of Maryland Baltimore.

4.1.2 Study design

Having established that the regimen of 5 doses of 1.35×10^5 PfSPZ was not adequate to meet the efficacy goal of >80% sterile protection at 6 months, we designed a study to assess whether increasing the dose of PfSPZ Vaccine from 1.35×10^5 to 2.7×10^5 PfSPZ per dose had an effect on VE. With this higher dose, we tested a three-dose (week 0, 4, and 20) or four-dose (week 0, 4, 8, and 20) regimen to determine how the number of immunizations influenced VE. Another group of subjects received

1.35×10^5 PfSPZ given four times followed by a fifth dose of 4.5×10^5 PfSPZ to see if a higher final dose improved VE compared to 5 doses of 1.35×10^5 PfSPZ. In each of these groups, PfSPZ Vaccine was administered by rapid IV injection.

As IV administration may pose logistic difficulties, this trial was also designed to assess route of vaccine administration, specifically whether IV administration is more efficient in conferring protection compared to the intramuscular (IM) route. Studies in non-human primates (NHP) and humans showed that IV administration of PfSPZ Vaccine is substantially more immunogenic and protective than subcutaneous (SC) or intradermal (ID) administration at a dose of 1.35×10^5 PfSPZ [141]. Studies in rodents showed that IM administration of radiation-attenuated SPZ is more protective than SC or ID administration, albeit significantly less than by IV administration [198]. Thus, we compared protective efficacy of 2.7×10^5 PfSPZ administered IV with 2.2×10^6 PfSPZ administered IM (an 8.1-fold higher dose) on the same four-dose regimen (weeks 0, 4, 8, and 20).

4.1.3 Study aims

In addition to the safety and efficacy data collected by the clinical team, in this study, I sought to:

1 Define antibody and cellular correlates of short-term and long-term sterile protection of PfSPZ Vaccine

2 Define the mechanism of protection of PfSPZ Vaccine

4.1.4 Authorship

The clinical study (VRC 314, ClinicalTrials.gov # NCT02015091) was designed by Robert A. Seder, Kirsten E. Lyke, Stephen L. Hoffman, Julie E. Ledgerwood, and myself. The efficacy data were collected by the clinical team led by KEL and JEL. I designed the human T cell, NHP study, and FRG study with R.A.S. I conducted the human T cell studies with technical assistance from Barbara Flynn and Ayako Yamamoto. I conducted the NHP study with technical assistance from Patricia

Darrah, Kailan Sierra-Davidson, Barbara Flynn, JP Todd, and Jay Norr. Brandon Sack and I conducted the FRG study. The antibody assays were run by Sumana Chakravarty. I performed all immunological analyses and statistical comparisons. SLH and Kim Lee Sim and their team at Sanaria provided aseptic PfSPZ and iRBCs for T cell assays and PfSPZ Vaccine for the NHP study.

4.1.5 Summary of findings

1 PfCSP responses correlate with durable sterile protection.

2 The pre-vaccine frequency of $V\gamma9^{+}V\delta2^{+}$ T cells correlate with durable sterile protection.

3 Sterile protection is maintained at 1 year despite reduced circulating antibody levels and PfSPZ-specific CD4 and CD8 T cells in blood.

4 Tissue-resident CD8 T cells in the liver are more prevalent in NHP vaccinated IV compared to 10-fold higher dose administered by IM or ID routes.

4.2 Results

4.2.1 Study population

101 subjects were enrolled from December 2013 to July 2015: 57 vaccine recipients, 32 CHMI controls, and 12 backup controls. Fifty-five of 57 (96%) subjects completed all scheduled vaccinations and, cumulatively, 224 vaccinations were administered. In total, 52/55 subjects (95%) who completed their vaccinations underwent at least 1 CHMI. At CHMI occurring 3 weeks, 21–25 weeks, and 59 weeks after final vaccination, there were 39, 31, and 5 participating vaccine recipients, respectively (**Fig. 4.1**).

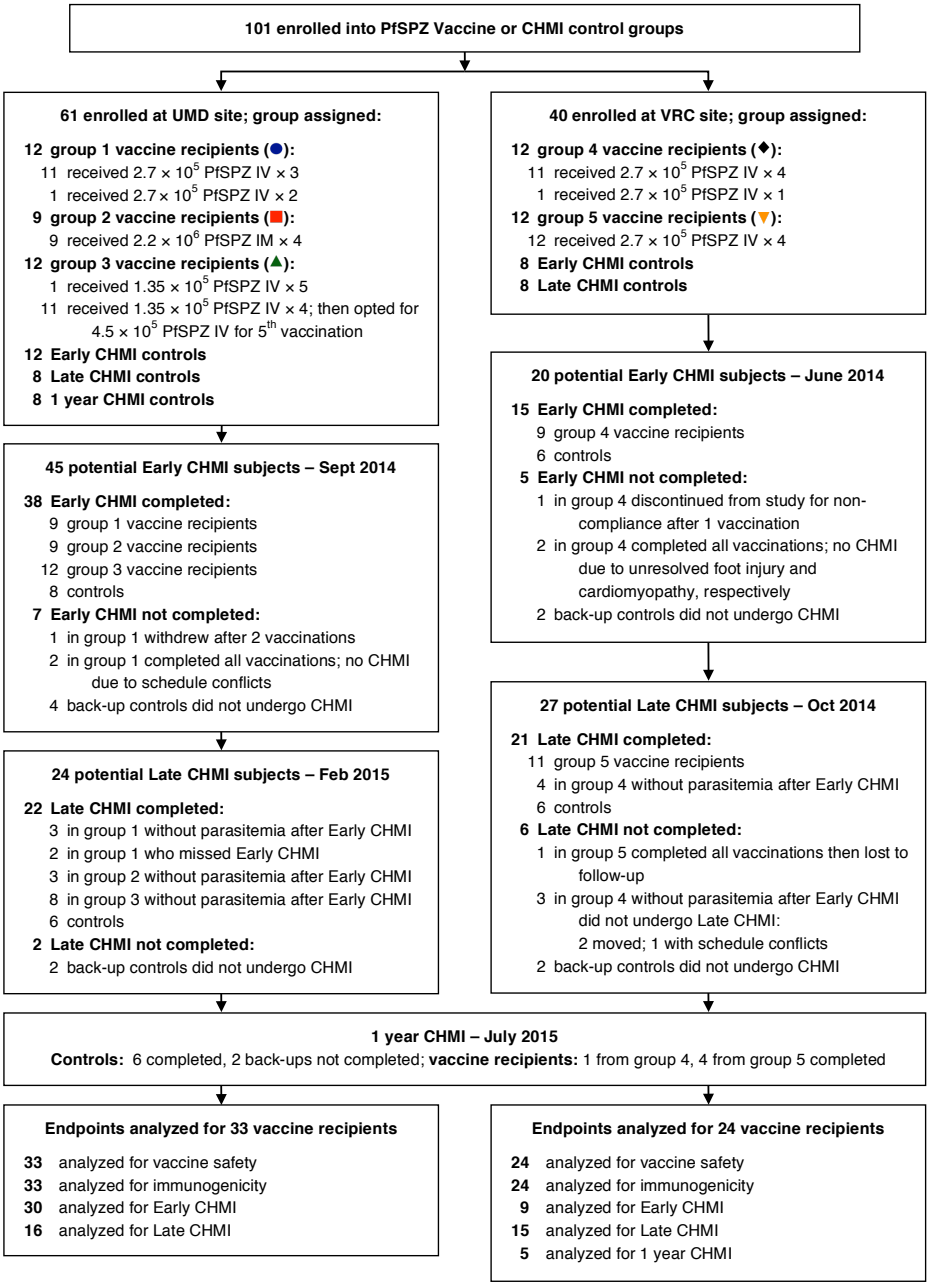
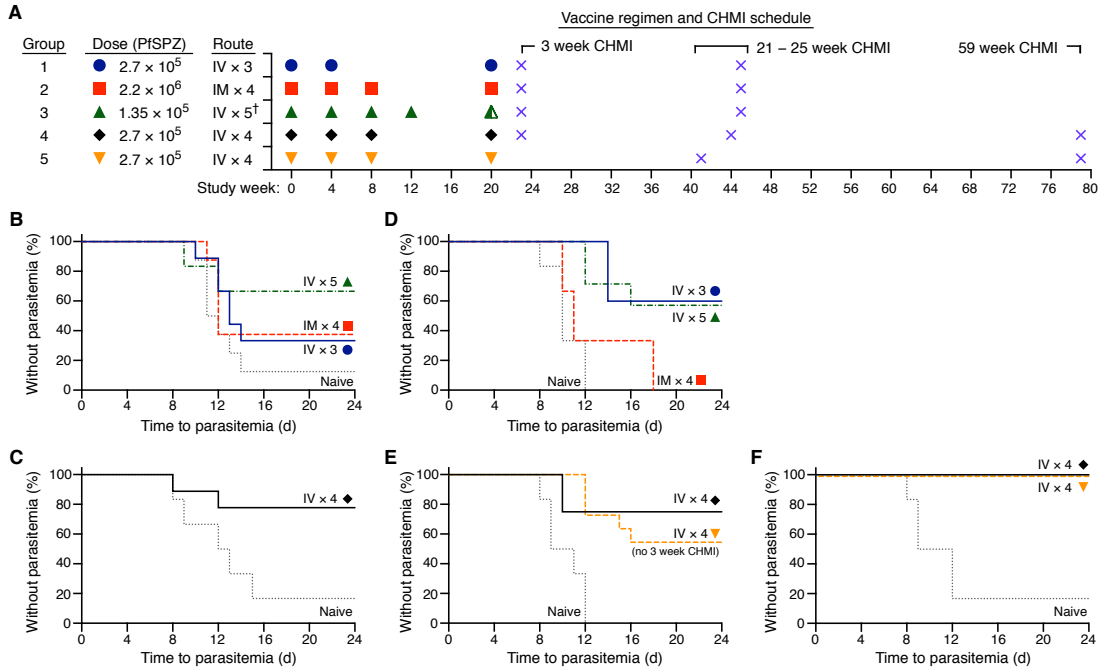


Figure 4.1: Enrollment, vaccinations, CHMIs, and study endpoints. "Early CHMI" occurred 3 weeks after final vaccination, "Late CHMI" occurred 21–25 weeks after final vaccination, and "1 year CHMI" occurred 59 weeks after final vaccination.



G

Group	Vaccination Dose	Inj. #	3 week CHMI # of subjects	3 week CHMI Parasite free	3 week CHMI First VE	21–25 week CHMI # of subjects	21–25 week CHMI Parasite free	21–25 week CHMI First VE	21–25 week CHMI Subgroup VE	21–25 week CHMI Cumulative VE	59 week CHMI # of subjects	59 week CHMI Parasite free	59 week CHMI Subgroup VE	59 week CHMI Cumulative VE
1	2.7 × 10^5	3	9	3	24%	3	2		67%	16%				
2	2.2 × 10^6	4	8	3	29%	3	0		0%	0%				
3	1.35 × 10^5	5†	12	8	62%	7	4		57%	35%				
Naive			8	1		6	0							
4	2.7 × 10^5	4	9	7	73%	4	3		75%	55%	1	1	> 100%	55%
5	2.7 × 10^5	4				11	6	55%		55%	4	4		
Naive			6	1		6	0				6	1		

Figure 4.2: (**A**) Timing of immunizations and CHMIs in groups 1–5 that received 3, 4, or 5 intravenous (IV) or intramuscular (IM) doses of PfSPZ Vaccine. Subjects underwent CHMI 3 (**B**,**C**), 21–25 (**D**,**E**), and/or 59 (**F**) weeks after final immunization. Kaplan-Meier curves showing the percent of volunteers who did not develop parasitemia after each of 5 separate CHMIs. New unvaccinated control subjects were enrolled for each CHMI. (**G**) Vaccine efficacy (VE, defined as 1 – relative risk) and 95% confidence intervals (c.i.) for each CHMI. Nine subjects in group 4 underwent CHMI at 3 weeks and first VE was 73% [95% c.i. for VE (0.05–0.93); $P = 0.035$, one-tailed Fisher's exact test]. Subjects in group 5 underwent CHMI for the first time 21 weeks after final immunization and *first* VE was 55% [95% c.i. for VE (0.13–0.76), $P = 0.037$]. Four subjects in group 4 (who had not developed parasitemia at 3 week CHMI) underwent repeat CHMI at 24 weeks. *Subgroup* VE was 75% and *cumulative* VE was 55% (see text for definitions). Five subjects from groups 4 and 5 underwent repeat CHMI 59 weeks after last immunization, and all were without parasitemia ($P = 0.013$). The five subjects had previously undergone one prior CHMI and had not developed parasitemia ($n = 1$ at 3 week CHMI, $n = 4$ at 21 week CHMI).

4.2.2 Vaccine efficacy over 1 year

VE at 3 weeks, IV administration

Subjects were immunized with 4 doses of 1.35×10^5 PfSPZ and a fifth dose of 4.5×10^5 PfSPZ (group 3) or with 3 or 4 doses of 2.7×10^5 PfSPZ (groups 1 and 4, respectively). Four of 12 subjects in group 3 and 6/9 subjects in group 1 developed parasitemia (**Fig. 4.2B**). In group 4, 2/9 vaccinated subjects developed parasitemia (**Fig. 4.2C**). *First* VE was estimated to be 62% for group 3 ($P = 0.025$). In comparing 3 or 4 doses of 2.7×10^5 PfSPZ, *first* VE was estimated to be 24% for 3 doses and 73% for 4 doses ($P = 0.035$).

VE at 21–25 weeks, IV administration

Only vaccine recipients who did not develop parasitemia after their first CHMI underwent repeat CHMI. Seven subjects from group 3 underwent repeat CHMI at 25 weeks after final vaccination, and 3/7 developed parasitemia compared to 6/6 controls (**Fig. 4.2D**). *Subgroup* VE was estimated as 57% and *cumulative* VE as 35%. These results were similar to the results from the VRC 312 study when CHMI was performed at 21 weeks [142]. Thus, increasing the final dose 3.3-fold did not improve short- or long-term protection compared to the five-dose regimen of 1.35×10^5 PfSPZ. Three subjects in group 1 (3 doses of 2.7×10^5 PfSPZ) underwent repeat CHMI at 25 weeks, and 1/3 developed parasitemia. *Subgroup* VE was estimated at 67% and *cumulative* VE was 16% (**Fig. 4.2D**).

Four subjects in group 4 (4 doses of 2.7×10^5 PfSPZ) underwent repeat CHMI at 24 weeks. One of 4 vaccinated subjects and 6/6 controls developed parasitemia. *Subgroup* VE was estimated to be 75%; when combined with *first* VE of 73%, *cumulative* VE was estimated to be 55% (**Fig. 4.2E**). A second group of subjects also received 4 doses of 2.7×10^5 PfSPZ and underwent their first CHMI at 21 weeks (group 5). Five of these 11 vaccinated subjects developed parasitemia; *first* VE of 55% ($P = 0.037$; **Fig. 4.2E**).

VE at 59 weeks, IV administration

Five subjects who received 4 doses of 2.7×10^5 PfSPZ ($n = 1$ from group 4, $n = 4$ from group 5), who had each undergone a single prior CHMI and not developed parasitemia, underwent a second CHMI 59 weeks after final immunization. None of the 5 vaccine recipients and 5/6 controls developed parasitemia ($P = 0.013$). *Subgroup* VE was 100% and estimated *cumulative* VE was 55% at 59 weeks (**Fig. 4.2F**).

VE at 3 and 25 weeks, IM administration

Subjects were immunized by the IM route (group 2) with 2.2×10^6 PfSPZ (8.1-fold higher dose than 2.7×10^5 PfSPZ IV) on the same administration schedule as groups 4 and 5. Five of 8 IM-vaccinated subjects developed parasitemia following CHMI 3 weeks after vaccination, *first* VE of 29% (**Fig. 4.2B**). The 3 subjects that did not develop parasitemia at 3 weeks underwent repeat CHMI at 25 weeks, and all developed parasitemia (**Fig. 4.2D**). Thus, PfSPZ administered IM at 8.1-fold higher dose was less efficient in inducing protection than IV administration (8/8 parasitemic in group 2 through 21–25 week CHMI vs. 5/11 in group 5; $P = 0.018$).

4.2.3 Immunogenicity

Antibody responses

Antibodies induced by attenuated SPZ vaccination can limit parasites from reaching the liver stage of infection in animal models [199, 200]. Therefore, antibodies against PfCSP and whole PfSPZ were determined by enzyme-linked immunosorbent assay (ELISA) and automated immunofluorescence assay (aIFA), respectively, two weeks after final vaccination. There were no differences in antibody levels among the groups that received IV regimens. However, subjects immunized IM had significantly lower antibody responses than did subjects immunized IV (**Fig. 4.3A,B**).

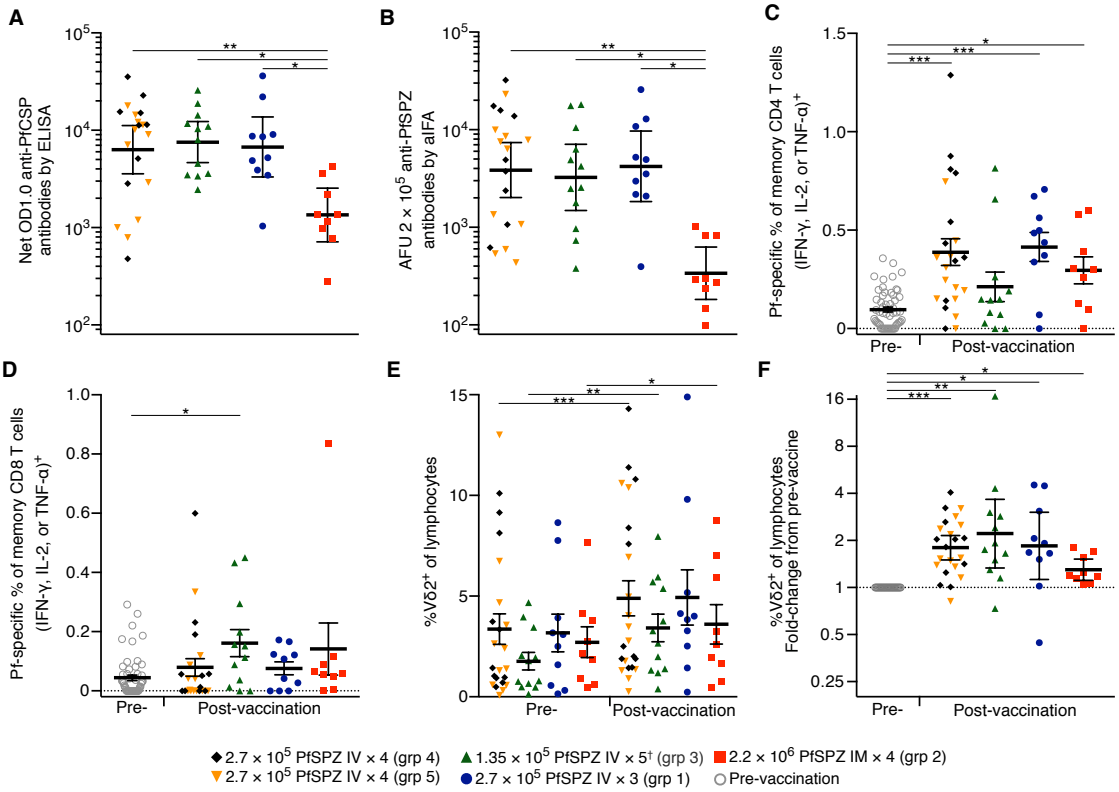


Figure 4.3: (**A**) Antibodies to PfCSP by ELISA. Antibody levels are the serum dilution at which the optical density was 1.0 (OD1.0); and net OD1.0 = OD1.0 of post-immunization serum – OD1.0 of pre-immunization serum. (**B**) Antibodies to PfSPZ by automated immunofluorescence assay (aIFA). Antibody levels are the serum dilution at which the arbitrary fluorescence units (AFU) was 2×10^5. (**C**) Pf-specific memory CD4 T cells secreting IFN-γ, IL-2, or TNF-α by intracellular cytokine staining (ICS). Results are the percent of cytokine producing cells after incubation with PfSPZ minus percent of cells after incubation with vaccine diluent (medium with 1% HSA) as control. (**D**) Pf-specific memory CD8 T cells secreting IFN-γ, IL-2, or TNF-α by ICS after incubation with Pf-infected red blood cells (PfRBCs) or uninfected RBCs as control. Results calculated as in **C**. (**E**) Absolute frequency of the Vγ9$^+$Vδ2$^+$ (hereafter Vδ2$^+$) sub-family of $\gamma\delta$ T cells out of total lymphocytes without incubation with PfSPZ or PfRBCs. (**F**) Fold change from pre- to post-vaccination in the frequency of Vδ2$^+$ T cells as a percentage of total lymphocytes. For **A**–**B**, between group differences were assessed by Kruskal-Wallis test with Dunn's correction for multiple comparisons. For **C**–**F**, there were no differences between groups in the post-vaccination responses by Kruskal-Wallis test. Difference from pre-vaccine was assessed by Wilcoxon signed rank test. For **C**–**F**, P-values were corrected for multiple comparisons by the Bonferroni method. * $P < 0.05$, ** $P < 0.01$, *** $P < 0.001$. Geometric mean ± 95% c.i. (**A**, **B**, **F**) or mean ± s.e.m. (**C**–**E**). †Group 3 received four doses of 1.35×10^5 PfSPZ and a fifth dose of 4.5×10^5 PfSPZ.

Cellular responses

Cellular immunity is critical for protective efficacy of live-attenuated SPZ vaccination in rodent and NHP models [201, 202, 203, 141]. While IFN-γ-producing CD8 T cells are necessary and sufficient in the majority of mouse and NHP studies, NK, $\gamma\delta$, and CD4 T cells also have a role in protection. Therefore, I used multi-parameter flow cytometry to assess the magnitude, quality, and phenotype of Pf-specific cellular responses.

Pf-specificity was determined by stimulating peripheral blood mononuclear cells (PBMCs) with either PfSPZ Vaccine (for CD4 T cell responses) or Pf-infected erythrocytes (for CD8 T cell responses), providing optimal sensitivity and specificity of the responses. While there was an increase in PfSPZ-specific CD4 T cell cytokine responses after final immunization in groups 1, 2, 4, and 5, there were no differences between the vaccine groups in the magnitude (**Fig. 4.3C**) or quality of the PfSPZ-specific CD4 cytokine responses (data not shown), including the IM group. The PfRBC-specific CD8 T cells were low or undetectable in PBMCs (**Fig. 4.3D**). Last, without any *in vitro* Pf-antigen stimulation, there was a vaccine-induced increase in the frequency of $\gamma\delta$ T cells but no differences between the groups (**Fig. 4.3E,F**).

The $\gamma\delta$ T cell expansion was restricted to the Vγ9$^+$Vδ2$^+$ family (hereafter Vδ2$^+$), which comprises 75% of $\gamma\delta$ T cells in blood (**Fig. 4.4A–F**). $\gamma\delta$ T cells showed upregulation of the activation markers CD38, the cytotoxic molecule perforin, and the liver-homing chemokine receptor CXCR6 after vaccination (**Fig. 4.4G–L**). Of note, $\gamma\delta$ T cells expressed IFN-γ when stimulated *ex vivo* with PfSPZ prior to immunization (**Fig. 4.4M**).

4.2.4 Correlates of sterile protection

To identify potential immune correlates of protection [204], I assessed whether there were associations between immune responses measured 2 weeks after the last immunization and outcome after the CHMIs (parasitemia vs. no parasitemia).

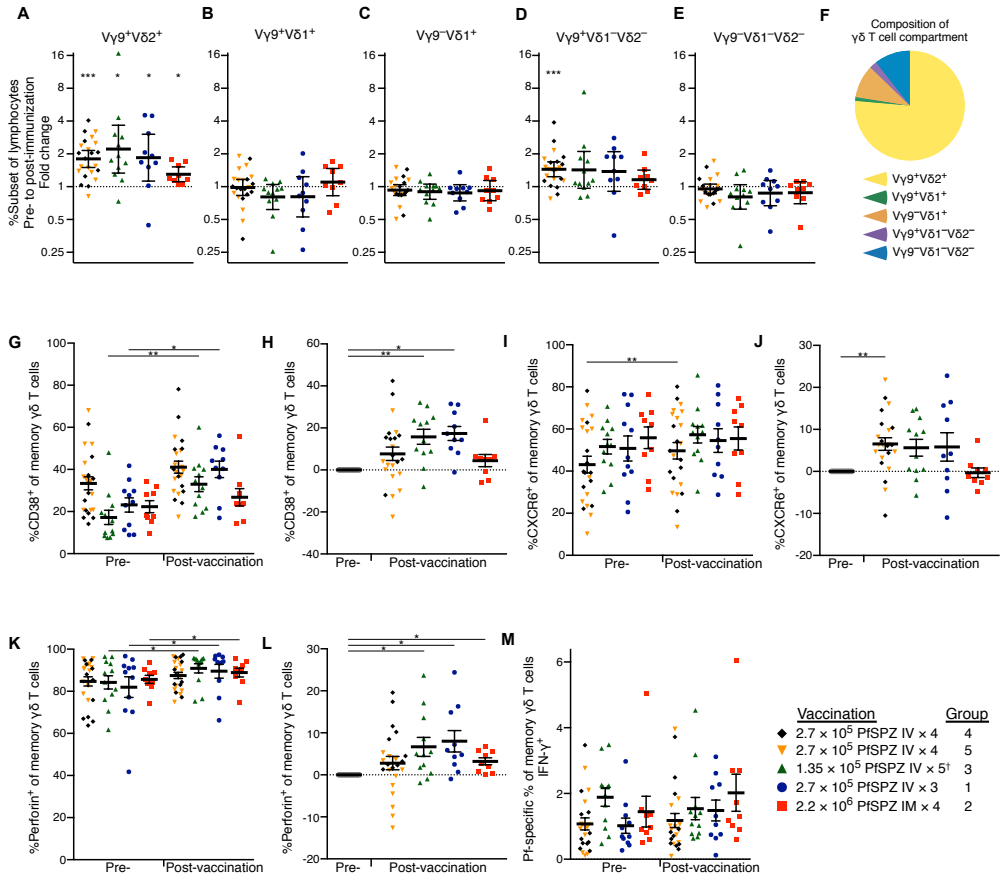


Figure 4.4: (**A**–**E**) The frequency of the circulating $\gamma\delta$ T cell subsets as a percentage of total lymphocytes was assessed in unstimulated PBMCs before the first immunization (pre-immunization) and 2 weeks after final immunization (post-immunization). Fold change from pre-vaccination to post-vaccination is shown for each of the $\gamma\delta$ T cell subfamilies. (**F**) Relative frequencies of $\gamma\delta$ T cell subsets in unstimulated PBMCs from 55 vaccine recipients from the pre-vaccination time point. (**G**–**I**) Total memory $\gamma\delta$ T cells were assessed pre- and post-immunization for the percent of cells expressing the activation marker CD38 (**G**,**H**), the liver-homing chemokine receptor CXCR6 (**I**,**J**), or the effector molecule perforin (**K**,**L**). The absolute frequencies are shown in **G**, **I**, and **K** and the change from pre- to post-vaccination is shown in **H**, **J**, and **L**. (**M**) Memory $\gamma\delta$ T cells secreting IFN-γ by ICS pre- and post-vaccination. Results are the percent of cytokine producing cells after incubation with PfSPZ minus percent of cells after incubation with vaccine diluent (medium with 1% HSA) as control. For **A**–**L**, difference from pre-vaccine was assessed by Wilcoxon signed rank test. *P*-values were corrected for multiple comparisons by the Bonferroni method. * $P < 0.05$, ** $P < 0.01$, *** $P < 0.001$. For **A**–**E**, data are geometric mean ± 95% c.i. For **G**–**M**, data are mean ± s.e.m.

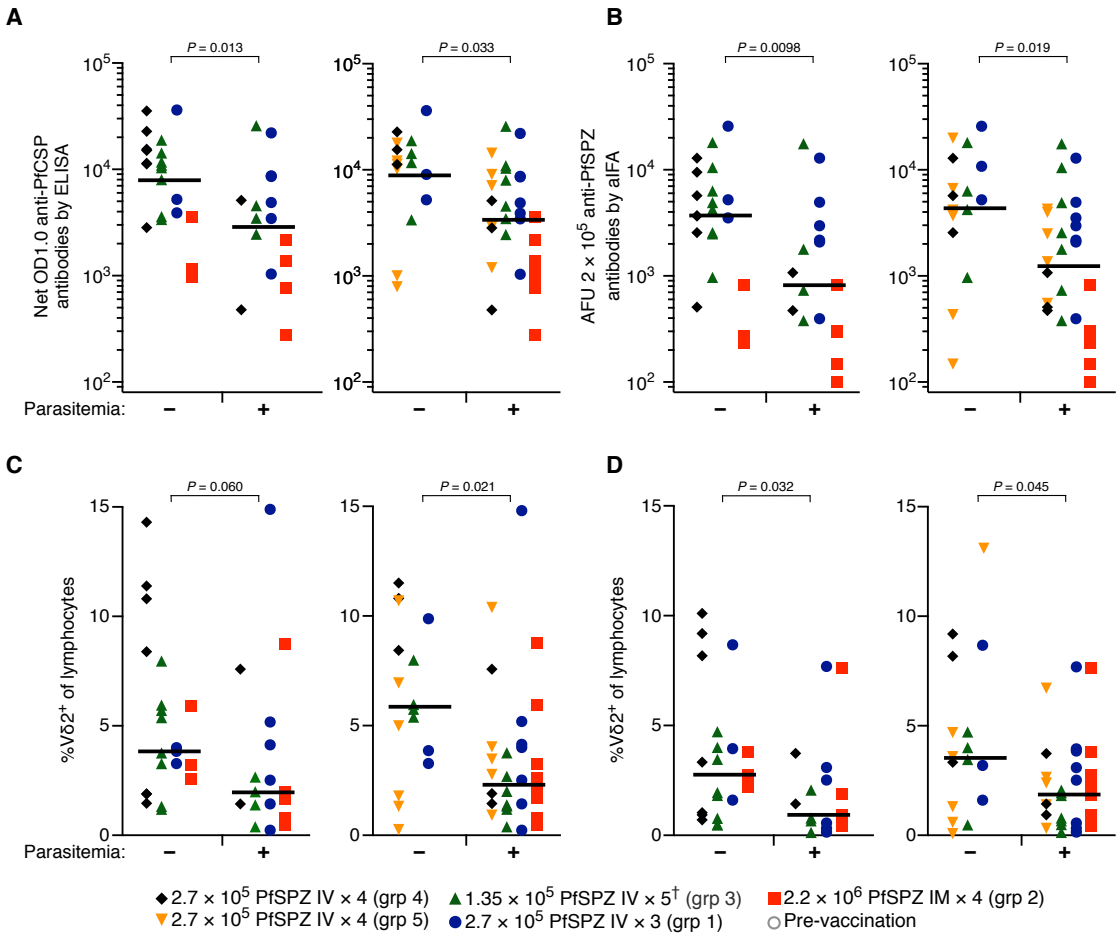


Figure 4.5: (**A**) Antibodies to PfCSP by ELISA (net OD1.0) 2 weeks after final immunization in subjects who did (+) and did not (–) develop parasitemia at 3 (left) and 21–25 (right) week CHMIs. Since we expected subjects who were parasitemic at 3 weeks to again be parasitemic at 21–25 weeks, the immune data from individuals who were parasitemic at 3 weeks were included in the 21–25 week analysis. (**B**) Antibodies to PfSPZ by aIFA (AFU 2×10^5) 2 weeks after final immunization in subjects who did (+) and did not (–) develop parasitemia at 3 (left) and 21–25 (right) week CHMIs. Subject inclusion was the same as in **A** above. (**C**) Frequency of V$\delta 2^+$ T cell subset 2 weeks after final immunization in subjects who did (+) and did not (–) develop parasitemia at 3 (left) and 21–25 (right) week CHMIs. Subject inclusion was the same as in **A** above. (**D**) Frequency of V$\delta 2^+$ T cell subset pre-immunization in subjects who did (+) and did not (–) develop parasitemia at 3 (left) and 21–25 (right) week CHMIs. Subject inclusion was the same as in **A** above. For **A**–**D**, statistical significance for all correlations was determined by stratified Wilcoxon test with vaccine regimen as co-variate. Bar denotes geometric mean (**A**–**B**) or median (**C**–**D**). †Group 3 received four doses of 1.35×10^5 PfSPZ and a fifth dose of 4.5×10^5 PfSPZ.

Antibody correlates

PfCSP and PfSPZ antibody responses correlated with outcome when CHMI occurred 3 weeks after final immunization (**Fig. 4.5A,B**). They also correlated with outcome after CHMI at 21–25 weeks (**Fig. 4.5A,B**). For this analysis, I assumed that subjects who developed parasitemia after the 3 week CHMI would also develop parasitemia after the 21–25 week CHMI, which is based on earlier findings [142].

Cellular correlates

The magnitude of Pf-specific CD4 and CD8 T cells in the blood did not correlate with outcome at the 3 or 21–25 week CHMIs (data not shown). However, the absolute frequency of unstimulated V$\delta 2^+$ T cells as a percentage of total lymphocytes correlated with outcome at the 21–25 week CHMI (**Fig. 4.5C**). Interestingly, the frequency of the V$\delta 2^+$ T cell subset measured before the first vaccination also correlated with outcome at the 3 and 21–25 week CHMIs (**Fig. 4.5D**).

4.2.5 Role of PfSPZ antibodies in protection

Pf-specific antibody levels over time

The finding that PfCSP- and PfSPZ-specific antibody levels 2 weeks after final immunization correlated with outcome of the 3 and 21–25 week CHMIs suggested that antibodies were a biomarker of a successful vaccine response; however, antibodies could also have a functional role in mediating protection by preventing PfSPZ from infecting hepatocytes [199, 200]. To investigate whether antibodies played a role in protection, I first measured the magnitude of antibodies at the time of the 21–25 and 59 week CHMIs. At 59 weeks, PfCSP antibody responses in the five subjects who did not develop parasitemia were 8.0-fold lower (PfCSP geometric mean (GM) = 1640) than the responses among subjects who did not develop parasitemia at 3 weeks (PfCSP GM = 13,200; $P = 0.0051$; **Fig. 4.6A**). Of note, the magnitude of the PfCSP antibody responses in the 5 subjects at 59 weeks (PfCSP GM = 1,640) was no different than antibody responses in subjects immunized with the same regimen who developed parasitemia at CHMI at 21–24

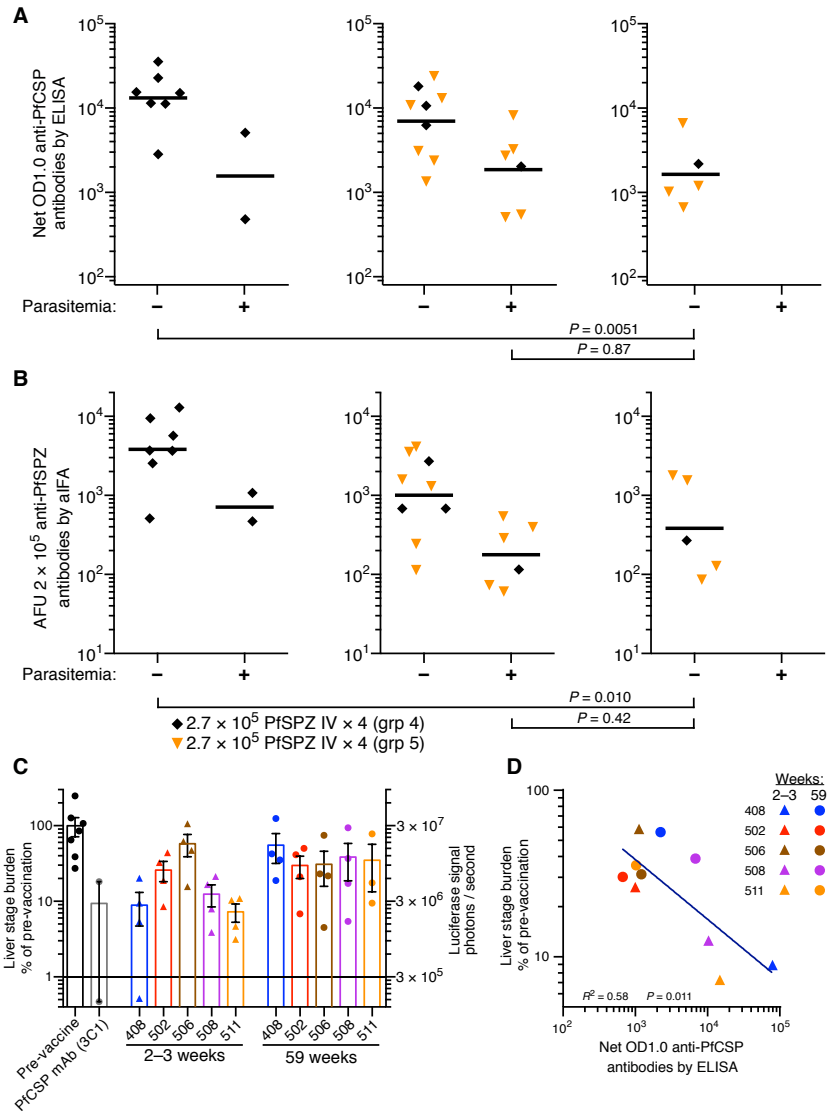


Figure 4.6: (**A**) Antibodies to PfCSP by ELISA (net OD1.0) measured at the time of each CHMI in subjects who received 4 doses of 2.7×10^5 PfSPZ IV and subsequently did (+) or did not (–) develop parasitemia at 3 (left), 21–24 (middle), or 59 (right) week CHMIs. (**B**) Antibodies to PfSPZ by aIFA (AFU = 2×10^5) measured at the time of each CHMI in subjects who received 4 doses of 2.7×10^5 PfSPZ IV and subsequently did (+) or did not (–) develop parasitemia at 3 (left), 21–24 (middle), or 59 (right) week CHMIs. For **A**–**B**, comparison between groups was assessed by Mann-Whitney U test. Bar denotes geometric mean. (**C**) Effect of passive transfer of purified IgG on liver stage burden assessed by IVIS. Right y-axis shows the raw luciferase signal. Left y-axis shows percent signal in mice that received the IgG from each of the 5 subjects at each of the two time points as compared to the signal in the mice that received pre-vaccination IgG, which was set to be 100%. (**D**) Correlation between PfCSP antibodies (net OD1.0) and liver-stage burden in the FRG-huHep mice.

weeks (PfCSP GM = 1,860; $P = 0.87$; **Fig. 4.6A**). These comparisons were extended to antibody responses against whole PfSPZ (**Fig. 4.6B**), revealing a similar decline in PfSPZ-specific antibodies over time.

Functional assessment of Pf-specific antibodies

To assess the *in vivo* functional activity of Pf-specific antibodies from subjects following immunization, immune deficient mice reconstituted with human hepatocytes (FRG-huHep mice) capable of supporting the liver stage development of Pf were used [185]. Total IgG from the 5 vaccine recipients that did not develop parasitemia following CHMI at 59 weeks was purified from plasma and serum obtained before vaccination, 2–3 weeks after the final vaccination, and on the day of the 59 week CHMI. The IgG was passively transferred to FRG-huHep mice, and they were challenged by exposure to 50 mosquitoes infected with luciferase-expressing PfSPZ. Liver stage burden was quantified by whole animal imaging. The negative control was pooled IgG from the 5 protected subjects before vaccination. Passive transfer of the positive control, 150 μg of the anti-PfCSP monoclonal antibody 3C1, reduced liver stage burden as compared to the negative control by 90%. Purified IgG from the 5 vaccinated subjects taken 3 weeks after vaccination significantly reduced liver stage burden by 88% (median), and IgG from 59 weeks after final immunization reduced liver stage burden by 65% (median) (**Fig. 4.6C**). There was higher inhibitory activity in IgG from 4/5 subjects at 2–3 weeks compared to 59 weeks. However, with this limited sample size, there was no significant difference in the reduction of liver stage burden by IgG collected at the 2–3 week and 59 week time points ($P > 0.05$ by Wilcoxon signed rank test); liver stage burden did correlate inversely with PfCSP antibody level (**Fig. 4.6D**).

4.2.6 PfSPZ-specific T cell activation after CHMI is dependent on timing of CHMI

To provide additional data into the potential mechanisms of protection, I assessed how CHMI affected PfSPZ-specific T cell responses over the course of 1 year. For this analysis, the expression of Ki-67 (a marker used to detect lymphocyte cell division

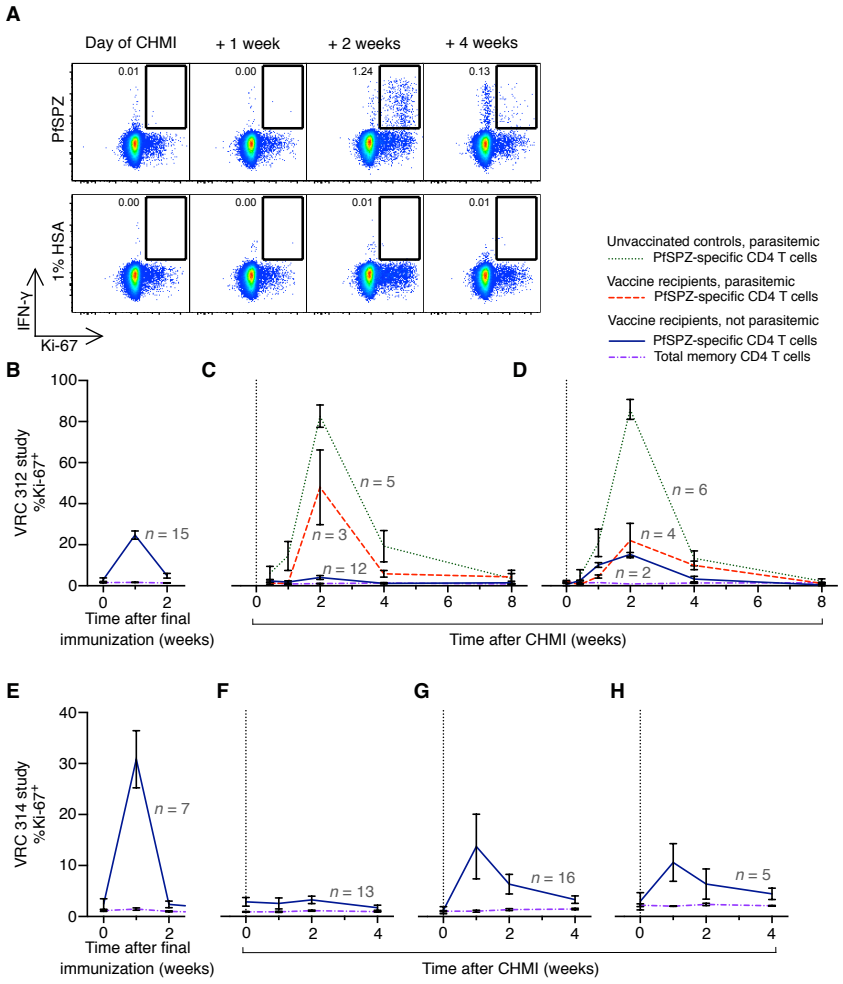


Figure 4.7: PBMCs acquired before and after the final vaccination and each CHMI from vaccinated subjects and unvaccinated controls in VRC 312 and VRC 314 were incubated with PfSPZ or vaccine diluent (1% HSA) and assessed by flow cytometry. (**A**) Gating example showing memory CD4 T cells at 0, 1, 2, and 4 weeks following CHMI in an unvaccinated control who developed parasitemia. PfSPZ-specific cells are identified by expression of IFN-γ following PfSPZ stimulation, and dividing cells are identified by Ki-67. (**B**) Frequency of cells expressing Ki-67 as a percentage of total memory CD4 T cells or PfSPZ-specific CD4 T cells in all vaccine recipients on the day of vaccination, and 1 and 2 weeks after vaccination. (**C**–**D**) Frequency of cells expressing Ki-67 in vaccine recipients who did or did not develop parasitemia following CHMI at 3 (**C**) and 21 (**D**) weeks after final vaccination. Unvaccinated controls are also shown. (**E**) Frequency of cells expressing Ki-67 in vaccine recipients on the day of vaccination, and 1 and 2 weeks after vaccination. (**F**–**H**) Frequency of cells expressing Ki-67 in IV-vaccinated subjects that remained without parasitemia following CHMI at 3 (**B**, 21–25 (**C**), and 59 (**D**) weeks after final vaccination. For **B**–**H**, PfSPZ-specific cells are identified by any combination of IFN-γ, IL-2, or TNF-α. Data are mean ± s.e.m. Gray numbers on graph denote number of subjects in each group.

[205]) in PBMCs (**Fig. 4.7A**) was used to assess response to PfSPZ exposure *in vivo* following vaccination and CHMI. One week after final immunization in the VRC 312 (**Fig. 4.7B**) [12] and VRC 314 (**Fig. 4.7E**) clinical trials, 20–30% of PfSPZ-specific CD4 T cells were Ki-67$^+$, demonstrating that vaccination induced T cell activation. Ki-67 was only detected in PfSPZ-specific CD4 T cells, not in total memory CD4 T cells (**Fig. 4.7B–H**), providing evidence for PfSPZ-specificity. One to 2 weeks following the 3 week CHMI, Ki-67 was detected in 40–60% of PfSPZ-specific CD4 T cells from parasitemic subjects (both vaccinated and unvaccinated subjects), showing that malaria infection was associated with activation of a high proportion of PfSPZ-specific CD4 T cells (**Fig. 4.7C,D**); in contrast, there were low to undetectable Ki-67$^+$ PfSPZ-specific CD4 T cells in PBMCs from the 25 subjects who did not develop parasitemia from VRC 312 ($n = 12$; **Fig. 4.7C**) and VRC 314 ($n = 13$; **Fig. 4.7F**) studies. Strikingly, 1–2 weeks after the 21–25 and 59 week CHMIs, 10–20% of PfSPZ-specific CD4 T cells from subjects who did not develop parasitemia were Ki-67$^+$ (**Fig. 4.7D,G,H**), compared to 0–1% on the day of the CHMI. These data suggest that there was differential antigen exposure *in vivo* when CHMI was done at 3 weeks compared to 21–25 or 59 weeks among subjects who remained without parasitemia. While these data demonstrate PfSPZ-specific CD4 T cell activation *in vivo*, the magnitude of Pf-specific CD4 or CD8 T cells in blood did not change after CHMI at any time in protected subjects, nor did PfCSP-specific antibody levels (data not shown).

4.2.7 Longitudinal T cell responses

The low level of Pf-specific antibody at 59 weeks when all 5 vaccinated subjects were not parasitemic after CHMI (**Fig. 4.8A,B**) strongly suggest that protection is not mediated by antibodies at this memory time point. Therefore, I assessed PfSPZ-specific T cell responses in blood through the course of vaccination and following CHMIs over the course of 1 year to determine their potential role in mediating protection.

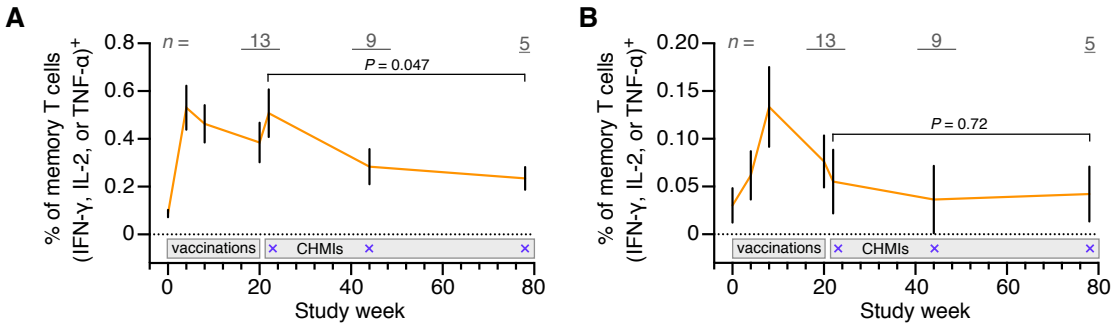


Figure 4.8: (**A**–**B**) Longitudinal assessment of PfSPZ-specific CD4 T cell responses (**A**) and PfRBC-specific CD8 T cell responses (**B**) in subjects who received 4 doses of 2.7×10^5 PfSPZ IV and did not develop parasitemia at the 3, 21–24 and 59 week CHMIs. Data are mean ± s.e.m. *P*-values are for comparisons between immune responses at 2 and 59 weeks after the final immunization by Mann-Whitney U test.

In PBMCs, CD4 T cell responses declined significantly over the course of 59 weeks in vaccinated subjects who remained without parasitemia (**Fig. 4.8A**), and CD8 T cell responses appeared during the vaccination series but returned to pre-vaccine levels shortly after final vaccination (**Fig. 4.8B**). Thus, Pf-specific T cells in the blood were also scarce in the 5 vaccinated subjects that were not parasitemic after CHMI at 59 weeks. Moreover, because Pf-specific T cell responses in PBMCs after final immunization were similar in subjects immunized IV and IM (**Fig. 4.3C,D**) despite the differences in short- and long-term VE, I hypothesized that the T cells resident in the liver played a critical role in protection.

4.2.8 Tissue-resident T cell responses in NHP.

As liver-resident cellular immunity could not be directly assessed in the human subjects, I assessed these responses in the blood and liver of NHPs following immunization with PfSPZ Vaccine using multi-parameter flow cytometry. Immunogenicity studies with PfSPZ Vaccine in NHP had already provided critical immune data that guided successful translation to humans. As Epstein *et al.* had previously shown that 1.35×10^5 PfSPZ administered SC did not induce detectable T cell responses in the blood or liver of NHPs, I administered 10-fold more PfSPZ in each of five doses administered by the IM or ID routes and compared the T cell responses to five IV doses of 1.35×10^5 PfSPZ and four IV doses of 2.7×10^5 PfSPZ (**Fig.**

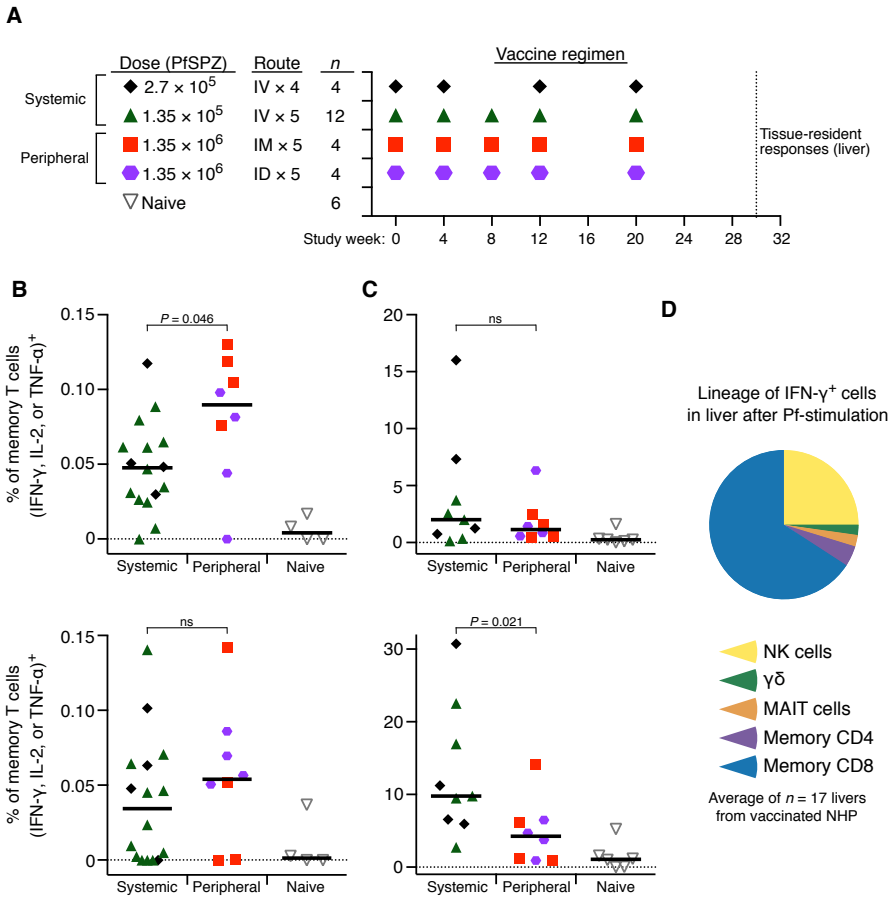


Figure 4.9: (**A**) NHP study outline. PfSPZ dose, route, number of injections, number of NHPs per group, and vaccine regimen. (**B**) PfSPZ-specific CD4 (top) and PfRBC-specific CD8 (bottom) T cell responses in PBMCs of NHPs 2 weeks after final vaccination. (**C**) PfSPZ-specific CD4 (top) and PfRBC-specific CD8 (bottom) T cell responses in livers of NHPs 10 weeks after final vaccination. (**D**) In vaccinated NHP, **D** shows the lineage of liver-resident lymphocytes expressing IFN-γ following stimulation with PfRBC. For **B**,**C**, bar denotes median, and between group comparisons were determined by Mann-Whitney U test. For **D**, the pie chart shows the arithmetic mean of the subset percentages. ns, not significant ($P > 0.05$).

4.9A), similar to the vaccination regimens in the human study. PfSPZ-specific CD4 T cell responses in PBMCs were modestly higher in NHPs vaccinated by the peripheral (IM/ID) routes as compared to the systemic (IV) route ($P = 0.046$), and there were no differences in PfRBC-specific CD8 T cell responses (**Fig. 4.9B**). In contrast, IV immunization induced 2-fold higher frequencies of PfRBC-specific CD8 T cells in the liver compared to peripheral (IM/ID) immunization, which used 6–10 fold higher total dose of PfSPZ (**Fig. 4.9C**). This indicates that the T cell responses in blood are not necessarily indicative of the liver-resident T cell responses.

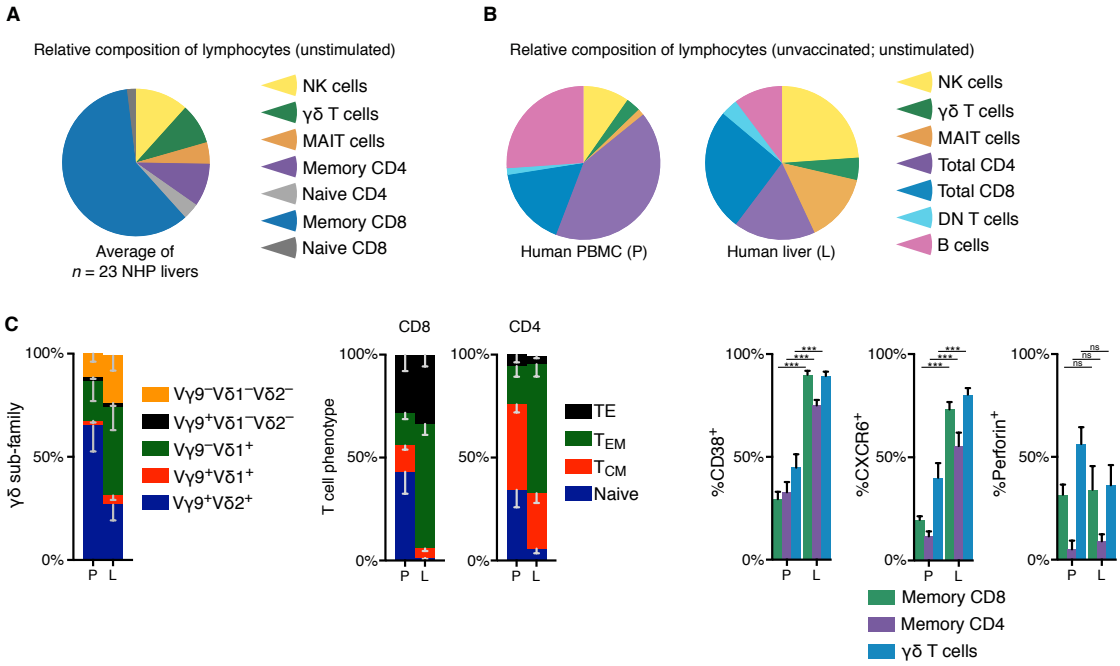


Figure 4.10: (**A**) Average relative proportions of lymphocyte populations (NK cells, $\gamma\delta$, MAIT, naive and memory CD4 and CD8 T cells) are shown for 23 rhesus livers. (**B**–**E**) Human PBMC ($n = 7$) and human intrahepatic mononuclear cells (liver; $n = 5$) were stained in parallel with the panels listed in Chapter 2. (**B**) Major lymphocyte subsets found in PBMC (P) and liver (L). DN = $CD3^{+}$TCR-$\gamma\delta^{-}$(MAIT marker)$^{-}CD4^{-}CD8^{-}$. (**C**) Proportions of $\gamma\delta$ sub-families in PBMC and liver. (**D**) Memory phenotype of total CD8 (left) and CD4 (right) T cells in PBMC and liver. (**E**) Expression of CD38, CXCR6, and perforin by memory CD8, CD4, and $\gamma\delta$ T cells in PBMC and liver. For **C**–**E**, data are mean ± s.e.m. For **E**, comparisons between PBMC and liver was by two-way ANOVA with Bonferroni correction. ns, not significant ($P > 0.05$); *** $P < 0.001$.

Importantly, the frequency of PfRBC-specific CD8 T cell responses in the liver were 100-fold higher than in PBMCs. Moreover, while multiple populations of IFN-γ-producing lymphocytes including NK, $\gamma\delta$, and CD4 T cells were identified in the liver of NHP, the majority (about 60%) were CD8 T cells (**Fig. 4.9D**).

Lymphocyte composition in human liver

The composition and differentiation state (*i.e.*, memory phenotype) of lymphocytes in NHP liver resembled that of unvaccinated human liver samples, underscoring the biological relevance of the NHP model (**Fig. 4.10**).

4.3 Discussion

4.3.1 Vaccine efficacy

The efficacy and T cell activation data presented herein show that PfSPZ Vaccine conferred approximately 55% sterilizing immunity through 59 weeks after four intravenous doses of 2.7×10^5 PfSPZ. This is the first clinical trial of a malaria vaccine in which the first CHMI in one of the vaccine groups was done more than four weeks after final immunization, representing a shift beyond a search for short-term protection towards trials that focus on dose and regimen optimization for durable sterilizing protection. The improvement in *cumulative* VE from an estimated 25% at 21 weeks after 4 or 5 doses of 1.35×10^5 PfSPZ to an estimated 55% at 21–24 and 59 weeks after 4 doses of 2.7×10^5 PfSPZ, suggests that additional increases in dose of PfSPZ Vaccine will further increase the magnitude and durability of protective efficacy.

The estimated VE of 3 doses of 2.7×10^5 PfSPZ against CHMI at 3 weeks was only 24%. The total PfSPZ Vaccine dosage (8.1×10^5 PfSPZ) was higher than the previously reported 5-dose regimen of 1.35×10^5 PfSPZ (total dose of 6.75×10^5 PfSPZ) that gave an estimated 100% VE against CHMI at 3 weeks [12]. These findings indicate that the total number of vaccinations is a key factor in induction of protective immunity, rather than simply the total dosage of PfSPZ Vaccine. Therefore, if fewer than 4 immunizations of PfSPZ Vaccine are used, higher doses per immunization and an alternative schedule will be required for long-lived immunity. Ongoing studies using 4.5×10^5 to 2.7×10^6 PfSPZ per dose will determine this directly.

4.3.2 Immunogenicity

The direct comparison of IM and IV administration of PfSPZ Vaccine addressed how systemic (IV) rather than peripheral (IM/ID) administration influenced immunogenicity and VE. Infectivity studies in mice show that >90% of SPZ administered IM/ID fail to reach the liver, and the parasite antigens are limited

to muscle- or skin-draining lymph nodes. Here, PfSPZ Vaccine administered by the IM route at an 8.1-fold higher dose compared to IV administration resulted in limited short-term and no durable protection. However, the frequency of circulating PfSPZ-specific CD4 T cells was not different when comparing IM and IV vaccinated subjects after the final immunization, and the levels of circulating CD8 T cells were uniformly low. In contrast, tissue-resident Pf-specific CD8 T cell responses in the liver of PfSPZ-vaccinated NHP were found to be highest after IV administration despite using 6–10 fold higher doses with the IM/ID routes. I hypothesized that this is because IV administration results in the efficient delivery of attenuated PfSPZ to the liver, where they mediate priming of T cells that remain as non-recirculating, liver-resident cells capable of efficient surveillance and rapid elimination of infected hepatocytes after CHMI. Importantly, the total level of PfSPZ-specific T cells in the blood predicted neither efficacy nor tissue-resident responses. Thus, for protective immunity mediated by direct T cell contact in infected tissues, vaccine development efforts may be misled by simply maximizing T cell responses in the blood without considering how the vaccination strategy affects T cell responses at the infection site.

4.3.3 Correlates of sterile protection

An unexpected finding was that the pre-vaccination frequency of circulating V$\delta 2^+$ T cells correlated with outcome of CHMI. V$\delta 2^+$ T cells recognize intracellular lipid metabolites (*i.e.*, HMBPP) from *Plasmodium*. Thus, it is possible that these cells play a role in the initial priming of adaptive immune responses through rapid Pf recognition and IFN-γ production at the time of immunization leading to enhanced CD8 T cell priming or by serving as antigen presenting cells. $\gamma\delta$ T cells can facilitate priming of protective immune responses against blood stage malaria by providing help to dendritic cells. In addition, a high frequency of circulating $\gamma\delta$ T cells express CXCR6, a chemokine receptor that facilitates surveillance of the liver sinusoids, and produce IFN-γ and perforin, two potent effector molecules shown to mediate killing of intracellular Pf. Given the importance of lipid metabolism to intrahepatic malaria, it is also possible V$\delta 2^+$ T cells mediate direct effector functions in the liver. Indeed, $\gamma\delta$

T cells have been shown to contribute to protection against pre-erythrocytic malaria in mouse models and are readily induced following whole sporozoite immunization. The correlation between $\gamma\delta$ T cell frequency and CHMI outcome described herein suggests that live-attenuated whole PfSPZ induces protective immunity through the recruitment of diverse and rarely considered T cell subsets, which may not occur after immunization with the most commonly used subunit vaccine approaches.

4.3.4 Mechanism of protection

To improve understanding of the immune mechanisms of protection, I studied antibody and cellular immune responses longitudinally in humans, cellular immune responses in NHP PBMCs and livers, and the *in vivo* function of antibodies from immunized subjects in humanized FRG-huHep mice. Based on the decrease in the magnitude (**Fig. 4.6A,B**) of PfSPZ antibodies over time, associated with an increase in Ki-67 expression in PfSPZ-specific CD4 T cells after CHMI at 21–25 (**Fig. 4.7D,G**) and 59 weeks (**Fig. 4.7H**), I hypothesize the following role for antibodies: at the time of early CHMIs (3 weeks), antibodies reduce the numbers of PfSPZ that successfully invaded hepatocytes, and this allowed for rapid elimination of the remaining parasites in the liver by cellular responses, and thus, low Ki-67 expression by PfSPZ-specific CD4 T cells of protected subjects (**Fig. 4.7C,F**). At the time of the later CHMIs (21–25 and 59 weeks), antibodies were lower (**Fig. 4.6A,B**), resulting in more parasites reaching the liver after CHMI, and thus, greater activation (Ki-67 expression) of PfSPZ-specific CD4 T cells during liver stage parasite clearance (**Fig. 4.7D,G,H**). These data, along with the findings that: (1) circulating Pf-specific T cell responses are low at 59 weeks in all subjects that are not parasitemic after CHMI (**Fig. 4.8A,B**), (2) there was no differences in the magnitude (**Fig. 4.3C,D**) or quality of the Pf-specific T cell responses in blood between IM vs. IV vaccinated subjects but no durable protection in the IM group, and (3) there were strikingly high numbers of Pf-specific CD8 T cells in the livers of IV-immunized NHPs (about 100-fold higher than in the PBMC; **Fig. 4.9D,E**), support the conclusion that - while antibodies can contribute to

protection early after final immunization - tissue-resident CD8 T cells are likely necessary for durable sterile protection.

4.3.5 Study limitations and future directions

These results underscore the importance of PfSPZ administration by the IV route in achieving protection with this vaccine. Completed studies in Mali, Tanzania, and Equatorial Guinea demonstrated the feasibility of routine direct venous inoculation (DVI) of PfSPZ Vaccine to adults in Africa, and field studies in Africa have begun to address DVI administration in young children and infants.

PfSPZ Vaccine conferred an estimated 55% sterile protective efficacy for 59 weeks, likely through the induction of long-lived tissue-resident T cells. I hypothesize that increases in the vaccine dose will further improve vaccine efficacy.

5

Immunogenicity and efficacy against heterologous PfSPZ

Contents

5.1 Introduction 98
5.1.1 Study aims 99
5.1.2 Authorship 100
5.1.3 Summary of findings 100
5.2 Results 100
5.2.1 Study population 100
5.2.2 Vaccine efficacy, homologous CHMI 100
5.2.3 Vaccine efficacy, heterologous CHMI 101
5.2.4 Antibody responses 102
5.2.5 CD8 and CD4 T cell responses 103
5.2.6 $\gamma\delta$ T cell responses 104
5.2.7 T cell responses against 7G8 106
5.3 Discussion 107
5.3.1 Efficacy 107
5.3.2 Immunogenicity 109
5.3.3 Study limitations and future directions 110

5.1 Introduction

In the previous chapter, PfSPZ Vaccine was shown to confer sterile protection against homologous CHMI for up to 14 months after final vaccination. No injectable

malaria vaccine has demonstrated high-level, long-term sterile protection against CHMI using Pf parasites heterologous to the vaccine strain.

Attenuated PfSPZ immunization consistently achieves high-level (>80%) sterile protection against CHMI with homologous Pf parasites [12, 142, 138, 143]. In addition, short-term protection against a heterologous CHMI has been demonstrated in a small number of subjects following irradiated PfSPZ immunization by mosquito bite [138]. In subjects who were previously protected against homologous CHMI following chloroquine prophylaxis administered with sporozoite (CPS) immunization by mosquito bite, protection was observed in 2/13 subjects overall and 1/2 in the highest dose group against CHMI with a heterologous CHMI strain 14 months post-vaccination [148]. High-level durable sterile protection against heterologous CHMI has not been achieved with any injectable malaria vaccine.

Based on the favorable safety profile and dose-dependent durable efficacy against homologous CHMI [12, 142], PfSPZ Vaccine dose escalation was continued to 9.0×10^5 PfSPZ per dose. A 3-dose regimen at 8-week intervals was selected based on data showing that an 8-week interval between immunizations resulted in enhanced immunogenicity in non-human primates (NHPs) [141]. Additionally, a clinical study showed that 4.5×10^5 PfSPZ given three times at 8-week intervals conferred 50% protection against homologous CHMI 24 weeks after vaccination, but minimal durable protection against heterologous CHMI (Epstein J, *et al.* In review).

5.1.1 Study aims

In this study, I sought to:

1 Assess the cellular immune activation in humans vaccinated three times with 9.0×10^5 PfSPZ IV

2 Determine the cross-reactivity of T cells between the vaccinating and heterologous CHMI strains

5.1.2 Authorship

The clinical study was designed by R.A.S., K.E.L., S.L.H., J.E.L., and myself, and conducted by the clinical team led by K.E.L. I designed the T cell immunological studies with R.A.S. I conducted the studies with technical assistance from B.F. The antibody assays were run by S.C. I performed all immunological analyses and statistical comparisons. S.L.H. and B.K.L.S. and their team at Sanaria provided aseptic NF54 and 7G8 PfSPZ.

5.1.3 Summary of findings

1 CD8 and CD4 T cell responses peak after the first immunization with minimal boosting despite subsequent immunizations.

2 PfSPZ Vaccine induces strain-transcending CD8, CD4, and $\gamma\delta$ T cells.

5.2 Results

5.2.1 Study population

Thirty-one volunteers were enrolled between December 2014 and February 2016: 15 vaccine recipients, 12 CHMI controls, and four back-up controls. Fifteen volunteers (100%) completed all three scheduled vaccinations. Fourteen volunteers underwent CHMI with homologous Pf parasites; one vaccine recipient withdrew prior to CHMI to attend medical school.

5.2.2 Vaccine efficacy, homologous CHMI

Vaccine efficacy was first assessed by CHMI with the Pf clone 3D7 by mosquito bite 19 weeks after final immunization. The vaccine is composed of the NF54 strain, which is likely of African origin [206]. 3D7 is a clone from the NF54 strain and thus homologous to the vaccine [207]. 3D7 has been used to evaluate efficacy in the majority of malaria vaccine trials using CHMI [12, 102, 104, 103, 130, 138, 146]. Nine of 14 vaccine recipients (64%; 95% CI: 35–87%) and none of the six non-vaccinated controls remained without parasitemia following homologous CHMI (P

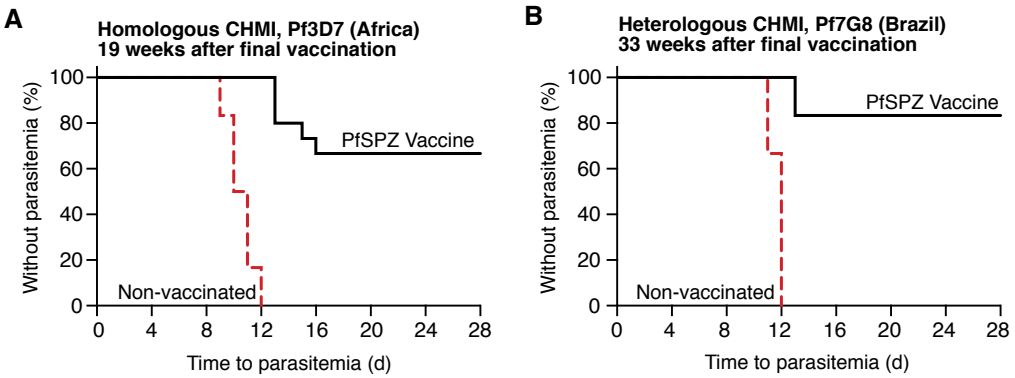


Figure 5.1: Kaplan-Meier curves showing the percent of volunteers remaining without parasitemia after CHMI with homologous Pf3D7 (**A**) or heterologous Pf7G8 (**B**). Six non-vaccinated controls were enrolled for each CHMI. In **A**, 9/14 (64%) vaccinated volunteers (black, solid line) and 0/6 non-vaccinated controls (red, dashed line) remained without parasitemia. In **B**, 5/6 (83%) vaccinated volunteers (black, solid line) and 0/6 non-vaccinated controls (red, dashed line) remained without parasitemia. Only vaccinated volunteers who remained without parasitemia after CHMI with the homologous strain, Pf3D7, underwent repeat CHMI with the heterologous strain, Pf7G8.

= 0.012) (**Fig. 5.1A**). In the five vaccinated volunteers who became parasitemic, the time to first positive malaria PCR ranged from 13–15 days compared to 8–11 days for the controls ($P < 0.0001$, controls vs. all vaccine recipients by log-rank).

5.2.3 Vaccine efficacy, heterologous CHMI

To assess the durability of the vaccine against heterologous CHMI, six of the nine vaccinated subjects who were not parasitemic after homologous CHMI underwent CHMI by the bite of mosquitoes infected with 7G8, a clone of Brazilian origin [208] approximately 33 weeks after final vaccination. As the heterologous CHMI was added as a protocol amendment after screening/enrollment, only six of nine eligible subjects were able to participate. The remaining three subjects were not able to undergo heterologous CHMI due to scheduling conflicts. The six subjects who underwent heterologous CHMI were not selected on the basis of any immunologic or other criteria. Sequential CHMIs are commonly used to assess the durability of vaccine efficacy [130, 145, 148, 142, 103]. Five of six vaccine recipients (83%; 95% CI: 36–99%) and none of the six non-vaccinated controls remained without parasitemia after heterologous CHMI (**Fig. 5.1B**).

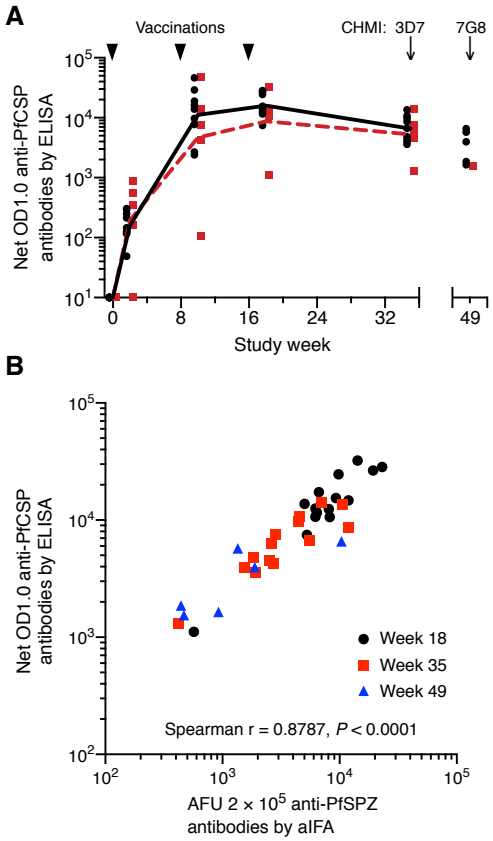


Figure 5.2: (**A**) Antibody responses to PfCSP by ELISA two weeks after each vaccination and at the time of homologous (3D7) and heterologous (7G8) CHMI. Subjects who were parasitemic (red, dashed line and red squares) or not parasitemic (black, solid line and black circles) are shown. Line is geometric mean. For weeks 0–35, data is stratified by outcome after homologous CHMI at study week 35. Data at week 49 is stratified by outcome after heterologous CHMI at study week 49. Individual points represent one subject. Arrowhead designates PfSPZ Vaccine administration, arrows designates time of CHMI with 3D7 or 7G8. (**B**) Antibody responses by automated immunofluorescence assay (aIFA) on whole PfSPZ (NF54). The comparison with PfCSP ELISA responses is shown for three time points. Spearman r was calculated using data from the three time points combined: $n = 15$ for study week 18 (two weeks after final vaccination; black circles), $n = 14$ for study week 35 (time of homologous CHMI; red squares), $n = 6$ for study week 49 (time of heterologous CHMI; blue triangles).

5.2.4 Antibody responses

I previously showed that antibody responses against PfCSP following immunization with PfSPZ Vaccine administered at lower doses have functional activity and may be a potential immune correlate of protection (**Chapter 4**). After the first vaccination, low-level PfCSP antibody responses were detected in 13/14 subjects (**Fig. 5.2A**; geometric mean (GM): 213.5). Such responses were substantially

boosted 40-fold after the second vaccination (14/14 subjects with PfCSP responses, GM: 9,336) with modest boosting after the third vaccination (GM: 13,066). There was a trend towards higher antibody responses among subjects who remained without parasitemia following homologous CHMI (GM 15,858 (not parasitemic) vs. 8,717 (parasitemic)). This comparison did not reach the threshold for statistical significance ($P = 0.23$) with this small sample size (9 not parasitemic vs. 5 parasitemic). Antibody responses were also assessed against whole PfSPZ measured by immunofluorescence assay (IFA) after the final vaccination and at the time of each CHMI. PfSPZ antibody responses were highly concordant with PfCSP antibody levels (Spearman r = 0.8787; $P < 0.0001$; **Fig. 5.2B**). These data showed that at doses of 9.0×10^5 PfSPZ, malaria specific antibody responses were induced in all subjects and did not easily discriminate between protected and unprotected subjects.

5.2.5 CD8 and CD4 T cell responses

T cell responses, primarily CD8 T cells, are critical for mediating protection following whole SPZ vaccination in mice and NHPs [202, 209, 201]. Here, following PfSPZ vaccination the frequency of PfSPZ-specific cytokine (IFN-γ, IL-2, or TNF-α) producing memory CD8 T cell responses peaked after the first immunization (0.38 $\pm$ 0.12%; mean $\pm$ standard error of the mean (SEM); $P = 0.002$ compared to pre-vaccine; **Fig. 5.3A**) as assessed by ICS following *in vitro* stimulation with PfSPZ. Of note, IFN-γ^+ CD8 T cell responses declined markedly after the second immunization, and were not different from pre-vaccine (background) levels two weeks after the third immunization ($P = 0.12$). The frequency of cytokine-producing PfSPZ-specific memory CD4 T cells was higher than CD8 T cell responses and also peaked after the first immunization (1.55 $\pm$ 0.38%; mean $\pm$ SEM; **Fig. 5.3B**). Such responses declined to 0.59 $\pm$ 0.08% and 0.51 $\pm$ 0.07% after the second and third immunizations, respectively. CD8 T cell responses were detected in 11/14 volunteers, and CD4 T cell responses were detected in 14/14 volunteers. The magnitude of the total PfSPZ-specific memory T cell cytokine responses did not significantly

differ among vaccinated subjects who did or did not develop parasitemia following homologous CHMI at the assessed time points.

Analysis of activation markers HLA-DR and CD38 on T cells without *ex vivo* antigen stimulation has been used as a sensitive measure of T cell activation in vivo following immunization (**Fig. 5.3C**) [210, 211]. The frequency of HLA-DR$^+$CD38$^+$ memory CD4 T cells increased by 1.69 ± 0.42 percentage points (mean ± SEM; $P < 0.001$; **Fig. 5.3D**) two weeks after first immunization compared to baseline (pre-vaccine). The mean increase was similar to the level of memory CD4 T cells that were determined to be PfSPZ-specific by the ICS assay (**Fig. 5.2B**) (*i.e.*, 1.55%), and individual responses were highly correlated (Spearman r = 0.8462; $P = 0.0003$; **Fig. 5.3E**), suggesting that the ICS assay used to assess the frequency of PfSPZ-specific T cell responses following *in vitro* stimulation with PfSPZ accurately reflects the absolute magnitude of *in vivo* CD4 T cell activation by PfSPZ vaccination. Interestingly, while circulating PfSPZ-specific CD4 T cells were detected at >0.5% by *in vitro* PfSPZ stimulation after the second and third vaccination, the frequency of HLA-DR$^+$CD38$^+$ memory CD4 T cells two weeks after second and third immunizations were only 0.17 ± 0.15 percentage points (mean ± SEM) and 0.25 ± 0.18 percentage points, respectively, above the pre-vaccination frequencies. This indicates a dramatic reduction in *in vivo* activation of circulating PfSPZ-specific CD4 T cells compared to the first vaccination.

5.2.6 $\gamma\delta$ T cell responses

Prior studies have shown that $\gamma\delta$ T cells expand after immunization with PfSPZ Vaccine [12, 142], and I showed that the frequency of the Vδ2$^+$ sub-family of $\gamma\delta$ T cells is a potential immune correlate of protection (**Chapter 4**). Here, I extend these findings and show that $\gamma\delta$ T cells have a high level of *in vivo* activation after vaccination as measured by HLA-DR$^+$CD38$^+$ co-expression (**Fig. 5.4A**). Activation peaked at a mean of 34% (compared to 6.4% at pre-vaccination) two weeks after second immunization (**Fig. 5.4B**). The frequency of circulating Vδ2$^+$ T cells increased after each vaccination (**Fig. 5.4C**). The frequency was 2.8-fold

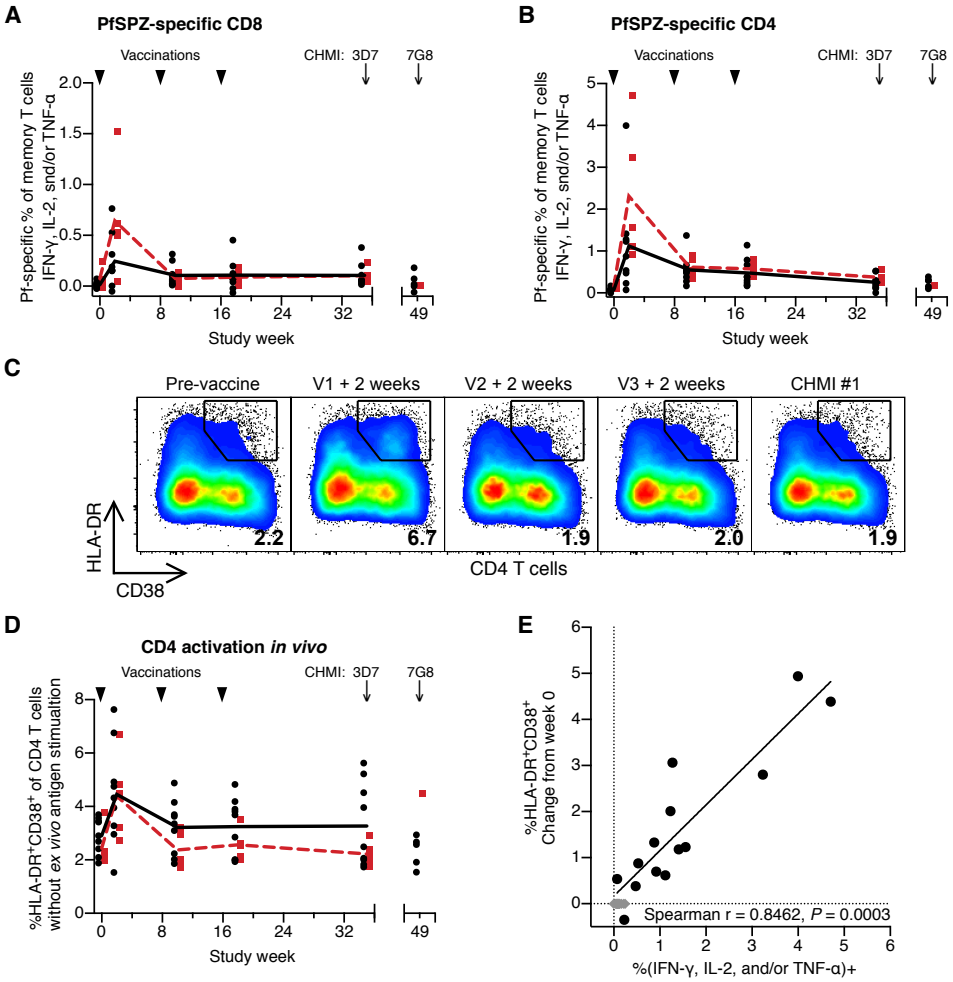


Figure 5.3: (**A**) Frequency of PfSPZ-specific cytokine-producing memory CD8 T cells. Results are the percentage of memory CD8 T cells producing IFN-γ, IL-2, and/or TNF-α following PfSPZ stimulation minus the percentage of cells following stimulation with vaccine diluent (1% human serum albumin in media). (**B**) Frequency of PfSPZ-specific cytokine-producing memory CD4 T cells. Results are calculated as in **A**. (**C**) Flow cytometry gating of CD4 T cell activation *in vivo* following vaccination. PBMCs were stained for the T cell activation markers HLA-DR and CD38 from vaccinated subjects without additional *in vitro* antigen stimulation. Representative gating examples of total memory CD4 T cells are shown before vaccination, two weeks after each vaccination (V1–V3), and at the time of homologous CHMI. (**D**) CD4 T cell activation *in vivo*. Results are the percentage of memory CD4 T cells expressing HLA-DR and CD38 as measured on PBMCs without antigen stimulation. (**E**) Correlation of CD4 T cell activation *in vivo* (HLA-DR$^+$CD38$^+$ induction) and frequency of PfSPZ-specific memory CD4 T cells by ICS. The y-axis shows the change in % of memory CD4 T cells expressing HLA-DR and CD38 from pre-vaccine to two weeks after vaccination 1. The x-axis shows the % of memory CD4 T cells expressing IFN-γ, IL-2, and/or TNF-α determined by ICS after *ex vivo* stimulation with PfSPZ. Black circles denote the frequency two weeks after vaccination 1; gray diamonds denote the frequency pre-vaccination. For each graph, n = 14 for study week 0 through 35 (time of homologous CHMI) and $n = 6$ at week 49 (time of heterologous CHMI). Arrowhead designates PfSPZ Vaccine administration, arrows designate time of CHMI with 3D7 or 7G8. For **A**, **B**, and **D**, data points are stratified as **Fig. 5.2A**, and lines are mean ± SEM. For **E**, Spearman r was calculated using post-vaccination data.

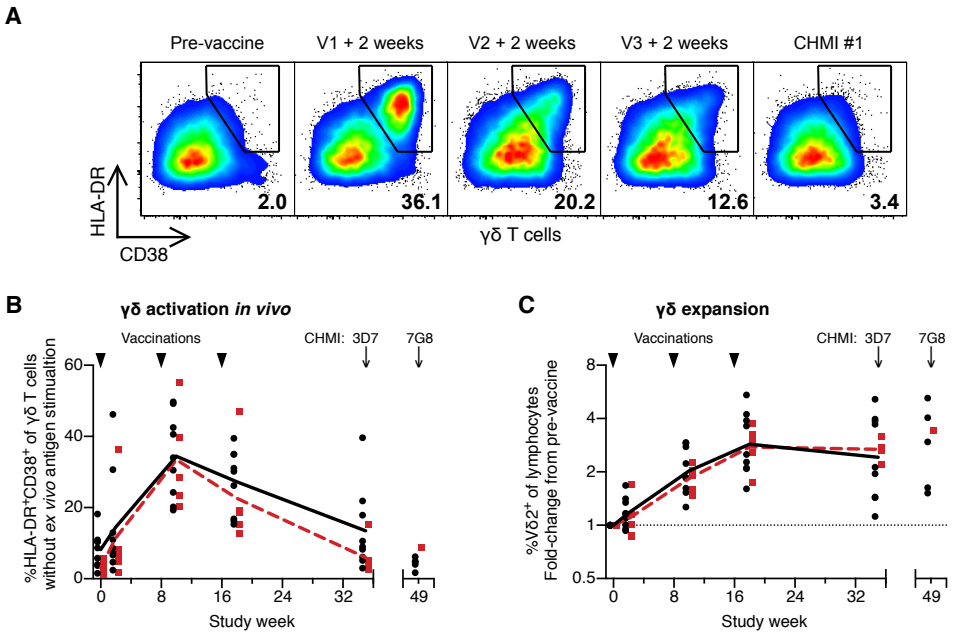


Figure 5.4: (**A**) Flow cytometry gating showing $\gamma\delta$ T cell activation *in vivo*. PBMCs were stained for the T cell activation markers HLA-DR and CD38 from vaccinated subjects without additional *in vitro* antigen stimulation. Representative gating examples of total memory $\gamma\delta$ T cells are shown before vaccination, two weeks after each vaccination (V1–V3), and at the time of homologous CHMI. (**B**) $\gamma\delta$ T cell activation *in vivo*. Results are the percentage of memory $\gamma\delta$ T cells expressing HLA-DR and CD38 as measured on PBMCs without antigen stimulation. (**C**) Frequency of V$\delta2^+$ T cells after immunization. Results are expressed as fold-change from the pre-vaccine frequency. For each graph, $n = 14$ for study week 0 through 35 (time of homologous CHMI) and $n = 6$ at week 49 (time of heterologous CHMI). Arrowhead designates PfSPZ Vaccine administration, arrows designate time of CHMI with 3D7 or 7G8. For **B** and **C**, data points are stratified as **Fig. 5.2A**, and lines are mean ± SEM (**B**) and geometric mean ± 95% CI (**C**).

higher than pre-vaccination and this increase persisted through follow-up (2.5-fold increase at the time of CHMI with 3D7).

5.2.7 T cell responses against 7G8

Since protection was observed against homologous and heterologous CHMI in subjects that received only the homologous NF54 vaccine strain, I assessed the PfSPZ-specific cytokine producing capacity from T cells against the heterologous 7G8 strain and compared them to responses against the homologous NF54 vaccine strain. There was a significant correlation in the magnitude of CD8 T cell cytokine responses to NF54 and 7G8 PfSPZ (Spearman r = 0.8052; $P = 0.0005$; **Fig. 5.5A**)

two weeks after the first immunization when such responses were measurable at detectable frequencies. CD8 T cell responses were also assessed by expression of the TNF-receptor superfamily member 4-1BB (also known as CD137). This marker has been used to identify antigen-specific CD8 T cells in the PBMC following *ex vivo* antigen stimulation [212]. Using this alternative assessment, CD8 T cell responses were also highly correlated (Spearman r = 0.9033; $P < 0.0001$; **Fig. 5.5B**). CD4 T cell cytokine responses also were significantly correlated between the two strains (**Fig. 5.5C**). Finally, $\gamma\delta$ T cell activation by the two strains (as measured by 4-1BB) was also highly correlated (**Fig. 5.5D**). Expression of 4-1BB in the $\gamma\delta$ T cell compartment in response to PfSPZ was evident in the pre-vaccine sample, as expected, as this lineage of cells is prevalent prior to vaccination, albeit at lower absolute frequencies than found after vaccination.

5.3 Discussion

5.3.1 Efficacy

The data presented here show that the PfSPZ Vaccine administered three times at a dose of 9.0×10^5 PfSPZ was highly immunogenic. The finding that 9/14 (64%) volunteers remained without parasitemia upon homologous CHMI at 19 weeks after final vaccination with a 3-dose regimen is higher than that previously achieved by 4 or 5 doses of 1.35×10^5 or 2.7×10^5 PfSPZ and further demonstrates the dose-dependent efficacy of PfSPZ Vaccine [12, 142]. The results after heterologous CHMI 33 weeks after final immunization provides the first evidence that durable protection can be induced against heterologous CHMI with an injectable vaccine. These data showing that higher immune responses and protective efficacy were induced with 9.0×10^5 PfSPZ support my hypothesis that higher PfSPZ Vaccine doses are required compared to the doses necessary for either long-term homologous [142] or short-term heterologous protection (Epstein JE, *et al.* In review).

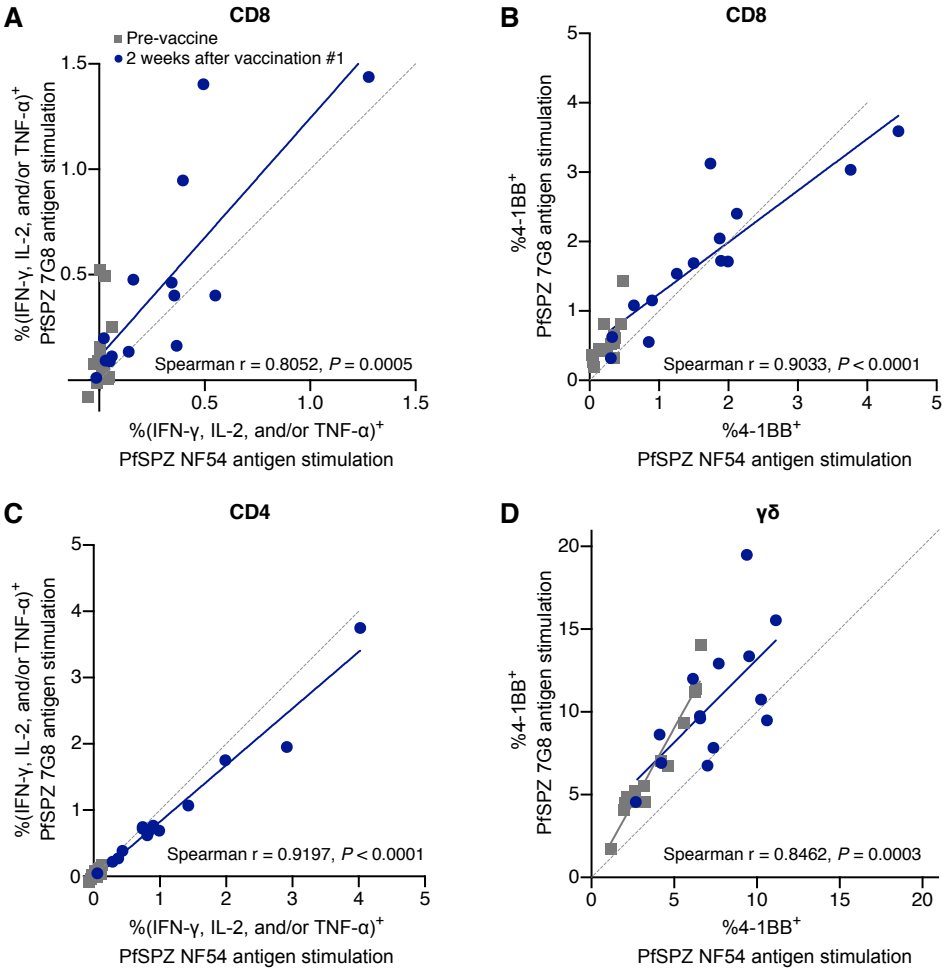


Figure 5.5: (**A**) Memory CD8 T cell cytokine production following *in vitro* PfSPZ 7G8 antigen stimulation compared to PfSPZ NF54. Results are the percentage of memory CD8 T cells producing IFN-γ, IL-2, and/or TNF-α following stimulation with PfSPZ 7G8 (y-axis) or PfSPZ NF54 (x-axis) after subtracting the percentage of cytokine-producing cells in PBMCs incubated with the vaccine diluent (1% human serum albumin in media). (**B**) Percentage of memory CD8 T cells expressing the activation marker 4-1BB following PfSPZ antigen stimulation as in **A**. (**C**) Memory CD4 T cell cytokine responses as in **A**. (**D**) Percentage of memory $\gamma\delta$ T cells expressing 4-1BB following PfSPZ antigen stimulation as in **B**. $n = 14$ for each time point. Each symbol represents an individual volunteer. Blue circles are samples two weeks after vaccination 1, and gray squares are pre-vaccine samples. Blue line is linear regression on post-vaccination sample percentages. Spearman r was calculated using post-vaccination data.

5.3.2 Immunogenicity

The consistent high-level protection observed with whole sporozoite vaccine approaches in CHMI studies suggest several critical differences in the immune responses induced by attenuated PfSPZ compared to subunit protein or viral vector vaccines. PfSPZ Vaccine primes antigenically-diverse T cell responses [12]. Moreover, I showed here that the vaccine induces strain-transcending CD8 and CD4 T cells (**Fig. 5.5**). In addition, the PfSPZ Vaccine induces activation and expansion of $\gamma\delta$ T cells [12, 142, 213], which are not induced by current subunit malaria vaccines. $\gamma\delta$ T cells recognize an invariant antigen from intracellular PfSPZ (phosphoantigens). Together, these characteristics of both antigenic and effector cell breadth may help limit vaccine escape mutants that may reduce protective efficacy of vaccines such as RTS,S/AS01 where immune responses are directed against a single protein [121].

Pf-specific T cell responses were induced in all vaccinated volunteers and were significantly higher than previously reported with lower doses of PfSPZ Vaccine (**Chapter 4** and [12]), providing additional evidence that increasing the vaccine dose enhanced immunity. CD8 and CD4 T cell responses in the blood were highest after the first immunization with limited boosting after the second and third immunizations. Previous data from non-human primates demonstrates that Pf-specific T cell responses resident in the liver are much higher than detected in the blood following immunization with PfSPZ Vaccine (**Chapter 4** and [141]). It is thus possible that boosting occurs after each immunization among non-recirculating tissue-resident T cells in the liver where responses cannot be easily measured in humans. Alternatively, as the goal of PfSPZ Vaccine administration is to induce immunity that interferes with the development of naturally-transmitted PfSPZ, rapid induction of anti-PfSPZ immunity may limit boosting by subsequent administrations of PfSPZ Vaccine especially at the higher vaccine doses used here compared to prior studies. Indeed, limited boosting following irradiated SPZ vaccination has been demonstrated in mouse models [214, 215]. These data raise the question of whether equivalent protective efficacy may be possible with fewer than three immunizations, especially with higher doses of the vaccine.

The frequency of PfSPZ-specific cytokine-producing CD8 and CD4 T cell responses were not different between subjects who were not parasitemic and parasitemic at the peak after vaccination or prior to the homologous CHMI. The lack of a significant correlation may be due to the small sample size studied here. Even though moderately detailed flow cytometric characterization was used, the small sample size precluded analysis of correlates of protection due to the high risk of Type I error from overfitting the data. Furthermore, protection may be mediated primarily by non-recirculating liver-resident T cells which cannot be directly measured in the blood (**Chapter 4**). Thus, identification of correlates of protection will require studies with much larger sample sizes and advanced immune monitoring that assesses the magnitude, antigenic breadth, and phenotype of the responses.

5.3.3 Study limitations and future directions

This study was done in malaria-naive US adults representative of travelers or military personnel who would benefit from a highly protective vaccine. Important considerations for successfully using this vaccine in Africa and other endemic areas include how pre-existing malaria exposure, age, and baseline health status influence immunogenicity and protection. Additionally, this study tested only one heterologous strain for CHMI. Future studies employing additional heterologous CHMI strains in conjunction with field studies against natural exposure will further establish the breadth of protective efficacy conferred by PfSPZ Vaccine.

The findings reported here suggest that sterile protection against homologous and heterologous CHMI can be achieved in malaria-naïve adults by a 3-dose regimen of PfSPZ Vaccine. Based on the favorable safety profile of the doses tested to date and the immune data reported here, further dose increases as well as fewer immunizations could be tested to determine if higher protective efficacy can be achieved, which will be necessary for travelers and for mass vaccination strategies aimed at interrupting transmission in endemic regions.

6

PfSPZ-CVac T cell immunology

Contents

6.1 Introduction 111
6.1.1 Clinical study design and efficacy 112
6.1.2 Immunogenicity study rationale 113
6.1.3 Study aims 113
6.1.4 Authorship 113
6.1.5 Summary of findings 114
6.2 Results 114
6.2.1 T cell immunogenicity 114
6.2.2 Correlates of sterile protection 120
6.3 Discussion 123
6.3.1 Immunogenicity 123
6.3.2 Correlates of sterile protection 123
6.3.3 Study limitations and future directions 123

6.1 Introduction

In the previous two chapters, the efficacy, immunogenicity, immune correlates of protection, and mechanism of protection of radiation-attenuated PfSPZ Vaccine is described.

P. falciparum is metabolically and transcriptionally active through multiple distinct life cycle stages in the mammalian host, and thus, there are multiple

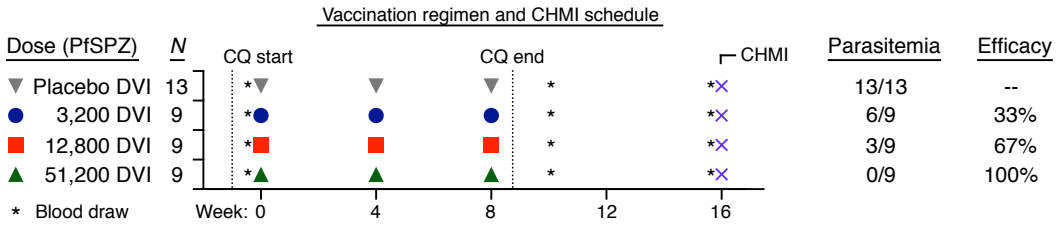


Figure 6.1: Dose groups, vaccination regimen, sampling schedule, time of CHMI, number of subjects that developed parasitemia after homologous challenge with Pf clone 3D7, and estimated efficacy.

potential opportunities for attenuation through distinct means [216].

Attenuation of the parasite at different stages induces qualitatively and quantitatively different immune responses [217], likely due to differences in the parasite proteome available to the immune system, differences in the pro-inflammatory environment that accompanies parasite arrest, and differences in the dose of protein antigen available due to replication of the parasite prior to arrest.

Specifically, radiation-attenuation sporozoites arrest early in the liver-stage of infection, prior to undergoing schizogony [217], whereas genetically-attenuated parasites can be programmed to undergo arrest at multiple points during the liver stage, including during the blood stage [218].

Roestenberg and colleagues initially described a strategy to arrest parasite development at the blood stage of infection using chloroquine, a drug that has specific anti-parasite activity only during the blood stage of infection [143]. This strategy is called chloroquine prophylaxis and sporozoites (CPS) immunization.

CPS immunization has several advantages over RAS immunization, including considerable dose-sparing, greater antigenic breadth, and longer durability of protective efficacy [143, 216, 138].

6.1.1 Clinical study design and efficacy

To determine whether non-attenuated Sanaria PfSPZ were safe, immunogenic, and protective when administered in a CPS regimen, investigators in Tübingen, Germany, conducted a randomized, double-blind, placebo-controlled, dose-escalation study with homologous CHMI in healthy malaria-naive volunteers.

The vaccine regimen was well tolerated. Sterile efficacy after CHMI was dose dependent. All 13 subjects that received placebo vaccination became infected. Six of 9 subjects (67%) that received 3,200 PfSPZ, 3 of 9 subjects (33%) that received 12,800 PfSPZ, and 0 of 9 subjects (0%) that received 51,200 PfSPZ developed parasitemia after CHMI (**Fig. 6.1**).

6.1.2 Immunogenicity study rationale

Sterile protection following CPS immunization is directed against the pre-erythrocytic stages in humans [146] and has been shown to be cell mediated [219]. However, antibodies may also play a role in partially reducing the liver-stage burden [220, 221]. Recently, evidence that the protection is mediated by blood stage immunity in some mouse strains has emerged [222].

To determine how the T cell immunogenicity of CPS immunization compares to RAS immunization, I examined the T cell response in this clinical study using multiparameter flow cytometry and cytokine bead array. I analyzed the data for signatures which associated with sterile protection.

6.1.3 Study aims

In this study, I sought to:

1 Describe the cellular immune activation in humans vaccinated with PfSPZ-CVac and compare this to humans vaccinated with PfSPZ Vaccine

2 Identify immune signatures that associate with sterile protection

6.1.4 Authorship

The clinical study was designed and conducted in Tübingen, Germany by Benjamin Mordmüller, Peter Kremsner, and colleagues. I designed the T cell immunological studies with R.A.S. I conducted the studies with technical assistance from B.F. I performed the T cell analysis and statistical comparisons with guidance from Mario Roederer.

6.1.5 Summary of findings

1 Pf-specific CD4, CD8, and $\gamma\delta$ T cell responses were dose-dependent.

2 CD4 T cell responses were considerably higher than the T cell responses in subjects that received RAS immunization at higher PfSPZ doses.

3 The frequency of circulating memory CD4 T cells simultaneously producing IFN-γ, IL-2, and TNF-α was identified as a potential correlate of sterile protection.

6.2 Results

6.2.1 T cell immunogenicity

On the basis of data generated in mouse and simian models, it is likely that after whole PfSPZ immunization, vaccine-induced antibodies reduce the number of non-attenuated PfSPZ from CHMI that effectively invade hepatocytes [220, 221], but cellular immune responses, particularly cells expressing CD8, are required for completely eliminating Pf-infected hepatocytes, and thereby preventing progression to disease [146, 219, 217].

To investigate T cell memory, 1.5×10^6 cryopreserved PBMCs acquired before first immunization (Pre-immunization), two weeks following completion of the immunization regimen (Post-immunization), and one day before CHMI (Pre-CHMI) were stimulated with either 1.5×10^5 PfSPZ, 2.0×10^5 Pf-infected red blood cells (PfRBC), or control antigens for 17 hours (See **Materials and methods** for additional details). Supernatants were sampled at the conclusion of the stimulation and assessed for the presence of secreted cytokines and chemokines by cytokine bead array. The stimulated PBMCs were then phenotyped by flow cytometry after intracellular cytokine staining.

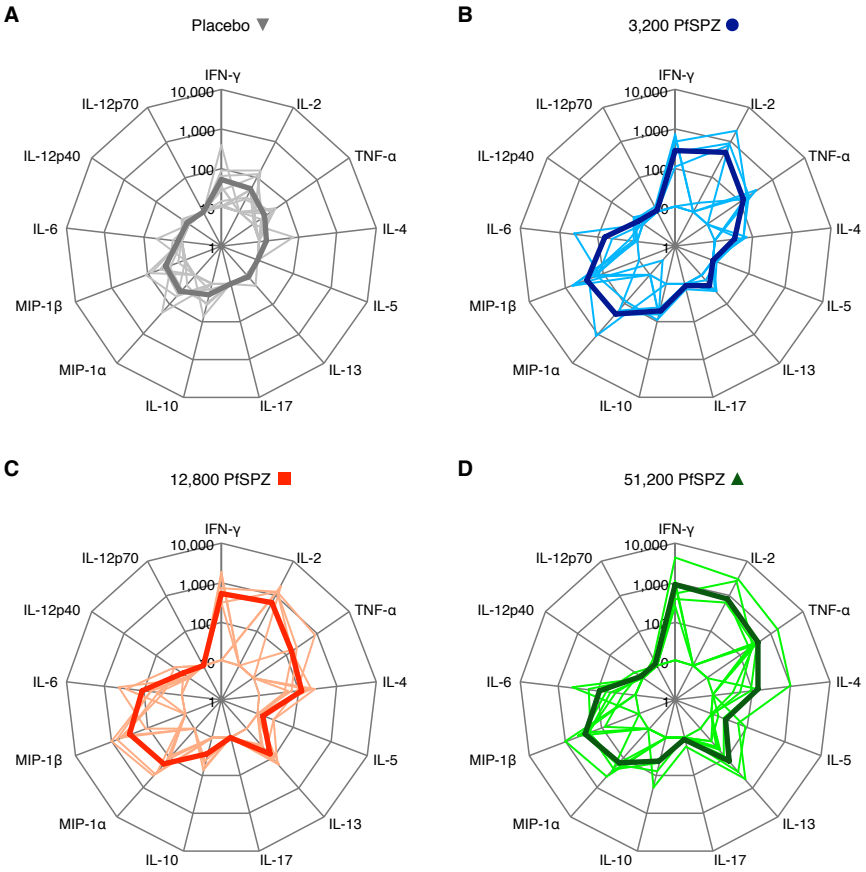


Figure 6.2: Culture supernatants from PBMCs stimulated with PfRBC were assessed for secreted cytokines by cytokine bead array. The spider plots show each subject by group, with light lines denoting each individual subject and heavy lines denoting the mean. Data are from two weeks after final vaccination. Analyte quantities are reported in pg/mL.

Supernatant cytokines

Supernatants from PfRBC-stimulated PBMCs are shown for each vaccine recipient two weeks after final vaccination. There is a dose-dependent increase in IFN-γ, IL-2, and TNF-α, cytokines that are often classified as T_H1 cytokines (**Fig. 6.2**). There is also a dose-dependent increase in IL-4, IL-5, and IL-13, the canonical T_H2 cytokines, though the amount of cytokine produced is generally lower than the T_H1 cytokines. IL-12p40 and IL-12p70 are below the limit of detection, indicating that IL-12-related bystander activation of non-malaria specific cells during this incubation period is likely minimal.

However, there are higher amounts of MIP-1α and MIP-1β in each of the

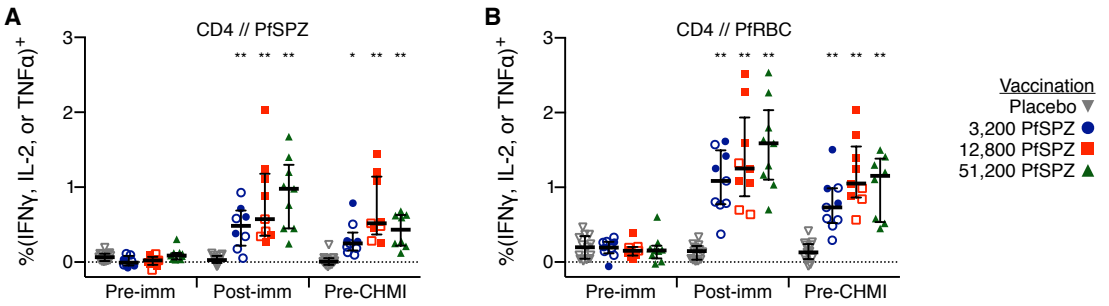


Figure 6.3: PBMCs were stimulated with PfSPZ or PfRBC and assessed by ICS. Memory CD4 T cells producing IFN-γ, IL-2, or TNF-α following PfSPZ (**A**) or PfRBC stimulation (**B**). Within a dose group, the difference from pre-immunization was assessed by two-way ANOVA with Bonferroni correction. * $P < 0.05$, ** $P < 0.01$. Data are median $\pm$ interquartile range.

vaccine groups, which at high enough levels can induce IL-6 and TNF-α secretion. Thus, while cytokine bead array of cultured supernatants confirms a clear dose response in the PfRBC-specific activation of the cellular components of blood following vaccination with PfSPZ-CVac, it does not allow for an understanding of the underlying cell types that are producing the cytokines of interest or their phenotypes.

CD4 T cell responses

Multiparameter flow cytometry revealed several unique aspects of the immune response following PfSPZ-CVac. The frequency of PfSPZ- and PfRBC-specific memory CD4 T cells expressing any combination of IFN-γ, IL-2, or TNF-α increased in a dose dependent manner (**Fig. 6.3**).

The CD4 T cell cytokine polyfunctionality is shown, revealing a trend towards higher polyfunctionality as dose increased (**Fig. 6.4**).

IL-4 producing CD4 T cells have been shown to contribute to the priming of CD8 T cell responses against liver stage parasites following radiation-attenuated sporozoite immunization in mouse models [223]. Thus, I assessed IL-4 expression in PBMCs following stimulation with PfRBC. There was a clear dose response in the percentage of memory CD4 T cells secreting IL-4. IL-10 producing CD4 T cell frequencies were also assessed, and such responses were also dose-dependent (**Fig. 6.5**).

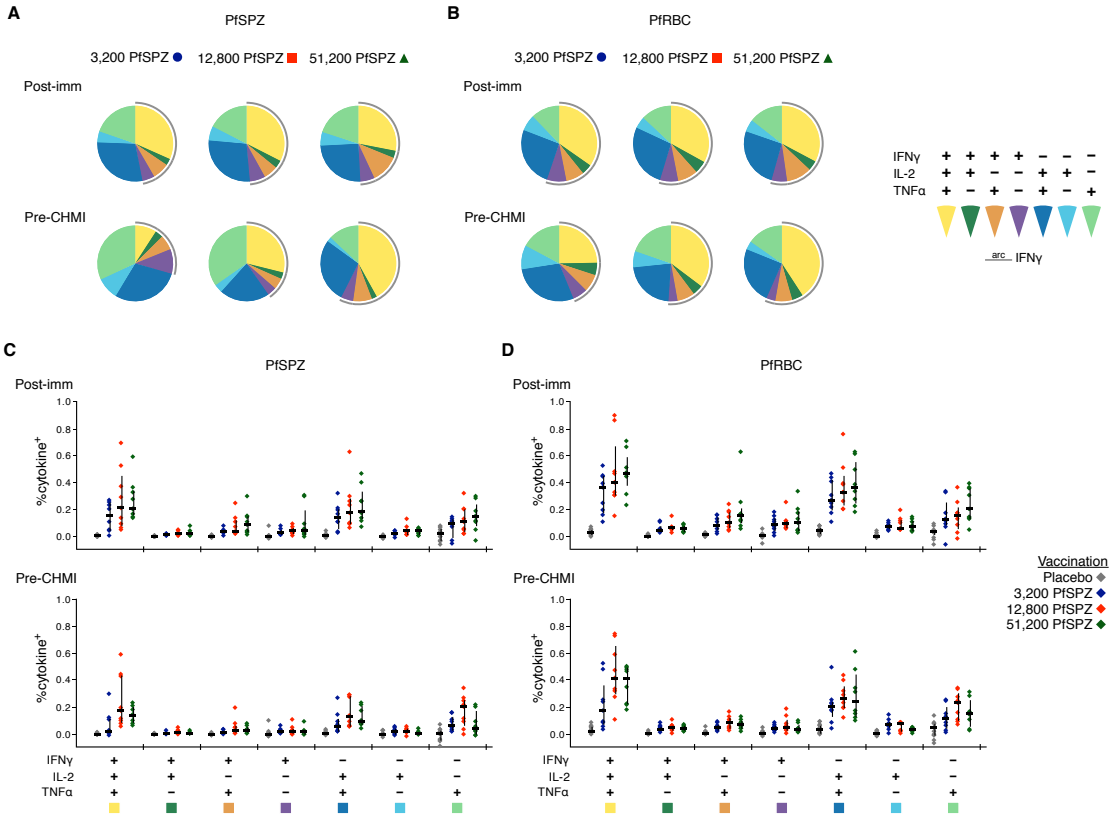


Figure 6.4: The pie charts (without thresholding) show the median proportion of memory CD4 T cells expressing any combination of IFN-γ, IL-2, or TNF-α for each dose group after stimulation with PfSPZ (**A**) or PfRBC (**B**). The magnitude of the memory CD4 T cell response for each combination of cytokines is shown in **C** and **D**. For **C**–**D**, bars are median ± interquartile range.

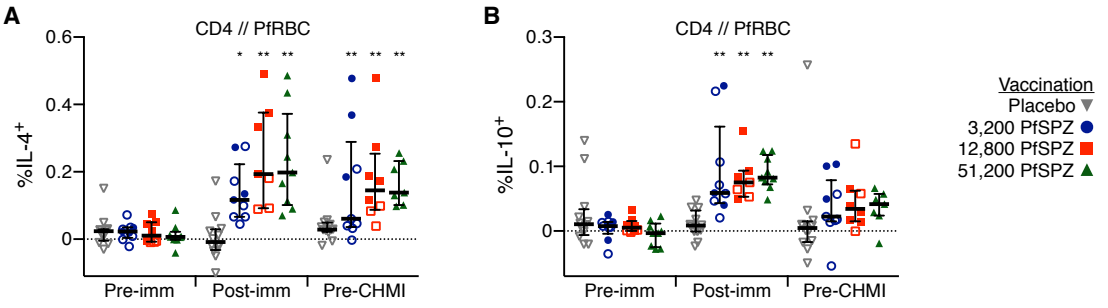


Figure 6.5: Memory CD4 T cells producing IL-4 (**A**) or IL-10 (**B**) is shown after stimulation with PfRBC. Within a dose group, the difference from pre-immunization was assessed by two-way ANOVA with Bonferroni correction. * $P < 0.05$, ** $P < 0.01$. Data are median ± interquartile range.

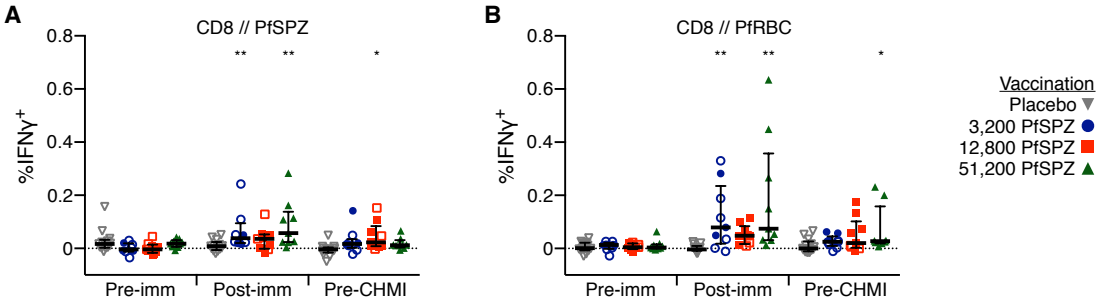


Figure 6.6: Memory CD8 T cells producing IFN-γ following PfSPZ (**A**) or PfRBC stimulation (**B**). Within a dose group, the difference from pre-immunization was assessed by two-way ANOVA with Bonferroni correction. * $P < 0.05$, ** $P < 0.01$. Data are median $\pm$ interquartile range.

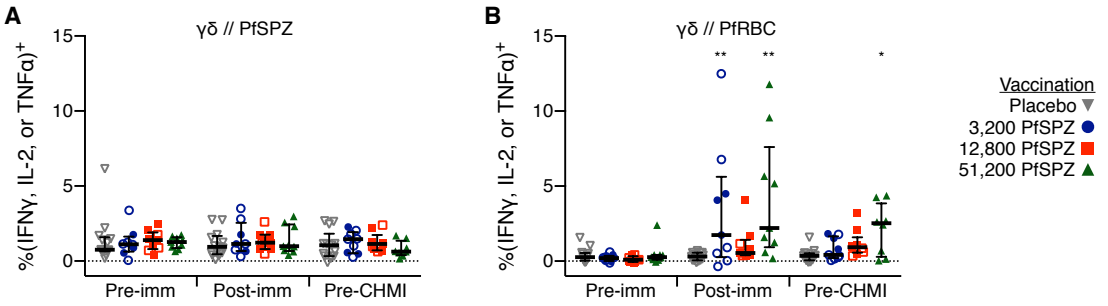


Figure 6.7: Memory $\gamma\delta$ T cells producing IFN-γ, IL-2, or TNF-α following PfSPZ (**A**) or PfRBC stimulation (**B**). Within a dose group, the difference from pre-immunization was assessed by two-way ANOVA with Bonferroni correction. * $P < 0.05$, ** $P < 0.01$. Data are median $\pm$ interquartile range.

CD8 T cell responses

PfSPZ- and PfRBC-specific CD8 T cells were detected after immunization, most reliably in the group that received 51,200 PfSPZ, but were lower in magnitude than comparable CD4 T cell responses (**Fig. 6.6**).

$\gamma\delta$ T cell responses

$\gamma\delta$ T cells prior to vaccination express IFN-γ when stimulated with PfSPZ, and the percent of $\gamma\delta$ T cells responding to PfSPZ did not change after immunization. However, there was a significant increase in the frequency of $\gamma\delta$ T cells responding to PfRBC after immunization (**Fig. 6.7**).

The frequency of circulating $\gamma\delta$ T cells (measured on PBMC without PfSPZ or PfRBC stimulation) increased in a dose-dependent manner. Expansion of $\gamma\delta$ T

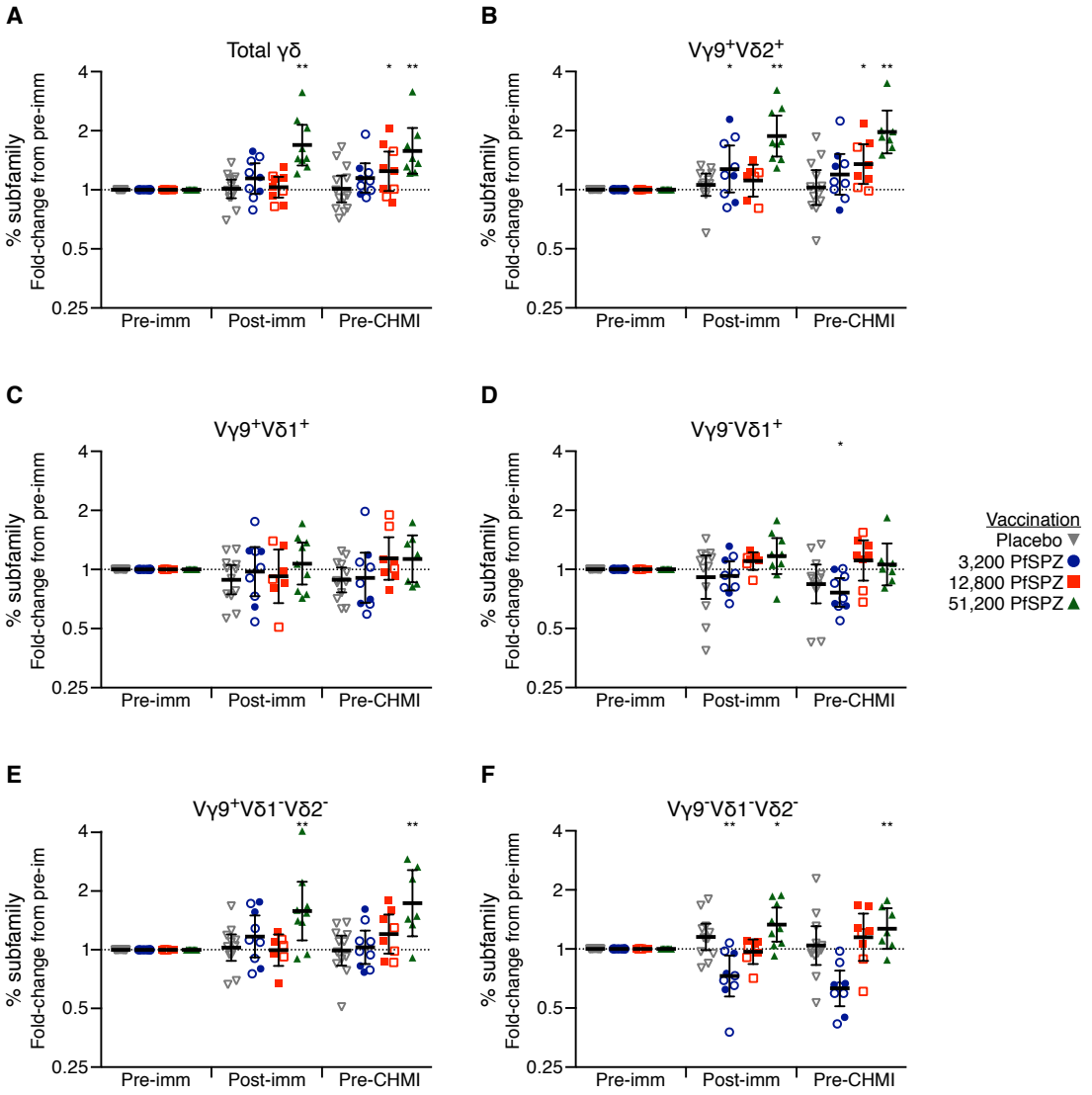


Figure 6.8: (**A**–**F**) The frequency of the circulating $\gamma\delta$ T cell sub-families as a percentage of total lymphocytes was assessed in unstimulated PBMCs before the first immunization (Pre-imm), 2 weeks after final immunization (Post-imm), and the day before CHMI (Pre-CHMI). Fold change compared to Pre-imm is shown for (**A**) total memory $\gamma\delta$ T cells, (**B**) V$\gamma9^{+}$V$\delta2^{+}$, (**C**) V$\gamma9^{+}$V$\delta1^{+}$, (**D**) V$\gamma9^{-}$V$\delta1^{+}$, (**E**) V$\gamma9^{+}$V$\delta1^{-}$V$\delta2^{-}$, and (**F**) V$\gamma9^{-}$V$\delta1^{-}$V$\delta2^{-}$ subfamilies. The frequency of V$\gamma9^{-}$V$\delta2^{+}$ subset is low to undetectable. Within a dose group, the difference from Pre-imm was assessed by two-way ANOVA with Bonferroni correction. * $P < 0.05$, ** $P < 0.01$. Data are geometric mean ± 95% c.i.

cells has been observed with other PfSPZ vaccines in humans [213, 12, 142]. This expansion was primarily restricted to the V$\gamma9^{+}$V$\delta2^{+}$ sub-family (**Fig. 6.8**).

Memory $\gamma\delta$ T cells showed an increase in the activation markers CD38 and a trend towards an increase in the liver-homing chemokine receptor CXCR6 (**Fig. 6.9**).

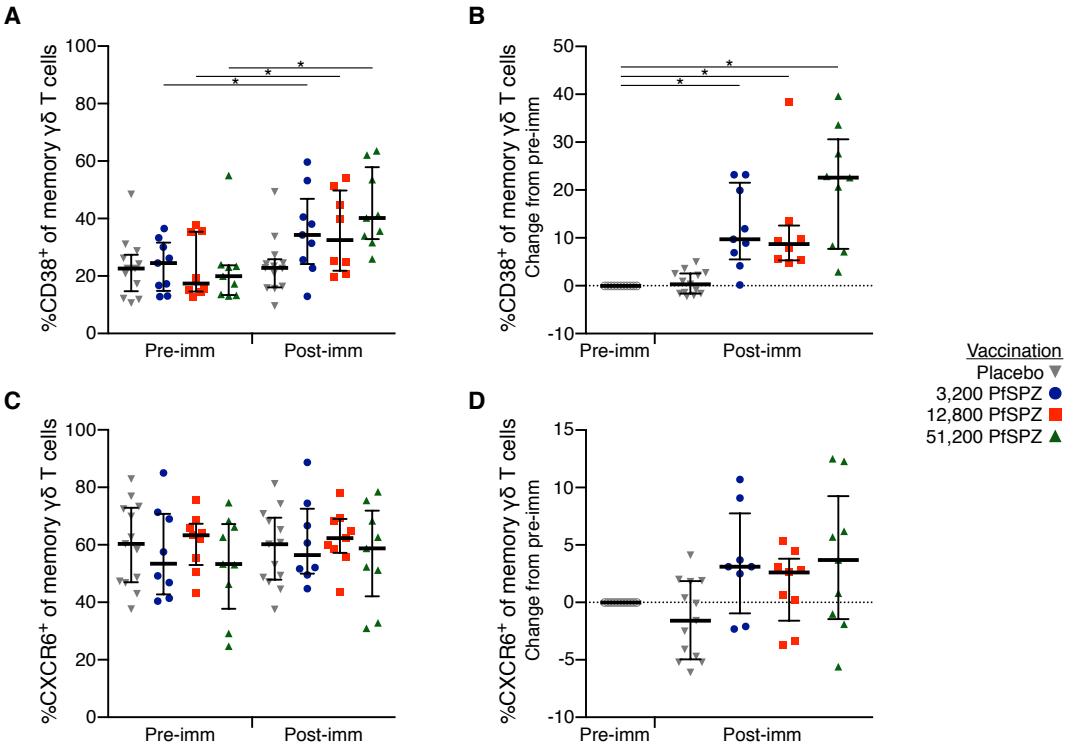


Figure 6.9: (**A**–**D**) Total memory $\gamma\delta$ T cells were assessed before immunization (Pre-imm) and 14 d after third immunization (Post-imm) for the percent of cells expressing the activation marker CD38 (**A**,**B**) and the liver-homing chemokine receptor CXCR6 (**C**,**D**). The absolute frequencies are shown in **A**,**C** and the change from pre-vaccination to post-vaccination is shown in **B**,**D**. Difference from Pre-imm was assessed by Wilcoxon signed rank test. *P*-values were corrected for multiple comparisons by the Bonferroni method. * $P < 0.05$. Data are median ± interquartile range.

6.2.2 Correlates of sterile protection

CD4 correlates

To identify correlates of protection, T cell responses were compared to outcome after CHMI using a stratified Wilcoxon test with vaccine dose as a co-variate. In this exploratory analysis of Phase I study samples, *P*-values were not corrected for multiple comparisons. Rather, the associations that yielded the lowest *P*-values are reported.

The magnitude of PfRBC-specific memory CD4 T cells producing IFN-γ correlated with sterile protection with an uncorrected *P*-value of 0.00043. Similarly, the magnitude of PfRBC-specific memory CD4 T cells simultaneously producing IFN-γ, IL-2, and TNF-α correlated with protection with an uncorrected *P*-value

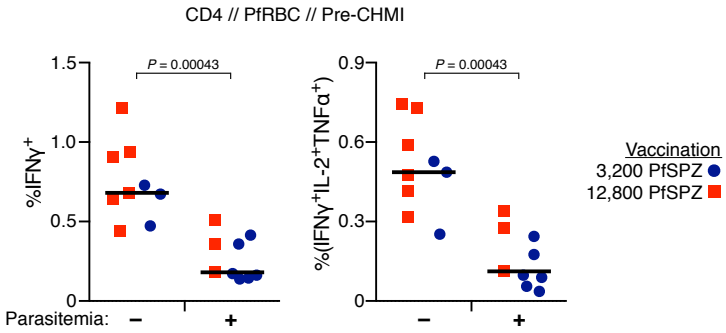


Figure 6.10: T cell responses measured before first immunization, two weeks after third immunization, or the day before CHMI were compared to outcome at CHMI (parasitemia or no parasitemia) in the 3,200 and 12,800 PfSPZ groups using a stratified Wilcoxon test controlling for vaccine dose as a co-variate. Since all subjects in the 51,200 PfSPZ group were protected, these subjects were not included in the analysis. PfRBC-specific CD4 T cells at the time of CHMI that produced IFN-γ^+ (left) or IFN-γ, IL-2, and TNF-α (right) correlated with sterile protection. Bar denotes overall median.

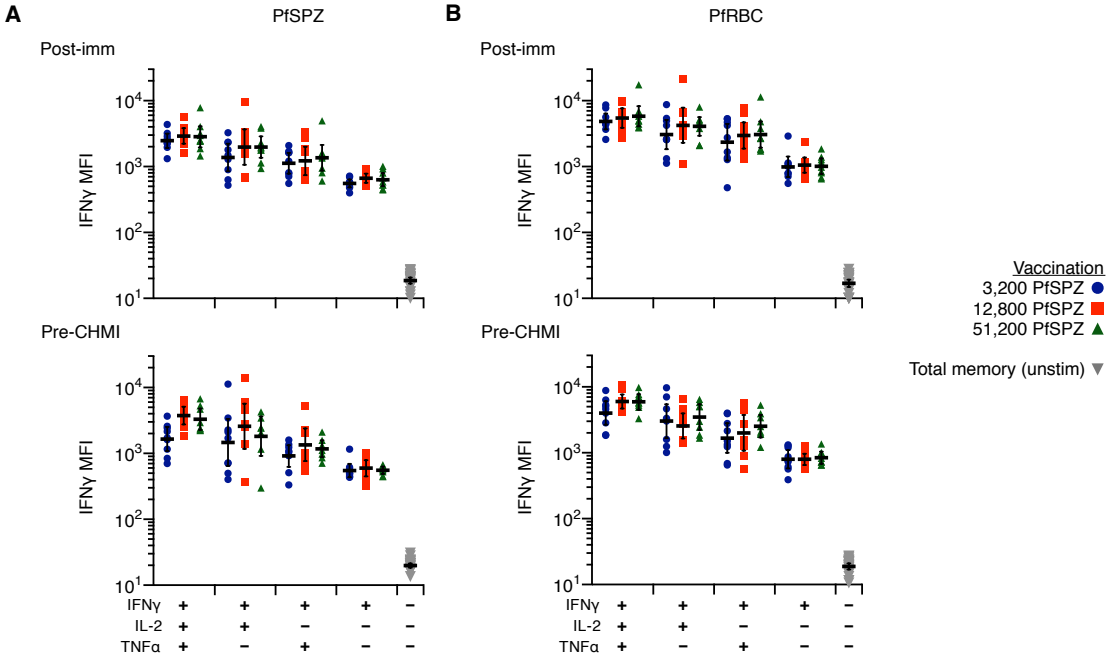


Figure 6.11: The median fluorescence intensity (MFI) for IFN-γ is shown for the different combination of IFN-γ^+ cells following PfSPZ or PfRBC stimulation. Cells that simultaneously produce IFN-γ, IL-2, and TNF-α have the highest IFN-γ MFI.

of 0.00043 (**Fig. 6.10**)

These polyfunctional cells produce the highest IFN-γ signal (MFI) (**Fig. 6.11**) and have been shown to correlate with protection in animals models of other parasitic infections [224].

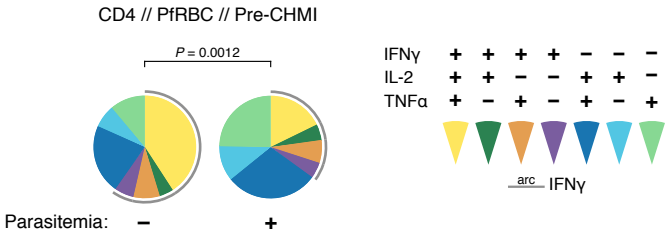


Figure 6.12: T cell responses measured before first immunization, two weeks after third immunization, or the day before CHMI were compared to outcome at CHMI (parasitemia or no parasitemia) in the 3,200 and 12,800 PfSPZ groups. PfRBC CD4 T cells responses at the time of CHMI from protected subjects were more polyfunctional than not protected subjects (3,200 and 12,800 dose groups combined).

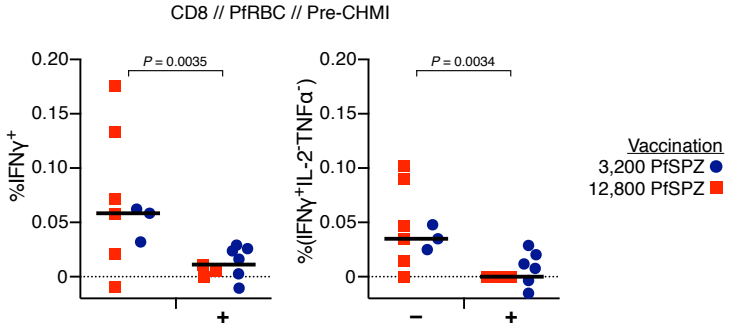


Figure 6.13: T cell responses measured before first immunization, two weeks after third immunization, or the day before CHMI were compared to outcome at CHMI (parasitemia or no parasitemia) in the 3,200 and 12,800 PfSPZ groups using a stratified Wilcoxon test controlling for vaccine dose as a co-variate. Since all subjects in the 51,200 PfSPZ group were protected, these subjects were not included in the analysis. PfRBC-specific CD8 T cells at the time of CHMI that produced IFN-γ with or without IL-2 or TNF-α (left) or produced IFN-γ only (right) correlated with sterile protection. Bar denotes overall median.

Similarly, the overall polyfunctionality of the CD4 T cell response to PfRBC was significantly higher when comparing protected and not protected subjects combined from the 3,200 and 12,800 PfSPZ dose groups (**Fig. 6.12**)

CD8 correlates

Within the CD8 T cell compartment, the magnitude of PfRBC-specific memory CD8 T cells producing IFN-γ correlated with sterile protection with an uncorrected P-value of 0.0035. The magnitude of single-positive IFN-γ^{+}IL-2^{-}TNF-α^{-} CD8 T cells also correlated with protection (**Fig. 6.13**).

A complete list of T cell correlates is shown in **Table 6.1**.

6.3 Discussion

6.3.1 Immunogenicity

CD4, CD8, and $\gamma\delta$ T cell responses showed a clear dose-dependency, confirming that PfSPZ is potent in the induction of multiple T cell lineages. The median T_H1 CD4 T cell response in the 51,200 PfSPZ dose group was 1.5% of the memory compartment 2 weeks after final immunization, which is considerably higher than the responses measured by identical methods observed in subjects two weeks after vaccination with radiation-attenuated PfSPZ at 270,000 PfSPZ per dose (See **Chapter 4, 5** and [12, 142]). This indicates that PfSPZ with CPS immunization is a more potent inducer of circulating T cells, which is consistent with studies in animal models [219, 220] and clinical trials [143, 138].

6.3.2 Correlates of sterile protection

CD4 and CD8 T cell responses at the time of CHMI correlated with sterile protection. These correlations should be considered hypothesis generating, requiring validation in large prospective studies. Nonetheless, their concordance with known biological mechanisms of protection following whole sporozoite vaccination suggests that T cell immunity is contributing to sterile immunity in these vaccinated human subjects. The correlation of polyfunctional CD4 T cells with protection indicates that the quality of the CD4 T cell response is an important factor in contributing to sterile protection. Interestingly, IFN-γ^+ CD8 T cells – the cell type known to be essential for protection in several animal models of whole sporozoite vaccination – detected following PfSPZ or PfRBC stimulation were low to undetectable by the time of CHMI in 7 of 9 of the protected subjects in the 51,200 PfSPZ dose group. Thus, if CD8 T cells are contributing to protection, they are likely localized in the tissues and not recirculating in substantial numbers.

6.3.3 Study limitations and future directions

This study of T cell responses following whole sporozoite vaccination with continuous chloroquine prophylaxis has several limitations.

CD4	Pre-immunization		Post-immunization		Pre-CHMI	
	PfSPZ	PfRBC	PfSPZ	PfRBC	PfSPZ	PfRBC
Boolean Sum	0.46620	0.28217	0.11522	0.00822	0.03982	0.00397
IFNγ+	0.55889	0.87613	0.21259	0.00369	0.03118	**0.00043**
IL-2+	0.82887	0.77735	0.12436	0.01247	0.04549	0.00213
TNFα+	0.51042	0.26148	0.10183	0.02013	0.03486	0.00652
γ+2+T+	0.97385	1.00000	0.10480	0.00992	0.03628	**0.00043**
γ+2+T-	0.70833	0.72874	0.53125	0.00524	0.51573	0.12684
γ+2-T+	0.49490	0.82752	0.41263	0.01134	0.04691	0.00354
γ+2-T-	0.18027	0.98866	0.71514	0.07285	0.48980	0.02820
γ-2+T+	0.64711	0.56448	0.11735	0.02664	0.04153	0.03685
γ-2+T-	0.53742	0.53430	0.44090	0.10799	0.74093	0.19005
γ-2-T+	0.37500	0.07937	0.22980	0.33702	0.77480	0.54011

CD8	Pre-immunization		Post-immunization		Pre-CHMI	
	PfSPZ	PfRBC	PfSPZ	PfRBC	PfSPZ	PfRBC
Boolean Sum	0.46088	0.76417	0.06101	0.21542	0.92687	0.06378
IFNγ+	0.19898	0.79719	0.19664	0.14286	0.50836	0.00354
IL-2+	0.20238	0.25156	0.71641	0.43552	0.65207	0.09892
TNFα+	0.54167	0.87628	0.30485	0.22832	0.87911	0.62996
γ+2+T+	0.60566	0.78699	0.91008	0.46641	0.01871	0.02183
γ+2+T-	1.00000	0.83333	0.16497	0.83900	0.90774	0.90859
γ+2-T+	0.07738	0.37642	0.77679	0.47208	0.50567	0.17730
γ+2-T-	0.35013	0.79294	0.03827	0.19402	0.43367	0.00340
γ-2+T+	0.31611	0.49603	0.60991	0.88691	0.94785	0.65079
γ-2+T-	0.74235	0.93325	0.48576	0.04932	0.33503	0.53671
γ-2-T+	0.57483	0.77749	0.07929	0.18169	0.82270	0.94983

γδ	Pre-immunization		Post-immunization		Pre-CHMI	
	PfSPZ	PfRBC	PfSPZ	PfRBC	PfSPZ	PfRBC
Boolean Sum	0.93608	0.16518	0.92928	0.36799	0.58688	0.01488
IFNγ+	0.74376	0.62436	0.94898	0.37181	0.67616	0.04932
IL-2+	0.72846	0.33440	0.52438	0.22045	0.46329	0.76658
TNFα+	1.00000	0.42836	0.92475	0.63988	0.43750	0.29826
γ+2+T+	0.43920	1.00000	0.75624	0.22619	0.39753	0.88520
γ+2+T-	0.32185	0.91071	0.82355	0.06250	0.59212	0.19792
γ+2-T+	0.52551	0.76658	0.75425	0.48236	0.54110	0.21620
γ+2-T-	0.59170	0.60672	0.81675	0.39435	0.72888	0.02381
γ-2+T+	0.56222	0.51807	0.40646	0.79103	0.86168	0.87351
γ-2+T-	0.50524	0.53933	0.06817	0.01722	0.26035	0.63244
γ-2-T+	0.82965	0.15306	0.56973	0.71280	0.27735	0.23554

$P > 0.01$
$P < 0.01$
$P < 0.001$

Table 6.1: Correlation of CD4, CD8, and $\gamma\delta$ T cell responses with sterile protection.

First, as is true for studies with RAS vaccination in humans, the analysis has been restricted to T cells in the blood, which are not representative in frequency or quality to Pf-specific cells in the tissues. Thus, each analysis is at least one level removed from the immunobiology at the site of infection and protective immunity.

Second, there was no sampling during the vaccination period. As I have seen in my studies with PfSPZ Vaccine, Pf-specific CD8 T cells are typically only readily detected after the first or second vaccination, depending on the dose used. The induction kinetics indicate that T cells redistribute into the tissues after an initial recirculation following the initial priming doses. Because samples were only avaliable two weeks after the final vaccination, it is likely that I missed the peak of the CD8 T cell response. Thus, opportunities to describe the CD8 T cell immunogenicity (for example, the cytokine and effector functionality, cellular differentiation, and other surface and intracellular markers of interest) and to describe Pf-specific CD8 T cell correlates is greatly reduced. Future studies would ideally sample more frequently, particularly 1 and 2 weeks after first immunization.

Third, the antigen stimulations for recalling antigen-specific T cell responses are limited. I used whole, live PfSPZ for one stimulation. As I have validated with subjects receiving PfSPZ Vaccine, PfSPZ stimulation is a comprehensive measure of the total T cell response following PfSPZ Vaccine administration (**Chapter 5**). The PfRBC stimulation consists of a lysate of >90% late stage schizonts. While these antigen stimulations share many proteins with sporozoite and early liver-stage forms (PfSPZ stimulation) or late liver-stage forms and infected RBCs (PfRBC stimulation), each antigen stimulation is only an approximation of the true antigens presented *in vivo*. Thus, it is possible that I am not being completely comprehensive in our efforts to measure the antigen-specific response, particularly following CPS immunization. Furthermore, my analysis provides no information on the identity of antigens recognized by protective or not protective T cell responses and provides no data on whether there are qualitative differences in the magnitude and quality of T cells specific for different antigens. Future analyses of the T cell immunogenicity

and correlates of protection would ideally identify protective antigens and describe the associated cellular and molecular features that correlate with protection.

Fourth, my correlates analysis was performed as a purely exploratory analysis. Thus, I examined numerous phenotypic subsets for correlations with protection. While I identified several potential correlates of protection that are consistent with known mechanisms of biological effects, in the absence of a validation cohort and a pre-specified statistical analysis plan, it is likely that my approach has introduced type I error (false discovery).

Additional immunological studies of PfSPZ-CVac will focus on mapping the T cell antigen repertoire, studying the T cell phenotype and function in greater depth using higher dimensional flow cytometry and single cell gene counting technologies, and identifying and validating correlates of protection against heterologous CHMI and heterogeneous field exposures.

7 Conclusions

Contents

7.1 Summary and conclusions 127
7.2 Future directions 130
7.2.1 RH5 vaccines 130
7.2.2 Immunological studies of PfSPZ Vaccine 130
7.2.3 PfSPZ Vaccine regimen optimizations 132

7.1 Summary and conclusions

Chapter 3 described my efforts to produce multimeric RH5 subunit vaccine constructs. The goal of these studies was to improve the quality and magnitude of the neutralizing activity of RH5 antibodies by multimerizing the truncated structural variant of RH5.

These efforts were largely unsuccessful, likely due to the instability of RH5-sv3 when arrayed as a multimer. First, the IMX313 heptameric construct was contaminated with degradation products. Second, the SpyTag-SpyCatcher approach resulted in VLP aggregation as soon as the RH5-sv3 was linked to the VLP. sv3 was designed originally with the goal of producing crystals for crystallography, and thus, all glycosylation sites were mutated away. Even the monomeric version of sv3 can be

unstable in solution, and it frequently aggregates even at moderate concentrations. It is possible that the lack of native glycosylation is aggravating the precipitation of the protein in solution. Strategies to address this are discussed in the next section.

Chapter 4 describes the efficacy, correlates of protection, and mechanism of protection of an initial dose escalation of the live attenuated PfSPZ Vaccine. With regard to efficacy, these studies showed that efficacy was dose dependent and that vaccination by the IM route results in no durable sterile efficacy.

Two potential correlates of protection were identified. The first could have been predicted on the basis of prior studies with RAS vaccination: PfCSP antibody level correlates with durable protection. The second, however, was unexpected: the pre-vaccine frequency of $V\gamma9^{+}V\delta2^{+}$ T cell correlated with durable sterile protection. This semi-innate T cell subset has been shown in mouse models to mediate effector functions against Pf-infected hepatocytes. Moreover, as the majority of the circulating $\gamma\delta$ T cells express CXCR6, the liver-homing chemokine receptor, it is possible that $\gamma\delta$ T cell recognition of infected hepatocytes is a crucial step in the induction of protective adaptive immunity. Studies in mice substantiate a potential role for $\gamma\delta$ T cells in antigen presentation [32, 33]. The induction of this atypical T cell subset and its apparent importance to the protective efficacy highlights one of the key advantages of using live-attenuated vaccines.

The studies in Chapter 4 also helped define the mechanism of protection. In one group, sterile protection was maintained for over 1 year even though antibody levels and PfSPZ-specific CD4 T cells in the blood had waned considerably. PfSPZ-specific CD8 T cells were undetectable in the blood but highly prevalent in the liver of non-human primates. These data and other data presented in that Chapter suggest that durable protection was mediated by long-lived liver-resident T cells. No licensed vaccine can yet claim to mediate protection through CD8 T cells.

Chapter 5 describes the immnuogenicity of three high doses (9.0×10^5) of PfSPZ Vaccine and describes the cross-reactivity of the T cell response to the heterologous CHMI strain. The T cell activation kinetics were notable because of the very high CD8 and CD4 T cell activation and expansion after the first vaccination that

was nearly absent after subsequent immunizations. This suggests that anti-PfSPZ immunity is interfering with subsequent PfSPZ Vaccine administrations, and that perhaps individuals would be better off receiving one or two large doses, rather than three or more split doses. Additionally, PfSPZ-specific T cells were highly cross-reactive between the vaccination strain and the heterologous CHMI strain. This cross-reactivity was observed across CD8, CD4, and $\gamma\delta$ T cell lineages. This feature of whole sporozoite vaccines – wherein the T cell response is spread across many different antigens – may help limit vaccine escape mutants.

Chapter 6 describes the immunogenicity and T cell correlates of protection of PfSPZ-CVac. With this alternative whole sporozoite vaccination approach, many of the T cell findings with PfSPZ Vaccine were substantiated. Importantly, the T cell responses seen here were higher that seen with PfSPZ Vaccine despite using lower PfSPZ doses with PfSPZ-CVac. Thus, the dose sparing effect on immunogenicity and protection is clear. Furthermore, the polyfunctionality of the CD4 T cell response was identified as a potential correlate of protection. This T_H1 correlate of protection is consistent with the immunobiology of the response it is understood from these and other studies on the mechanism of protection.

CD4 T cells are helper T cells, and thus, recirculation through the blood to secondary lymphoid organs is entirely consistent with their function. PfSPZ-specific CD4 T cells persistently circulate in the blood after vaccination. Consistent with a role of active tissue surveillance, however, liver-resident CD8 T cells do not recirculate to secondary lymphoid organs and are nearly undetectable in the blood. Determining that the magnitude of the T_H1 CD4 response correlated with protection is entirely consistent with a role for IFN-γ CD8 T cells mediating protection in the liver. I would posit that the T_H1 CD4 T cells response is closely correlated with the magnitude of the IFN-γ CD8 T cell response, but the only thing that can be reasonably measured at the time of CHMI is the CD4 T cell response.

7.2 Future directions

7.2.1 RH5 vaccines

In its native form, RH5 is not expressed alone. To be present on the surface of the merozoite, it must be bound through quaternary interactions to Ripr and CyRPA. To continue to advance the RH5 as an immunogen will likely require the structure-based re-design of the immunogen. Solubility could be improved by the addition of glycans or hydrophilic amino acids on the solvent-exposed surface of the protein without interfering with the domains that bind neutralizing antibodies.

Flexibility in the protein can also cause instability. The RH5 molecule consists of multiple bundled alpha helices, and these could be stabilized by disulfide bridges, salt bridges, or the removal of side groups that cause partial steric clash. Such studies are currently ongoing in collaboration with a structural vaccinology group in Oxford.

Secondarily, solubility could be improved with the use of alternative carriers. Efforts are also underway to covalently link RH5-sv3 antigen as it is to a fully water-soluble polymer nanoscaffold that also carries potent TLR agonists. The polymer nanoscaffold selected for this work contains a short polymeric section that is responsive to changes in temperature. This thermo-responsive section collapses on itself at elevated (*i.e.*, body) temperature, spontaneously forming multimeric particles upon injection. Whether the sv3-thermoresponsive nanoscaffold unit will remain soluble prior to injection remains to be empirically determined.

7.2.2 Immunological studies of PfSPZ Vaccine

Immunologically, there is still much to be learned about the nature of the immune response to PfSPZ Vaccine in humans.

First, it is unknown what antigens are being recognized by the vaccine-induced CD8 and CD4 T cells. Malaria sporozoites and early liver stage forms express about 2000 antigens. A comprehensive mapping effort would require overcoming large technical hurdles. Mapping would require the development of an unbiased antigen library encoding the entire sporozoite and liver stage proteomes. A second

generation library would ideally encode the entire blood stage proteome given the need to study the immunogenic antigens in patients undergoing CPS immunization. The screening would require HLA-matched presentation of the library to T cells. This could be accomplished using patient derived antigen-presentation cells, which are relatively scarce. Importantly, both large patient samples (likely pre- and post-vaccine leukapheresis) and large numbers of patients with known efficacy outcomes would be required to detect meaningful signals from such a large antigen screen. Yet, the importance of such an effort is clear. Antigen mapping would be able to tell us what the targets of pre-erythrocytic immunity are, allowing us to predict the efficacy of whole sporozoite vaccines against currently circulating strains. Moreover, such an effort could reveal new antigenic targets to include in the next generation of subunit vaccines, which could be more scalable than whole sporozoite vaccines.

Second, it is not known how the vaccine will translate to infant immune systems or semi-immune populations. Of particular interest is how vaccine dose affects safety, immunogenicity, and efficacy in children and young infants. Given the large differences in $\gamma\delta$ T cell subsets in infants compared to adults [29], it will be interested to see how these cells respond to vaccination. Additionally, the presence of regulatory T cells that are specific to malaria proteins could adversely affect the immunogenicity of the PfSPZ Vaccine. Other factors – such as a history of helminth infection or other chronic infections – could adversely affect the ability of individuals living in endemic areas to respond to the vaccine. As the vaccine will have the greatest impact when deployed to these populations, determining whether the vaccination regimen is being adversely affected by such factors will be essential.

Third, protection – on the basis of data from animal models and data from this thesis – is believed to be mediated by CD8 T cells. However, in the studies where sufficient numbers of protected and not protected subjects were available for analysis (Chapters 4 and 6), the blood was not sampled at a time point that would allow me to effectively study the vaccine-induced CD8 T cell response. Subsequent efficacy studies would ideally samples frequently after the first vaccination to provide the greatest window for studying the immunobiology of a protective CD8

T cell response. This could inform the vaccine regimen by clearly defining a mechanistic correlate of protection.

Fourth, the precise interplay of multiple lymphocyte effectors at the site of immunity needs to be defined. While I hypothesize that durable sterile protection is mediated by long-lived liver-resident CD8 T cells on the basis of their frequency compared to other antigen-specific cells in the liver, it is possible that CD4 or $\gamma\delta$ T cells are contributing to the elimination of parasite-infected hepatocytes. Such studies could be accomplished using advanced fluorescent microscopy on non-human primates livers. This data could better inform vaccine delivery by clearly establishing the mechanism of protection following whole sporozoite vaccination.

7.2.3 PfSPZ Vaccine regimen optimizations

In terms of the vaccine regimen, the T cell data presented in Chapter 5 suggest that vaccination regimens with fewer than 3 immunizations should be tested. The rapid activation and expansion of T cells highlights the importance of the priming immunization. The size of the dose during priming is likely to be the most important factor in determining the efficacy against heterogenous field exposures. The lack of activation of circulating T cells after the second and third vaccinations suggests that these vaccinations are rapidly neutralized and contribute minimally to the induction of protective immunity.

The evidence for testing single or two dose vaccination strategy is compelling: (1) single dose RAS vaccination can confer 100% protection in some mouse models [216]; (2) there is minimal evidence of boosting of CD4 or CD8 T cells after the second or third vaccination in humans receiving 9.0×10^5 PfSPZ three times; and (3) there is demonstrable narrowing of antigenic breadth in some mouse models of repetitive sporozoite immunization [214].

Alternatively, a vaccine regimen with a sub-protective prime (*e.g.*, 2.0×10^5 PfSPZ) followed by a very large booster dose (*e.g.*, 10^7 PfSPZ) could have the benefit of expanding the antigen-specific T cell frequency to a level that is insufficient to eliminate the second, much larger booster vaccination.

Finally, combination vaccine regimens should also be tested. As PfSPZ Vaccine appears to mediate protection through CD8 T cells targeting liver stage parasites, there may be synergy with a vaccine that induces high titer antibodies directed against the sporozoite, such as RTS,S/AS01. Such a combination strategy could extend the duration of sterile protection against field transmission enough that focused elimination campaigns are credible.

Bibliography

[1] D. A. Henderson. The eradication of smallpox–an overview of the past, present, and future. *Vaccine*, 29 Suppl 4:D7–9, 2011.

[2] J. John. Role of injectable and oral polio vaccines in polio eradication. *Expert Rev Vaccines*, 8(1):5–8, 2009.

[3] W. J. Moss and D. E. Griffin. Global measles elimination. *Nat Rev Microbiol*, 4(12):900–8, 2006.

[4] M. H. Roper, J. H. Vandelaer, and F. L. Gasse. Maternal and neonatal tetanus. *Lancet*, 370(9603):1947–59, 2007.

[5] P. E. Farmer. Shattuck Lecture. Chronic infectious disease and the future of health care delivery. *N Engl J Med*, 369(25):2424–36, 2013.

[6] E. De Gregorio and R. Rappuoli. From empiricism to rational design: a personal perspective of the evolution of vaccine development. *Nat Rev Immunol*, 14(7):505–14, 2014.

[7] A. J. McMichael and B. F. Haynes. Lessons learned from HIV-1 vaccine trials: new priorities and directions. *Nat Immunol*, 13(5):423–7, 2012.

[8] H. A. Fletcher and L. Schrager. TB vaccine development and the End TB Strategy: importance and current status. *Trans R Soc Trop Med Hyg*, 110(4):212–8, 2016.

[9] U.S. Food and Drug Administration. Vaccines licensed for use in the United States. *www.fda.gov/BiologicsBloodVaccines/Vaccines/ApprovedProducts/ucm093833.htm*, Accessed 20 Dec 2016.

[10] W. C. Koff, D. R. Burton, P. R. Johnson, B. D. Walker, C. R. King, G. J. Nabel, R. Ahmed, M. K. Bhan, and S. A. Plotkin. Accelerating next-generation vaccine development for global disease prevention. *Science*, 340(6136):1232910, 2013.

[11] J. B. Ulmer, U. Valley, and R. Rappuoli. Vaccine manufacturing: challenges and solutions. *Nat Biotechnol*, 24(11):1377–83, 2006.

[12] R. A. Seder, L. J. Chang, M. E. Enama, K. L. Zephir, U. N. Sarwar, I. J. Gordon, L. A. Holman, E. R. James, P. F. Billingsley, A. Gunasekera, A. Richman, S. Chakravarty, A. Manoj, S. Velmurugan, M. Li, A. J. Ruben, T. Li, A. G. Eappen, R. E. Stafford, S. H. Plummer, C. S. Hendel, L. Novik, P. J. Costner, F. H. Mendoza, J. G. Saunders, M. C. Nason, J. H. Richardson, J. Murphy, S. A. Davidson, T. L. Richie, M. Sedegah, A. Sutamihardja, G. A. Fahle, K. E. Lyke, M. B. Laurens, M. Roederer, K. Tewari, J. E. Epstein, B. K. Sim, J. E. Ledgerwood, B. S. Graham, S. L. Hoffman, and the VRC 312 Study Team. Protection against malaria by intravenous immunization with a nonreplicating sporozoite vaccine. *Science*, 341(6152):1359–65, 2013.

[13] P. D. Kwong, J. R. Mascola, and G. J. Nabel. Rational design of vaccines to elicit broadly neutralizing antibodies to HIV-1. *Cold Spring Harb Perspect Med*, 1(1):a007278, 2011.

[14] N. S. Laursen and I. A. Wilson. Broadly neutralizing antibodies against influenza viruses. *Antiviral Res*, 98(3):476–83, 2013.

[15] B. M. Nkowane, S. G. Wassilak, W. A. Orenstein, K. J. Bart, L. B. Schonberger, A. R. Hinman, and O. M. Kew. Vaccine-associated paralytic poliomyelitis. United States: 1973 through 1984. *JAMA*, 257(10):1335–40, 1987.

[16] L. G. Rubin, M. J. Levin, P. Ljungman, E. G. Davies, R. Avery, M. Tomblyn, A. Bousvaros, S. Dhanireddy, L. Sung, H. Keyserling, I. Kang, and the Infectious Diseases Society of America. 2013 IDSA clinical practice guideline

for vaccination of the immunocompromised host. *Clin Infect Dis*, 58(3):e44–100, 2014.

[17] G. J. Nabel. Designing tomorrow's vaccines. *N Engl J Med*, 368(6):551–60, 2013.

[18] S. J. Draper and J. L. Heeney. Viruses as vaccine vectors for infectious diseases and cancer. *Nat Rev Microbiol*, 8(1):62–73, 2010.

[19] D. R. Casimiro, L. Chen, T. M. Fu, R. K. Evans, M. J. Caulfield, M. E. Davies, A. Tang, M. Chen, L. Huang, V. Harris, D. C. Freed, K. A. Wilson, S. Dubey, D. M. Zhu, D. Nawrocki, H. Mach, R. Troutman, L. Isopi, D. Williams, W. Hurni, Z. Xu, J. G. Smith, S. Wang, X. Liu, L. Guan, R. Long, W. Trigona, G. J. Heidecker, H. C. Perry, N. Persaud, T. J. Toner, Q. Su, X. Liang, R. Youil, M. Chastain, A. J. Bett, D. B. Volkin, E. A. Emini, and J. W. Shiver. Comparative immunogenicity in rhesus monkeys of DNA plasmid, recombinant vaccinia virus, and replication-defective adenovirus vectors expressing a human immunodeficiency virus type 1 gag gene. *J Virol*, 77(11):6305–13, 2003.

[20] R. W. Lindsay, P. A. Darrah, K. M. Quinn, U. Wille-Reece, L. M. Mattei, A. Iwasaki, S. P. Kasturi, B. Pulendran, J. G. Gall, A. G. Spies, and R. A. Seder. CD8+ T cell responses following replication-defective adenovirus serotype 5 immunization are dependent on CD11c+ dendritic cells but show redundancy in their requirement of TLR and nucleotide-binding oligomerization domain-like receptor signaling. *J Immunol*, 185(3):1513–21, 2010.

[21] D. M. Roberts, A. Nanda, M. J. Havenga, P. Abbink, D. M. Lynch, B. A. Ewald, J. Liu, A. R. Thorner, P. E. Swanson, D. A. Gorgone, M. A. Lifton, A. A. Lemckert, L. Holterman, B. Chen, A. Dilraj, A. Carville, K. G. Mansfield, J. Goudsmit, and D. H. Barouch. Hexon-chimaeric adenovirus serotype 5 vectors circumvent pre-existing anti-vector immunity. *Nature*, 441(7090):239–43, 2006.

[22] R. L. Coffman, A. Sher, and R. A. Seder. Vaccine adjuvants: putting innate immunity to work. *Immunity*, 33(4):492–503, 2010.

[23] M. F. Bachmann and G. T. Jennings. Vaccine delivery: a matter of size, geometry, kinetics and molecular patterns. *Nat Rev Immunol*, 10(11):787–96, 2010.

[24] W. H. Gerlich. Medical virology of hepatitis B: how it began and where we are now. *Virol J*, 10:239, 2013.

[25] D. M. Harper, E. L. Franco, C. Wheeler, D. G. Ferris, D. Jenkins, A. Schuind, T. Zahaf, B. Innis, P. Naud, N. S. De Carvalho, C. M. Roteli-Martins, J. Teixeira, M. M. Blatter, A. P. Korn, W. Quint, G. Dubin, and the GlaxoSmithKline HPV Vaccine Study Group. Efficacy of a bivalent L1 virus-like particle vaccine in prevention of infection with human papillomavirus types 16 and 18 in young women: a randomised controlled trial. *Lancet*, 364(9447):1757–65, 2004.

[26] S. Akira, S. Uematsu, and O. Takeuchi. Pathogen recognition and innate immunity. *Cell*, 124(4):783–801, 2006.

[27] R. M. Steinman. The dendritic cell system and its role in immunogenicity. *Annu Rev Immunol*, 9:271–96, 1991.

[28] M. Bonneville, R. L. O'Brien, and W. K. Born. Gammadelta T cell effector functions: a blend of innate programming and acquired plasticity. *Nat Rev Immunol*, 10(7):467–78, 2010.

[29] S. C. De Rosa, J. P. Andrus, S. P. Perfetto, J. J. Mantovani, L. A. Herzenberg, L. A. Herzenberg, and M. Roederer. Ontogeny of gamma delta T cells in humans. *J Immunol*, 172(3):1637–45, 2004.

[30] Z. W. Chen. Multifunctional immune responses of HMBPP-specific Vgamma2Vdelta2 T cells in *M. tuberculosis* and other infections. *Cell Mol Immunol*, 10(1):58–64, 2013.

[31] C. T. Morita, C. Jin, G. Sarikonda, and H. Wang. Nonpeptide antigens, presentation mechanisms, and immunological memory of human Vgamma2Vdelta2 T cells: discriminating friend from foe through the recognition of prenyl pyrophosphate antigens. *Immunol Rev*, 215:59–76, 2007.

[32] M. Brandes, K. Willimann, and B. Moser. Professional antigen-presentation function by human gammadelta T cells. *Science*, 309(5732):264–8, 2005.

[33] M. Brandes, K. Willimann, G. Bioley, N. Levy, M. Eberl, M. Luo, R. Tampe, F. Levy, P. Romero, and B. Moser. Cross-presenting human gammadelta T cells induce robust CD8+ alphabeta T cell responses. *Proc Natl Acad Sci U S A*, 106(7):2307–12, 2009.

[34] S. Inoue, M. Niikura, S. Takeo, S. Mineo, Y. Kawakami, A. Uchida, S. Kamiya, and F. Kobayashi. Enhancement of dendritic cell activation via CD40 ligand-expressing gammadelta T cells is responsible for protective immunity to *Plasmodium* parasites. *Proc Natl Acad Sci U S A*, 109(30):12129–34, 2012.

[35] M. C. D'Ombrain, L. J. Robinson, D. I. Stanisic, J. Taraika, N. Bernard, P. Michon, I. Mueller, and L. Schofield. Association of early interferon-gamma production with immunity to clinical malaria: a longitudinal study among Papua New Guinean children. *Clin Infect Dis*, 47(11):1380–7, 2008.

[36] J. Rossjohn, D. G. Pellicci, O. Patel, L. Gapin, and D. I. Godfrey. Recognition of CD1d-restricted antigens by natural killer T cells. *Nat Rev Immunol*, 12(12):845–57, 2012.

[37] M. C. Gold and D. M. Lewinsohn. Co-dependents: MR1-restricted MAIT cells and their antimicrobial function. *Nat Rev Microbiol*, 11(1):14–9, 2013.

[38] K. van Nierop and C. de Groot. Human follicular dendritic cells: function, origin and development. *Semin Immunol*, 14(4):251–7, 2002.

[39] D. Breitfeld, L. Ohl, E. Kremmer, J. Ellwart, F. Sallusto, M. Lipp, and R. Forster. Follicular B helper T cells express CXC chemokine receptor 5, localize to B cell follicles, and support immunoglobulin production. *J Exp Med*, 192(11):1545–52, 2000.

[40] A. Lalvani, R. Brookes, S. Hambleton, W. J. Britton, A. V. Hill, and A. J. McMichael. Rapid effector function in CD8+ memory T cells. *J Exp Med*, 186(6):859–65, 1997.

[41] P. Wong and E. G. Pamer. CD8 T cell responses to infectious pathogens. *Annu Rev Immunol*, 21:29–70, 2003.

[42] R. A. Seder and W. E. Paul. Acquisition of lymphokine-producing phenotype by CD4+ T cells. *Annu Rev Immunol*, 12:635–73, 1994.

[43] W. E. Paul and R. A. Seder. Lymphocyte responses and cytokines. *Cell*, 76(2):241–51, 1994.

[44] S. Romagnani. Th1/Th2 cells. *Inflamm Bowel Dis*, 5(4):285–94, 1999.

[45] K. N. Couper, D. G. Blount, and E. M. Riley. IL-10: the master regulator of immunity to infection. *J Immunol*, 180(9):5771–7, 2008.

[46] D. Masopust, V. Vezys, A. L. Marzo, and L. Lefrancois. Preferential localization of effector memory cells in nonlymphoid tissue. *Science*, 291(5512):2413–7, 2001.

[47] T. Sathaliyawala, M. Kubota, N. Yudanin, D. Turner, P. Camp, J. J. Thome, K. L. Bickham, H. Lerner, M. Goldstein, M. Sykes, T. Kato, and D. L. Farber. Distribution and compartmentalization of human circulating and tissue-resident memory T cell subsets. *Immunity*, 38(1):187–97, 2013.

[48] G. Stary, A. Olive, A. F. Radovic-Moreno, D. Gondek, D. Alvarez, P. A. Basto, M. Perro, V. D. Vrbanac, A. M. Tager, J. Shi, J. A. Yethon, O. C. Farokhzad, R. Langer, M. N. Starnbach, and U. H. von Andrian. A mucosal vaccine

against *Chlamydia trachomatis* generates two waves of protective memory T cells. *Science*, 348(6241):aaa8205, 2015.

[49] D. Fernandez-Ruiz, W. Y. Ng, L. E. Holz, J. Z. Ma, A. Zaid, Y. C. Wong, L. S. Lau, V. Mollard, A. Cozijnsen, N. Collins, J. Li, G. M. Davey, Y. Kato, S. Devi, R. Skandari, M. Pauley, J. H. Manton, D. I. Godfrey, A. Braun, S. S. Tay, P. S. Tan, D. G. Bowen, F. Koch-Nolte, B. Rissiek, F. R. Carbone, B. S. Crabb, M. Lahoud, I. A. Cockburn, S. N. Mueller, P. Bertolino, G. I. McFadden, I. Caminschi, and W. R. Heath. Liver-resident memory CD8+ T cells form a front-line defense against malaria liver-stage infection. *Immunity*, 2016.

[50] N. J. White. *Plasmodium knowlesi*: the fifth human malaria parasite. *Clin Infect Dis*, 46(2):172–3, 2008.

[51] C. J. Murray, K. F. Ortblad, C. Guinovart, S. S. Lim, T. M. Wolock, D. A. Roberts, E. A. Dansereau, N. Graetz, R. M. Barber, J. C. Brown, H. Wang, H. C. Duber, M. Naghavi, D. Dicker, L. Dandona, J. A. Salomon, K. R. Heuton, K. Foreman, D. E. Phillips, T. D. Fleming, A. D. Flaxman, B. K. Phillips, E. K. Johnson, M. S. Coggeshall, F. Abd-Allah, S. F. Abera, J. P. Abraham, I. Abubakar, L. J. Abu-Raddad, N. M. Abu-Rmeileh, T. Achoki, A. O. Adeyemo, A. K. Adou, J. C. Adsuar, E. E. Agardh, D. Akena, M. J. Al Kahbouri, D. Alasfoor, M. I. Albittar, G. Alcala-Cerra, M. A. Alegretti, Z. A. Alemu, R. Alfonso-Cristancho, S. Alhabib, R. Ali, F. Alla, P. J. Allen, U. Alsharif, E. Alvarez, N. Alvis-Guzman, A. A. Amankwaa, A. T. Amare, H. Amini, W. Ammar, B. O. Anderson, C. A. Antonio, P. Anwari, J. Arnlov, V. S. Arsenijevic, A. Artaman, R. J. Asghar, R. Assadi, L. S. Atkins, A. Badawi, K. Balakrishnan, A. Banerjee, S. Basu, J. Beardsley, T. Bekele, M. L. Bell, E. Bernabe, T. J. Beyene, N. Bhala, A. Bhalla, Z. A. Bhutta, A. B. Abdulhak, A. Binagwaho, J. D. Blore, B. B. Basara, D. Bose, M. Brainin, N. Breitborde, C. A. Castaneda-Orjuela, F. Catala-Lopez, V. K. Chadha, J. C. Chang, P. P. Chiang, T. W. Chuang, M. Colomar, L. T.

Cooper, C. Cooper, K. J. Courville, B. C. Cowie, M. H. Criqui, R. Dandona, A. Dayama, D. De Leo, L. Degenhardt, B. Del Pozo-Cruz, K. Deribe, et al. Global, regional, and national incidence and mortality for HIV, tuberculosis, and malaria during 1990-2013: a systematic analysis for the Global Burden of Disease Study 2013. *Lancet*, 384(9947):1005–70, 2014.

[52] J. G. Breman, M. S. Alilio, and A. Mills. Conquering the intolerable burden of malaria: what's new, what's needed: a summary. *Am J Trop Med Hyg*, 71(2 Suppl):1–15, 2004.

[53] J. L. Gallup and J. D. Sachs. The economic burden of malaria. *Am J Trop Med Hyg*, 64(1-2 Suppl):85–96, 2001.

[54] R. Amino, S. Thiberge, B. Martin, S. Celli, S. Shorte, F. Frischknecht, and R. Menard. Quantitative imaging of *Plasmodium* transmission from mosquito to mammal. *Nat Med*, 12(2):220–4, 2006.

[55] J. P. Vanderberg and U. Frevert. Intravital microscopy demonstrating antibody-mediated immobilisation of *Plasmodium berghei* sporozoites injected into skin by mosquitoes. *Int J Parasitol*, 34(9):991–6, 2004.

[56] M. J. Stewart and J. P. Vanderberg. Malaria sporozoites release circumsporozoite protein from their apical end and translocate it along their surface. *J Protozool*, 38(4):411–21, 1991.

[57] M. J. Stewart and J. P. Vanderberg. Malaria sporozoites leave behind trails of circumsporozoite protein during gliding motility. *J Protozool*, 35(3):389–93, 1988.

[58] M. J. Stewart, R. J. Nawrot, S. Schulman, and J. P. Vanderberg. *Plasmodium berghei* sporozoite invasion is blocked *in vitro* by sporozoite-immobilizing antibodies. *Infect Immun*, 51(3):859–64, 1986.

[59] U. Frevert, S. Engelmann, S. Zougbede, J. Stange, B. Ng, K. Matuschewski, L. Liebes, and H. Yee. Intravital observation of *Plasmodium berghei* sporozoite infection of the liver. *PLoS Biol*, 3(6):e192, 2005.

[60] I. Usynin, C. Klotz, and U. Frevert. Malaria circumsporozoite protein inhibits the respiratory burst in Kupffer cells. *Cell Microbiol*, 9(11):2610–28, 2007.

[61] C. Klotz and U. Frevert. *Plasmodium yoelii* sporozoites modulate cytokine profile and induce apoptosis in murine Kupffer cells. *Int J Parasitol*, 38(14):1639–50, 2008.

[62] M. M. Mota, J. C. Hafalla, and A. Rodriguez. Migration through host cells activates *Plasmodium* sporozoites for infection. *Nat Med*, 8(11):1318–22, 2002.

[63] K. E. Rankin, S. Graewe, V. T. Heussler, and R. R. Stanway. Imaging liver-stage malaria parasites. *Cell Microbiol*, 12(5):569–79, 2010.

[64] G. J. Wright and J. C. Rayner. *Plasmodium falciparum* erythrocyte invasion: combining function with immune evasion. *PLoS Pathog*, 10(3):e1003943, 2014.

[65] J. P. Vanderberg. Development of infectivity by the *Plasmodium berghei* sporozoite. *J Parasitol*, 61(1):43–50, 1975.

[66] K. Haldar, S. C. Murphy, D. A. Milner, and T. E. Taylor. Malaria: mechanisms of erythrocytic infection and pathological correlates of severe disease. *Annu Rev Pathol*, 2:217–49, 2007.

[67] B. P. Goncalves, C. Y. Huang, R. Morrison, S. Holte, E. Kabyemela, D. R. Prevots, M. Fried, and P. E. Duffy. Parasite burden and severity of malaria in Tanzanian children. *N Engl J Med*, 370(19):1799–808, 2014.

[68] G. E. Grau, P. F. Piguet, P. Vassalli, and P. H. Lambert. Tumor-necrosis factor and other cytokines in cerebral malaria: experimental and clinical data. *Immunol Rev*, 112:49–70, 1989.

[69] M. Hensmann and D. Kwiatkowski. Cellular basis of early cytokine response to *Plasmodium falciparum*. *Infect Immun*, 69(4):2364–71, 2001.

[70] M. Marti, R. T. Good, M. Rug, E. Knuepfer, and A. F. Cowman. Targeting malaria virulence and remodeling proteins to the host erythrocyte. *Science*, 306(5703):1930–3, 2004.

[71] T. F. de Koning-Ward, P. R. Gilson, J. A. Boddey, M. Rug, B. J. Smith, A. T. Papenfuss, P. R. Sanders, R. J. Lundie, A. G. Maier, A. F. Cowman, and B. S. Crabb. A newly discovered protein export machine in malaria parasites. *Nature*, 459(7249):945–9, 2009.

[72] L. H. Miller, D. I. Baruch, K. Marsh, and O. K. Doumbo. The pathogenic basis of malaria. *Nature*, 415(6872):673–9, 2002.

[73] B. S. Lowe, M. Mosobo, and P. C. Bull. All four species of human malaria parasites form rosettes. *Trans R Soc Trop Med Hyg*, 92(5):526, 1998.

[74] S. M. Kraemer and J. D. Smith. A family affair: var genes, PfEMP1 binding, and malaria disease. *Curr Opin Microbiol*, 9(4):374–80, 2006.

[75] M. Kaviratne, S. M. Khan, W. Jarra, and P. R. Preiser. Small variant STEVOR antigen is uniquely located within Maurer's clefts in *Plasmodium falciparum*-infected red blood cells. *Eukaryot Cell*, 1(6):926–35, 2002.

[76] V. Fernandez, M. Hommel, Q. Chen, P. Hagblom, and M. Wahlgren. Small, clonally variant antigens expressed on the surface of the *Plasmodium falciparum*-infected erythrocyte are encoded by the rif gene family and are the target of human immune responses. *J Exp Med*, 190(10):1393–404, 1999.

[77] D. L. Doolan, C. Dobano, and J. K. Baird. Acquired immunity to malaria. *Clin Microbiol Rev*, 22(1):13–36, Table of Contents, 2009.

[78] J. K. Baird, Krisin, M. J. Barcus, I. R. Elyazar, M. J. Bangs, J. D. Maguire, D. J. Fryauff, T. L. Richie, Sekartuti, and W. Kalalo. Onset of clinical immunity to *Plasmodium falciparum* among Javanese migrants to Indonesian Papua. *Ann Trop Med Parasitol*, 97(6):557–64, 2003.

[79] P. C. Bull, B. S. Lowe, M. Kortok, C. S. Molyneux, C. I. Newbold, and K. Marsh. Parasite antigens on the infected red cell surface are targets for naturally acquired immunity to malaria. *Nat Med*, 4(3):358–60, 1998.

[80] V. Udhayakumar, S. Kariuki, M. Kolczack, M. Girma, J. M. Roberts, A. J. Oloo, B. L. Nahlen, and A. A. Lal. Longitudinal study of natural immune responses to the *Plasmodium falciparum* apical membrane antigen (AMA-1) in a holoendemic region of malaria in western Kenya: Asembo Bay Cohort Project VIII. *Am J Trop Med Hyg*, 65(2):100–7, 2001.

[81] A. F. Egan, J. Morris, G. Barnish, S. Allen, B. M. Greenwood, D. C. Kaslow, A. A. Holder, and E. M. Riley. Clinical immunity to *Plasmodium falciparum* malaria is associated with serum antibodies to the 19-kDa C-terminal fragment of the merozoite surface antigen, PfMSP-1. *J Infect Dis*, 173(3):765–9, 1996.

[82] A. F. Egan, P. Burghaus, P. Druilhe, A. A. Holder, and E. M. Riley. Human antibodies to the 19kDa C-terminal fragment of *Plasmodium falciparum* merozoite surface protein 1 inhibit parasite growth *in vitro*. *Parasite Immunol*, 21(3):133–9, 1999.

[83] B. A. Okech, P. H. Corran, J. Todd, A. Joynson-Hicks, C. Uthaipibull, T. G. Egwang, A. A. Holder, and E. M. Riley. Fine specificity of serum antibodies to *Plasmodium falciparum* merozoite surface protein, PfMSP-1(19), predicts protection from malaria infection and high-density parasitemia. *Infect Immun*, 72(3):1557–67, 2004.

[84] Y. P. Shi, U. Sayed, S. H. Qari, J. M. Roberts, V. Udhayakumar, A. J. Oloo, W. A. Hawley, D. C. Kaslow, B. L. Nahlen, and A. A. Lal. Natural immune

response to the C-terminal 19-kilodalton domain of *Plasmodium falciparum* merozoite surface protein 1. *Infect Immun*, 64(7):2716–23, 1996.

[85] R. R. Taylor, S. J. Allen, B. M. Greenwood, and E. M. Riley. IgG3 antibodies to *Plasmodium falciparum* merozoite surface protein 2 (MSP2): increasing prevalence with age and association with clinical immunity to malaria. *Am J Trop Med Hyg*, 58(4):406–13, 1998.

[86] A. Baumann, M. M. Magris, M. L. Urbaez, S. Vivas-Martinez, R. Duran, T. Nieves, M. Esen, B. G. Mordmuller, M. Theisen, L. Avilan, and W. G. Metzger. Naturally acquired immune responses to malaria vaccine candidate antigens MSP3 and GLURP in Guahibo and Piaroa indigenous communities of the Venezuelan Amazon. *Malar J*, 11:46, 2012.

[87] D. Dodoo, M. Theisen, J. A. Kurtzhals, B. D. Akanmori, K. A. Koram, S. Jepsen, F. K. Nkrumah, T. G. Theander, and L. Hviid. Naturally acquired antibodies to the glutamate-rich protein are associated with protection against *Plasmodium falciparum* malaria. *J Infect Dis*, 181(3):1202–5, 2000.

[88] A. D. Douglas, A. R. Williams, J. J. Illingworth, G. Kamuyu, S. Biswas, A. L. Goodman, D. H. Wyllie, C. Crosnier, K. Miura, G. J. Wright, C. A. Long, F. H. Osier, K. Marsh, A. V. Turner, A. V. Hill, and S. J. Draper. The blood-stage malaria antigen PfRH5 is susceptible to vaccine-inducible cross-strain neutralizing antibody. *Nat Commun*, 2:601, 2011.

[89] T. M. Tran, A. Ongoiba, J. Coursen, C. Crosnier, A. Diouf, C. Y. Huang, S. Li, S. Doumbo, D. Doumtabe, Y. Kone, A. Bathily, S. Dia, M. Niangaly, C. Dara, J. Sangala, L. H. Miller, O. K. Doumbo, K. Kayentao, C. A. Long, K. Miura, G. J. Wright, B. Traore, and P. D. Crompton. Naturally acquired antibodies specific for *Plasmodium falciparum* reticulocyte-binding protein homologue 5 inhibit parasite growth and predict protection from malaria. *J Infect Dis*, 209(5):789–98, 2014.

[90] S. D. Patel, A. D. Ahouidi, A. K. Bei, T. N. Dieye, S. Mboup, S. C. Harrison, and M. T. Duraisingh. *Plasmodium falciparum* merozoite surface antigen, PfRH5, elicits detectable levels of invasion-inhibiting antibodies in humans. *J Infect Dis*, 208(10):1679–87, 2013.

[91] S. Bhatt, D. J. Weiss, E. Cameron, D. Bisanzio, B. Mappin, U. Dalrymple, K. E. Battle, C. L. Moyes, A. Henry, P. A. Eckhoff, E. A. Wenger, O. Briet, M. A. Penny, T. A. Smith, A. Bennett, J. Yukich, T. P. Eisele, J. T. Griffin, C. A. Fergus, M. Lynch, F. Lindgren, J. M. Cohen, C. L. Murray, D. L. Smith, S. I. Hay, R. E. Cibulskis, and P. W. Gething. The effect of malaria control on *Plasmodium falciparum* in Africa between 2000 and 2015. *Nature*, 526(7572):207–11, 2015.

[92] P. L. Alonso, S. W. Lindsay, J. R. Armstrong, M. Conteh, A. G. Hill, P. H. David, G. Fegan, A. de Francisco, A. J. Hall, F. C. Shenton, and et al. The effect of insecticide-treated bed nets on mortality of Gambian children. *Lancet*, 337(8756):1499–502, 1991.

[93] C. G. Nevill, E. S. Some, V. O. Mung'ala, W. Mutemi, L. New, K. Marsh, C. Lengeler, and R. W. Snow. Insecticide-treated bednets reduce mortality and severe morbidity from malaria among children on the Kenyan coast. *Trop Med Int Health*, 1(2):139–46, 1996.

[94] M. L. Mabaso, B. Sharp, and C. Lengeler. Historical review of malarial control in southern African with emphasis on the use of indoor residual house-spraying. *Trop Med Int Health*, 9(8):846–56, 2004.

[95] R. N'Guessan, V. Corbel, M. Akogbeto, and M. Rowland. Reduced efficacy of insecticide-treated nets and indoor residual spraying for malaria control in pyrethroid resistance area, Benin. *Emerg Infect Dis*, 13(2):199–206, 2007.

[96] D. Payne. Spread of chloroquine resistance in *Plasmodium falciparum*. *Parasitol Today*, 3(8):241–6, 1987.

[97] A. M. Dondorp, F. Nosten, P. Yi, D. Das, A. P. Phyo, J. Tarning, K. M. Lwin, F. Ariey, W. Hanpithakpong, S. J. Lee, P. Ringwald, K. Silamut, M. Imwong, K. Chotivanich, P. Lim, T. Herdman, S. S. An, S. Yeung, P. Singhasivanon, N. P. Day, N. Lindegardh, D. Socheat, and N. J. White. Artemisinin resistance in *Plasmodium falciparum* malaria. *N Engl J Med*, 361(5):455–67, 2009.

[98] E. A. Ashley, M. Dhorda, R. M. Fairhurst, C. Amaratunga, P. Lim, S. Suon, S. Sreng, J. M. Anderson, S. Mao, B. Sam, C. Sopha, C. M. Chuor, C. Nguon, S. Sovannaroth, S. Pukrittayakamee, P. Jittamala, K. Chotivanich, K. Chutasmit, C. Suchatsoonthorn, R. Runcharoen, T. T. Hien, N. T. Thuy-Nhien, N. V. Thanh, N. H. Phu, Y. Htut, K. T. Han, K. H. Aye, O. A. Mokuolu, R. R. Olaosebikan, O. O. Folaranmi, M. Mayxay, M. Khanthavong, B. Hongvanthong, P. N. Newton, M. A. Onyamboko, C. I. Fanello, A. K. Tshefu, N. Mishra, N. Valecha, A. P. Phyo, F. Nosten, P. Yi, R. Tripura, S. Borrmann, M. Bashraheil, J. Peshu, M. A. Faiz, A. Ghose, M. A. Hossain, R. Samad, M. R. Rahman, M. M. Hasan, A. Islam, O. Miotto, R. Amato, B. MacInnis, J. Stalker, D. P. Kwiatkowski, Z. Bozdech, A. Jeeyapant, P. Y. Cheah, T. Sakulthaew, J. Chalk, B. Intharabut, K. Silamut, S. J. Lee, B. Vihokhern, C. Kunasol, M. Imwong, J. Tarning, W. J. Taylor, S. Yeung, C. J. Woodrow, J. A. Flegg, D. Das, J. Smith, M. Venkatesan, C. V. Plowe, K. Stepniewska, P. J. Guerin, A. M. Dondorp, N. P. Day, N. J. White, and the Tracking Resistance to Artemisinin Collaboration. Spread of artemisinin resistance in *Plasmodium falciparum* malaria. *N Engl J Med*, 371(5):411–23, 2014.

[99] E. M. Riley and V. A. Stewart. Immune mechanisms in malaria: new insights in vaccine development. *Nat Med*, 19(2):168–78, 2013.

[100] J. B. Dame, J. L. Williams, T. F. McCutchan, J. L. Weber, R. A. Wirtz, W. T. Hockmeyer, W. L. Maloy, J. D. Haynes, I. Schneider, and D. Roberts. Structure of the gene encoding the immunodominant surface antigen on the

sporozoite of the human malaria parasite *Plasmodium falciparum*. *Science*, 225(4662):593–9, 1984.

[101] D. M. Gordon, T. W. McGovern, U. Krzych, J. C. Cohen, I. Schneider, R. LaChance, D. G. Heppner, G. Yuan, M. Hollingdale, and M. Slaoui. Safety, immunogenicity, and efficacy of a recombinantly produced *Plasmodium falciparum* circumsporozoite protein-hepatitis B surface antigen subunit vaccine. *J Infect Dis*, 171(6):1576–85, 1995.

[102] J. A. Stoute, M. Slaoui, D. G. Heppner, P. Momin, K. E. Kester, P. Desmons, B. T. Wellde, N. Garcon, U. Krzych, and M. Marchand. A preliminary evaluation of a recombinant circumsporozoite protein vaccine against *Plasmodium falciparum* malaria. RTS,S Malaria Vaccine Evaluation Group. *N Engl J Med*, 336(2):86–91, 1997.

[103] K. E. Kester, J. F. Cummings, O. Ofori-Anyinam, C. F. Ockenhouse, U. Krzych, P. Moris, R. Schwenk, R. A. Nielsen, Z. Debebe, E. Pinelis, L. Juompan, J. Williams, M. Dowler, V. A. Stewart, R. A. Wirtz, M. C. Dubois, M. Lievens, J. Cohen, W. R. Ballou, Jr. Heppner, D. G., and the RTS,S Vaccine Evaluation Group. Randomized, double-blind, phase 2a trial of falciparum malaria vaccines RTS,S/AS01B and RTS,S/AS02A in malaria-naive adults: safety, efficacy, and immunologic associates of protection. *J Infect Dis*, 200(3):337–46, 2009.

[104] K. E. Kester, D. A. McKinney, N. Tornieporth, C. F. Ockenhouse, D. G. Heppner, T. Hall, U. Krzych, M. Delchambre, G. Voss, M. G. Dowler, J. Palensky, J. Wittes, J. Cohen, W. R. Ballou, and the RTS,S Malaria Vaccine Evaluation Group. Efficacy of recombinant circumsporozoite protein vaccine regimens against experimental *Plasmodium falciparum* malaria. *J Infect Dis*, 183(4):640–7, 2001.

[105] K. E. Kester, D. A. McKinney, N. Tornieporth, C. F. Ockenhouse, Jr. Heppner, D. G., T. Hall, B. T. Wellde, K. White, P. Sun, R. Schwenk, U. Krzych,

M. Delchambre, G. Voss, M. C. Dubois, Jr. Gasser, R. A., M. G. Dowler, M. O'Brien, J. Wittes, R. Wirtz, J. Cohen, W. R. Ballou, and the RTS,S Malaria Vaccine Evaluation Group. A phase i/iia safety, immunogenicity, and efficacy bridging randomized study of a two-dose regimen of liquid and lyophilized formulations of the candidate malaria vaccine RTS,S/AS02A in malaria-naive adults. *Vaccine*, 25(29):5359–66, 2007.

[106] K. E. Kester, J. F. Cummings, C. F. Ockenhouse, R. Nielsen, B. T. Hall, D. M. Gordon, R. J. Schwenk, U. Krzych, C. A. Holland, G. Richmond, M. G. Dowler, J. Williams, R. A. Wirtz, N. Tornieporth, L. Vigneron, M. Delchambre, M. A. Demoitie, W. R. Ballou, J. Cohen, Jr. Heppner, D. G., and the RTS,S Malaria Vaccine Evaluation Group. Phase 2a trial of 0, 1, and 3 month and 0, 7, and 28 day immunization schedules of malaria vaccine RTS,S/AS02 in malaria-naive adults at the Walter Reed Army Institute of Research. *Vaccine*, 26(18):2191–202, 2008.

[107] C. F. Ockenhouse, J. Regules, D. Tosh, J. Cowden, A. Kathcart, J. Cummings, K. Paolino, J. Moon, J. Komisar, E. Kamau, T. Oliver, A. Chhoeu, J. Murphy, K. Lyke, M. Laurens, A. Birkett, C. Lee, R. Weltzin, U. Wille-Reece, M. Sedegah, J. Hendriks, I. Versteege, M. G. Pau, J. Sadoff, Y. Vanloubbeeck, M. Lievens, D. Heerwegh, P. Moris, Y. Guerra Mendoza, E. Jongert, J. Cohen, G. Voss, W. R. Ballou, and J. Vekemans. Ad35.CS.01-RTS,S/AS01 heterologous prime boost vaccine efficacy against sporozoite challenge in healthy malaria-naive adults. *PLoS One*, 10(7):e0131571, 2015.

[108] P. Bejon, J. Lusingu, A. Olotu, A. Leach, M. Lievens, J. Vekemans, S. Mshamu, T. Lang, J. Gould, M. C. Dubois, M. A. Demoitie, J. F. Stallaert, P. Vansadia, T. Carter, P. Njuguna, K. O. Awuondo, A. Malabeja, O. Abdul, S. Gesase, N. Mturi, C. J. Drakeley, B. Savarese, T. Villafana, W. R. Ballou, J. Cohen, E. M. Riley, M. M. Lemnge, K. Marsh, and L. von Seidlein. Efficacy of RTS,S/AS01E vaccine against malaria in children 5 to 17 months of age. *N Engl J Med*, 359(24):2521–32, 2008.

[109] A. Olotu, J. Lusingu, A. Leach, M. Lievens, J. Vekemans, S. Msham, T. Lang, J. Gould, M. C. Dubois, E. Jongert, P. Vansadia, T. Carter, P. Njuguna, K. O. Awuondo, A. Malabeja, O. Abdul, S. Gesase, N. Mturi, C. J. Drakeley, B. Savarese, T. Villafana, D. Lapierre, W. R. Ballou, J. Cohen, M. M. Lemnge, N. Peshu, K. Marsh, E. M. Riley, L. von Seidlein, and P. Bejon. Efficacy of RTS,S/AS01E malaria vaccine and exploratory analysis on anti-circumsporozoite antibody titres and protection in children aged 5-17 months in Kenya and Tanzania: a randomised controlled trial. *Lancet Infect Dis*, 11(2):102–9, 2011.

[110] S. T. Agnandji, B. Lell, S. S. Soulanoudjingar, J. F. Fernandes, B. P. Abossolo, C. Conzelmann, B. G. Methogo, Y. Doucka, A. Flamen, B. Mordmuller, S. Issifou, P. G. Kremsner, J. Sacarlal, P. Aide, M. Lanaspa, J. J. Aponte, A. Nhamuave, D. Quelhas, Q. Bassat, S. Mandjate, E. Macete, P. Alonso, S. Abdulla, N. Salim, O. Juma, M. Shomari, K. Shubis, F. Machera, A. S. Hamad, R. Minja, A. Mtoro, A. Sykes, S. Ahmed, A. M. Urassa, A. M. Ali, G. Mwangoka, M. Tanner, H. Tinto, U. D'Alessandro, H. Sorgho, I. Valea, M. C. Tahita, W. Kabore, S. Ouedraogo, Y. Sandrine, R. T. Guiguemde, J. B. Ouedraogo, M. J. Hamel, S. Kariuki, C. Odero, M. Oneko, K. Otieno, N. Awino, J. Omoto, J. Williamson, V. Muturi-Kioi, K. F. Laserson, L. Slutsker, W. Otieno, L. Otieno, O. Nekoye, S. Gondi, A. Otieno, B. Ogutu, R. Wasuna, V. Owira, D. Jones, A. A. Onyango, P. Njuguna, R. Chilengi, P. Akoo, C. Kerubo, J. Gitaka, C. Maingi, T. Lang, A. Olotu, B. Tsofa, P. Bejon, N. Peshu, K. Marsh, S. Owusu-Agyei, K. P. Asante, K. Osei-Kwakye, O. Boahen, S. Ayamba, K. Kayan, R. Owusu-Ofori, D. Dosoo, I. Asante, G. Adjei, G. Adjei, D. Chandramohan, B. Greenwood, J. Lusingu, S. Gesase, A. Malabeja, O. Abdul, H. Kilavo, C. Mahende, E. Liheluka, et al. First results of phase 3 trial of RTS,S/AS01 malaria vaccine in African children. *N Engl J Med*, 365(20):1863–75, 2011.

[111] S. Clinical Trials Partnership Rts, S. T. Agnandji, B. Lell, J. F. Fernandes, B. P. Abossolo, B. G. Methogo, A. L. Kabwende, A. A. Adegnika, B. Mordmuller, S. Issifou, P. G. Kremsner, J. Sacarlal, P. Aide, M. Lanaspa, J. J. Aponte, S. Machevo, S. Acacio, H. Bulo, B. Sigauque, E. Macete, P. Alonso, S. Abdulla, N. Salim, R. Minja, M. Mpina, S. Ahmed, A. M. Ali, A. T. Mtoro, A. S. Hamad, P. Mutani, M. Tanner, H. Tinto, U. D'Alessandro, H. Sorgho, I. Valea, B. Bihoun, I. Guiraud, B. Kabore, O. Sombie, R. T. Guiguemde, J. B. Ouedraogo, M. J. Hamel, S. Kariuki, M. Oneko, C. Odero, K. Otieno, N. Awino, M. McMorrow, V. Muturi-Kioi, K. F. Laserson, L. Slutsker, W. Otieno, L. Otieno, N. Otsyula, S. Gondi, A. Otieno, V. Owira, E. Oguk, G. Odongo, J. B. Woods, B. Ogutu, P. Njuguna, R. Chilengi, P. Akoo, C. Kerubo, C. Maingi, T. Lang, A. Olotu, P. Bejon, K. Marsh, G. Mwambingu, S. Owusu-Agyei, K. P. Asante, K. Osei-Kwakye, O. Boahen, D. Dosoo, I. Asante, G. Adjei, E. Kwara, D. Chandramohan, B. Greenwood, J. Lusingu, S. Gesase, A. Malabeja, O. Abdul, C. Mahende, E. Liheluka, L. Malle, M. Lemnge, T. G. Theander, C. Drakeley, D. Ansong, T. Agbenyega, S. Adjei, H. O. Boateng, T. Rettig, J. Bawa, J. Sylverken, D. Sambian, A. Sarfo, et al. A phase 3 trial of RTS,S/AS01 malaria vaccine in African infants. *N Engl J Med*, 367(24):2284–95, 2012.

[112] RTS,S Clinical Trials Partnership. Efficacy and safety of RTS,S/AS01 malaria vaccine with or without a booster dose in infants and children in Africa: final results of a phase 3, individually randomised, controlled trial. *Lancet*, 386(9988):31–45, 2015.

[113] M. A. Penny, R. Verity, C. A. Bever, C. Sauboin, K. Galactionova, S. Flasche, M. T. White, E. A. Wenger, N. Van de Velde, P. Pemberton-Ross, J. T. Griffin, T. A. Smith, P. A. Eckhoff, F. Muhib, M. Jit, and A. C. Ghani. Public health impact and cost-effectiveness of the RTS,S/AS01 malaria vaccine: a systematic comparison of predictions from four mathematical models. *Lancet*, 387(10016):367–75, 2016.

[114] A. Olotu, G. Fegan, J. Wambua, G. Nyangweso, K. O. Awuondo, A. Leach, M. Lievens, D. Leboulleux, P. Njuguna, N. Peshu, K. Marsh, and P. Bejon. Four-year efficacy of RTS,S/AS01E and its interaction with malaria exposure. *N Engl J Med*, 368(12):1111–20, 2013.

[115] A. Olotu, G. Fegan, J. Wambua, G. Nyangweso, A. Leach, M. Lievens, D. C. Kaslow, P. Njuguna, K. Marsh, and P. Bejon. Seven-year efficacy of RTS,S/AS01 malaria vaccine among young African children. *N Engl J Med*, 374(26):2519–29, 2016.

[116] H. Reyburn, R. Mbatia, C. Drakeley, J. Bruce, I. Carneiro, R. Olomi, J. Cox, W. M. Nkya, M. Lemnge, B. M. Greenwood, and E. M. Riley. Association of transmission intensity and age with clinical manifestations and case fatality of severe *Plasmodium falciparum* malaria. *JAMA*, 293(12):1461–70, 2005.

[117] M. T. White, P. Bejon, A. Olotu, J. T. Griffin, E. M. Riley, K. E. Kester, C. F. Ockenhouse, and A. C. Ghani. The relationship between RTS,S vaccine-induced antibodies, CD4(+) T cell responses and protection against *Plasmodium falciparum* infection. *PLoS One*, 8(4):e61395, 2013.

[118] A. L. Cunningham, H. Lal, M. Kovac, R. Chlibek, S. J. Hwang, J. Diez-Domingo, O. Godeaux, M. J. Levin, J. E. McElhaney, J. Puig-Barbera, C. Vanden Abeele, T. Vesikari, D. Watanabe, T. Zahaf, A. Ahonen, E. Athan, J. F. Barba-Gomez, L. Campora, F. de Looze, H. J. Downey, W. Ghesquiere, I. Gorfinkel, T. Korhonen, E. Leung, S. A. McNeil, L. Oostvogels, L. Rombo, J. Smetana, L. Weckx, W. Yeo, T. C. Heineman, and Z. O. E. Study Group. Efficacy of the herpes zoster subunit vaccine in adults 70 years of age or older. *N Engl J Med*, 375(11):1019–32, 2016.

[119] H. Lal, A. L. Cunningham, O. Godeaux, R. Chlibek, J. Diez-Domingo, S. J. Hwang, M. J. Levin, J. E. McElhaney, A. Poder, J. Puig-Barbera, T. Vesikari, D. Watanabe, L. Weckx, T. Zahaf, and T. C. Heineman. Efficacy of an

adjuvanted herpes zoster subunit vaccine in older adults. *N Engl J Med*, 372(22):2087–96, 2015.

[120] S. L. Klein, F. Shann, W. J. Moss, C. S. Benn, and P. Aaby. RTS,S malaria vaccine and increased mortality in girls. *MBio*, 7(2):e00514–16, 2016.

[121] D. E. Neafsey, M. Juraska, T. Bedford, D. Benkeser, C. Valim, A. Griggs, M. Lievens, S. Abdulla, S. Adjei, T. Agbenyega, S. T. Agnandji, P. Aide, S. Anderson, D. Ansong, J. J. Aponte, K. P. Asante, P. Bejon, A. J. Birkett, M. Bruls, K. M. Connolly, U. D'Alessandro, C. Dobano, S. Gesase, B. Greenwood, J. Grimsby, H. Tinto, M. J. Hamel, I. Hoffman, P. Kamthunzi, S. Kariuki, P. G. Kremsner, A. Leach, B. Lell, N. J. Lennon, J. Lusingu, K. Marsh, F. Martinson, J. T. Molel, E. L. Moss, P. Njuguna, C. F. Ockenhouse, B. R. Ogutu, W. Otieno, L. Otieno, K. Otieno, S. Owusu-Agyei, D. J. Park, K. Pelle, D. Robbins, C. Russ, E. M. Ryan, J. Sacarlal, B. Sogoloff, H. Sorgho, M. Tanner, T. Theander, I. Valea, S. K. Volkman, Q. Yu, D. Lapierre, B. W. Birren, P. B. Gilbert, and D. F. Wirth. Genetic diversity and protective efficacy of the RTS,S/AS01 malaria vaccine. *N Engl J Med*, 373(21):2025–37, 2015.

[122] J. A. Regules, S. B. Cicatelli, J. W. Bennett, K. M. Paolino, P. S. Twomey, J. E. Moon, A. K. Kathcart, K. D. Hauns, J. L. Komisar, A. N. Qabar, S. A. Davidson, S. Dutta, M. E. Griffith, C. D. Magee, M. Wojnarski, J. R. Livezey, A. T. Kress, P. E. Waterman, E. Jongert, U. Wille-Reece, W. Volkmuth, D. Emerling, W. H. Robinson, M. Lievens, D. Morelle, C. K. Lee, B. Yassin-Rajkumar, R. Weltzin, J. Cohen, R. M. Paris, N. C. Waters, A. J. Birkett, D. C. Kaslow, W. R. Ballou, C. F. Ockenhouse, and J. Vekemans. Fractional third and fourth dose of RTS,S/AS01 malaria candidate vaccine: A phase 2a controlled human malaria parasite infection and immunogenicity study. *J Infect Dis*, 214(5):762–71, 2016.

[123] S. J. McConkey, W. H. Reece, V. S. Moorthy, D. Webster, S. Dunachie, G. Butcher, J. M. Vuola, T. J. Blanchard, P. Gothard, K. Watkins, C. M. Hannan, S. Everaere, K. Brown, K. E. Kester, J. Cummings, J. Williams, D. G. Heppner, A. Pathan, K. Flanagan, N. Arulanantham, M. T. Roberts, M. Roy, G. L. Smith, J. Schneider, T. Peto, R. E. Sinden, S. C. Gilbert, and A. V. Hill. Enhanced T-cell immunogenicity of plasmid DNA vaccines boosted by recombinant modified vaccinia virus Ankara in humans. *Nat Med*, 9(6):729–35, 2003.

[124] D. P. Webster, S. Dunachie, J. M. Vuola, T. Berthoud, S. Keating, S. M. Laidlaw, S. J. McConkey, I. Poulton, L. Andrews, R. F. Andersen, P. Bejon, G. Butcher, R. Sinden, M. A. Skinner, S. C. Gilbert, and A. V. Hill. Enhanced T cell-mediated protection against malaria in human challenges by using the recombinant poxviruses FP9 and modified vaccinia virus Ankara. *Proc Natl Acad Sci U S A*, 102(13):4836–41, 2005.

[125] M. Walther, F. M. Thompson, S. Dunachie, S. Keating, S. Todryk, T. Berthoud, L. Andrews, R. F. Andersen, A. Moore, S. C. Gilbert, I. Poulton, F. Dubovsky, E. Tierney, S. Correa, A. Huntcooke, G. Butcher, J. Williams, R. E. Sinden, and A. V. Hill. Safety, immunogenicity, and efficacy of prime-boost immunization with recombinant poxvirus FP9 and modified vaccinia virus Ankara encoding the full-length *Plasmodium falciparum* circumsporozoite protein. *Infect Immun*, 74(5):2706–16, 2006.

[126] S. J. Dunachie, M. Walther, J. E. Epstein, S. Keating, T. Berthoud, L. Andrews, R. F. Andersen, P. Bejon, N. Goonetilleke, I. Poulton, D. P. Webster, G. Butcher, K. Watkins, R. E. Sinden, G. L. Levine, T. L. Richie, J. Schneider, D. Kaslow, S. C. Gilbert, D. J. Carucci, and A. V. Hill. A DNA prime-modified vaccinia virus Ankara boost vaccine encoding thrombospondin-related adhesion protein but not circumsporozoite protein partially protects healthy malaria-naive adults against *Plasmodium falciparum* sporozoite challenge. *Infect Immun*, 74(10):5933–42, 2006.

[127] G. A. O'Hara, C. J. Duncan, K. J. Ewer, K. A. Collins, S. C. Elias, F. D. Halstead, A. L. Goodman, N. J. Edwards, A. Reyes-Sandoval, P. Bird, R. Rowland, S. H. Sheehy, I. D. Poulton, C. Hutchings, S. Todryk, L. Andrews, A. Folgori, E. Berrie, S. Moyle, A. Nicosia, S. Colloca, R. Cortese, L. Siani, A. M. Lawrie, S. C. Gilbert, and A. V. Hill. Clinical assessment of a recombinant simian adenovirus ChAd63: a potent new vaccine vector. *J Infect Dis*, 205(5):772–81, 2012.

[128] C. Ogwang, M. Afolabi, D. Kimani, Y. J. Jagne, S. H. Sheehy, C. M. Bliss, C. J. Duncan, K. A. Collins, M. A. Garcia Knight, E. Kimani, N. A. Anagnostou, E. Berrie, S. Moyle, S. C. Gilbert, A. J. Spencer, P. Soipei, J. Mueller, J. Okebe, S. Colloca, R. Cortese, N. K. Viebig, R. Roberts, K. Gantlett, A. M. Lawrie, A. Nicosia, E. B. Imoukhuede, P. Bejon, B. C. Urban, K. L. Flanagan, K. J. Ewer, R. Chilengi, A. V. Hill, and K. Bojang. Safety and immunogenicity of heterologous prime-boost immunisation with *Plasmodium falciparum* malaria candidate vaccines, ChAd63 ME-TRAP and MVA ME-TRAP, in healthy Gambian and Kenyan adults. *PLoS One*, 8(3):e57726, 2013.

[129] S. H. Hodgson, K. J. Ewer, C. M. Bliss, N. J. Edwards, T. Rampling, N. A. Anagnostou, E. de Barra, T. Havelock, G. Bowyer, I. D. Poulton, S. de Cassan, R. Longley, J. J. Illingworth, A. D. Douglas, P. B. Mange, K. A. Collins, R. Roberts, S. Gerry, E. Berrie, S. Moyle, S. Colloca, R. Cortese, R. E. Sinden, S. C. Gilbert, P. Bejon, A. M. Lawrie, A. Nicosia, S. N. Faust, and A. V. Hill. Evaluation of the efficacy of ChAd63-MVA vectored vaccines expressing circumsporozoite protein and ME-TRAP against controlled human malaria infection in malaria-naive individuals. *J Infect Dis*, 211(7):1076–86, 2015.

[130] K. J. Ewer, G. A. O'Hara, C. J. Duncan, K. A. Collins, S. H. Sheehy, A. Reyes-Sandoval, A. L. Goodman, N. J. Edwards, S. C. Elias, F. D. Halstead, R. J. Longley, R. Rowland, I. D. Poulton, S. J. Draper, A. M. Blagborough, E. Berrie, S. Moyle, N. Williams, L. Siani, A. Folgori, S. Colloca, R. E. Sinden, A. M. Lawrie, R. Cortese, S. C. Gilbert, A. Nicosia, and A. V. Hill.

Protective CD8+ T-cell immunity to human malaria induced by chimpanzee adenovirus-MVA immunisation. *Nat Commun*, 4:2836, 2013.

[131] C. Ogwang, D. Kimani, N. J. Edwards, R. Roberts, J. Mwacharo, G. Bowyer, C. Bliss, S. H. Hodgson, P. Njuguna, N. K. Viebig, A. Nicosia, E. Gitau, S. Douglas, J. Illingworth, K. Marsh, A. Lawrie, E. B. Imoukhuede, K. Ewer, B. C. Urban, S. Hill AV, and P. Bejon. Prime-boost vaccination with chimpanzee adenovirus and modified vaccinia Ankara encoding TRAP provides partial protection against *Plasmodium falciparum* infection in Kenyan adults. *Sci Transl Med*, 7(286):286re5, 2015.

[132] C. Tamminga, M. Sedegah, D. Regis, I. Chuang, J. E. Epstein, M. Spring, J. Mendoza-Silveiras, S. McGrath, S. Maiolatesi, S. Reyes, V. Steinbeiss, C. Fedders, K. Smith, B. House, H. Ganeshan, J. Lejano, E. Abot, G. J. Banania, R. Sayo, F. Farooq, M. Belmonte, J. Murphy, J. Komisar, J. Williams, M. Shi, D. Brambilla, N. Manohar, N. O. Richie, C. Wood, K. Limbach, N. B. Patterson, J. T. Bruder, D. L. Doolan, C. R. King, C. Diggs, L. Soisson, D. Carucci, G. Levine, S. Dutta, M. R. Hollingdale, C. F. Ockenhouse, and T. L. Richie. Adenovirus-5-vectored *P. falciparum* vaccine expressing CSP and AMA1. Part B: safety, immunogenicity and protective efficacy of the CSP component. *PLoS One*, 6(10):e25868, 2011.

[133] C. Tamminga, M. Sedegah, S. Maiolatesi, C. Fedders, S. Reyes, A. Reyes, C. Vasquez, Y. Alcorta, I. Chuang, M. Spring, M. Kavanaugh, H. Ganeshan, J. Huang, M. Belmonte, E. Abot, A. Belmonte, J. Banania, F. Farooq, J. Murphy, J. Komisar, N. O. Richie, J. Bennett, K. Limbach, N. B. Patterson, J. T. Bruder, M. Shi, E. Miller, S. Dutta, C. Diggs, L. A. Soisson, M. R. Hollingdale, J. E. Epstein, and T. L. Richie. Human adenovirus 5-vectored *Plasmodium falciparum* NMRC-M3V-Ad-PfCA vaccine encoding CSP and AMA1 is safe, well-tolerated and immunogenic but does not protect against controlled human malaria infection. *Hum Vaccin Immunother*, 9(10):2165–77, 2013.

[134] I. Chuang, M. Sedegah, S. Cicatelli, M. Spring, M. Polhemus, C. Tamminga, N. Patterson, M. Guerrero, J. W. Bennett, S. McGrath, H. Ganeshan, M. Belmonte, F. Farooq, E. Abot, J. G. Banania, J. Huang, R. Newcomer, L. Rein, D. Litilit, N. O. Richie, C. Wood, J. Murphy, R. Sauerwein, C. C. Hermsen, A. J. McCoy, E. Kamau, J. Cummings, J. Komisar, A. Sutamihardja, M. Shi, J. E. Epstein, S. Maiolatesi, D. Tosh, K. Limbach, E. Angov, E. Bergmann-Leitner, J. T. Bruder, D. L. Doolan, C. R. King, D. Carucci, S. Dutta, L. Soisson, C. Diggs, M. R. Hollingdale, C. F. Ockenhouse, and T. L. Richie. DNA prime/adenovirus boost malaria vaccine encoding *P. falciparum* CSP and AMA1 induces sterile protection associated with cell-mediated immunity. *PLoS One*, 8(2):e55571, 2013.

[135] T. L. Richie, Y. Charoenvit, R. Wang, J. E. Epstein, R. C. Hedstrom, S. Kumar, T. C. Luke, D. A. Freilich, J. C. Aguiar, Jr. Sacci, J. B., M. Sedegah, Jr. Nosek, R. A., P. De La Vega, M. P. Berzins, V. F. Majam, E. N. Abot, H. Ganeshan, N. O. Richie, J. G. Banania, M. F. Baraceros, T. G. Geter, R. Mere, L. Bebris, K. Limbach, B. W. Hickey, D. E. Lanar, J. Ng, M. Shi, P. M. Hobart, J. A. Norman, L. A. Soisson, M. R. Hollingdale, W. O. Rogers, D. L. Doolan, and S. L. Hoffman. Clinical trial in healthy malaria-naive adults to evaluate the safety, tolerability, immunogenicity and efficacy of MuStDO5, a five-gene, sporozoite/hepatic stage *Plasmodium falciparum* DNA vaccine combined with escalating dose human GM-CSF DNA. *Hum Vaccin Immunother*, 8(11):1564–84, 2012.

[136] K. E. Kester, Jr. Gray Heppner, D., P. Moris, O. Ofori-Anyinam, U. Krzych, N. Tornieporth, D. McKinney, M. Delchambre, C. F. Ockenhouse, G. Voss, C. Holland, J. P. Beckey, W. R. Ballou, J. Cohen, and the RTS,S-Trap Group. Sequential phase 1 and phase 2 randomized, controlled trials of the safety, immunogenicity and efficacy of combined pre-erythrocytic vaccine antigens RTS,S and TRAP formulated with AS02 adjuvant system in healthy, malaria naive adults. *Vaccine*, 32(49):6683–91, 2014.

[137] D. F. Clyde, H. Most, V. C. McCarthy, and J. P. Vanderberg. Immunization of man against sporozite-induced falciparum malaria. *Am J Med Sci*, 266(3):169–77, 1973.

[138] S. L. Hoffman, L. M. Goh, T. C. Luke, I. Schneider, T. P. Le, D. L. Doolan, J. Sacci, P. de la Vega, M. Dowler, C. Paul, D. M. Gordon, J. A. Stoute, L. W. Church, M. Sedegah, D. G. Heppner, W. R. Ballou, and T. L. Richie. Protection of humans against malaria by immunization with radiation-attenuated *Plasmodium falciparum* sporozoites. *J Infect Dis*, 185(8):1155–64, 2002.

[139] T. C. Luke and S. L. Hoffman. Rationale and plans for developing a non-replicating, metabolically active, radiation-attenuated *Plasmodium falciparum* sporozoite vaccine. *J Exp Biol*, 206(Pt 21):3803–8, 2003.

[140] S. L. Hoffman, P. F. Billingsley, E. James, A. Richman, M. Loyevsky, T. Li, S. Chakravarty, A. Gunasekera, R. Chattopadhyay, M. Li, R. Stafford, A. Ahumada, J. E. Epstein, M. Sedegah, S. Reyes, T. L. Richie, K. E. Lyke, R. Edelman, M. B. Laurens, C. V. Plowe, and B. K. Sim. Development of a metabolically active, non-replicating sporozoite vaccine to prevent *Plasmodium falciparum* malaria. *Hum Vaccin*, 6(1):97–106, 2010.

[141] J. E. Epstein, K. Tewari, K. E. Lyke, B. K. Sim, P. F. Billingsley, M. B. Laurens, A. Gunasekera, S. Chakravarty, E. R. James, M. Sedegah, A. Richman, S. Velmurugan, S. Reyes, M. Li, K. Tucker, A. Ahumada, A. J. Ruben, T. Li, R. Stafford, A. G. Eappen, C. Tamminga, J. W. Bennett, C. F. Ockenhouse, J. R. Murphy, J. Komisar, N. Thomas, M. Loyevsky, A. Birkett, C. V. Plowe, C. Loucq, R. Edelman, T. L. Richie, R. A. Seder, and S. L. Hoffman. Live attenuated malaria vaccine designed to protect through hepatic CD8(+) T cell immunity. *Science*, 334(6055):475–80, 2011.

[142] A. S. Ishizuka, K. E. Lyke, A. DeZure, A. A. Berry, T. L. Richie, F. H. Mendoza, M. E. Enama, I. J. Gordon, L. J. Chang, U. N. Sarwar, K. L. Zephir,

L. A. Holman, E. R. James, P. F. Billingsley, A. Gunasekera, S. Chakravarty, A. Manoj, M. Li, A. J. Ruben, T. Li, A. G. Eappen, R. E. Stafford, C. N. K, T. Murshedkar, H. DeCederfelt, S. H. Plummer, C. S. Hendel, L. Novik, P. J. Costner, J. G. Saunders, M. B. Laurens, C. V. Plowe, B. Flynn, W. R. Whalen, J. P. Todd, J. Noor, S. Rao, K. Sierra-Davidson, G. M. Lynn, J. E. Epstein, M. A. Kemp, G. A. Fahle, S. A. Mikolajczak, M. Fishbaugher, B. K. Sack, S. H. Kappe, S. A. Davidson, L. S. Garver, N. K. Bjorkstrom, M. C. Nason, B. S. Graham, M. Roederer, B. K. Sim, S. L. Hoffman, J. E. Ledgerwood, and R. A. Seder. Protection against malaria at 1 year and immune correlates following PfSPZ vaccination. *Nat Med*, 22(6):614–23, 2016.

[143] M. Roestenberg, M. McCall, J. Hopman, J. Wiersma, A. J. Luty, G. J. van Gemert, M. van de Vegte-Bolmer, B. van Schaijk, K. Teelen, T. Arens, L. Spaarman, Q. de Mast, W. Roeffen, G. Snounou, L. Renia, A. van der Ven, C. C. Hermsen, and R. Sauerwein. Protection against a malaria challenge by sporozoite inoculation. *N Engl J Med*, 361(5):468–77, 2009.

[144] Jr. Sullivan, D. J., I. Y. Gluzman, D. G. Russell, and D. E. Goldberg. On the molecular mechanism of chloroquine's antimalarial action. *Proc Natl Acad Sci U S A*, 93(21):11865–70, 1996.

[145] M. Roestenberg, A. C. Teirlinck, M. B. McCall, K. Teelen, K. N. Makamdop, J. Wiersma, T. Arens, P. Beckers, G. van Gemert, M. van de Vegte-Bolmer, A. J. van der Ven, A. J. Luty, C. C. Hermsen, and R. W. Sauerwein. Long-term protection against malaria after experimental sporozoite inoculation: an open-label follow-up study. *Lancet*, 377(9779):1770–6, 2011.

[146] E. M. Bijker, G. J. Bastiaens, A. C. Teirlinck, G. J. van Gemert, W. Graumans, M. van de Vegte-Bolmer, R. Siebelink-Stoter, T. Arens, K. Teelen, W. Nahrendorf, E. J. Remarque, W. Roeffen, A. Jansens, D. Zimmerman, M. Vos, B. C. van Schaijk, J. Wiersma, A. J. van der Ven, Q. de Mast, L. van Lieshout, J. J. Verweij, C. C. Hermsen, A. Scholzen, and R. W. Sauerwein.

Protection against malaria after immunization by chloroquine prophylaxis and sporozoites is mediated by preerythrocytic immunity. *Proc Natl Acad Sci U S A*, 110(19):7862–7, 2013.

[147] E. M. Bijker, R. Schats, J. M. Obiero, M. C. Behet, G. J. van Gemert, M. van de Vegte-Bolmer, W. Graumans, L. van Lieshout, G. J. Bastiaens, K. Teelen, C. C. Hermsen, A. Scholzen, L. G. Visser, and R. W. Sauerwein. Sporozoite immunization of human volunteers under mefloquine prophylaxis is safe, immunogenic and protective: a double-blind randomized controlled clinical trial. *PLoS One*, 9(11):e112910, 2014.

[148] R. Schats, E. M. Bijker, G. J. van Gemert, W. Graumans, M. van de Vegte-Bolmer, L. van Lieshout, M. C. Haks, C. C. Hermsen, A. Scholzen, L. G. Visser, and R. W. Sauerwein. Heterologous protection against malaria after immunization with *Plasmodium falciparum* sporozoites. *PLoS One*, 10(5):e0124243, 2015.

[149] M. Spring, J. Murphy, R. Nielsen, M. Dowler, J. W. Bennett, S. Zarling, J. Williams, P. de la Vega, L. Ware, J. Komisar, M. Polhemus, T. L. Richie, J. Epstein, C. Tamminga, I. Chuang, N. Richie, M. O'Neil, D. G. Heppner, J. Healer, M. O'Neill, H. Smithers, O. C. Finney, S. A. Mikolajczak, R. Wang, A. Cowman, C. Ockenhouse, U. Krzych, and S. H. Kappe. First-in-human evaluation of genetically attenuated *Plasmodium falciparum* sporozoites administered by bite of *Anopheles* mosquitoes to adult volunteers. *Vaccine*, 31(43):4975–83, 2013.

[150] K. M. VanBuskirk, M. T. O'Neill, P. De La Vega, A. G. Maier, U. Krzych, J. Williams, M. G. Dowler, Jr. Sacci, J. B., N. Kangwanrangsan, T. Tsuboi, N. M. Kneteman, Jr. Heppner, D. G., B. A. Murdock, S. A. Mikolajczak, A. S. Aly, A. F. Cowman, and S. H. Kappe. Preerythrocytic, live-attenuated *Plasmodium falciparum* vaccine candidates by design. *Proc Natl Acad Sci U S A*, 106(31):13004–9, 2009.

[151] S. A. Mikolajczak, V. Lakshmanan, M. Fishbaugher, N. Camargo, A. Harupa, A. Kaushansky, A. N. Douglass, M. Baldwin, J. Healer, M. O'Neill, T. Phuong, A. Cowman, and S. H. Kappe. A next-generation genetically attenuated *Plasmodium falciparum* parasite created by triple gene deletion. *Mol Ther*, 22(9):1707–15, 2014.

[152] S. Cohen, Gregor Ia Mc, and S. Carrington. Gamma-globulin and acquired immunity to human malaria. *Nature*, 192:733–7, 1961.

[153] A. Sabchareon, T. Burnouf, D. Ouattara, P. Attanath, H. Bouharoun-Tayoun, P. Chantavanich, C. Foucault, T. Chongsuphajaisiddhi, and P. Druilhe. Parasitologic and clinical human response to immunoglobulin administration in *falciparum* malaria. *Am J Trop Med Hyg*, 45(3):297–308, 1991.

[154] D. I. Baruch, J. A. Gormely, C. Ma, R. J. Howard, and B. L. Pasloske. *Plasmodium falciparum* erythrocyte membrane protein 1 is a parasitized erythrocyte receptor for adherence to CD36, thrombospondin, and intercellular adhesion molecule 1. *Proc Natl Acad Sci U S A*, 93(8):3497–502, 1996.

[155] H. Groux and J. Gysin. Opsonization as an effector mechanism in human protection against asexual blood stages of *Plasmodium falciparum*: functional role of IgG subclasses. *Res Immunol*, 141(6):529–42, 1990.

[156] H. Bouharoun-Tayoun, P. Attanath, A. Sabchareon, T. Chongsuphajaisiddhi, and P. Druilhe. Antibodies that protect humans against *Plasmodium falciparum* blood stages do not on their own inhibit parasite growth and invasion *in vitro*, but act in cooperation with monocytes. *J Exp Med*, 172(6):1633–41, 1990.

[157] E. Malkin, J. Hu, Z. Li, Z. Chen, X. Bi, Z. Reed, F. Dubovsky, J. Liu, Q. Wang, X. Pan, T. Chen, B. Giersing, Y. Xu, X. Kang, J. Gu, Q. Shen, K. Tucker, E. Tierney, W. Pan, C. Long, and Z. Cao. A phase 1 trial of PfCP2.9: an AMA1/MSP1 chimeric recombinant protein vaccine for *Plasmodium falciparum* malaria. *Vaccine*, 26(52):6864–73, 2008.

[158] I. Sagara, A. Dicko, R. D. Ellis, M. P. Fay, S. I. Diawara, M. H. Assadou, M. S. Sissoko, M. Kone, A. I. Diallo, R. Saye, M. A. Guindo, O. Kante, M. B. Niambele, K. Miura, G. E. Mullen, M. Pierce, L. B. Martin, A. Dolo, D. A. Diallo, O. K. Doumbo, L. H. Miller, and A. Saul. A randomized controlled phase 2 trial of the blood stage AMA1-C1/Alhydrogel malaria vaccine in children in Mali. *Vaccine*, 27(23):3090–8, 2009.

[159] B. R. Ogutu, O. J. Apollo, D. McKinney, W. Okoth, J. Siangla, F. Dubovsky, K. Tucker, J. N. Waitumbi, C. Diggs, J. Wittes, E. Malkin, A. Leach, L. A. Soisson, J. B. Milman, L. Otieno, C. A. Holland, M. Polhemus, S. A. Remich, C. F. Ockenhouse, J. Cohen, W. R. Ballou, S. K. Martin, E. Angov, V. A. Stewart, J. A. Lyon, D. G. Heppner, M. R. Withers, and M. S. P. Malaria Vaccine Working Group. Blood stage malaria vaccine eliciting high antigen-specific antibody concentrations confers no protection to young children in Western Kenya. *PLoS One*, 4(3):e4708, 2009.

[160] M. D. Spring, J. F. Cummings, C. F. Ockenhouse, S. Dutta, R. Reidler, E. Angov, E. Bergmann-Leitner, V. A. Stewart, S. Bittner, L. Juompan, M. G. Kortepeter, R. Nielsen, U. Krzych, E. Tierney, L. A. Ware, M. Dowler, C. C. Hermsen, R. W. Sauerwein, S. J. de Vlas, O. Ofori-Anyinam, D. E. Lanar, J. L. Williams, K. E. Kester, K. Tucker, M. Shi, E. Malkin, C. Long, C. L. Diggs, L. Soisson, M. C. Dubois, W. R. Ballou, J. Cohen, and Jr. Heppner, D. G. Phase 1/2a study of the malaria vaccine candidate apical membrane antigen-1 (AMA-1) administered in adjuvant system AS01B or AS02A. *PLoS One*, 4(4):e5254, 2009.

[161] S. Biswas, M. D. Dicks, C. A. Long, E. J. Remarque, L. Siani, S. Colloca, M. G. Cottingham, A. A. Holder, S. C. Gilbert, A. V. Hill, and S. J. Draper. Transgene optimization, immunogenicity and *in vitro* efficacy of viral vectored vaccines expressing two alleles of *Plasmodium falciparum* AMA1. *PLoS One*, 6(6):e20977, 2011.

[162] S. H. Sheehy, C. J. Duncan, S. C. Elias, K. A. Collins, K. J. Ewer, A. J. Spencer, A. R. Williams, F. D. Halstead, S. E. Moretz, K. Miura, C. Epp, M. D. Dicks, I. D. Poulton, A. M. Lawrie, E. Berrie, S. Moyle, C. A. Long, S. Colloca, R. Cortese, S. C. Gilbert, A. Nicosia, A. V. Hill, and S. J. Draper. Phase Ia clinical evaluation of the *Plasmodium falciparum* blood-stage antigen MSP1 in ChAd63 and MVA vaccine vectors. *Mol Ther*, 19(12):2269–76, 2011.

[163] S. L. Takala and C. V. Plowe. Genetic diversity and malaria vaccine design, testing and efficacy: preventing and overcoming 'vaccine resistant malaria'. *Parasite Immunol*, 31(9):560–73, 2009.

[164] M. A. Thera, O. K. Doumbo, D. Coulibaly, M. B. Laurens, A. Ouattara, A. K. Kone, A. B. Guindo, K. Traore, I. Traore, B. Kouriba, D. A. Diallo, I. Diarra, M. Daou, A. Dolo, Y. Tolo, M. S. Sissoko, A. Niangaly, M. Sissoko, S. Takala-Harrison, K. E. Lyke, Y. Wu, W. C. Blackwelder, O. Godeaux, J. Vekemans, M. C. Dubois, W. R. Ballou, J. Cohen, D. Thompson, T. Dube, L. Soisson, C. L. Diggs, B. House, D. E. Lanar, S. Dutta, Jr. Heppner, D. G., and C. V. Plowe. A field trial to assess a blood-stage malaria vaccine. *N Engl J Med*, 365(11):1004–13, 2011.

[165] A. Saul, G. Lawrence, A. Smillie, C. M. Rzepczyk, C. Reed, D. Taylor, K. Anderson, A. Stowers, R. Kemp, A. Allworth, R. F. Anders, G. V. Brown, D. Pye, P. Schoofs, D. O. Irving, S. L. Dyer, G. C. Woodrow, W. R. Briggs, R. Reber, and D. Sturchler. Human phase I vaccine trials of 3 recombinant asexual stage malaria antigens with Montanide ISA720 adjuvant. *Vaccine*, 17(23-24):3145–59, 1999.

[166] B. Genton, I. Betuela, I. Felger, F. Al-Yaman, R. F. Anders, A. Saul, L. Rare, M. Baisor, K. Lorry, G. V. Brown, D. Pye, D. O. Irving, T. A. Smith, H. P. Beck, and M. P. Alpers. A recombinant blood-stage malaria vaccine reduces *Plasmodium falciparum* density and exerts selective pressure on parasite populations in a phase 1-2b trial in Papua New Guinea. *J Infect Dis*, 185(6):820–7, 2002.

[167] B. Mordmuller, K. Szywon, B. Greutelaers, M. Esen, L. Mewono, C. Treut, R. E. Murbeth, R. Chilengi, R. Noor, W. L. Kilama, E. B. Imoukhuede, N. Imbault, O. Leroy, M. Theisen, S. Jepsen, P. Milligan, R. Fendel, P. G. Kremsner, and S. Issifou. Safety and immunogenicity of the malaria vaccine candidate GMZ2 in malaria-exposed, adult individuals from Lambarene, Gabon. *Vaccine*, 28(41):6698–703, 2010.

[168] S. B. Sirima, B. Mordmuller, P. Milligan, U. A. Ngoa, F. Kironde, F. Atuguba, A. B. Tiono, S. Issifou, M. Kaddumukasa, O. Bangre, C. Flach, M. Christiansen, P. Bang, R. Chilengi, S. Jepsen, P. G. Kremsner, M. Theisen, and the GMZ Trial Study Group. A phase 2b randomized, controlled trial of the efficacy of the GMZ2 malaria vaccine in African children. *Vaccine*, 34(38):4536–42, 2016.

[169] K. A. Koram, B. Adu, J. Ocran, Y. S. Karikari, S. Adu-Amankwah, M. Ntiri, B. Abuaku, D. Dodoo, B. Gyan, K. C. Kronmann, and F. Nkrumah. Safety and immunogenicity of EBA-175 RII-NG malaria vaccine administered intramuscularly in semi-immune adults: A phase 1, double-blinded placebo controlled dosage escalation study. *PLoS One*, 11(9):e0163066, 2016.

[170] J. Baum, L. Chen, J. Healer, S. Lopaticki, M. Boyle, T. Triglia, F. Ehlgen, S. A. Ralph, J. G. Beeson, and A. F. Cowman. Reticulocyte-binding protein homologue 5 - an essential adhesin involved in invasion of human erythrocytes by *Plasmodium falciparum*. *Int J Parasitol*, 39(3):371–80, 2009.

[171] L. Y. Bustamante, S. J. Bartholdson, C. Crosnier, M. G. Campos, M. Wanaguru, C. Nguon, D. P. Kwiatkowski, G. J. Wright, and J. C. Rayner. A full-length recombinant *Plasmodium falciparum* PfRH5 protein induces inhibitory antibodies that are effective across common PfRH5 genetic variants. *Vaccine*, 31(2):373–9, 2013.

[172] C. Crosnier, L. Y. Bustamante, S. J. Bartholdson, A. K. Bei, M. Theron, M. Uchikawa, S. Mboup, O. Ndir, D. P. Kwiatkowski, M. T. Duraisingh, J. C.

Rayner, and G. J. Wright. Basigin is a receptor essential for erythrocyte invasion by *Plasmodium falciparum*. *Nature*, 480(7378):534–7, 2011.

[173] L. Chen, S. Lopaticki, D. T. Riglar, C. Dekiwadia, A. D. Uboldi, W. H. Tham, M. T. O'Neill, D. Richard, J. Baum, S. A. Ralph, and A. F. Cowman. An EGF-like protein forms a complex with PfRH5 and is required for invasion of human erythrocytes by *Plasmodium falciparum*. *PLoS Pathog*, 7(9):e1002199, 2011.

[174] K. S. Reddy, E. Amlabu, A. K. Pandey, P. Mitra, V. S. Chauhan, and D. Gaur. Multiprotein complex between the GPI-anchored CyRPA with PfRH5 and PfRipr is crucial for *Plasmodium falciparum* erythrocyte invasion. *Proc Natl Acad Sci U S A*, 112(4):1179–84, 2015.

[175] A. D. Douglas, G. C. Baldeviano, C. M. Lucas, L. A. Lugo-Roman, C. Crosnier, S. J. Bartholdson, A. Diouf, K. Miura, L. E. Lambert, J. A. Ventocilla, K. P. Leiva, K. H. Milne, J. J. Illingworth, A. J. Spencer, K. A. Hjerrild, D. G. Alanine, A. V. Turner, J. T. Moorhead, K. A. Edgel, Y. Wu, C. A. Long, G. J. Wright, A. G. Lescano, and S. J. Draper. A PfRH5-based vaccine is efficacious against heterologous strain blood-stage *Plasmodium falciparum* infection in *Aotus* monkeys. *Cell Host Microbe*, 17(1):130–9, 2015.

[176] R. Carter. Transmission blocking malaria vaccines. *Vaccine*, 19(17-19):2309–14, 2001.

[177] Y. Li, D. B. Leneghan, K. Miura, D. Nikolaeva, I. J. Brian, M. D. Dicks, A. J. Fyfe, S. E. Zakutansky, S. de Cassan, C. A. Long, S. J. Draper, A. V. Hill, F. Hill, and S. Biswas. Enhancing immunogenicity and transmission-blocking activity of malaria vaccines by fusing Pfs25 to IMX313 multimerization technology. *Sci Rep*, 6:18848, 2016.

[178] T. S. Churcher, A. M. Blagborough, M. Delves, C. Ramakrishnan, M. C. Kapulu, A. R. Williams, S. Biswas, D. F. Da, A. Cohuet, and R. E. Sinden.

Measuring the blockade of malaria transmission–an analysis of the Standard Membrane Feeding Assay. *Int J Parasitol*, 42(11):1037–44, 2012.

[179] K. E. Wright, K. A. Hjerrild, J. Bartlett, A. D. Douglas, J. Jin, R. E. Brown, J. J. Illingworth, R. Ashfield, S. B. Clemmensen, W. A. de Jongh, S. J. Draper, and M. K. Higgins. Structure of malaria invasion protein RH5 with erythrocyte basigin and blocking antibodies. *Nature*, 515(7527):427–30, 2014.

[180] S. A. Ogun, L. Dumon-Seignovert, J. B. Marchand, A. A. Holder, and F. Hill. The oligomerization domain of C4-binding protein (C4bp) acts as an adjuvant, and the fusion protein comprised of the 19-kilodalton merozoite surface protein 1 fused with the murine C4bp domain protects mice against malaria. *Infect Immun*, 76(8):3817–23, 2008.

[181] K. D. Brune, D. B. Leneghan, I. J. Brian, A. S. Ishizuka, M. F. Bachmann, S. J. Draper, S. Biswas, and M. Howarth. Plug-and-Display: decoration of virus-like particles via isopeptide bonds for modular immunization. *Sci Rep*, 6:19234, 2016.

[182] L. Li, J. O. Fierer, T. A. Rapoport, and M. Howarth. Structural analysis and optimization of the covalent association between SpyCatcher and a peptide Tag. *J Mol Biol*, 426(2):309–17, 2014.

[183] L. Lamoreaux, M. Roederer, and R. Koup. Intracellular cytokine optimization and standard operating procedure. *Nat Protoc*, 1(3):1507–16, 2006.

[184] A. M. Vaughan, S. A. Mikolajczak, N. Camargo, V. Lakshmanan, M. Kennedy, S. E. Lindner, J. L. Miller, J. C. Hume, and S. H. Kappe. A transgenic *Plasmodium falciparum* NF54 strain that expresses GFP-luciferase throughout the parasite life cycle. *Mol Biochem Parasitol*, 186(2):143–7, 2012.

[185] B. K. Sack, J. L. Miller, A. M. Vaughan, A. Douglass, A. Kaushansky, S. Mikolajczak, A. Coppi, G. Gonzalez-Aseguinolaza, M. Tsuji, F. Zavala, P. Sinnis, and S. H. Kappe. Model for *in vivo* assessment of humoral protection

against malaria sporozoite challenge by passive transfer of monoclonal antibodies and immune serum. *Infect Immun*, 82(2):808–17, 2014.

[186] M. Roederer, J. L. Nozzi, and M. C. Nason. SPICE: exploration and analysis of post-cytometric complex multivariate datasets. *Cytometry A*, 79(2):167–74, 2011.

[187] A. F. Cowman and B. S. Crabb. Invasion of red blood cells by malaria parasites. *Cell*, 124(4):755–66, 2006.

[188] K. A. Hjerrild, J. Jin, K. E. Wright, R. E. Brown, J. M. Marshall, G. M. Labbe, S. E. Silk, C. J. Cherry, S. B. Clemmensen, T. Jorgensen, J. J. Illingworth, D. G. Alanine, K. H. Milne, R. Ashfield, W. A. de Jongh, A. D. Douglas, M. K. Higgins, and S. J. Draper. Production of full-length soluble *Plasmodium falciparum* RH5 protein vaccine using a *Drosophila melanogaster* Schneider 2 stable cell line system. *Sci Rep*, 6:30357, 2016.

[189] B. Zakeri, J. O. Fierer, E. Celik, E. C. Chittock, U. Schwarz-Linek, V. T. Moy, and M. Howarth. Peptide tag forming a rapid covalent bond to a protein, through engineering a bacterial adhesin. *Proc Natl Acad Sci U S A*, 109(12):E690–7, 2012.

[190] K. E. Sapsford, W. R. Algar, L. Berti, K. B. Gemmill, B. J. Casey, E. Oh, M. H. Stewart, and I. L. Medintz. Functionalizing nanoparticles with biological molecules: developing chemistries that facilitate nanotechnology. *Chem Rev*, 113(3):1904–2074, 2013.

[191] M. T. Smith, A. K. Hawes, and B. C. Bundy. Reengineering viruses and virus-like particles through chemical functionalization strategies. *Curr Opin Biotechnol*, 24(4):620–6, 2013.

[192] A. Walker, C. Skamel, and M. Nassal. SplitCore: an exceptionally versatile viral nanoparticle for native whole protein display regardless of 3D structure. *Sci Rep*, 1:5, 2011.

[193] A. Jegerlehner, A. Tissot, F. Lechner, P. Sebbel, I. Erdmann, T. Kundig, T. Bachi, T. Storni, G. Jennings, P. Pumpens, W. A. Renner, and M. F. Bachmann. A molecular assembly system that renders antigens of choice highly repetitive for induction of protective B cell responses. *Vaccine*, 20(25-26):3104–12, 2002.

[194] L. K. Pattenden, A. P. Middelberg, M. Niebert, and D. I. Lipin. Towards the preparative and large-scale precision manufacture of virus-like particles. *Trends Biotechnol*, 23(10):523–9, 2005.

[195] Q. Zhao, Y. Wang, D. Freed, T. M. Fu, J. A. Gimenez, R. D. Sitrin, and M. W. Washabaugh. Maturation of recombinant hepatitis B virus surface antigen particles. *Hum Vaccin*, 2(4):174–80, 2006.

[196] D. B. Craig and A. A. Dombkowski. Disulfide by Design 2.0: a web-based tool for disulfide engineering in proteins. *BMC Bioinformatics*, 14:346, 2013.

[197] G. M. Lynn, R. Laga, P. A. Darrah, A. S. Ishizuka, A. J. Balaci, A. E. Dulcey, M. Pechar, R. Pola, M. Y. Gerner, A. Yamamoto, C. R. Buechler, K. M. Quinn, M. G. Smelkinson, O. Vanek, R. Cawood, T. Hills, O. Vasalatiy, K. Kastenmuller, J. R. Francica, L. Stutts, J. K. Tom, K. A. Ryu, A. P. Esser-Kahn, T. Etrych, K. D. Fisher, L. W. Seymour, and R. A. Seder. *In vivo* characterization of the physicochemical properties of polymer-linked TLR agonists that enhance vaccine immunogenicity. *Nat Biotechnol*, 33(11):1201–10, 2015.

[198] K. Nganou-Makamdop, I. Ploemen, M. Behet, G. J. Van Gemert, C. Hermsen, M. Roestenberg, and R. W. Sauerwein. Reduced *Plasmodium berghei* sporozoite liver load associates with low protective efficacy after intradermal immunization. *Parasite Immunol*, 34(12):562–9, 2012.

[199] P. Potocnjak, N. Yoshida, R. S. Nussenzweig, and V. Nussenzweig. Monovalent fragments (Fab) of monoclonal antibodies to a sporozoite surface antigen

(Pb44) protect mice against malarial infection. *J Exp Med*, 151(6):1504–13, 1980.

[200] Y. Charoenvit, S. Mellouk, C. Cole, R. Bechara, M. F. Leef, M. Sedegah, L. F. Yuan, F. A. Robey, R. L. Beaudoin, and S. L. Hoffman. Monoclonal, but not polyclonal, antibodies protect against *Plasmodium yoelii* sporozoites. *J Immunol*, 146(3):1020–5, 1991.

[201] L. Schofield, J. Villaquiran, A. Ferreira, H. Schellekens, R. Nussenzweig, and V. Nussenzweig. Gamma interferon, CD8+ T cells and antibodies required for immunity to malaria sporozoites. *Nature*, 330(6149):664–6, 1987.

[202] W. R. Weiss, M. Sedegah, R. L. Beaudoin, L. H. Miller, and M. F. Good. CD8+ T cells (cytotoxic/suppressors) are required for protection in mice immunized with malaria sporozoites. *Proc Natl Acad Sci U S A*, 85(2):573–6, 1988.

[203] D. L. Doolan and S. L. Hoffman. The complexity of protective immunity against liver-stage malaria. *J Immunol*, 165(3):1453–62, 2000.

[204] S. A. Plotkin. Immunologic correlates of protection induced by vaccination. *Pediatr Infect Dis J*, 20(1):63–75, 2001.

[205] A. K. McElroy, R. S. Akondy, C. W. Davis, A. H. Ellebedy, A. K. Mehta, C. S. Kraft, G. M. Lyon, B. S. Ribner, J. Varkey, J. Sidney, A. Sette, S. Campbell, U. Stroher, I. Damon, S. T. Nichol, C. F. Spiropoulou, and R. Ahmed. Human Ebola virus infection results in substantial immune activation. *Proc Natl Acad Sci U S A*, 112(15):4719–24, 2015.

[206] M. D. Preston, S. Campino, S. A. Assefa, D. F. Echeverry, H. Ocholla, A. Amambua-Ngwa, L. B. Stewart, D. J. Conway, S. Borrmann, P. Michon, I. Zongo, J. B. Ouedraogo, A. A. Djimde, O. K. Doumbo, F. Nosten, A. Pain, T. Bousema, C. J. Drakeley, R. M. Fairhurst, C. J. Sutherland, C. Roper, and T. G. Clark. A barcode of organellar genome polymorphisms identifies the

geographic origin of *Plasmodium falciparum* strains. *Nat Commun*, 5:4052, 2014.

[207] D. Walliker, I. A. Quakyi, T. E. Wellems, T. F. McCutchan, A. Szarfman, W. T. London, L. M. Corcoran, T. R. Burkot, and R. Carter. Genetic analysis of the human malaria parasite *Plasmodium falciparum*. *Science*, 236(4809):1661–6, 1987.

[208] T. R. Burkot, J. L. Williams, and I. Schneider. Infectivity to mosquitoes of *Plasmodium falciparum* clones grown *in vitro* from the same isolate. *Trans R Soc Trop Med Hyg*, 78(3):339–41, 1984.

[209] W. R. Weiss and C. G. Jiang. Protective CD8+ T lymphocytes in primates immunized with malaria sporozoites. *PLoS One*, 7(2):e31247, 2012.

[210] J. D. Miller, R. G. van der Most, R. S. Akondy, J. T. Glidewell, S. Albott, D. Masopust, K. Murali-Krishna, P. L. Mahar, S. Edupuganti, S. Lalor, S. Germon, C. Del Rio, M. J. Mulligan, S. I. Staprans, J. D. Altman, M. B. Feinberg, and R. Ahmed. Human effector and memory CD8+ T cell responses to smallpox and yellow fever vaccines. *Immunity*, 28(5):710–22, 2008.

[211] R. Schwenk, G. Banania, J. Epstein, Y. Kim, B. Peters, M. Belmonte, H. Ganeshan, J. Huang, S. Reyes, A. Stryhn, C. F. Ockenhouse, S. Buus, T. L. Richie, and M. Sedegah. *Ex vivo* tetramer staining and cell surface phenotyping for early activation markers CD38 and HLA-DR to enumerate and characterize malaria antigen-specific CD8+ T-cells induced in human volunteers immunized with a *Plasmodium falciparum* adenovirus-vectored malaria vaccine expressing AMA1. *Malar J*, 12:376, 2013.

[212] A. Gros, M. R. Parkhurst, E. Tran, A. Pasetto, P. F. Robbins, S. Ilyas, T. D. Prickett, J. J. Gartner, J. S. Crystal, I. M. Roberts, K. Trebska-McGowan, J. R. Wunderlich, J. C. Yang, and S. A. Rosenberg. Prospective identification of neoantigen-specific lymphocytes in the peripheral blood of melanoma patients. *Nat Med*, 22(4):433–8, 2016.

[213] A. C. Teirlinck, M. B. McCall, M. Roestenberg, A. Scholzen, R. Woestenenk, Q. de Mast, A. J. van der Ven, C. C. Hermsen, A. J. Luty, and R. W. Sauerwein. Longevity and composition of cellular immune responses following experimental *Plasmodium falciparum* malaria infection in humans. *PLoS Pathog*, 7(12):e1002389, 2011.

[214] S. C. Murphy, A. Kas, B. C. Stone, and M. J. Bevan. A T-cell response to a liver-stage *Plasmodium* antigen is not boosted by repeated sporozoite immunizations. *Proc Natl Acad Sci U S A*, 110(15):6055–60, 2013.

[215] I. A. Cockburn, S. Chakravarty, M. G. Overstreet, A. Garcia-Sastre, and F. Zavala. Memory CD8+ T cell responses expand when antigen presentation overcomes T cell self-regulation. *J Immunol*, 180(1):64–71, 2008.

[216] K. Nganou-Makamdop and R. W. Sauerwein. Liver or blood-stage arrest during malaria sporozoite immunization: the later the better? *Trends Parasitol*, 29(6):304–10, 2013.

[217] N. S. Butler, N. W. Schmidt, A. M. Vaughan, A. S. Aly, S. H. Kappe, and J. T. Harty. Superior antimalarial immunity after vaccination with late liver stage-arresting genetically attenuated parasites. *Cell Host Microbe*, 9(6):451–62, 2011.

[218] C. Demarta-Gatsi, L. Smith, S. Thiberge, R. Peronet, P. H. Commere, M. Matondo, L. Apetoh, P. Bruhns, R. Menard, and S. Mecheri. Protection against malaria in mice is induced by blood stage-arresting histamine-releasing factor (HRF)-deficient parasites. *J Exp Med*, 213(8):1419–28, 2016.

[219] E. Belnoue, F. T. Costa, T. Frankenberg, A. M. Vigario, T. Voza, N. Leroy, M. M. Rodrigues, I. Landau, G. Snounou, and L. Renia. Protective T cell immunity against malaria liver stage after vaccination with live sporozoites under chloroquine treatment. *J Immunol*, 172(4):2487–95, 2004.

[220] K. L. Doll, N. S. Butler, and J. T. Harty. CD8 T cell independent immunity after single dose infection-treatment-vaccination (ITV) against *Plasmodium yoelii*. *Vaccine*, 32(4):483–91, 2014.

[221] M. C. Behet, L. Foquet, G. J. van Gemert, E. M. Bijker, P. Meuleman, G. Leroux-Roels, C. C. Hermsen, A. Scholzen, and R. W. Sauerwein. Sporozoite immunization of human volunteers under chemoprophylaxis induces functional antibodies against pre-erythrocytic stages of *Plasmodium falciparum*. *Malar J*, 13:136, 2014.

[222] W. Nahrendorf, P. J. Spence, I. Tumwine, P. Levy, W. Jarra, R. W. Sauerwein, and J. Langhorne. Blood-stage immunity to *Plasmodium chabaudi* malaria following chemoprophylaxis and sporozoite immunization. *Elife*, 4, 2015.

[223] L. H. Carvalho, G. Sano, J. C. Hafalla, A. Morrot, M. A. Curotto de Lafaille, and F. Zavala. IL-4-secreting CD4+ T cells are crucial to the development of CD8+ T-cell responses against malaria liver stages. *Nat Med*, 8(2):166–70, 2002.

[224] P. A. Darrah, D. T. Patel, P. M. De Luca, R. W. Lindsay, D. F. Davey, B. J. Flynn, S. T. Hoff, P. Andersen, S. G. Reed, S. L. Morris, M. Roederer, and R. A. Seder. Multifunctional TH1 cells define a correlate of vaccine-mediated protection against *Leishmania major*. *Nat Med*, 13(7):843–50, 2007.